UNIVERSITÀ DEGLI STUDI DELL'INSUBRIA
DIPARTIMENTO DI SCIENZA ED ALTA TECNOLOGIA

Dottorato in Informatica e Matematica del Calcolo
(Ciclo XXIX)

Construction and Analysis of Subdivision Schemes from a Linear Algebra Perspective

PhD Thesis of: **Paola Novara**

Matr.: 722957

Advisor: **Prof.ssa Lucia Romani**

Co-Advisor: **Prof. Marco Donatelli**

Academic Year 2015–2016

Music was my first love and it will be my last.
Music of the future and music of the past.
To live without my music would be impossible to do.
In this world of troubles, my music pulls me through.

Music, John Miles.

Alle mie Nonne

Contents

Introduction

Subdivision schemes are efficient tools for generating smooth curves and surfaces as limit of an iterative algorithm based on simple refinement rules starting from few control points defining a polyline (curve case) or a mesh (surface case). The basic ideas behind subdivision are very old and can be dated back to the papers of de Rham, in which he proposed the so-called 'corner cutting' to describe smooth curves [35]. Some years later, the publication of the papers by Catmull and Clark [14] and Doo and Sabin [48] marked the beginning of subdivision for surface modeling. In fact, subdivision surfaces are currently extensively used in animated features, computer-generated animated movies, computer graphics and video games design, and they have recently started to appear also in the geometric kernels of modeling and CAD systems. The great success of subdivision schemes is due to the many advantages they offer such as computational efficiency and freedom in movements and shapes. In fact, only the initial control points has to be stored and just few iterations are needed to get a 'graphically smooth' limit curve or surface. Moreover, using meshes with arbitrary manifold topology we can include in the limit surface sharp edges, creases, cusps and any desired feature. Recently, subdivision schemes have become of interest also in biomedical imaging applications, due to their potential usefulness in efficiently representing active surfaces for the segmentation of 2D and 3D biomedical images [38]. As a consequence, the widely use in many different application fields has led to the definition of many different subdivision schemes and to the development of tools for the analysis of the main properties characterizing the schemes and the limit curves or surfaces produced. Many of these tools are based on algebra and linear algebra structures.

Aim of this thesis is to give a complete framework regarding the tools used for the analysis of subdivision schemes and to exploit them to construct new subdivision schemes improving many results appeared in literature. In particular, we focus our attention on some linear algebra structures that allow to give an exhaustive characterization regarding the analysis of convergence and smoothness of the limit curves and surfaces produced. In fact, it is well-known that for stationary subdivision surfaces constructed on an arbitrary manifold topology mesh, the smoothness analysis near extraordinary vertices and faces could be investigated by studying the eigenproperties of a block-circulant matrix and by applying a block diagonalization via a unitary matrix which involves the discrete Fourier transform [112, 117, 138]. Block-circulant matrices form an algebra and represent a subspace of block-Toeplitz used for their approximation in many numerical methods such as multigrid methods, preconditioned Krylov methods [33, 80] and, as we will extensively see in Chapter 5, in subdivision analysis. If the literature gives us all the necessary tools for the analysis of stationary subdivision surfaces on arbitrary manifold topology meshes, which are all summarized in Section 2.3, no

general methods have ever been proposed for the study of non-stationary subdivision surfaces near extraordinary vertices or faces. In this thesis (cf. Section 3.2.2), we propose general sufficient conditions to check the convergence of non-stationary subdivision schemes on arbitrary manifold topology meshes, exploiting again the eigenproperties of a block-circulant matrix.
The design of these linear algebra tools are thus fundamental for the construction and analysis of stationary and non-stationary subdivision schemes on arbitrary manifold topology meshes. The use of this kind of meshes, described by triangular or quadrilateral faces, is extremely important for the application of subdivision surfaces. In fact, using only regular meshes, we would not be able to design the complex models used in computer aided design as well as in biomedical imaging segmentation. Moreover, non-stationary subdivision schemes allow us to design particular shapes such as ellipsoids, tori and cylinders, thanks to their capability of generating or reproducing not only polynomials, as the stationary schemes, but also exponential polynomials. Chapters 5 and 6 deeply analyze these topics.
Regarding the univariate setting, the regularity analysis of stationary subdivision curves is usually developed using algebraic conditions on a Laurent polynomial associated to the subdivision scheme [52, 53, 57]. However, this technique provides only sufficient conditions ensuring C^r convergence. To work out necessary and sufficient conditions for the C^r continuity of a subdivision scheme, we should exploit a linear algebra tool that involves the joint spectral radius of a set of matrices [18, 22, 32, 115, 118, 121]. This technique has been already used in some papers (see e.g [13, 62, 74]), since it allows to compute the Hölder regularity of the limit curves. In this thesis, we are not interested in finding the Hölder exponent [20]; on the contrary, in Section 4.1, we exploit the joint spectral radius technique, to find the exact ranges of variation of the free parameters that define the refinement rules of a subdivision scheme.
We now describe in more details the contents of each chapter.

- Chapters 1, 2 and 3 recall the main notions regarding subdivision schemes. In particular, Chapter 1 gives a classification of subdivision schemes, focusing on the features we will consider in this thesis and explaining the terminology we will meet in the following chapters. In Chapter 2, we present stationary subdivision schemes, together with all the properties and methods proposed in literature for their analysis. Particular attention is given to the description of the linear algebra technique based on the joint spectral radius (Section 2.2.1), and to the construction and analysis of the block-circulant matrix associated to the subdivision scheme (Section 2.3). In a similar way, Chapter 3 contains the main notions on non-stationary subdivision schemes. We focus our attention on the first general method to check convergence of non-stationary subdivision schemes near extraordinary vertices and faces in Section 3.2.2.

- Chapter 4 deals with univariate subdivision. In literature, many algorithms for high quality curve design have been proposed during the years (e.g. [16, 35, 42, 72, 74, 90]). In this chapter, we would not present new subdivision schemes, but we show some generalizations of existent schemes in order to provide a complete framework and to extend their use for more applications. In Section 4.1, we present a 4-point parameter-dependent subdivision scheme which results to contain numerous independent schemes appeared in the last years as special cases [71, 72, 66, 109, 67, 116]. Exploiting the joint spectral radius technique, we show the complete range of variability of the free

parameters in order to obtain limit curves of class C^2 and C^3. This method allows us to improve the result given in [109]. To require not only high smoothness, but also the capability of reproducing a large space of polynomials, we need to consider a 5-point subdivision scheme. In Section 4.2, we study the interpolatory 5-point subdivision scheme proposed in [136], focusing on the property of convexity preservation, and we generalize this scheme to the non-stationary setting, thus allowing for the reproduction of exponential polynomials, i.e. reproduction of conic sections. These properties lead to the construction of a piecewise-uniform scheme able to produce C^2 limit curves containing segments of curve preserving the convexity of the initial data and segments reproducing conic sections arcs. The advantages given by the use of non-stationary rules prompt us to study a generalization of some fundamental families of subdivision schemes [42, 74, 90] to the non-stationary setting. These extensions are presented in Section 4.3.

- In Chapter 5, we consider stationary subdivision surfaces defined on arbitrary manifold topology meshes. The goal is to study how to choose the free weights of the extraordinary stencils in order to obtain limit surfaces of class C^1 and with bounded curvature. In Section 5.1, we study an interpolatory subdivision scheme generalizing the tensor-product version of the Dubuc-Deslauriers 4-point scheme [42] to quadrilateral meshes of arbitrary manifold topology. Requiring special conditions on eigenvalues and eigenvectors of the block-circulant matrix associated to the scheme (cf. Section 2.3), we find which conditions have to be satisfied by the stencil weights to produce surfaces with the desired properties. We also propose a particular choice for these weights to improve the schemes in [39, 84, 93]. The technique used to find the stencil weights of this particular scheme could be generalized to be applied to any subdivision scheme, described on triangular or quadrilateral meshes of arbitrary manifold topology. In Section 5.2, we propose a general computational strategy for this purpose, focusing on the case of primal schemes associated to hybrid block-circulant matrices. We apply this strategy to two schemes improving the properties of well-known Loop's scheme [95] and we obtain new ranges of variability for the stencil weights which satisfy the necessary conditions for C^1 continuity and bounded curvature.

- Chapter 6 studies non-stationary subdivision schemes and their application in biomedical imaging segmentation. An important challenge in biomedical imaging is the segmentation of closed 3D structures. Since objects in biomedical images generally have an ellipsoidal shape, non-stationary subdivision schemes turn out to be useful in this field. In this chapter, we propose novel explicit definitions of 3D deformable models based on two different non-stationary subdivision schemes both defined on triangular meshes. In Section 6.1, we construct a non-stationary subdivision scheme defined on regular triangular meshes and providing exact reproduction of ellipsoids; while in Section 6.2 we propose a non-stationary subdivision scheme defined on arbitrary manifold topology triangular meshes and able to produce a good approximation of an ellipsoid. We compare these two proposals, highlighting positive and negative aspects. Tests on real biomedical images are shown.

- In Chapter 7, we propose a general algorithm to design interpolatory curves and surfaces using stationary and non-stationary approximating subdivision schemes. The key

element of this algorithm is the use of the so-called limit stencil which indicates the position of the control points at the end of the subdivision process. In the stationary case, the computation of the limit stencil is obtained exploiting once again linear algebra tools; in particular, we use the Jordan decomposition of the so-called local subdivision matrix. In the non-stationary case, there is not a general method to find the limit stencil, but we show two different ways to compute it based on linear algebra and geometrical approaches. Many examples of interpolatory curves and surfaces are shown using both stationary and non-stationary approximating subdivision schemes.

The papers that supply material for this thesis are the following. For the convergence analysis of non-stationary subdivision schemes near extraordinary elements see [45], currently in preparation. For the study of univariate schemes see [103, 105, 106]. For the analysis of stationary subdivision schemes on arbitrary manifold topology meshes see [46, 104], while for the use of non-stationary subdivision schemes for biomedical imaging segmentation see [108] and [6], in preparation. Finally, for the interpolatory algorithm, a first example based on non-stationary Chaikin's scheme is presented in [102], while an extended generalization is in preparation (see [107]).

Chapter 1

Classification of subdivision schemes

In this thesis we study univariate and bivariate subdivision schemes to design smooth curves and surfaces. We consider only linear and scalar subdivision schemes, that is subdivision schemes whose refinement rules are described as a linear combination of points. Thus, we exclude from this treatment subdivision schemes defined by non-linear or geometrical rules as well as subdivision schemes applied to vectors (see e.g. [17, 43, 60] and [26, 50, 79]).
Among linear scalar subdivision schemes, we can distinguish between stationary and non-stationary schemes. Stationary schemes are characterized by refinement rules which are independent from the subdivision level, thus they are the same at each step of the refinement process. On the contrary, non-stationary schemes have refinement rules that change with the subdivision level, hence they are level-dependent. As we will see in the following, non-stationary subdivision could be seen as a generalization of the stationary setting. In this thesis we study both stationary and non-stationary subdivision schemes.
Another distinction regards the uniformity of the subdivision rules. A subdivision scheme is called uniform if the same refinement rules are applied to all control points of the initial polyline or mesh, otherwise it is called non-uniform. In general, in this thesis we consider uniform scheme, except for a piecewise-uniform scheme studied in Section 4.2 and the definition of the so-called extraordinary vertices and faces in the surface case presented in Chapter 5, since they usually require special refinement rules. Thus, where it is do not explicitly specify, we imply that the considered scheme is uniform.
Summarizing, in this thesis we focus on subdivision schemes which are

- univariate or bivariate,
- linear,
- scalar,
- stationary or non-stationary,
- uniform or non-uniform.

Since we have talked about extraordinary vertices and faces, in the following we describe in detail the elements that compose a mesh and their properties.

1.1 Regular and arbitrary manifold topology meshes

In general, a mesh is defined by vertices and polygonal faces identified by the so-called vertex valence, i.e. the number of edges incident on a vertex, and face valence, i.e. the number of edges delimiting a face. For a quadrilateral mesh, vertices and faces are called regular if they have valence 4 (see Figure 1.1 (a)). Differently, for a triangular mesh, regular vertices are the ones with valence 6, while regular faces have valence 3 (see Figure 1.1 (b)). In this thesis, we use the term regular mesh to refer to a mesh that contains regular vertices and regular faces only. The irregular vertices and faces are called extraordinary vertices/faces and, whenever

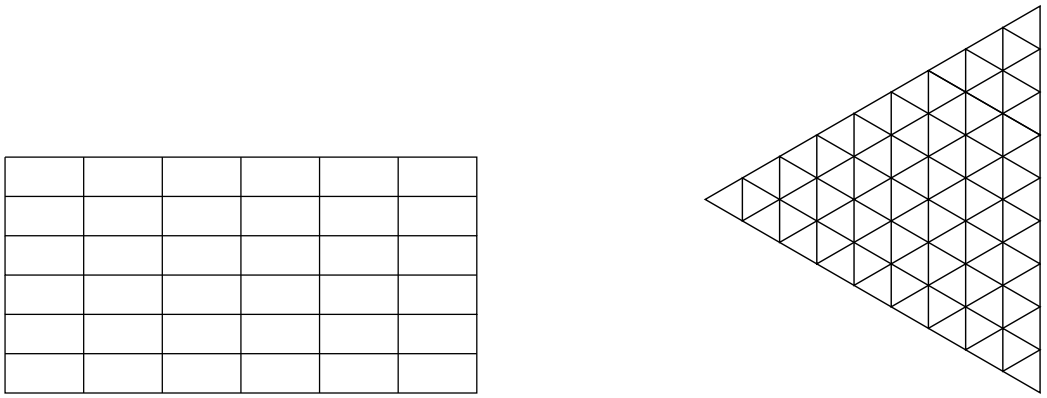

(a) Regular quadrilateral mesh

(b) Regular triangular mesh

Figure 1.1: Regular meshes.

they appear, the mesh is said to be irregular or of arbitrary manifold topology (see Figure 1.2).

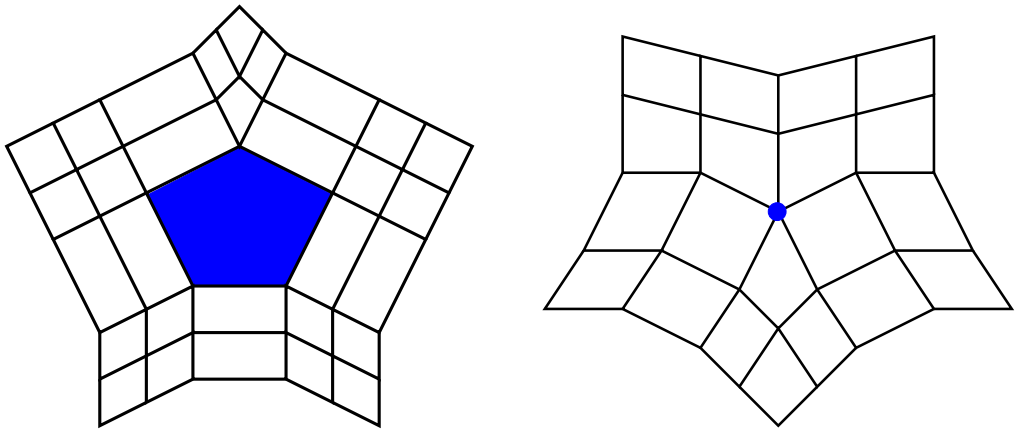

(a) Extraordinary face

(b) Extraordinary vertex

Figure 1.2: Extraordinary elements in a quadrilateral mesh.

In literature, there are also subdivision schemes defined on quad/triangle meshes, i.e. meshes defined both by triangles and quadrilaterals (see e.g. [81, 98]). However, this kind of schemes are not studied in this thesis.

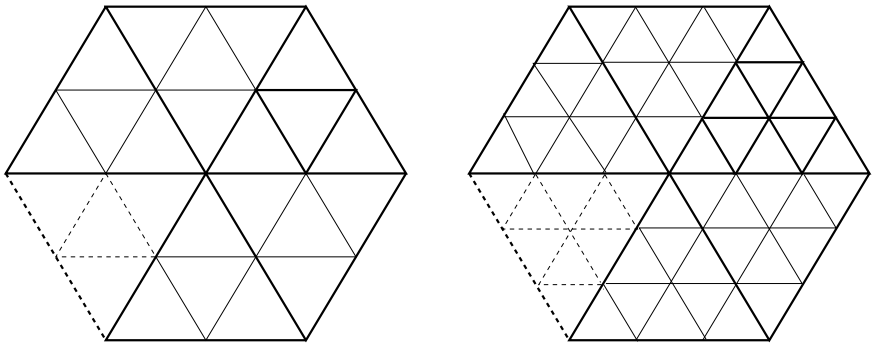

(a) Binary scheme (b) Ternary scheme

Figure 1.3: Examples of bivariate binary and ternary schemes on triangular meshes.

1.2 Main characteristics of subdivision schemes

There are other common terms to classify subdivision schemes. The arity $m \geq 2$ indicates the rate with which the control polyline or mesh is subdivided. Precisely, a univariate subdivision scheme of arity m inserts m new vertices in correspondence of an old vertex or edge, while a bivariate subdivision scheme splits each old polygonal face in m^2 new faces, as shown in Figure 1.3. In this thesis we study binary ($m = 2$) and ternary ($m = 3$) subdivision schemes.

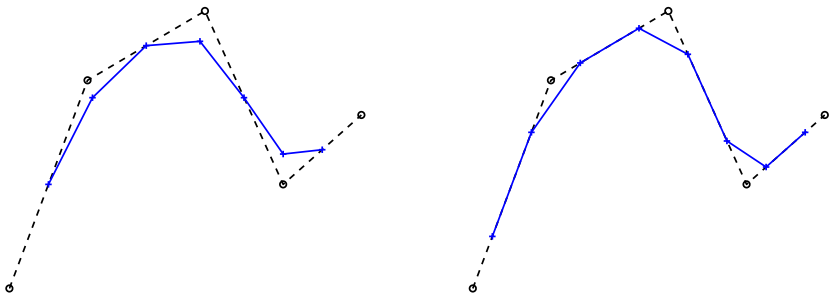

(a) Univariate primal scheme (b) Univariate dual scheme

Figure 1.4: Univariate binary primal and dual schemes.

A m-arity univariate subdivision scheme is said to be primal if it retains or modifies the old vertices and create $m-1$ new vertices at each old edge of the control polyline (see Figure 1.4 (a)), while it is said to be dual if it creates m new vertices at the old edges and discards the old vertices (see Figure 1.4(b)). In a similar way, a bivariate subdivision scheme is said to be

primal if it performs a face split as explained in Figure 1.5 (a), while it is said to be dual if it performs a vertex split as shown in Figure 1.5 (b).

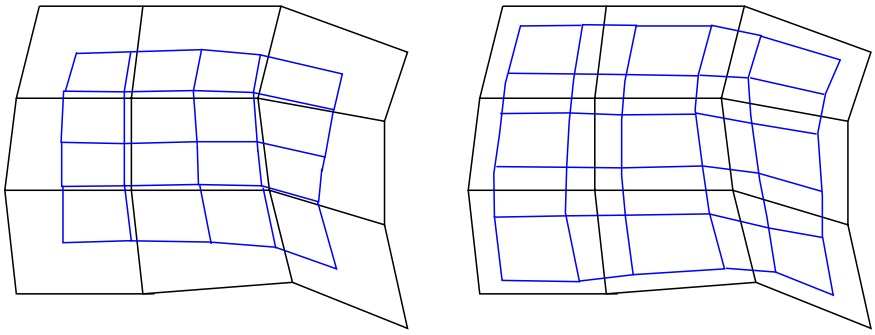

(a) Bivariate primal scheme (b) Bivariate dual scheme

Figure 1.5: Bivariate binary primal and dual schemes.

During the subdivision process, for each vertex of the initial control polyline or mesh, a sequence of vertices corresponding to different subdivision levels is defined. If all the vertices in the sequence are the same, the scheme is called interpolatory, otherwise it is termed approximating. In practice, an interpolatory scheme retains all the old vertices and introduces new ones, so that the limit curve or surface passes through the initial control points see Figure 1.6 (a). On the contrary, an approximating scheme deletes the old vertices and creates new ones, thus the limit curve or surface follows the shape of the initial control polyline or mesh without interpolating the starting vertices, as shown in Figure 1.6 (b).

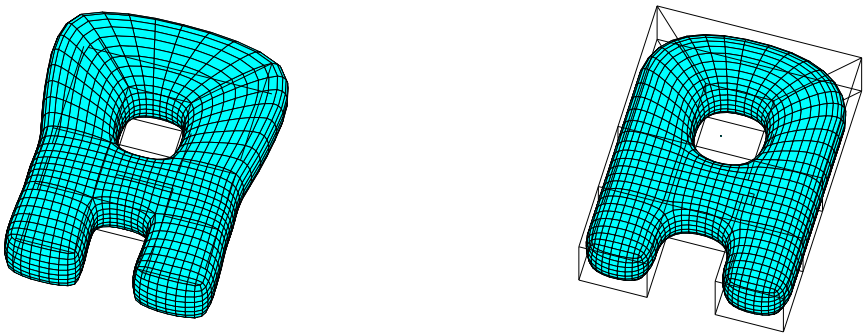

(a) Interpolatory surface (b) Approximating surface

Figure 1.6: Subdivision surfaces produced by approximating and interpolatory schemes.

We point out that all the interpolatory schemes are primal, since they retain the old vertices.

Chapter 2

Stationary subdivision schemes

This chapter is devoted to recalling the main notions on stationary subdivision schemes: the formalism and the notation, the important properties that characterize a stationary subdivision scheme, the main tools used to develop the analysis of the limit curves or surfaces generated.
A stationary subdivision scheme is denoted by $\mathcal{S}$. The term 'stationary' is important to distinguish this kind of schemes from those studied in Chapter 3, and it underlines that the refinement rules characterizing the scheme $\mathcal{S}$ are the same at each step of the subdivision process, namely they do not depend on the subdivision level $k \in \mathbb{N}_0 = \mathbb{N} \cup \{0\}$. Thus, a stationary subdivision scheme is an iterative algorithm that generates the refined data sequence $\mathbf{f}^{(k+1)} = \{f_{\mathbf{i}}^{(k+1)}, \mathbf{i} \in \mathbb{Z}^s\}$, starting from a set of control points $\mathbf{f}^{(0)} = \{f_{\mathbf{i}}^{(0)}, \mathbf{i} \in \mathbb{Z}^s\}$, by applying the same refinement rules at each subdivision step.
When we study a stationary subdivision scheme, we have to pay attention not only to its refinement rules but also to the set of initial control points and the topology with which they are connected, especially in the bivariate case. In fact, in the univariate setting ($s = 1$), the set of control points $\mathbf{f}^{(0)}$ is just a sequence of ordered vertices, connected by edges, and thus defining a control polyline. The control polyline could be open or close. In the bivariate setting ($s = 2$), the control points $\mathbf{f}^{(0)}$ define a mesh composed by polygonal faces, vertices and edges. As we have seen in Section 1.1, we could distinguish between regular or arbitrary manifold topology meshes defined on quadrilateral or triangular grids. Open polylines and meshes require special conditions on the boundary, which are not the main goal of this thesis. Thus, to avoid any problems on boundaries, when an open curve or surface is studied we consider it as a truncation of a more extended one.
The kind of mesh on which we apply a subdivision scheme $\mathcal{S}$ influences the refinement rules of the subdivision algorithm and the tools useful for the analysis of the limit surface. In particular, in the univariate setting and on regular meshes, the action of the subdivision scheme $\mathcal{S}$ is described by the subdivision mask

$$\mathbf{a} = \{\mathrm{a}_{\mathbf{i}}, \mathbf{i} \in \mathbb{Z}^s\}. \tag{2.1}$$

To emphasize the connection with the subdivision mask, when the subdivision scheme $\mathcal{S}$ is a univariate scheme or a bivariate scheme defined on regular meshes, we refer to it as $\mathcal{S}_{\mathbf{a}}$. In this case, a stationary scheme $\mathcal{S}_{\mathbf{a}}$ is described by the refinement rules

$$f_{\mathbf{i}}^{(k+1)} = \sum_{\mathbf{j} \in \mathbb{Z}^s} \mathrm{a}_{\mathbf{i}-m\mathbf{j}}\, f_{\mathbf{j}}^{(k)}, \quad \mathbf{i} \in \mathbb{Z}^s, \quad k \in \mathbb{N}_0, \tag{2.2}$$

which generate the sequence of points at level $k+1$ starting from the points at level k. In particular, $s=1$ for curves and $s=2$ for surfaces, while m indicates the arity of the scheme (see Section 1.2). The coefficients of the mask in (2.1) define the so-called subdivision symbol

$$\mathrm{a}(\boldsymbol{z}) := \sum_{\mathbf{i}\in\mathbb{Z}^s} \mathrm{a}_{\mathbf{i}} \boldsymbol{z}^{\mathbf{i}}, \quad \boldsymbol{z} \in (\mathbb{C}\backslash\{\mathbf{0}\})^s, \tag{2.3}$$

with $\boldsymbol{z}^{\mathbf{i}} = z_1^{i_1} z_2^{i_2}$, in case $s=2$. Since the schemes we consider have finite support $supp(\mathbf{a}) = \{\mathbf{i} \in \mathbb{Z}^s \mid \mathrm{a}_{\mathbf{i}} \neq 0\}$, the corresponding symbols are Laurent polynomials, namely polynomials in positive and negative powers of the variables.
On the other hand, in the irregular regions of a mesh, i.e. in the neighborhood of an extraordinary vertex or face, the action of the subdivision scheme $\mathcal{S}$ is described by the local subdivision matrix S (see Section 2.3). Near an extraordinary vertex/face, the subdivision rules which relates the vertices of the k-th level mesh with those of the next level are encoded in the rows of the local subdivision matrix S, resulting in

$$\mathbf{f}^{(k+1)} = S\mathbf{f}^{(k)} = S^2\mathbf{f}^{(k-1)} = \ldots = S^{k+1}\mathbf{f}^{(0)}. \tag{2.4}$$

Important properties of subdivision schemes are convergence, polynomial generation and reproduction, approximation order and regularity of the limit curve or surface. In particular, in literature there are tools for the study of polynomial generation and reproduction related only to regular case [19, 25, 91], while regarding convergence and regularity analysis different methods have been proposed for both the case of regular meshes (see e.g. [52, 53, 57, 62, 74]) and arbitrary manifold topology meshes (see e.g. [112, 111, 117]).
In the following sections we recall the main results regarding these important properties.

2.1 Generation and reproduction of polynomials

We start by denoting with Π_d^s the space of s-variate polynomials up to degree d. Polynomial generation of degree d is the capability of a subdivision scheme $\mathcal{S}_{\mathbf{a}}$ to generate the full space Π_d^s, while polynomial reproduction of degree d is the capability to produce in the limit exactly the same d-degree polynomial from which the data are sampled. To give more details, we first need to recall the notion of convergence and non-singularity of a stationary subdivision scheme $\mathcal{S}_{\mathbf{a}}$.

Definition 2.1 *A stationary subdivision scheme $\mathcal{S}_{\mathbf{a}}$ is called uniformly convergent if, for any initial data $\mathbf{f}^{(0)} \in \ell(\mathbb{Z}^s)$, there exists a limit function $g_{\mathbf{f}^{(0)}} \in C(\mathbb{R}^s)$ (which is nonzero for at least one initial nonzero sequence $\mathbf{f}^{(0)}$) such that the sequence of continuous functions $F^{(k)}$ interpolating the data $\mathbf{f}^{(k)}$ at the parameter values $\frac{\mathbf{i}}{m^k}$, $\mathbf{i} \in \mathbb{Z}^s$, converges to $g_{\mathbf{f}^{(0)}}$ as $k \to +\infty$, i.e.*

$$g_{\mathbf{f}^{(0)}} := \lim_{k\to+\infty} \mathcal{S}_{\mathbf{a}}^k \mathbf{f}^{(0)} = \lim_{k\to+\infty} F^{(k)},$$

uniformly. The stationary subdivision scheme $\mathcal{S}_{\mathbf{a}}$ is called C^r convergent, $r \in \mathbb{N}_0$, if $g_{\mathbf{f}^{(0)}} \in C^r(\mathbb{R}^s)$.

Definition 2.2 *The limit function $\phi := g_{\boldsymbol{\delta}}$ with initial data*

$$\delta_{\mathbf{i}} = \begin{cases} 1, & \mathbf{i} = \mathbf{0}, \\ 0, & otherwise, \end{cases} \qquad \mathbf{i} \in \mathbb{Z}^s \tag{2.5}$$

is called the basic limit function of the subdivision scheme and it is compactly supported.

Definition 2.3 *[19] A stationary subdivision scheme is called non-singular if it is convergent and* $g_{\mathbf{f}^{(0)}} = 0$ *if and only if* $\mathbf{f}^{(0)}$ *is the zero sequence, namely* $f_{\mathbf{i}}^{(0)} = 0$ *for all* $\mathbf{i} \in \mathbb{Z}^s$.

In particular, the notion of non-singularity is equivalent to the notion of linear independence of the integer shifts of the correspondent basic limit function [19, Proposition 1.3].
The differences between polynomial generation and polynomial reproduction have been studied in [25] for the univariate case, and in [19] for the surface case. We underline these differences in the following definitions.

Definition 2.4 *A convergent stationary subdivision scheme* $\mathcal{S}_{\mathbf{a}}$ *generates polynomials up to degree* d *if for any polynomial* $\pi \in \Pi_d^s$ *there exists some initial data* $\mathbf{f}^{(0)} \in \ell(\mathbb{Z}^s)$ *such that* $\mathcal{S}_{\mathbf{a}}^{\infty}\mathbf{f}^{(0)} = \pi$.

Many properties of a subdivision scheme do not depend on the choice of the associated parameter values $\mathbf{t}_{\mathbf{i}}^{(k)}, \mathbf{i} \in \mathbb{Z}^s$, to which the data $f_{\mathbf{i}}^{(k)}$ are attached. Thus, these are usually set to

$$\mathbf{t}_{\mathbf{i}}^{(k)} := \frac{\mathbf{i}}{m^k}, \quad \mathbf{i} \in \mathbb{Z}^s,\ k \in \mathbb{N}_0,$$

which is called the standard parametrization. However, for the analysis of polynomial reproduction it turns out that a better parametrization is given by $\{\mathbf{T}^{(k)}, k \in \mathbb{N}_0\}$ such that

$$\mathbf{T}^{(k)} = \left\{ \mathbf{t}_{\mathbf{i}}^{(k)} = \frac{\mathbf{i} + \boldsymbol{\tau}}{m^k}, \mathbf{i} \in \mathbb{Z}^s \right\}, \tag{2.6}$$

with a suitable $\boldsymbol{\tau} \in \mathbb{R}^s$. The sequence $\{\mathbf{T}^{(k)}, k \in \mathbb{N}_0\}$ in (2.6) is called the sequence of parameter values associated with the subdivision scheme.

Definition 2.5 *A convergent stationary subdivision scheme* $\mathcal{S}_{\mathbf{a}}$ *with associated parametrization in* (2.6) *reproduces polynomials up to degree* d *if for any polynomial* $\pi \in \Pi_d^s$ *and for the initial data* $\mathbf{f}^{(0)} = \{\pi(\mathbf{t}_{\mathbf{i}}^{(0)}), \mathbf{i} \in \mathbb{Z}^s\}$ *the limit of the subdivision satisfies* $\mathcal{S}_{\mathbf{a}}^{\infty}\mathbf{f}^{(0)} = \pi$.

Another important property of stationary subdivision is the so-called step-wise polynomial reproduction.

Definition 2.6 *A convergent stationary subdivision scheme* $\mathcal{S}_{\mathbf{a}}$ *with associated parametrization in* (2.6) *is step-wise polynomial reproducing up to degree* d *if for any polynomial* $\pi \in \Pi_d^s$ *and for the data* $\mathbf{f}^{(k)} = \{\pi(\mathbf{t}_{\mathbf{i}}^{(k)}), \mathbf{i} \in \mathbb{Z}^s\}$

$$\mathbf{f}^{(k+1)} = \mathcal{S}_{\mathbf{a}}\mathbf{f}^{(k)} \quad \textit{or, equivalently,} \quad \pi(\mathbf{t}_{\mathbf{i}}^{(k+1)}) = \sum_{\mathbf{j} \in \mathbb{Z}^s} \mathrm{a}_{\mathbf{i}-m\mathbf{j}}\ \pi(\mathbf{t}_{\mathbf{j}}^{(k)}), \quad \mathbf{i} \in \mathbb{Z}^s.$$

For a non-singular subdivision scheme the concepts of polynomial reproduction and step-wise polynomial reproduction are equivalent [19, Proposition 1.7].
In [19], sufficient algebraic conditions on the subdivision symbol $\mathrm{a}(\boldsymbol{z})$ of a convergent stationary subdivision scheme $\mathcal{S}_{\mathbf{a}}$ are proposed to guarantee generation and reproduction of Π_d^s. They could be seen as a multivariate extension of the conditions shown in [25]. We denote with

$$E := \{0, \ldots, m-1\}^s, \tag{2.7}$$

the set of the representatives of $\mathbb{Z}^s/m\mathbb{Z}^s$ containing $\mathbf{0} = \{0, \dots, 0\}$ and let Ξ be the set

$$\Xi = \{\boldsymbol{\epsilon} = e^{-\mathrm{i}\frac{2\pi}{m}\boldsymbol{e}} \ : \ \boldsymbol{e} \in E\}, \tag{2.8}$$

containing $\mathbf{1} = (1, 1, \dots, 1)$, while

$$\Xi' := \Xi \backslash \{\mathbf{1}\}. \tag{2.9}$$

Finally, by $D^{\boldsymbol{\gamma}}$ we denote the directional derivative along $\boldsymbol{\gamma} = (\gamma_1, \dots, \gamma_s) \in \mathbb{N}_0^s$, that is

$$D^{\boldsymbol{\gamma}} := \frac{\partial^{\gamma_1}}{\partial z_1^{\gamma_1}} \ \cdots \ \frac{\partial^{\gamma_s}}{\partial z_s^{\gamma_s}}, \tag{2.10}$$

and $|\boldsymbol{\gamma}| = \sum_{j=1}^{s} \gamma_j$.

Proposition 2.7 *A convergent stationary subdivision scheme with symbol* $\mathrm{a}(\boldsymbol{z})$ *generates polynomials up to degree* d *if*

$$D^{\boldsymbol{\gamma}}\mathrm{a}(\boldsymbol{\epsilon}) = 0, \qquad \forall \ \boldsymbol{\epsilon} \in \Xi', \quad |\boldsymbol{\gamma}| \leq d.$$

Polynomial generation of degree d implies that the associated refinable function has accuracy of order d [78], but it is only a necessary condition for the corresponding shift-invariant space to have approximation order $d + 1$. Moreover, the condition of polynomial generation is strictly connected with the notion of sum rules (see e.g. [20]).

Definition 2.8 *A stationary subdivision scheme* $\mathcal{S}_{\mathbf{a}}$ *satisfies sum rules of order d+1 if*

$$\mathrm{a}(1) = m^s \qquad \textit{and} \qquad \max_{|\boldsymbol{\gamma}| \leq d} \max_{\boldsymbol{\epsilon} \in \Xi'} |D^{\boldsymbol{\gamma}}\mathrm{a}(\boldsymbol{\epsilon})| = 0.$$

Proposition 2.9 *A convergent stationary subdivision scheme, with symbol* $\mathrm{a}(\boldsymbol{z})$ *and associated parametrization in* (2.6) *with some* $\boldsymbol{\tau} \in \mathbb{R}^s$*, reproduces polynomials up to degree* d *if*

$$D^{\boldsymbol{\gamma}}\mathrm{a}(\mathbf{1}) = m^s \mathrm{q}_{\mathbf{j}}(\boldsymbol{\tau}) \quad \textit{and} \quad D^{\boldsymbol{\gamma}}\mathrm{a}(\boldsymbol{\epsilon}) = 0, \ \ \forall \ \boldsymbol{\epsilon} \in \Xi', \ |\boldsymbol{\gamma}| \leq d,$$

where

$$\mathrm{q}_{\mathbf{0}}(\boldsymbol{z}) := 1, \quad \mathrm{q}_{\mathbf{j}}(z_1, \dots, z_s) = \prod_{i=1}^{s} \prod_{\ell_i=0}^{j_i-1} (z_i - \ell_i), \quad \mathbf{j} = (j_1, \dots, j_s).$$

The results in [91, Proposition 3.5] state that sufficient condition to have approximation order $d + 1$ is given by the polynomial reproduction of degree d.

Proposition 2.10 *If a stationary subdivision scheme reproduces* Π_d^s*, then it has approximation order* $d + 1$*.*

Another important property required by a stationary subdivision scheme is the affine invariance. If we moved all the control points simultaneously by the same amount, we would expect the curve or surface defined by these control points to move in the same way as a rigid object, i.e. the curve/surface should be invariant under distance-preserving transformations, such as translation and rotation. It follows from linearity of subdivision that if subdivision is invariant with respect to distance-preserving transformations, it also should be invariant under any affine transformations. The family of affine transformations in addition to distance-preserving transformations, contains shears.

Proposition 2.11 *[5, 112] If a stationary subdivision scheme $\mathcal{S}_{\mathbf{a}}$ reproduces Π_1^s, then it has the property of affine invariance.*

Finally, we consider the particular case of an interpolatory subdivision scheme. If $\mathcal{S}_{\mathbf{a}}$ is interpolatory, then it satisfies

$$\sum_{\mathbf{j}\in J} \mathrm{a}(e^{\frac{2\pi \mathrm{i}}{m}\mathbf{j}}\boldsymbol{z}) = m^s, \qquad \text{with} \quad J = \{(j_1,\ldots,j_s), 0 \le j_i \le m-1, \forall i = 1,\ldots,s\}. \tag{2.11}$$

Corollary 2.12 *Let $\mathcal{S}_{\mathbf{a}}$ be an interpolatory subdivision scheme Π_d^s-generating. Then $\mathcal{S}_{\mathbf{a}}$ is also Π_d^s-reproducing with respect to the parametrization in* (2.6).

2.2 Convergence and smoothness analysis of subdivision curves and surfaces defined on regular meshes

To recall the main notions regarding convergence and smoothness analysis of stationary subdivision schemes, we first focus on the univariate case ($s = 1$), and then we study the case of subdivision surfaces defined on regular meshes ($s = 2$). Most of the following results are taken from [52, 53, 57].

2.2.1 Convergence and smoothness analysis of subdivision curves

Let $s = 1$. If $\mathcal{S}_{\mathbf{a}}$ is convergent, than the subdivision mask $\mathbf{a}$ in (2.1) satisfies

$$\sum_{i\in\mathbb{Z}} \mathrm{a}_{mi+j} = 1, \quad \text{for all } j = 0,\ldots m-1,$$

[53, Theorem 1] and thus the subdivision symbol in (2.3) could be factorized into

$$\mathrm{a}(z) = (1 + z + \ldots + z^{m-1})\mathrm{q}(z), \qquad \mathrm{q}(1) = 1. \tag{2.12}$$

Theorem 2.13 *Let $\mathcal{S}_{\mathbf{a}}$ be a stationary subdivision scheme with symbol $\mathrm{a}(z)$ and denote by $\Delta\mathbf{f}^{(0)} = \{(\Delta f^{(0)})_i = f_i^{(0)} - f_{i-1}^{(0)} \ : i \in \mathbb{Z}\}$, for $\mathbf{f}^{(0)} = \{f_i^{(0)} \ : i \in \mathbb{Z}\}$. If* (2.12) *holds, then*

$$\Delta(\mathcal{S}_{\mathbf{a}}\mathbf{f}^{(k)}) = \mathcal{S}_{\mathbf{q}}\Delta\mathbf{f}^{(k)}.$$

$\Delta\mathbf{f}^{(k)}$ is called the divided difference scheme of order 1, with associated symbol given by the Laurent polynomial $\mathrm{q}(z)$ in (2.12). It is clear that if $\mathcal{S}_{\mathbf{a}}$ is convergent, $\Delta\mathbf{f}^{(0)}$ tends to $\mathbf{0}$ as $k \to +\infty$. The opposite direction is also true.

Theorem 2.14 *A stationary subdivision scheme $\mathcal{S}_{\mathbf{a}}$ is convergent if and only if for all initial data $\mathbf{f}^{(0)}$*

$$\lim_{k\to+\infty} \mathcal{S}_{\mathbf{q}}^k \mathbf{f}^{(0)} = \mathbf{0}. \tag{2.13}$$

If (2.13) holds for any initial data $\mathbf{f}^{(0)}$, the subdivision scheme $\mathcal{S}_{\mathbf{q}}$ is called 'contractive' and the check of the convergence of $\mathcal{S}_{\mathbf{a}}$ is equivalent to checking whether $\mathcal{S}_{\mathbf{q}}$ is contractive. This means that, we first compute the symbol

$$\mathrm{q}^{[L]}(z) := \mathrm{q}(z)\,\mathrm{q}(z^m)\,\ldots\,\mathrm{q}(z^{m^{L-1}}),$$

of the iterated scheme $\mathcal{S}_{\mathbf{q}}^L$ and then check the C^r convergence of $\mathcal{S}_{\mathbf{a}}$ showing that there exists $L \in \mathbb{N}$ (reasonably $L \leq 10$) such that

$$\|S_{\mathbf{q}}^L\|_\infty = \max\left\{\sum_i |\mathrm{q}_{i-m^L j}| : 0 \leq i < m^L\right\} < 1, \quad \text{for some } L \in \mathbb{N}. \tag{2.14}$$

In the following, to simplify the notation, we denote $\|\cdot\| = \|\cdot\|_\infty$.
The smoothness analysis is similar.

Theorem 2.15 *Let* $\mathrm{a}(z) = \left(\frac{1+z+\ldots+z^{m-1}}{2}\right)^r \mathrm{b}^{[r]}(z)$. *If* $\mathcal{S}_{\mathbf{b}^{[r]}}$ *is convergent, then* $\mathcal{S}_{\mathbf{a}}^\infty \mathbf{f}^{(0)} \in C^r(\mathbb{R})$ *for any initial data* $\mathbf{f}^{(0)}$.

Thus, C^r continuity of the subdivision scheme $\mathcal{S}_{\mathbf{a}}$ follows from the convergence of the subdivision scheme $\mathcal{S}_{\mathbf{b}^{[r]}}$ and hence from the contractivity of the scheme $\mathcal{S}_{\mathbf{b}^{[r+1]}}$ associated to the symbol $\mathrm{b}^{[r+1]}(z)$ such that $\mathrm{b}^{[r]}(z) = (1+z+\ldots+z^{m-1})\mathrm{b}^{[r+1]}(z)$, i.e the symbol of the divided difference scheme of order $r+1$ defined recursively as $\Delta^{r+1}\mathbf{f}^{(0)} = \Delta(\Delta^r \mathbf{f}^{(0)})$.

Joint spectral radius

Studying the contractivity of $\mathcal{S}_{\mathbf{b}^{[r+1]}}$, we can derive sufficient conditions ensuring C^r continuity of the scheme $\mathcal{S}_{\mathbf{a}}$ Differently, to work out necessary and sufficient conditions for the C^r continuity of a subdivision scheme $\mathcal{S}_{\mathbf{a}}$, we can exploit the joint spectral radius approach introduced in [32]. In particular, we here recall the result in [22, Theorem 4.1].

Proposition 2.16 *Assume that* $\mathbf{b}^{[r+1]}$ *has finite support of dimension* $n \in \mathbb{N}$ *and let*

$$\begin{aligned}\rho :&= \rho(B_0^{[r+1]}, \ldots, B_{m-1}^{[r+1]}) \\ &= \limsup_{\ell\to\infty} \left(\max\left\{\|B_{\epsilon_\ell}^{[r+1]} \cdots B_{\epsilon_2}^{[r+1]}\, B_{\epsilon_1}^{[r+1]}\|^{1/\ell} \,:\, \epsilon_i \in \{0,\ldots,m-1\},\ i = 1,...,\ell\right\}\right)\end{aligned}$$

denote the joint spectral radius (JSR) (see [121]) of the set $\{B_0^{[r+1]}, \ldots, B_{m-1}^{[r+1]}\}$ *of* $n \times n$ *matrices given by*

$$B_\epsilon^{[r+1]} = \left(\mathrm{b}^{[r+1]}_{n+i-mj+\epsilon}\right)_{i,j=0,\ldots,n-1}, \quad \epsilon = 0,\ldots,m-1,$$

(see e.g. [32, 18, 115, 118]). The subdivision scheme $\mathcal{S}_{\mathbf{a}}$ *is* C^r *continuous if and only if it satisfies sum rules of order* $r+1$ *and* $\rho \in [1, m)$.

Taking into account that (see, e.g., [89])

$$\max\{\rho(B_0^{[r+1]}), \ldots, \rho(B_{m-1}^{[r+1]})\} \leq \rho \leq \max\{\|B_0^{[r+1]}\|, \ldots, \|B_{m-1}^{[r+1]}\|\}, \tag{2.15}$$

whenever the upper and lower bounds in (2.15) coincide, we can provide explicit formulas for the joint spectral radius ρ.
This method will be used in Section 4.1 to determine the complete regions of C^2 and C^3 continuity of a combined ternary scheme.

2.2.2 Convergence and smoothness analysis of subdivision surfaces on regular meshes

The analysis of convergence and smoothness of a bivariate subdivision scheme ($s = 2$) on regular meshes could be easily deduced from the univariate case if the symbol factorizes into univariate smoothing factors. Otherwise, a more complex method involving matrix symbols is required, as shown in [57].
In the following, we assume to deal with binary subdivision scheme, i.e. $m = 2$, since the bivariate subdivision scheme on regular meshes studied in this thesis are all binary schemes. However, the generalization to any arity m is immediate.
Let us start by considering the easier case of a stationary subdivision scheme $\mathcal{S}_{\mathbf{a}}$ with factorizable symbols $\mathrm{a}(\boldsymbol{z})$, and suppose to consider a quadrilateral regular mesh. Necessary condition for the convergence of $\mathcal{S}_{\mathbf{a}}$ is

$$\sum_{\mathbf{j}\in\mathbb{Z}^2} \mathrm{a}_{\mathbf{i}-2\mathbf{j}} = 1, \quad \mathbf{i} = \{(0,0),(0,1),(1,0),(1,1)\}.$$

In contrast to the univariate case (see (2.12)), this necessary condition does not imply a factorization of the symbol. If the symbol is factorizable, then the two following theorems state convergence and C^r smoothness of $\mathcal{S}_{\mathbf{a}}$ [57, Theorems 4.23 and 4.24].

Theorem 2.17 *Let $\mathcal{S}_{\mathbf{a}}$ have a symbol of the form $\mathrm{a}(\boldsymbol{z}) = \mathrm{a}(z_1,z_2) = (1+z_1)(1+z_2)\mathrm{b}(z_1,z_2)$. If the schemes with the symbols $\mathrm{a}_1(z_1,z_2) = \frac{\mathrm{a}(z_1,z_2)}{1+z_1}$, $\mathrm{a}_2(z_1,z_2) = \frac{\mathrm{a}(z_1,z_2)}{1+z_2}$ are both contractive, then $\mathcal{S}_{\mathbf{a}}$ is convergent. Conversely, if $\mathcal{S}_{\mathbf{a}}$ is convergent, then $\mathcal{S}_{\mathbf{a}_1}$ and $\mathcal{S}_{\mathbf{a}_2}$ are contractive.*

Theorem 2.18 *Let $\mathcal{S}_{\mathbf{a}}$ have a symbol of the form $\mathrm{a}(\boldsymbol{z}) = \mathrm{a}(z_1,z_2) = (1+z_1)^{r_1}(1+z_2)^{r_2}\mathrm{b}(z_1,z_2)$. If the schemes with symbols*

$$\mathrm{a}_{r_1,r_2}(z_1,z_2) = \frac{2^{r_1+r_2}\mathrm{a}(z_1,z_2)}{(1+z_1)^{r_1}(1+z_2)^{r_2}}, \quad r_1,r_2 = 0,\dots,r,$$

are convergent, then $\mathcal{S}_{\mathbf{a}}$ is C^r.

Remark 2.19 *The previous analysis applies also to tensor product schemes, but it is not needed, since $\mathrm{a}(z_1,z_2) = \mathrm{a}_1(z_1)\mathrm{a}_2(z_2)$ is the symbol of a tensor product scheme and thus its smoothness properties derived from those of the associated univariate schemes $\mathcal{S}_{\mathbf{a}_1}$ and $\mathcal{S}_{\mathbf{a}_2}$.*

A similar analysis could be done also for schemes defined on triangular meshes, where the correspondent symbols, if factorizable, have the form

$$\mathrm{a}(z_1,z_2) = (1+z_1)^{r_1}(1+z_2)^{r_2}(1+z_1z_2)^{r_3}\mathrm{b}(z_1,z_2).$$

Theorem 2.20 *Let $\mathcal{S}_{\mathbf{a}}$ have a symbol of the form $\mathrm{a}(z_1,z_2) = (1+z_1)(1+z_2)(1+z_1z_2)\mathrm{b}(z_1,z_2)$. Then $\mathcal{S}_{\mathbf{a}}$ is convergent if and only if the schemes with symbols*

$$\mathrm{a}_1 = \frac{\mathrm{a}(z_1,z_2)}{1+z_1}, \quad \mathrm{a}_2 = \frac{\mathrm{a}(z_1,z_2)}{1+z_2}, \quad \mathrm{a}_3 = \frac{\mathrm{a}(z_1,z_2)}{1+z_1z_2},$$

are contractive. If any two of these schemes are contractive, then the third is also contractive.

We can generalize the proposed method for the smoothness analysis of a subdivision scheme with a factorizable symbol, to the case of non factorizable symbols as shown in [57]. We proceed as follows. Choose $\mathcal{Z}_{r+1} \subset \{(i,j,\ell) \in \mathbb{N}_0^3 : i+j+\ell = r+1\}$ such that $\#\mathcal{Z}_{r+1} = r+2$, where $\ell = 0$ on quadrilateral meshes and $\ell \geq 0$ on triangular meshes. If $\mathrm{a}(z_1, z_2)$ satisfies

$$\left((1-z_1)^i(1-z_2)^j(1-z_1z_2)^\ell\right)_{(i,j,\ell)\in\mathcal{Z}_{r+1}} \mathrm{a}(z_1,z_2) = \mathrm{b}^{[r+1]}(z_1,z_2)\left((1-z_1^2)^i(1-z_2^2)^j(1-z_1^2z_2^2)^\ell\right)_{(i,j,\ell)\in\mathcal{Z}_{r+1}} \tag{2.16}$$

then $\mathrm{b}^{[r+1]}(z_1, z_2)$ is the $(r+2)\times(r+2)$ matrix symbol of the $(r+1)$-th order difference scheme $\mathcal{S}_{\mathbf{b}^{[r+1]}}$. It satisfies

$$\nabla^{r+1}\,\mathcal{S}_{\mathbf{a}} = \mathcal{S}_{\mathbf{b}^{[r+1]}}\,\nabla^{r+1}$$

with $\nabla^{r+1} : \ell(\mathbb{Z}^2) \to \ell^{r+2}(\mathbb{Z}^2)$ consisting of $r+2$ independent backward differences of order $r+1$, defined by $\mathcal{Z}_{r+1}$. For instance, when $r = 0$, $\nabla = \begin{pmatrix} \nabla_1 \\ \nabla_2 \end{pmatrix}$ and we can alternatively choose

- $\mathcal{Z}_1 = \{(1,0,0),(0,1,0)\}$ and $\nabla_1\mathbf{c} = \mathbf{c} - \mathbf{c}(\cdot-1,\cdot)$, $\nabla_2\mathbf{c} = \mathbf{c} - \mathbf{c}(\cdot,\cdot-1)$, both on quadrilateral and triangular meshes,
- $\mathcal{Z}_1 = \{(1,0,0),(0,0,1)\}$ and $\nabla_1\mathbf{c} = \mathbf{c}-\mathbf{c}(\cdot-1,\cdot)$, $\nabla_2\mathbf{c} = \mathbf{c}-\mathbf{c}(\cdot-1,\cdot-1)$, on triangular meshes,
- $\mathcal{Z}_1 = \{(0,1,0),(0,0,1)\}$ and $\nabla_1\mathbf{c} = \mathbf{c}-\mathbf{c}(\cdot,\cdot-1)$, $\nabla_2\mathbf{c} = \mathbf{c}-\mathbf{c}(\cdot-1,\cdot-1)$, on triangular meshes.

The straightforward generalization of the approach in [57] for checking C^r convergence, $r \in \mathbb{N}_0$, of $\mathcal{S}_{\mathbf{a}}$ is based on verifying the contractivity of the $(r+1)$-th order difference scheme $\mathcal{S}_{\mathbf{b}^{[r+1]}}$. This means that, we first compute the symbol

$$(\mathrm{b}^{[r+1]})^{[L]}(\boldsymbol{z}) := \mathrm{b}^{[r+1]}(\boldsymbol{z})\,\mathrm{b}^{[r+1]}(\boldsymbol{z}^2)\,\ldots\,\mathrm{b}^{[r+1]}(\boldsymbol{z}^{2^{L-1}}),$$

with $\boldsymbol{z} = (z_1, z_2) \in (\mathbb{C}\backslash\{0\})^2$, of the iterated scheme $\mathcal{S}^L_{\mathbf{b}^{[r+1]}}$ and then check the C^r convergence of $\mathcal{S}_{\mathbf{a}}$ showing that there exists $L \in \mathbb{N}$ (reasonably $L \leq 10$) such that

$$||\mathcal{S}^L_{\mathbf{b}^{[r+1]}}|| = \max_{\mathbf{i}\in[0,2^L-1]^2\cap\mathbb{N}_0^2} \left\| \sum_{\mathbf{j}\in\mathbb{Z}^2} |(\mathrm{b}^{[r+1]})^{[L]}(\mathbf{i}-2^L\mathbf{j})| \right\| < \frac{1}{2^r}. \tag{2.17}$$

2.3 Extraordinary vertices and faces

Section 2.2.2 deals with convergence and smoothness analysis of bivariate subdivision schemes defined on regular meshes. As we have seen, the tools used for these analysis are the subdivision symbol and the contractivity of the divided difference masks. On arbitrary manifold topology meshes, we need to use different tools to study convergence and regularity of the limit surfaces at the limit of extraordinary elements of the mesh, that is extraordinary vertices and faces.

First of all, we always suppose that the extraordinary elements are isolated. We focus our attention on the local configuration of the control points near an extraordinary element, since it influences the structure of the subdivision matrix S. The subdivision matrix S describes

the action of the subdivision scheme $\mathcal{S}$ near extraordinary elements.
A primal scheme is influenced by the presence of extraordinary vertices. In this case, the local configuration of the points of the mesh is given by a central vertex of valence n plus a certain number of vertices lying on rings with increasing radial distance from it (see Figure 2.1 (a)). Near an extraordinary vertex, primal subdivision algorithms are characterized by a local subdivision matrix S of size $(pn+1) \times (pn+1)$, exactly in view of the fact that their refinement rules involve the central vertex of valence n, and n sectors with p vertices each coming from the rings around it. A dual scheme is influenced by the presence of an extraordinary face. The local configuration of the points of the mesh is given by a central face of valence n surrounded by a certain number of vertices lying on rings with increasing radial distance from it (see Figure 2.1 (b)). From this configuration it follows that near an extraordinary face dual subdivision algorithms are described by a local subdivision matrix S of size $pn \times pn$. In order to keep the matrix size as small as possible, we emphasize that it

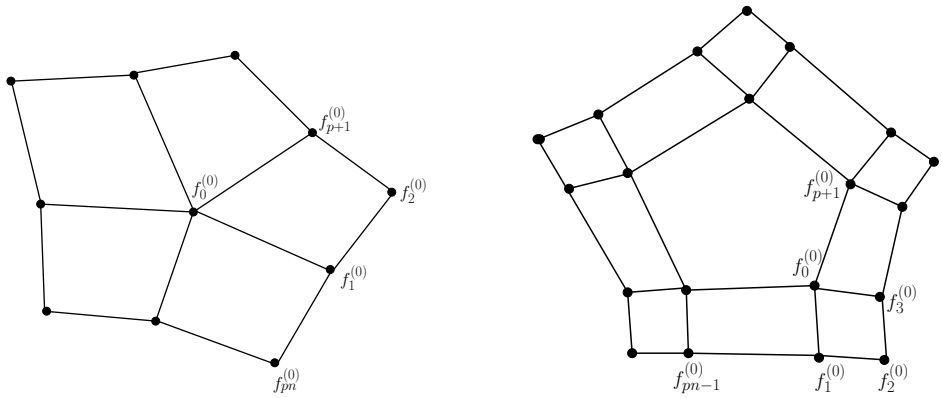

(a) Extraordinary vertex (b) Extraordinary face

Figure 2.1: Local configurations of the points near an extraordinary vertex or face in case of quadrilateral meshes.

is convenient to derive the value of p considering the exact number of rings required by the subdivision rules. Precisely, for subdivision schemes defined on triangular meshes by r-ring rules, the number p of points contained in each sector is

$$p = \frac{r(r+1)}{2}, \tag{2.18}$$

while for quadrilateral meshes we have

$$p = \begin{cases} r(r+1) & \text{for primal schemes,} \\ r^2 & \text{for dual schemes.} \end{cases} \tag{2.19}$$

Moreover, it is of crucial importance to know that, having labeled both the old and the new vertices in a symmetric way around the central vertex or face, the structure of the matrix S changes depending on the ordering of the entries of the vectors $\mathbf{f}^{(k)}$ and $\mathbf{f}^{(k+1)}$ in (2.4). Precisely:

Order 1. Primal scheme: ordering the vertices outwards from the central vertex, that is on successive rings with increasing radial distance, yields a matrix S that, discarded the first row and column, is a $p \times p$ block-matrix where each block, of size $n \times n$, is circulant;
Dual scheme: ordering the vertices outwards from one of the vertices of the central face, that is on successive rings with increasing radial distance, yields a matrix S that is a $p \times p$ block-matrix where each block, of size $n \times n$, is circulant;

Order 2. Primal scheme: ordering the vertices starting from the central vertex and outwards within each sector, before moving on to the next, and labeling compatibly within the sectors, gives a matrix S that, discarded the first row and column, is a $n \times n$ block-circulant matrix with blocks of size $p \times p$;
Dual scheme: ordering the vertices starting from one of the vertices of the central face and outwards within each sector, before moving on to the next, and labeling compatibly within the sectors, gives a matrix S that is a $n \times n$ block-circulant matrix with blocks of size $p \times p$.

Doo and Sabin [48] were the first to show that many properties of the limit surface can be investigated by studying the eigenproperties of the matrix S. Depending on the ordering of points that has been chosen, the following different methods have appeared in the literature to analyze the spectrum of S.

Method 1. Originally presented by Doo and Sabin [48] and successively exploited by Ball and Storry [7] and by Zorin [137], it applies a similarity transform to S given by the matrix $\left[\begin{array}{c|c} 1 & 0 \\ \hline 0 & I_p \otimes F_n \end{array}\right]$ for primal schemes, and $I_p \otimes F_n$ for dual schemes, with I_p denoting the identity matrix of size p and F_n the Fourier matrix $F_n = \frac{1}{\sqrt{n}} \left[\mathrm{e}^{-\frac{2\pi i j \ell}{n}}\right]_{j,\ell=0}^{n-1}$. Then, once a matrix with diagonal blocks is obtained, a permutation is applied to finally reduce the local subdivision matrix into a block-diagonal matrix containing one block of size $(p+1) \times (p+1)$ and $n-1$ blocks each of size $p \times p$ for primal schemes, or n blocks each of size $p \times p$ for dual schemes.

Method 2. Introduced by Peters and Reif [112], if the scheme is primal, it artificially extends each block of size $p \times p$ by one row and one column such that the local subdivision matrix assumes a standard block-circulant structure, and then diagonalizes it by applying the block-Fourier matrix $F_n \otimes I_{p+1}$, while if the scheme is dual the extension is not necessary and a diagonalization is obtained by applying the block-Fourier matrix $F_n \otimes I_p$.

In Section 5.2, we will show a general strategy for the eigen-analysis of S, while in this chapter we order the points of the mesh as in Order 2 and we follow Method 2 to study the eigenproperties of the subdivision matrix, as we show in the following.
If $\mathcal{S}$ is a dual scheme, near an extraordinary face the subdivision matrix has the form

$$S = \begin{bmatrix} M_0 & M_1 & \cdots & M_{n-1} \\ M_{n-1} & M_0 & \cdots & M_{n-2} \\ \vdots & \vdots & \ddots & \vdots \\ M_1 & \cdots & M_{n-1} & M_0 \end{bmatrix}, \tag{2.20}$$

where $M_i \in \mathbb{R}^{p\times p}$, $i = 0, \dots, n-1$. Thus $S \in \mathbb{R}^{N\times N}$ with $N = np$ and it has a block-circulant structure. For short we write $S := \mathrm{circ}(M_0, \dots, M_{n-1})$. On the other hand, if $\mathcal{S}$ is a primal scheme, near an extraordinary vertex we construct a matrix $\tilde{S}$ of the form

$$\tilde{S} = \begin{bmatrix} \tilde{a} & \tilde{\mathbf{b}}^T & \tilde{\mathbf{b}}^T & \cdots & \tilde{\mathbf{b}}^T \\ \tilde{\mathbf{c}} & \tilde{M}_0 & \tilde{M}_1 & \cdots & \tilde{M}_{n-1} \\ \tilde{\mathbf{c}} & \tilde{M}_{n-1} & \tilde{M}_0 & \cdots & \tilde{M}_{n-2} \\ \vdots & \vdots & \vdots & \ddots & \vdots \\ \tilde{\mathbf{c}} & \tilde{M}_1 & \cdots & \tilde{M}_{n-1} & \tilde{M}_0 \end{bmatrix}, \tag{2.21}$$

where $\tilde{a} \in \mathbb{R}$, $\tilde{\mathbf{b}}, \tilde{\mathbf{c}} \in \mathbb{R}^p$ and $\tilde{M}_i \in \mathbb{R}^{p\times p}$, $i = 0, \dots, n-1$. Then, following the method shown in [112, Example 5.14], we transform the matrix $\tilde{S}$ in a block-circulant matrix S of the form

$$S := \mathrm{circ}(M_0, \dots, M_{n-1}) \quad \text{with} \quad M_j = \begin{pmatrix} \frac{\tilde{a}}{n} & \tilde{\mathbf{b}}^T \\ \frac{\tilde{\mathbf{c}}}{n} & \tilde{M}_j \end{pmatrix}, \quad j = 0, \dots, n-1. \tag{2.22}$$

It follows that $S \in \mathbb{R}^{N\times N}$ with $N = n(p+1)$ and again it has a block-circulant structure. Without loss of generality, we can thus always assume that the local subdivision matrix S has a block-circulant structure with blocks of dimension $\overline{p} \times \overline{p}$, where $\overline{p} = p$ if the mesh contains an extraordinary face and $\overline{p} = p + 1$ if it contains an extraordinary vertex.
Following the notation in [112, 117, 131], we also assume that near an isolated extraordinary vertex or face the regular subdivision surface $\mathbf{r}$ is defined on the local domain $\mathbf{D}_n = \Omega \times \mathbb{Z}_n$ and described as $\mathbf{r} : \mathbf{D}_n \to \mathbb{R}^3$. If we apply one step of refinement to the local domain $\mathbf{D}_n$, we obtain a new domain with $4n$ cells: $3n$ outer ordinary cells and n inner cells that contain the extraordinary elements. The restriction $\mathbf{r}_0$ of $\mathbf{r}$ to the outer cells is called ring. Moreover, $\mathbf{r}$ could be divided into n patches $\mathbf{r}^i, i = 0, \dots, n-1$, and the n parts of the ring corresponding to the initial patches are called segments. Let us denote with $\tilde{\mathbf{r}}$ the inner part of $\mathbf{r}$, that is $\tilde{\mathbf{r}} = \mathbf{r}\backslash\mathbf{r}_0$. We repeat the refinement process only for $\tilde{\mathbf{r}}$ to obtain a second ring $\mathbf{r}_1$ and an even smaller inner part. Hence, iterated refinement generates a sequence of rings $\{\mathbf{r}_k, k \in \mathbb{N}_0\}$ which covers all of the surface except for the central point (limit of the extraordinary vertex or face), that hereinafter we denote by $\mathbf{r}_c$ (see Figure 2.2). Precisely, assuming the central point to be placed at $\mathbf{0}$ and introducing the notation

$$\Omega_0 := \Omega\backslash\tilde{\Omega}, \qquad \Omega_k := 2^{-k}\Omega_0, \qquad \mathbf{D}_{n,k} := \Omega_k \times \mathbb{Z}_n, \quad k \in \mathbb{N}_0,$$

by exploiting the refinement process we can represent Ω and $\mathbf{D}_n$ as

$$\Omega = \bigcup_{k\in\mathbb{N}_0} \Omega_k \cup \{\mathbf{0}\}, \qquad \mathbf{D}_n = \bigcup_{k\in\mathbb{N}_0} \mathbf{D}_{n,k} \cup \{\mathbf{0}\}. \tag{2.23}$$

In particular, we can explicitly write $\Omega_k = \{(u, v) \in \mathbb{R}^2 \,|\, u, v \geq 0 \text{ and } 2^{1-k} \leq u + v \leq 2^{2-k}\}$ in the case of triangular meshes while $\Omega_k = \{(u, v) \in \mathbb{R}^2 \,|\, u, v \geq 0 \text{ and } 2^{1-k} \leq \max\{u, v\} \leq 2^{2-k}\}$ in the case of quadrilateral meshes (see Figure 2.3).
The segment $\mathbf{r}^i_k$ corresponds to the restriction of the patch $\mathbf{r}^i$ to the set Ω_k, i.e.

$$\mathbf{r}^i_k(\Omega_1) = \mathbf{r}^i(\Omega_k), \quad i = 0, \dots, n-1, \quad k \in \mathbb{N}_0,$$

as shown in Figure 2.4 (bottom), while the ring $\mathbf{r}_k$ corresponds to the restriction of the regular subdivision surface $\mathbf{r}$ to the set $\mathbf{D}_{n,k}$, i.e.

$$\mathbf{r}_k(\mathbf{D}_{n,1}) = \mathbf{r}(\mathbf{D}_{n,k}), \quad k \in \mathbb{N}_0,$$

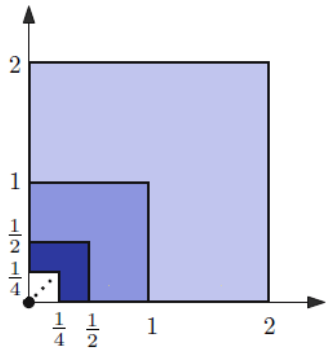

Figure 2.2: Domains $\Omega_0, \Omega_1, \Omega_2$ corresponding to three subdivision steps in the case of a quadrilateral mesh containing an extraordinary vertex.

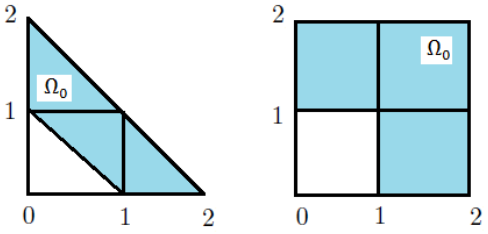

Figure 2.3: Domain Ω_0 in the case of a triangular (left) and a quadrilateral (right) mesh containing an extraordinary vertex.

(see Figure 2.4 (top)). This implies

$$\mathbf{r}^i(\Omega) = \bigcup_{k\in\mathbb{N}_0,} \mathbf{r}_k^i(\Omega_1) \cup \{\mathbf{r}_c\}, \quad \mathbf{r}(\mathbf{D}_n) = \bigcup_{k\in\mathbb{N}_0,} \mathbf{r}_k(\mathbf{D}_{n,1}) \cup \{\mathbf{r}_c\},$$

where $\mathbf{r}_c = \mathbf{r}(\mathbf{0})$ is the central point.
Now, we denote by $\mathbf{f}^{(k)} \in \mathbb{R}^{N\times 3}$ the vector of vertices (points in $\mathbb{R}^3$) of each ring $\mathbf{r}_k$, and with $\mathbf{\Phi}(u,v) \in \mathbb{R}^N$ the vector with the associated basic limit functions (see Definition 2.2), resulting in

$$\begin{aligned} \mathbf{r}_k : \mathbf{D}_{n,k} = \Omega_k \times \mathbb{Z}_n &\to \mathbb{R}^3 \\ (u,v) &\longmapsto \mathbf{r}_k(u,v) = (\mathbf{f}^{(k)})^T\, \mathbf{\Phi}(u,v). \end{aligned} \tag{2.24}$$

Remark 2.21 *If the subdivision algorithm is convergent, then the N functions collected in $\mathbf{\Phi}(u,v)$ satisfy the property of partition of unity, i.e. they sum up to 1 for all values of $(u,v) \in \mathbb{R}^2$, namely $\mathbf{\Phi}(u,v)^T \boldsymbol{x}_0 = 1$ for all $(u,v) \in \mathbb{R}^2$, with $\boldsymbol{x}_0 = [1,\dots,1]^T$.*

Now, exploiting the definition of k-th level ring $\mathbf{r}_k$ given in (2.24), we can finally introduce the notion of convergence of a stationary subdivision scheme $\mathcal{S}$ in correspondence to irregular regions of the mesh (see [117] for more details).

Definition 2.22 *[117, Definition 2.1] Let $\mathcal{S}$ be a stationary subdivision scheme whose action in correspondence to extraordinary elements of the mesh is described by the matrix S. $\mathcal{S}$ is*

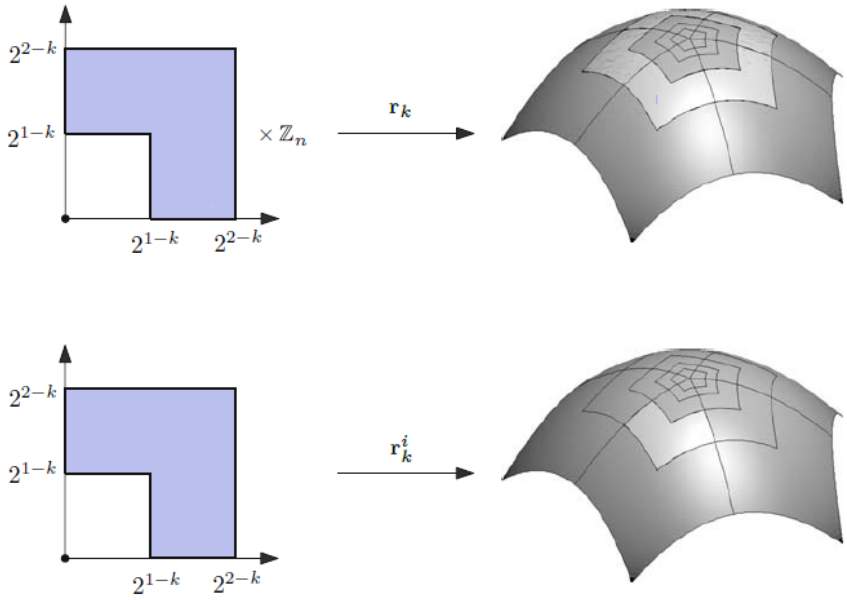

Figure 2.4: Ring $\mathbf{r}_k$ (top), segment $\mathbf{r}_k^i$ (bottom) in the case of a quadrilateral mesh with an extraordinary vertex (figure taken from [112]).

said to be convergent in the vicinity of an extraordinary vertex/face if, for all bounded initial data $\mathbf{f}^{(0)} \in \mathbb{R}^{N\times 3}$*, there exists a limit point* $\mathbf{r}_c \in \mathbb{R}^3$ *such that*

$$\lim_{k\to+\infty} \mathbf{r}_k = \mathbf{r}_c, \tag{2.25}$$

with $\mathbf{r}_k$ *defined according to* (2.24) *and*

$$\mathbf{f}^{(k)} = S\mathbf{f}^{(k-1)} = ... = S^k\mathbf{f}^{(0)}. \tag{2.26}$$

If the subdivision scheme $\mathcal{S}$ converges, then $\mathbf{r} = \bigcup_{k\in\mathbb{N}_0,} \mathbf{r}_k \cup \{\mathbf{r}_c\}$ is a surface without gap, i.e. $\mathbf{r}$ is a surface which is continuous at all points including $\mathbf{r}_c$. We call $\mathbf{r}$ the limit surface of the subdivision scheme $\mathcal{S}$. For $\mathbf{r}$ we can provide a weaker definition of C^1 continuity at the limit point $\mathbf{r}_c$, called *tangent plane continuity*, which reads as follows.

Definition 2.23 *[117, Definition 2.2] Let* $n(\mathbf{r}_c)$ *denote the normal vector at the limit point* $\mathbf{r}_c$*. A subdivision surface* $\mathbf{r}$ *is called tangent plane continuous at* $\mathbf{r}_c$ *if there is a unique vector* $n(\mathbf{r}_c)$ *such that for all sequences of normal vectors* $\{\mathbf{n}_k := \frac{\partial_u \mathbf{r}_k \wedge \partial_v \mathbf{r}_k}{\|\partial_u \mathbf{r}_k \wedge \partial_v \mathbf{r}_k\|_2}, k \in \mathbb{N}_0, \}$*,*

$$\lim_{k\to+\infty} \mathbf{n}_k = n(\mathbf{r}_c).$$

2.3.1 Linear algebra tools: Jordan decomposition

The convergence of a stationary subdivision scheme near an extraordinary element is described by the formula in (2.26), which leads to the study of S^k. We assume that $S \in \mathbb{R}^{N\times N}$ has $\overline{r}+1$ different eigenvalues λ_r, $r = 0, \ldots, \overline{r}$, $0 \le \overline{r} \le N-1$, sorted in decreasing order according to their magnitude, i.e. $|\lambda_0| \ge |\lambda_1| \ge \ldots \ge |\lambda_{\overline{r}}|$, and we denote by $\ell_r + 1$, $\ell_r \ge 0$

the algebraic multiplicity of λ_r.
In order to study the properties of S^k, it is convenient to use its Jordan decomposition. Firstly, the Jordan decomposition of S is $S = XJX^{-1}$ with $J = \mathrm{diag}(J_0, J_1, \ldots, J_{\overline{r}})$, where the r-th Jordan block J_r corresponding to the eigenvalue λ_r has dimension $(\ell_r+1)\times(\ell_r+1)$ and is defined as

$$J_r = \begin{pmatrix} \lambda_r & 1 & 0 & \cdots & 0 \\ 0 & \lambda_r & 1 & \cdots & 0 \\ \vdots & \ddots & \ddots & \ddots & \vdots \\ 0 & \cdots & 0 & \lambda_r & 1 \\ 0 & \cdots & 0 & 0 & \lambda_r \end{pmatrix}.$$

According to the block structure of J, the matrix X is partitioned as $X = [X_0, X_1, \ldots, X_{\overline{r}}]$ with $X_r = [\boldsymbol{x}_r^0, \ldots, \boldsymbol{x}_r^{\ell_r}]$. The vectors $\boldsymbol{x}_r^\ell,\ r = 0, \ldots, \overline{r},\ \ell = 0, \ldots, \ell_r$ form the set $\{\boldsymbol{x}_0^0, \ldots \boldsymbol{x}_0^{\ell_0}, \ldots, \boldsymbol{x}_{\overline{r}}^0, \ldots, \boldsymbol{x}_{\overline{r}}^{\ell_{\overline{r}}}\}$ of generalized eigenvectors. Moreover, for any $\mathbf{v} \in \mathbb{R}^{N\times 3}$ and $\mathbf{p} := X^{-1}\mathbf{v}$, in view of the structure of X we can write $\mathbf{p} = [\mathbf{p}_0^T, \mathbf{p}_1^T, \ldots, \mathbf{p}_{\overline{r}}^T]^T$ with $\mathbf{p}_r = [p_r^0, p_r^1, \ldots, p_r^{\ell_r}]^T$. Thus, since $S^k = XJ^kX^{-1}$ with $J^k = \mathrm{diag}(J_0^k, J_1^k, \ldots, J_{\overline{r}}^k)$ and

$$J_r^k = \begin{pmatrix} \lambda_r^{k,0} & \lambda_r^{k,1} & \lambda_r^{k,2} & \cdots & \lambda_r^{k,\ell_r} \\ 0 & \lambda_r^{k,0} & \lambda_r^{k,1} & \cdots & \lambda_r^{k,\ell_r-1} \\ \vdots & \ddots & \ddots & \ddots & \vdots \\ 0 & \cdots & 0 & \lambda_r^{k,0} & \lambda_r^{k,1} \\ 0 & \cdots & 0 & 0 & \lambda_r^{k,0} \end{pmatrix} \tag{2.27}$$

where

$$\lambda_r^{k,j} := \begin{cases} \binom{k}{j}\lambda_r^{k-j} & \text{if } \lambda_r \neq 0 \text{ and } 0 \leq j \leq k, \\ 1 & \text{if } \lambda_r = 0 \text{ and } j = k, \\ 0 & \text{otherwise,} \end{cases} \tag{2.28}$$

we have

$$S^k\mathbf{v} = XJ^k\mathbf{p} = \sum_{r=0}^{\overline{r}} \sum_{\ell=0}^{\ell_r} \lambda_r^{k,\ell} \sum_{i=\ell}^{\ell_r} \boldsymbol{x}_r^{i-\ell} p_r^i. \tag{2.29}$$

Remark 2.24 *Note that, the definition of $\lambda_r^{k,j}$ in (2.28) implies that, if $\ell_r = 0$, then $\lambda_r^{k,0} = \lambda_r^k$. Moreover, the terms $\lambda_r^{k,\ell}$, $r = 1, \ldots, \overline{r}$, decay to zero as $k \to +\infty$ (see [112, Section 4.5]).*

2.3.2 Sufficient smoothness conditions

In this section, we show that the smoothness properties of the limit surface produced by the stationary subdivision scheme $\mathcal{S}$ near extraordinary elements can be detected from the leading eigenvalues of the subdivision matrix S and an associated characteristic map $\boldsymbol{\Psi}$. The following results are taken from [112, 117, 138].

Theorem 2.25 *A stationary subdivision scheme $\mathcal{S}$ associated to the subdivision matrix S converges if $1 = \lambda_0 > |\lambda_r|$, for all $r = 1, \ldots, \overline{r}$ and $\boldsymbol{x}_0 = [1, ..., 1]^T$.*

Remark 2.26 *It is a well-known fact that a subdivision scheme $\mathcal{S}$ is affinely invariant in the neighborhood of extraordinary vertices if the elements in each row of S sum up to 1 [5].*

The further smoothness properties of the limit surface can be derived from the leading eigenvalues of S and a map $\mathbf{\Psi}$ which depends only on the corresponding eigenvectors of S and the basic limit functions. Therefore, $\mathbf{\Psi}$ is called the characteristic map of the subdivision process.

Definition 2.27 *For a stationary subdivision matrix S with $1 = \lambda_0 > \lambda_1 > |\lambda_r|$, for all $r = 2, \ldots, \overline{r}$, with λ_1 positive real and double and associated linear independent eigenvectors $\boldsymbol{x}_1^0, \boldsymbol{x}_1^1$, the characteristic map is defined by $\mathbf{\Psi}(u,v) := \mathbf{\Phi}[\boldsymbol{x}_1^0, \boldsymbol{x}_1^1]$. $\mathbf{\Psi}$ is called regular if*

$$\det(D\mathbf{\Psi}(u,v)^T) = \det \begin{pmatrix} \partial_u \mathbf{\Psi}(u,v)^T \\ \partial_v \mathbf{\Psi}(u,v)^T \end{pmatrix} \neq 0, \qquad \forall (u,v) \in \mathbb{R}^2$$

or equivalently $\operatorname{sign}(\det(D\mathbf{\Psi}(u,v)^T))$ *is constant.*

Of course, the characteristic map is subjected to the ambiguity in the choice of the vectors $\boldsymbol{x}_1^0, \boldsymbol{x}_1^1$, however, all of its crucial properties are well defined as proved in [117, Lemma 3.4] from which injectivity and regularity of the characteristic map do not depend on the particular choice of the vectors $\boldsymbol{x}_1^0, \boldsymbol{x}_1^1$. The next theorem gives a sufficient condition for the tangent plane continuity of a subdivision algorithm.

Theorem 2.28 *If $1 = \lambda_0 > \lambda_1 > |\lambda_r|$, for all $r = 2, \ldots, \overline{r}$, with $\lambda_1 \in \mathbb{R}^+$ with algebraic and geometric multiplicity 2 and if the characteristic map $\mathbf{\Psi}$ is regular, then the limit surface is tangent plane continuous at the limit points of an extraordinary element for almost every initial vector $\mathbf{f}^{(0)}$ of control points.*

Requiring the injectivity of the characteristic map we gain the C^1 continuity of the limit surfaces in the limit points of an extraordinary element.

Theorem 2.29 *If $1 = \lambda_0 > \lambda_1 > |\lambda_r|$, for all $r = 2, \ldots, \overline{r}$, with $\lambda_1 \in \mathbb{R}^+$ with algebraic and geometric multiplicity 2 and if the characteristic map $\mathbf{\Psi}$ is regular and injective, then the limit surface is C^1 continuous at the limit points of an extraordinary element for almost every initial vector $\mathbf{f}^{(0)}$ of control points.*

Method 2 proposes a useful and extensively used strategy (see e.g. [48, 65, 96, 137]) to study the eigenvalues of the subdivision matrix S which consists in applying a block diagonalization to S via the discrete Fourier transform $F_n \otimes I_{\overline{p}}$. It means that starting from the subdivision matrix $S = \operatorname{circ}(M_0, M_1, \ldots, M_{n-1})$, we compute

$$\hat{S}_\nu = \sum_{j=0}^{n} M_j \omega^{j\nu}, \quad \nu = 0, \ldots, n-1, \quad \omega = e^{\frac{2\pi \mathrm{i}}{n}},$$

thus defining the diagonal matrix

$$\hat{S} = diag(\hat{S}_0, \hat{S}_1, \ldots, \hat{S}_{n-1}).$$

Definition 2.30 *For any $\nu = 0, \ldots, n-1$, if λ_i is an eigenvalue of $\hat{S}_\nu$ we call ν the Fourier index of λ_i and we write $\mathcal{F}(\lambda_i) = \nu$.*

Remark 2.31 *If the double eigenvalue λ_1 is an eigenvalue of the blocks $\hat{S}_1$ and $\hat{S}_{n-1}$, i.e. $\mathcal{F}(\lambda_1) = \{1, n-1\}$, and the characteristic map $\mathbf{\Psi}$ is regular, then the injectivity of $\mathbf{\Psi}$ follows immediately [112, Chapter 5].*

The spectral properties of the subdivision matrix S expressed in Theorems 2.25 and 2.29 regards convergence and C^1 continuity. However, to design limit surfaces with higher quality in correspondence to extraordinary elements, the properties of boundedness of curvature and of optimal shrinkage of the local configuration of points are also required. All these properties could be obtaining requiring special necessary conditions on the eigenvalues of S, and could be written as follows (see [48, 112, 111, 117, 138]).

(I) *Requirements for convergence:*
Apart from $\lambda_0 = 1$ which must have Fourier index 0, all other eigenvalues of S have to be less than 1 in modulus, i.e.

$$1 = \lambda_0 > |\lambda_1|, \qquad \text{with} \quad \mathcal{F}(1) = 0.$$

(II) *Requirements for tangent plane continuity:*
The sub-dominant eigenvalue has to be double, equal to a real positive λ, with Fourier indices $1, n-1$, and all other eigenvalues have to be less than λ in modulus, i.e.

$$1 = \lambda_0 > \lambda := \lambda_1 = \lambda_2 > |\lambda_3|, \quad \lambda \in \mathbb{R}^+, \quad \mathcal{F}(\lambda) = \{1,\, n-1\}.$$

(III) *Requirements for boundedness of curvature:*
The subsub-dominant eigenvalue has to be triple, equal to $\mu = \lambda^2$, with Fourier indices $0, 2, n-2$, and all other eigenvalues have to be not larger than λ^2 in modulus, i.e.

$$1 = \lambda_0 > \lambda := \lambda_1 = \lambda_2 > \mu := \lambda_3 = \lambda_4 = \lambda_5 \geq |\lambda_6|, \quad \mathcal{F}(\mu) \supseteq \{0,\, 2,\, n-2\}.$$

(IV) *Requirements for optimal shrinkage:*
The sub-dominant eigenvalue λ has to be equal to $\frac{1}{m}$ (or the closest possible to $\frac{1}{m}$), where m is the arity of the subdivision scheme.

Now, for any $\nu = 0, \ldots, n-1$, let λ_r^ν be the r-th eigenvalue of $\hat{M}_\nu$. In this way, properties (I)-(IV) can be summarized as in Table 2.1.

Conditions required on the eigenvalues of S
(i) $\lambda_0^0 = 1$, $\lambda_1^0 = \lambda^2$
(ii) $\lambda_0^1 = \lambda$, $\lambda_0^{n-1} = \lambda$
(iii) $\lambda_0^2 = \lambda^2$, $\lambda_0^{n-2} = \lambda^2$
(iv) the modulus of all the other eigenvalues is not larger than λ^2
(v) $\lambda = \frac{1}{m}$ $\quad$ (m = arity of the subdivision scheme).

Table 2.1: Conditions to be satisfied by the eigenvalues of S.

2.3.3 Important valences

Extraordinary elements of a triangular mesh with valence less than 5 or greater than 7 are also problematic for many mesh processing tasks. However, vertices with valence equal to 6 everywhere is most often impossible due to either surface topology or surface feature preservation, that is why 567-meshes are particularly of interest.
Many authors [1, 23, 127, 134, 133] have developed (complex) strategies to either drastically reduce the number of extraordinary elements of a triangular mesh or at least avoid too irregular ones (with valences less than 5 or greater than 7). 567-remeshing algorithm, proposed in [1] and improved in [133], falls in the latter category and has gained particular attention since it can resolve all issues regarding edge collapse, artifacts and distortion in the limit surfaces. This algorithm locally retriangulates a mesh containing extraordinary elements of any valence to obtain a mesh with only valences $n = 5, 6, 7$ which closely approximates the original mesh geometrically, e.g. in terms of feature preservation, and has a comparable vertex count as the original mesh. Thus, thanks to this algorithm any arbitrary manifold topology mesh can be transformed into a 567-mesh.
The same reasoning could be applied to quadrilateral meshes, thus focusing on the valences $n = 3, 4, 5$ and producing a 345-remeshing. However, to the best of our knowledge there are no results in this field in literature and this topic is not one of the purposes of the thesis.

2.4 Review of some stationary subdivision schemes in literature

In this section we recall the most famous binary bivariate subdivision schemes proposed in literature and their main properties. This is not a complete list of all the subdivision schemes appeared during the years, but we here present only the schemes that will be useful in the following chapters for comparisons or generalizations. In particular, among the schemes defined on triangular meshes, we recall Loop's scheme, firstly proposed in [95], and the interpolatory Butterfly scheme [54] defined only on regular meshes and then generalized to the case of arbitrary manifold topology meshes [139]. Among the subdivision schemes defined on quadrilateral meshes, we recall Doo-Sabin's and Catmull-Clark's schemes [48, 14] which are a generalization of the bi-quadratic and bi-cubic splines, respectively, and Kobbelt's interpolatory scheme [84]. Other subdivision schemes not considered in this thesis are for example the Simplest scheme [110], the $\sqrt{3}$-scheme [85], the 4-8 scheme [132] and the 3-4 scheme [113].

2.4.1 Loop's scheme

Loop's scheme is a primal approximating subdivision scheme originally proposed in [95] and described by the stencils in Figure 2.5, with $\delta = \left(\frac{3}{8} + \frac{1}{4}\cos\frac{2\pi}{n}\right)^2 + \frac{3}{8}$. This scheme produces C^2 limit surfaces on regular meshes and C^1 in correspondence of extraordinary vertices. During the years, many variants of Loop's scheme appeared requiring an adjusted edge-point stencil to gain the boundedness of curvature at extraordinary vertices [65, 96, 97]. However, the property of optimal shrinkage is never satisfied in a neighborhood of an extraordinary vertex. We will study Loop's scheme and its variants in Section 5.2.

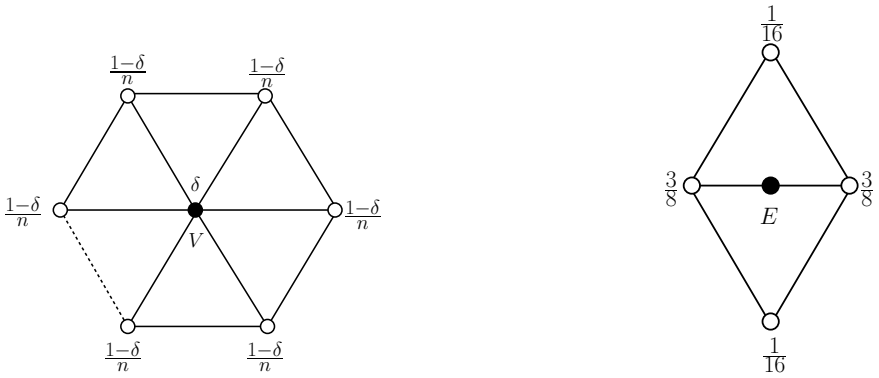

(a) Vertex-point stencil (b) Edge-point stencil

Figure 2.5: Stencils for the vertex-point rule and the edge-point rule of Loop's subdivision scheme at vertices of valence n.

2.4.2 Butterfly scheme and modified Butterfly scheme

The Butterfly scheme is an interpolatory subdivision scheme proposed in [54] defined on regular triangular mesh. Some years later, Zorin et al. [139] proposed a generalization of the Butterfly scheme, calling it the modified Butterfly scheme. The rule for the vertex-point computation is trivial since the scheme is interpolatory, so all the old points are retained in the new mesh, while the edge-point stencil is shown in Figure 2.6 (a) with

$$\alpha_0 = \frac{1}{2} - w, \quad \alpha_1 = w, \quad \alpha_2 = -\frac{1}{16} - w, \quad \alpha_3 = \frac{1}{8} + 2w,$$

where w is chosen in $[-0.03, 0)$ to produce C^1 limit surfaces (see [73]). The original Butterfly scheme is obtained with $w = 0$. Zorin et al. also proposed an extension to meshes with arbitrary manifold topology with an adjusted rule for the edge-point computation near an extraordinary vertex described by the stencil in Figure 2.6 (b), with

$$\begin{aligned}
&\sigma_0 = \frac{5}{12}, \quad \sigma_1 = \sigma_2 = -\frac{1}{12}, && \text{if } n = 3,\\
&\sigma_0 = \frac{3}{8}, \quad , \sigma_1 = \sigma_3 = 0, \quad \sigma_2 = -\frac{1}{8}, && \text{if } n = 4,\\
&\sigma_j = \frac{1}{n}\left(\frac{1}{4} + \cos\frac{2\pi j}{n} + \frac{1}{2}\cos\frac{4\pi j}{n}\right), \quad j = 0, \ldots, n-1, && \text{if } n \geq 5.
\end{aligned}$$

This scheme produces C^1 limit surfaces also at extraordinary vertices, but it has neither bounded curvature nor optimal shrinkage at extraordinary vertices. In Section 6.1 we will recall the main properties of the Butterfly scheme and we will propose a new scheme improving its smoothness and accuracy.

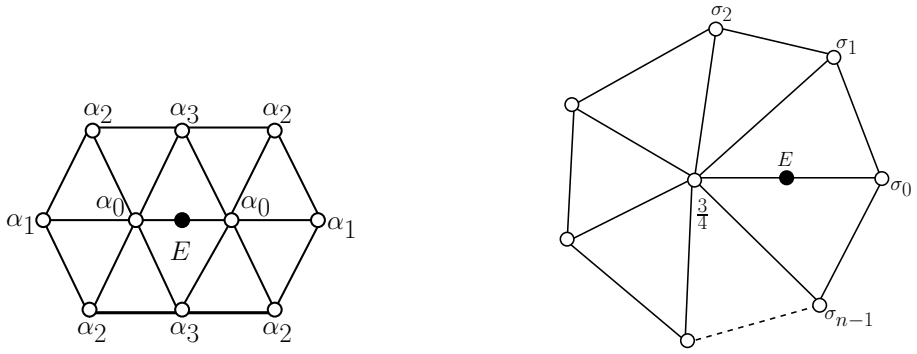

(a) Regular edge-point stencil

(b) Extraordinary edge-point stencil

Figure 2.6: Edge-point stencils of (a) Butterfly subdivision scheme for regular vertices, (b) modified Butterfly subdivision scheme for extraordinary vertices of valence $n \neq 6$.

2.4.3 Doo-Sabin's scheme

Doo-Sabin's scheme [48] is a dual approximating subdivision scheme whose rules for the computation of the new points are described by the stencil in Figure 2.7, with

$$\alpha_0 = \frac{1}{4} + \frac{5}{4n}, \quad \alpha_j = \frac{3 + 2\cos\frac{2\pi j}{n}}{4n}, \; j = 1, \ldots, n-1.$$

When $n = 4$, the rules reduce to the tensor-product of the quadratic B-spline, thus implying the C^1 continuity of the limit surface on regular meshes. Moreover, this choice of stencil coefficients guarantees C^1 continuous limit surfaces, with bounded curvature and optimal shrinkage also at extraordinary faces.
Catmull and Clark proposed a variant of this scheme, which is known as the quadratic Catmull-Clark's scheme to underline the main difference with the well-known Catmull-Clark's scheme based on cubics and recalled in the next section. The stencil coefficients they proposed are

$$\alpha_0 = \frac{1}{2} + \frac{1}{4n}, \quad \alpha_1 = \alpha_{n-1} = \frac{1}{8} + \frac{1}{4n}, \quad \alpha_j = \frac{1}{4n}, \; j = 2, \ldots, n-2,$$

which for $n = 4$ reduce to the coefficients of the tensor-product quadratic B-spline, thus implying the C^1 continuity of the limit surface on regular meshes.However, these coefficients do not allow for bounded curvature and optimal shrinkage at extraordinary faces.
A level-dependent variant of Doo-Sabin's scheme will be studied in Chapter 7 to produce interpolating limit surfaces after a suitable preprocessing of the initial control mesh.

2.4.4 Catmull-Clark's scheme

Catmull-Clark's scheme [14] is a primal approximating subdivision scheme whose rules for the computation of the new vertex- edge- and face-point are described in Figure 2.8 with

$$\alpha = 1 - \frac{7}{4n}, \qquad \beta = \frac{3}{2n^2}, \qquad \gamma = \frac{1}{4n^2}.$$

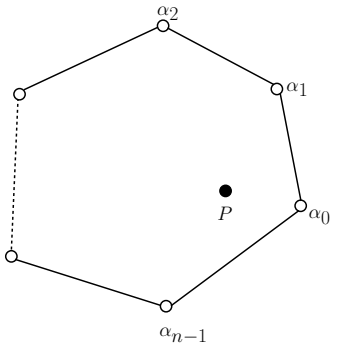

Figure 2.7: Stencil for the computation of a new vertex of Doo-Sabin's scheme.

When $n = 4$, the rules reduce to the tensor-product of the cubic B-spline, thus implying the C^2 continuity of the limit surfaces on regular meshes. At extraordinary vertices, the limit surfaces are only C^1, with neither bounded curvature nor optimal shrinkage. Catmull-Clark's

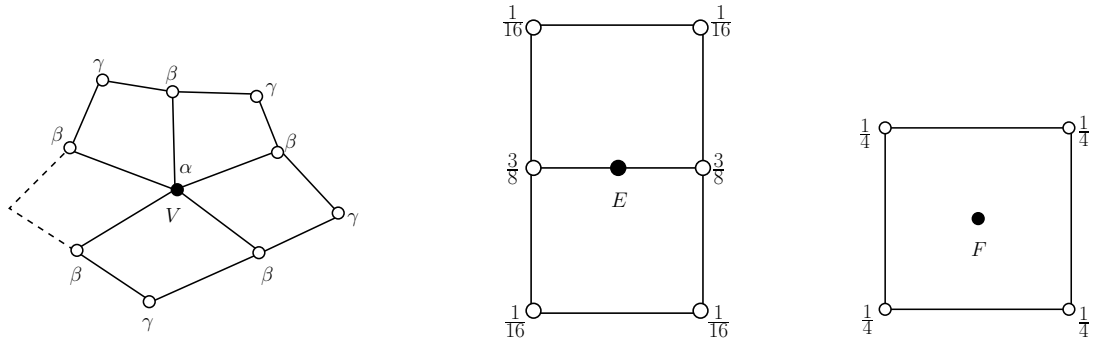

(a) Vertex point (b) Edge point (c) Face point

Figure 2.8: Stencils for the computation of (a) the vertex-point, (b) the edge-point, (c) the face-point, of Catmull-Clark's subdivision scheme.

scheme will be used in Chapter 7 to produce interpolating limit surfaces.

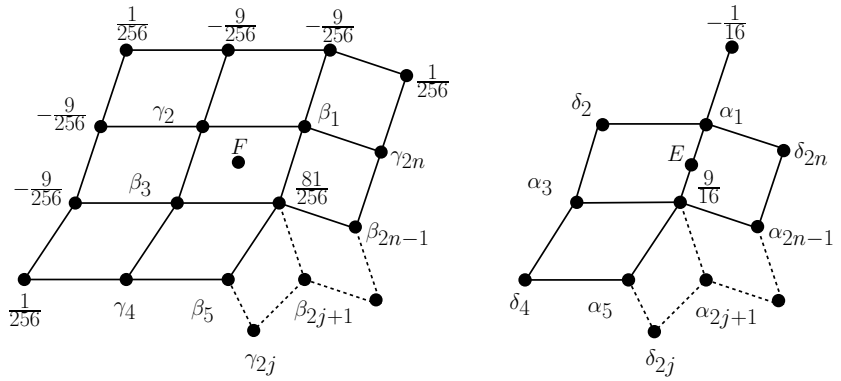

(a) Face point (b) Edge point

Figure 2.9: Stencils for the computation of (a) the face-point, (b) the edge-point, of Kobbelt's subdivision scheme.

2.4.5 Kobbelt's scheme

Kobbelt's scheme [84] is an interpolatory subdivision scheme. Its stencils for the computation of the edge- and face-point are shown in Figure 2.9 with

$$\alpha_1 = \frac{5}{8} + \frac{1}{4n}, \qquad \alpha_3 = \alpha_{2n-1} = \frac{1}{16} - \frac{1}{4n}, \qquad \alpha_{2j+1} = -\frac{1}{4n},\ j = 2, \dots, n-2,$$
$$\beta_1 = \beta_3 = \frac{45}{128} - \frac{9}{45n}, \qquad \beta_{2j+1} = -\frac{9}{64n},\ j = 2, \dots, n-1,$$
$$\gamma_2 = \frac{5}{16} + \frac{1}{64n}, \qquad \gamma_4 = \gamma_{2n} = -\frac{5}{128} + \frac{1}{64n}, \qquad \gamma_{2j} = \frac{1}{64n},\ j = 2, \dots, n-2,$$
$$\delta_2 = \delta_4 = \delta_{2n-2} = \delta_{2n} = \frac{1}{36n} - \frac{1}{144}, \qquad \delta_{2j} = \frac{1}{36n},\ j = 2, \dots, n-3.$$

Since the scheme is interpolatory, the computation of the vertex-point is trivial. When $n = 4$, the rules reduce to the tensor-product of the 4-point scheme.This scheme produce C^1 continuous limit surfaces with bounded curvature and optimal shrinkage on regular meshes, but it is only C^1 at extraordinary vertices. Improvements of this scheme have been proposed in [39, 93] which gain bounded curvature and optimal shrinkage also at extraordinary vertices. These variants will be studied in Section 5.1.

Chapter 3

Non-stationary subdivision schemes

In this chapter we recall the main notions, properties and tools regarding non-stationary subdivision schemes. A non-stationary subdivision scheme is denoted by $\{\mathcal{S}_k, k \in \mathbb{N}_0\}$. The subscript k, with $k \in \mathbb{N}_0$, and the term 'non-stationary' underline the main difference with the stationary subdivision schemes introduced in Chapter 2, that is the fact that subdivision rules change with the subdivision level k, namely they are level-dependent. Thus, a non stationary subdivision scheme is an iterative algorithm that generates the refined data sequence $\mathbf{f}^{(k+1)} = \{f_{\mathbf{i}}^{(k+1)}, \mathbf{i} \in \mathbb{Z}^s\}$, $k \in \mathbb{N}_0$, starting from a set of control points $\mathbf{f}^{(0)} = \{f_{\mathbf{i}}^{(0)}, \mathbf{i} \in \mathbb{Z}^s\}$, by applying refinement rules that depend on the subdivision level.
As in the stationary case, when we study a non-stationary subdivision scheme we have to pay attention not only to the subdivision rules, but also to set of initial control points $\mathbf{f}^{(0)}$, in particular in the bivariate setting where the control mesh could be regular or could contain extraordinary elements. In fact, different tools are used to analyze non-stationary subdivision schemes on regular meshes and on arbitrary manifold topology meshes.
In the univariate setting and on regular meshes, the action of a non-stationary subdivision scheme $\{\mathcal{S}_k, k \in \mathbb{N}_0\}$ is described by the k-level subdivision mask

$$\mathbf{a}^{(k)} = \{\mathrm{a}_{\mathbf{i}}^{(k)}, \mathbf{i} \in \mathbb{Z}^s\}. \tag{3.1}$$

To emphasize the connection with the k-level subdivision mask when the subdivision scheme $\{\mathcal{S}_k, k \in \mathbb{N}_0\}$ is a univariate scheme or a bivariate scheme defined on regular meshes, we refer to it as $\{\mathcal{S}_{\mathbf{a}^{(k)}}, k \in \mathbb{N}_0\}$. In this case, a non-stationary scheme $\{\mathcal{S}_{\mathbf{a}^{(k)}}, k \in \mathbb{N}_0\}$ is described by the refinement rules

$$f_{\mathbf{i}}^{(k+1)} = \sum_{\mathbf{j} \in \mathbb{Z}^s} \mathrm{a}_{\mathbf{i}-m\mathbf{j}}^{(k)} \, f_{\mathbf{j}}^{(k)}, \quad \mathbf{i} \in \mathbb{Z}^s, \quad k \in \mathbb{N}_0, \tag{3.2}$$

which generate the sequence of points at level $k+1$ starting from the points at level k. The coefficients of the k-th level mask $\mathbf{a}^{(k)}$ in (3.1) define the so-called k-th level subdivision symbol

$$\mathrm{a}^{(k)}(\boldsymbol{z}) := \sum_{\mathbf{i} \in \mathbb{Z}^s} \mathrm{a}_{\mathbf{i}}^{(k)} \boldsymbol{z}^{\mathbf{i}}, \quad \boldsymbol{z} \in (\mathbb{C}\backslash\{0\})^s. \tag{3.3}$$

On the other hand, in the irregular regions of a mesh, i.e. in the neighborhood of an extraordinary vertex or face, the action of the non-stationary subdivision scheme $\{\mathcal{S}_k, k \in \mathbb{N}_0\}$ is described by a sequence of local subdivision matrices $\{S_k, k \in \mathbb{N}_0\}$. Near an extraordinary

vertex/face, the subdivision rules which relate the vertices of the k-th level mesh with those of the next level are encoded in the rows of the local subdivision matrix S_k, resulting in

$$\mathbf{f}^{(k+1)} = S_k \mathbf{f}^{(k)} = S_k S_{k-1} \mathbf{f}^{(k-1)} = \ldots = S^{(k+1)} \mathbf{f}^{(0)}, \tag{3.4}$$

with

$$S^{(k+1)} = S_k \; S_{k-1} \cdots S_0, \tag{3.5}$$

Important properties of non-stationary subdivision schemes are convergence, exponential polynomial generation and reproduction, approximation order and regularity of the limit curves or surfaces. In particular, in literature there are tools for the study of exponential polynomial generation and reproduction [21] and for the smoothness analysis of the limit curves/surfaces produced by univariate non-stationary subdivision schemes or bivariate non-stationary subdivision schemes defined on regular meshes (see e.g. [20, 24, 56]). In the following, we recall these results and we also show the first proposed method of sufficient conditions to check the convergence of the limit surface produced by a non-stationary subdivision scheme near extraordinary vertices and faces. The latter is one of the main contributions of this thesis.

3.1 Generation and reproduction of exponential polynomials

We start by adapting the general definition of the space of s-variate exponential polynomials, given in [21, Definition 3.1], to the specific context of our interest.

Definition 3.1 *Let $d \in \mathbb{N}_0$. Let also*

$$\Gamma_d := \left\{ \boldsymbol{\gamma} = (\gamma_1, \ldots, \gamma_s) \in \mathbb{N}_0^s \;:\; 0 \leq \sum_{j=1}^{s} \gamma_j \leq d \right\}, \qquad \#\Gamma_d = \frac{(d+1)(d+2)}{2}, \tag{3.6}$$

$$\Lambda_t := \left\{ 0,\, t,\, -t \;:\; t \in \left(0, \frac{m}{2}\pi\right) \cup \mathrm{i}\mathbb{R}^+ \right\}, \quad \#\Lambda_t = 3 \qquad \textit{and} \qquad \Theta \subseteq \underbrace{\Lambda_t \times \Lambda_t \times \ldots \times \Lambda_t}_{s \text{ times}}. \tag{3.7}$$

We define the space of bivariate exponential polynomials as

$$EP^s_{(\Gamma_d, \Theta)} := \mathrm{span}\{ \boldsymbol{x}^{\boldsymbol{\gamma}} e^{\boldsymbol{\theta} \cdot \boldsymbol{x}} \;:\; \boldsymbol{x} \in \mathbb{R}^s,\; \boldsymbol{\gamma} \in \Gamma_d,\; \boldsymbol{\theta} \in \Theta \}. \tag{3.8}$$

Remark 3.2 *We underline that $EP^s_{(\Gamma_d, \mathbf{0})} = \Pi^s_d$, that is the space of s-variate polynomials of degree d.*

For the analysis of the non-stationary subdivision schemes proposed in the following chapters, we denote by $\mathcal{W}_d$ the subspace of $EP^s_{(\Gamma_d, \Theta)}$ defined as

$$\mathcal{W}^s_d := span\{ \boldsymbol{x}^{\boldsymbol{\gamma}} \in \mathbb{R}^s \, \boldsymbol{\gamma} \in \Gamma_d \} \cup \{ e^{\boldsymbol{\theta} \cdot \boldsymbol{x}},\; \boldsymbol{\theta} \in \Theta \} \subset EP^s_{(\Gamma_d, \Theta)}. \tag{3.9}$$

The definition of convergence of a non-stationary subdivision scheme $\{\mathcal{S}_{\mathbf{a}^{(k)}}, k \in \mathbb{N}_0\}$ is very close to Definition 2.1.

Definition 3.3 *A non-stationary subdivision scheme* $\{\mathcal{S}_{\mathbf{a}^{(k)}}, k \in \mathbb{N}_0\}$ *is called uniformly convergent if, for any initial data* $\mathbf{f}^{(0)} \in \ell(\mathbb{Z}^s)$*, there exists a limit function* $g_{\mathbf{f}^{(0)}} \in C(\mathbb{R}^s)$ *(which is nonzero for at least one initial nonzero sequence* $\mathbf{f}^{(0)}$*) such that the sequence of continuous functions* $F^{(k)}$ *interpolating the data* $\mathbf{f}^{(k)}$ *at the parameter values* $\frac{\mathbf{i}}{m^k}$*,* $\mathbf{i} \in \mathbb{Z}^s$*, converges to* $g_{\mathbf{f}^{(0)}}$ *as* $k \to +\infty$*, i.e.*

$$g_{\mathbf{f}^{(0)}} := \lim_{k\to+\infty} \mathcal{S}_{\mathbf{a}^{(k+\ell)}} \mathcal{S}_{\mathbf{a}^{(k+\ell-1)}} \cdots \mathcal{S}_{\mathbf{a}^{(\ell)}} \mathbf{f}^{(0)} = \lim_{k\to+\infty} F^{(k)}, \quad \ell \in \mathbb{N}_0,$$

uniformly. The subdivision scheme $\{\mathcal{S}_{\mathbf{a}^{(k)}}, k \in \mathbb{N}_0\}$ *is called* C^r *convergent,* $r \in \mathbb{N}_0$*, if* $g_{\mathbf{f}^{(0)}} \in C^r(\mathbb{R}^s)$*.*

The following definitions stress the difference between the notions of generation and reproduction of the space of exponential polynomials $EP^s_{(\Gamma_{\mathrm{d}},\,\Theta)}$.

Definition 3.4 *A convergent non-stationary subdivision scheme* $\{\mathcal{S}_{\mathbf{a}^{(k)}}, k \in \mathbb{N}_0\}$ *is said to be* $EP^s_{(\Gamma_d,\,\Theta)}$*-generating if there exists a parametrization* $\{\mathbf{T}^{(k)}, k \in \mathbb{N}_0\}$ *as in* (2.6)*, such that for all initial data* $\mathbf{f}^{(0)} = \{\pi(\mathbf{t}^{(0)}_{\mathbf{i}}), \mathbf{i} \in \mathbb{Z}^s\}$*,* $\pi \in EP^s_{(\Gamma_d,\,\Theta)}$*, we have*

$$\lim_{k\to+\infty} \mathcal{S}_{\mathbf{a}^{(\ell+k)}} \mathcal{S}_{\mathbf{a}^{(\ell+k-1)}} \cdots \mathcal{S}_{\mathbf{a}^{(\ell)}} \mathbf{f}^{(0)} \in EP^s_{(\Gamma_d,\,\Theta)}, \qquad \forall \ell \in \mathbb{N}_0.$$

Definition 3.5 *A convergent non-stationary subdivision scheme* $\{\mathcal{S}_{\mathbf{a}^{(k)}}, k \in \mathbb{N}_0\}$ *is said to be* $EP^s_{(\Gamma_L,\,\Theta)}$*-reproducing if there exists a parametrization* $\{\mathbf{T}^{(k)}, k \in \mathbb{N}_0\}$ *as in* (2.6)*, such that for all initial data* $\mathbf{f}^{(0)} = \{\pi(\mathbf{t}^{(0)}_{\mathbf{i}}), \mathbf{i} \in \mathbb{Z}^s\}$*,* $\pi \in EP^s_{(\Gamma_d,\,\Theta)}$*, we have*

$$\lim_{k\to+\infty} \mathcal{S}_{\mathbf{a}^{(\ell+k)}} \mathcal{S}_{\mathbf{a}^{(\ell+k-1)}} \cdots \mathcal{S}_{\mathbf{a}^{(\ell)}} \mathbf{f}^{(0)} = \pi, \qquad \forall \ell \in \mathbb{N}_0.$$

Note that generation and reproduction properties are independent of the starting level ℓ. Next, we recall from [21] sufficient conditions on the k-th level symbol of a convergent non-stationary subdivision scheme that guarantee generation and reproduction of $EP^s_{(\Gamma_{\mathrm{d}},\,\Theta)}$. For Θ as in (3.7) and Ξ' as in (2.9), in the next propositions we denote by $\mathcal{V}_{k,\Theta}$ the subset of $\mathbb{C}^2$ defined by

$$\begin{aligned} \mathcal{V}_{k,\Theta} := \quad & \{(\nu_1, \ldots, \nu_s) \in \mathbb{C}^s \,:\, \nu_j = \epsilon_j e^{-\frac{\theta_j}{m^{k+1}}},\ j = 1, \ldots, s \\ & \boldsymbol{\theta} = (\theta_1, \ldots, \theta_s) \in \Theta,\, \boldsymbol{\epsilon} = (\epsilon_1, \ldots, \epsilon_s) \in \Xi'\}. \end{aligned} \tag{3.10}$$

Moreover, we denote with $D^{\boldsymbol{\gamma}}$ the directional derivative along $\boldsymbol{\gamma} = (\gamma_1, \ldots, \gamma_s) \in \mathbb{N}_0^s$, as in (2.10).

Proposition 3.6 *[21, Proposition 4.2] Let* Γ_d *and* Θ *be the sets in* (3.6)*,* (3.7)*, respectively, and* $\mathcal{V}_{k,\Theta}$ *be the subset of* $\mathbb{C}^s$ *in* (3.10)*. If a convergent non-stationary subdivision scheme* $\{\mathcal{S}_{\mathbf{a}^{(k)}}, k \in \mathbb{N}_0\}$ *has a k-th level symbol* $\mathrm{a}^{(k)}(\boldsymbol{z})$ *such that*

$$D^{\boldsymbol{\gamma}} \mathrm{a}^{(k)}(\boldsymbol{\nu}) = 0, \qquad \forall \boldsymbol{\nu} \in \mathcal{V}_{k,\Theta}, \quad \boldsymbol{\gamma} \in \Gamma_d, \quad k \in \mathbb{N}_0,$$

then it is $EP^s_{(\Gamma_d,\,\Theta)}$*-generating.*

Proposition 3.7 *[21, Theorem 4.4] Let Γ_d and Θ be the sets in* (3.6), (3.7)*, respectively. If a convergent, non-stationary, subdivision scheme $\{\mathcal{S}_{\mathbf{a}^{(k)}}, k \in \mathbb{N}_0\}$ is $EP^s_{(\Gamma_d,\Theta)}$-generating and its k-th level symbol $\mathrm{a}^{(k)}(\boldsymbol{z})$ satisfies*

$$D^{\boldsymbol{\gamma}}\,\mathrm{a}^{(k)}(\boldsymbol{\nu}) = m^s \prod_{j=1}^{s}\prod_{\ell=1}^{2} \nu_j^{\tau_j-\gamma_j}\mathrm{q}_{\gamma_\ell}(\tau_\ell), \qquad \mathrm{q}_{\gamma_\ell}(\tau_\ell) = \begin{cases} \prod_{h=0}^{\gamma_\ell-1}(\tau_\ell - h) & \text{if} \quad \gamma_\ell \in \mathbb{N}, \\ 1 & \text{if} \quad \gamma_\ell = 0 \end{cases}$$

for all $\boldsymbol{\nu} \in \{\boldsymbol{\nu} \in \mathbb{C}^s : \nu_j = \epsilon_j e^{-\frac{\theta_j}{m^{k+1}}},\ \boldsymbol{\theta} \in \Theta, \boldsymbol{\epsilon} \in \Xi\}$, $\boldsymbol{\gamma} \in \Gamma_d$ and $k \in \mathbb{N}_0$, then it is $EP^s_{(\Gamma_d,\Theta)}$-reproducing with respect to the parametrization $\{\mathbf{T}^{(k)}, k \in \mathbb{N}_0\}$ in (2.6).

Another important property of non-stationary subdivision schemes is the so-called step-wise exponential polynomial reproduction.

Proposition 3.8 *A non-stationary subdivision scheme $\{\mathcal{S}_{\mathbf{a}^{(k)}}, k \in \mathbb{N}_0\}$ is step-wise $EP^s_{(\Gamma_d,\Theta)}$-reproducing if and only if there exists a shift parameter $\boldsymbol{\tau} \in \mathbb{R}^s$ such that*

$$\sum_{\mathbf{j}\in\mathbb{Z}^s} \mathrm{a}^{(k)}_{m\mathbf{j}+\boldsymbol{e}} \left(\frac{\mathbf{j}}{m^k}\right)^{\boldsymbol{\gamma}'} \boldsymbol{\nu}^{m\mathbf{j}+\boldsymbol{e}} = \boldsymbol{\nu}^{m\boldsymbol{\tau}-\boldsymbol{\tau}}\boldsymbol{\epsilon}^{-m\boldsymbol{\tau}+\boldsymbol{\tau}+\boldsymbol{e}} \left(\frac{m\boldsymbol{\tau}-\boldsymbol{\tau}-\boldsymbol{e}}{m^{k+1}}\right)^{\boldsymbol{\gamma}'}$$

is satisfied for all $\boldsymbol{\nu} \in \{(v_1,\dots,v_s) : v_j = \epsilon_j e^{-\frac{\theta_j}{m^{k+1}}},\ \boldsymbol{\theta} \in \Theta, \boldsymbol{\epsilon} \in \Xi\},\ k \in \mathbb{N}_0,\ \mathbf{0} \le \boldsymbol{\gamma}' \le \boldsymbol{\gamma},\ \boldsymbol{\gamma} \in \Gamma_d, \boldsymbol{e} \in E$ [1].

Remark 3.9 *The property of affine invariance of a non-stationary subdivision scheme $\{\mathcal{S}_{\mathbf{a}^{(k)}}, k \in \mathbb{N}_0\}$ is exactly the same of the stationary case, thus if $\{\mathcal{S}_{\mathbf{a}^{(k)}}, k \in \mathbb{N}_0\}$ reproduces Π^s_1, then it is affine invariant (see Proposition 2.11).*

Finally, we consider the particular case of an interpolatory subdivision scheme. If $\{\mathcal{S}_{\mathbf{a}^{(k)}}, k \in \mathbb{N}_0\}$ is interpolatory, then it satisfies the interpolation property in (2.11).

Corollary 3.10 *[21, Corollary 5.1] Let $\{\mathcal{S}_{\mathbf{a}^{(k)}}, k \in \mathbb{N}_0\}$ be a non-stationary interpolatory subdivision scheme that is $EP^s_{(\Gamma_d,\Theta)}$-generating. Then $\{\mathcal{S}_{\mathbf{a}^{(k)}}, k \in \mathbb{N}_0\}$ is also $EP^s_{(\Gamma_d,\Theta)}$-reproducing with respect to the parametrization in* (2.6) *with $\boldsymbol{\tau} = 0$.*

3.1.1 The tension parameter t

In the non-stationary setting, the rules of the subdivision schemes depend on a free parameter $t \in [0, \frac{m}{2}\pi) \cup \mathrm{i}\mathbb{R}^+$, which defines the exponential space $EP^s_{(\Gamma_d,\Theta)}$ in (3.8). Generally, the refinement rules are expressed in terms of the parameter sequence $\{v^{(k)}, k \in \mathbb{N}_0\}$ which contains the parameters t as

$$v^{(k)} = \frac{1}{2}\left(e^{\mathrm{i}\frac{t}{m^{k+1}}} + e^{-\mathrm{i}\frac{t}{m^{k+1}}}\right), \quad k \in \mathbb{N}_0, \tag{3.11}$$

[1] The expression $\mathbf{0} \le \boldsymbol{\gamma}' \le \boldsymbol{\gamma}$, i.e. $(0,\dots,0) \le (\gamma_1',\dots,\gamma_s') \le (\gamma_1,\dots,\gamma_s)$ means that $0 \le \gamma_j' \le \gamma_j$ for all $j = 1,\dots,s$ (see [21])

where m is the arity of the subdivision scheme. In particular, in the binary case ($m = 2$), we have that, after choosing an arbitrary $v^{(0)} \in \mathbb{R}^+$ defined as

$$v^{(0)} := \cos\left(\frac{t}{2}\right) = \begin{cases} \cos\left(\frac{s}{2}\right) \in (0,1) & \text{if } \ t = s, \quad s \in (0,\pi), \\ 1 & \text{if } \ t = 0, \\ \cosh\left(\frac{s}{2}\right) \in (1,+\infty) & \text{if } \ t = is, \quad s \in \mathbb{R}^+, \end{cases} \tag{3.12}$$

we can equivalently compute the value of $v^{(k)}$ in (3.11) via the recursive formula (see [8, Proposition 2])

$$v^{(k+1)} = \sqrt{\frac{v^{(k)}+1}{2}}, \qquad \forall\, k \in \mathbb{N}_0. \tag{3.13}$$

In the ternary case ($m = 3$), choosing an arbitrary $v^{(0)} \in \mathbb{R}^+$ specifically of the form

$$v^{(0)} := \cos\left(\frac{t}{3}\right) = \begin{cases} \cos\left(\frac{s}{3}\right) \in (0,1) & \text{if } \ s = t, \ t \in \left(0, \frac{3}{2}\pi\right), \\ 1 & \text{if } \ t = 0, \\ \cosh\left(\frac{s}{3}\right) \in (1,+\infty) & \text{if } \ t = \mathrm{i}s, \ s \in \mathbb{R}^+. \end{cases} \tag{3.14}$$

we can equivalently compute the value of $v^{(k)}$ in (3.11) using the recurrence relation

$$v^{(k)} = \frac{1}{2}\,\mathrm{Re}\left(\left(v^{(k-1)} + \sqrt{\left(v^{(k-1)}\right)^2 - 1}\right)^{\frac{1}{3}} + \left(v^{(k-1)} + \sqrt{\left(v^{(k-1)}\right)^2 - 1}\right)^{-\frac{1}{3}}\right). \tag{3.15}$$

In both the cases, it follows that the parameter sequence $\{v^{(k)},\, k \in \mathbb{N}_0\}$ is such that

$$\lim_{k\to\infty} v^{(k)} = 1 \qquad \text{and} \qquad |1 - v^{(k)}| \le c\, m^{-2k}, \tag{3.16}$$

for $k \to \infty$ with some constant $c > 0$ (see [8, Remark 3]).
The parameter $t \in \left[0, \frac{m}{2}\pi\right) \cup \mathrm{i}\mathbb{R}^+$ has a tension role, as shown in [8] and as we will see in Section 4.2 and in Chapter 7.

3.2 Convergence and smoothness analysis of non-stationary subdivision schemes

As in the stationary case, we have to distinguish the smoothness properties on regular meshes from those at extraordinary vertices and faces. We start by recalling the main results regarding regular meshes.

3.2.1 Smoothness analysis of curves and surfaces on regular meshes

The analysis of convergence and smoothness of univariate non-stationary subdivision schemes and bivariate non-stationary subdivision schemes defined on regular meshes was first studied in [56] and it is based on the concept of asymptotic equivalence.

Definition 3.11 *Let $\mathcal{S}_{\mathbf{a}}$ and $\{\mathcal{S}_{\mathbf{a}^{(k)}}, k \in \mathbb{N}_0\}$ be subdivision schemes defined on regular meshes by the subdivision masks $\mathbf{a} \in \ell(\mathbb{Z}^s)$ and $\mathbf{a}^{(k)} \in \ell(\mathbb{Z}^s)$, $k \in \mathbb{N}_0$,respectively. If*

$$\sum_{k=0}^{+\infty} \|\mathbf{a}^{(k)} - \mathbf{a}\| < +\infty, \tag{3.17}$$

then $\mathcal{S}_{\mathbf{a}}$ and $\{\mathcal{S}_{\mathbf{a}^{(k)}}, k \in \mathbb{N}_0\}$ are said to be asymptotically equivalent schemes.

Theorem 3.12 *[56, Theorems 7] Let $\mathcal{S}_{\mathbf{a}}$ and $\{\mathcal{S}_{\mathbf{a}^{(k)}}, k \in \mathbb{N}_0\}$ be asymptotically equivalent subdivision schemes defined on regular meshes by the subdivision masks $\mathbf{a} \in \ell(\mathbb{Z}^s)$ and $\mathbf{a}^{(k)} \in \ell(\mathbb{Z}^s)$, $k \in \mathbb{N}_0$, respectively. If $\mathcal{S}_{\mathbf{a}}$ is convergent, then $\{\mathcal{S}_{\mathbf{a}^{(k)}}, k \in \mathbb{N}_0\}$ is also convergent.*

Remark 3.13 *From Theorem 3.12 it follows that [56, Lemma 15]*

$$\lim_{k \to +\infty} \mathbf{\Phi}_k(u, v) = \mathbf{\Phi}(u, v), \quad \text{uniformly on } \mathbb{R}^s, \tag{3.18}$$

where $\mathbf{\Phi}(u, v)$ is the basic limit function vector of $\mathcal{S}_{\mathbf{a}}$ and $\mathbf{\Phi}_k(u, v)$, $k \in \mathbb{N}_0$ the family of basic limit function vectors of $\{\mathcal{S}_{\mathbf{a}^{(k)}}, k \in \mathbb{N}_0\}$.

Theorem 3.14 *[56, Theorems 8] Let $\mathcal{S}_{\mathbf{a}}$ and $\{\mathcal{S}_{\mathbf{a}^{(k)}}, k \in \mathbb{N}_0\}$ be asymptotically equivalent subdivision schemes defined on regular meshes by the subdivision masks $\mathbf{a} \in \ell(\mathbb{Z}^s)$ and $\mathbf{a}^{(k)} \in \ell(\mathbb{Z}^s)$, $k \in \mathbb{N}_0$, respectively. If $\mathcal{S}_{\mathbf{a}}$ is of class C^r and*

$$\sum_{k=1}^{+\infty} 2^{rk} \|\mathbf{a}^{(k)} - \mathbf{a}\| < +\infty, \tag{3.19}$$

then $\{\mathcal{S}_{\mathbf{a}^{(k)}}, k \in \mathbb{N}_0\}$ is also of class C^r.

Thus the smoothness analysis of a non-stationary subdivision scheme is checked by comparison with a stationary one whose convergence and regularity properties are known. The conditions required by Theorem 3.12 could be relaxed as proposed in [20, 24].

Definition 3.15 *[20, Definition 3] Let Ξ' be defined as in (2.9), $\boldsymbol{\gamma} \in \mathbb{N}_0^s$ and $D^{\boldsymbol{\gamma}}$ as in (2.10). A non-stationary subdivision scheme $\{\mathcal{S}_{\mathbf{a}^{(k)}}, k \in \mathbb{N}_0\}$ is said to satisfy the approximate sum rules of order $r+1$, $r \in \mathbb{N}_0$, if the sequences $\{\mu_k,\, k \in \mathbb{N}_0\}$ and $\{\delta_k,\, k \in \mathbb{N}_0\}$ with*

$$\mu_k := \left| \mathrm{a}^{(k)}(\mathbf{1}) - m \right| \qquad \text{and} \qquad \delta_k := \max_{0 \le |\boldsymbol{\gamma}| \le r} \max_{\boldsymbol{\epsilon} \in \Xi'} m^{-k|\boldsymbol{\gamma}|} \left| D^{\boldsymbol{\gamma}} \mathrm{a}^{(k)}(\boldsymbol{\epsilon}) \right|$$

satisfy

$$\sum_{k=0}^{\infty} \mu_k < +\infty \qquad \text{and} \qquad \sum_{k=0}^{\infty} m^{kr}\, \delta_k < +\infty.$$

Definition 3.16 *[24, Definition 7] A stationary subdivision scheme $\mathcal{S}_{\mathbf{a}}$ and a non-stationary one $\{\mathcal{S}_{\mathbf{a}^{(k)}}, k \in \mathbb{N}_0\}$ are termed asymptotically similar if the sequence of subdivision masks $\mathbf{a}^{(k)}$, $k \in \mathbb{N}_0$, and $\mathbf{a}$ have the same support $\mathcal{J}$ (i.e. $\mathrm{a}_{\mathbf{i}}^{(k)} = \mathrm{a}_{\mathbf{i}} = 0$ for all $\mathbf{i} \notin \mathcal{J}$) and satisfy*

$$\lim_{k \to +\infty} \mathrm{a}_{\mathbf{i}}^{(k)} = \mathrm{a}_{\mathbf{i}}, \quad \forall \mathbf{i} \in \mathcal{J}.$$

These two notions allow us to check convergence and smoothness of a non-stationary scheme by comparing it with a stationary scheme whose convergence, regularity and polynomial generation properties are known. More precisely, in [20, Corollary 4] the following result is given.

Proposition 3.17 *Assume that the non-stationary subdivision scheme $\{\mathcal{S}_{\mathbf{a}^{(k)}}, k \in \mathbb{N}_0\}$ satisfies approximate sum rules of order $r+1$, $r \in \mathbb{N}_0$, and is asymptotically similar to a convergent stationary subdivision scheme $\mathcal{S}_{\mathbf{a}}$ whose refinable basic limit function is C^r. Then the limits of the non-stationary scheme $\{\mathcal{S}_{\mathbf{a}^{(k)}}, k \in \mathbb{N}_0\}$ are C^r.*

The notions of asymptotical similarity and reproduction of exponential polynomials are useful for the study of the approximation order of a non-stationary subdivision scheme [30, Theorem 20].

Proposition 3.18 *Assume that the non-stationary subdivision scheme* $\{\mathcal{S}_{\mathbf{a}^{(k)}}, k \in \mathbb{N}_0\}$ *reproduces a d-dimentional space of exponential polynomials and is asymptotically similar to a convergent stationary subdivision scheme* $\mathcal{S}_{\mathbf{a}}$*. Then, the non-stationary subdivision scheme* $\{\mathcal{S}_{\mathbf{a}^{(k)}}, k \in \mathbb{N}_0\}$ *has approximation order d.*

3.2.2 Convergence at extraordinary vertices and faces

As in the stationary case, near an extraordinary vertex or face the convergence analysis is performed using the subdivision matrix. In the non-stationary setting, the subdivision scheme $\{\mathcal{S}_k, k \in \mathbb{N}_0\}$ is not associated to one subdivision matrix, but to a sequence of matrices $\{S_k, k \in \mathbb{N}_0\}$, since the subdivision rules depend on the subdivision level k. However, the construction and structure of the matrices is the same shown in the stationary case. Precisely, we order the points as explained in Order 2 and thus we construct the k-th level subdivision matrix S_k as shown in Section 2.3. It results that S_k near an extraordinary elements of valence n has the form in (2.20) if $\{\mathcal{S}_k, k \in \mathbb{N}_0\}$ is dual, and it is as in (2.21) if $\{\mathcal{S}_k, k \in \mathbb{N}_0\}$ is primal. In general, we have that, for all $k \in \mathbb{N}_0$, S_k is a block-circulant matrix of the form

$$S_k = \operatorname{circ}(M_{0,k}, M_{1,k}, \ldots, M_{n-1,k}) \in \mathbb{R}^{N\times N}.$$

Near an isolated vertex or face, the regular subdivision surface produced by a non-stationary subdivision scheme $\{\mathcal{S}_k, k \in \mathbb{N}_0\}$ is denoted by $\overline{\mathbf{r}}$ which is defined on the local domain $\mathbf{D}_n = \Omega \times \mathbb{Z}_n$ and described as $\overline{\mathbf{r}} : \mathbf{D}_n \to \mathbb{R}^3$ (see Section 2.3). In this case, we define the ring $\overline{\mathbf{r}}_k$ as the restriction of the regular subdivision surface $\overline{\mathbf{r}}$ to the set $\mathbf{D}_{n,k}$, i.e.

$$\overline{\mathbf{r}}_k(\mathbf{D}_{n,1}) = \overline{\mathbf{r}}(\mathbf{D}_{n,k}), \quad k \in \mathbb{N}_0,$$

which implies

$$\overline{\mathbf{r}}(\mathbf{D}_n) = \bigcup_{k\in\mathbb{N}_0} \overline{\mathbf{r}}_k(\mathbf{D}_{n,1}) \cup \{\overline{\mathbf{r}}_c\},$$

where $\overline{\mathbf{r}}_c = \overline{\mathbf{r}}(\mathbf{0})$ is the central point.
Let $\mathbf{\Phi}_k(u,v) \in \mathbb{R}^N$ be the vector with the associated basic limit functions and let $\mathbf{f}^{(k)} \in \mathbb{R}^{N\times 3}$ be the vector of vertices of each ring $\overline{\mathbf{r}}_k$, then

$$\begin{aligned} \overline{\mathbf{r}}_k : \mathbf{D}_{n,k} = \Omega_k \times \mathbb{Z}_n &\to \mathbb{R}^3 \\ (u,v) &\longmapsto \overline{\mathbf{r}}_k(u,v) = (\mathbf{f}^{(k)})^T\, \mathbf{\Phi}_k(u,v). \end{aligned} \tag{3.20}$$

Remark 3.19 *For all* $k \geq 1$, $\mathbf{\Phi}_k(u,v)^T \boldsymbol{x}_0 = \alpha_k$ *with* $\alpha_k \in \mathbb{R}$*. Note that* $\mathbf{\Phi}_k(u,v)^T \boldsymbol{x}_0 = 1$ *for all* $k \geq 1$*, if and only if the non-stationary subdivision scheme has the property of step-wise reproduction of constants (see Definition 3.8).*

The definition of convergence of a non-stationary subdivision scheme $\{\mathcal{S}_k, k \in \mathbb{N}_0\}$ near an extraordinary element is the same shown in the stationary case (see Definitions 2.22), where equation (2.26) changes as in (3.4).

Remark 3.20 *The property of affine invariance of a non-stationary subdivision scheme near extraordinary elements is exactly the same as in the stationary case, i.e. if the elements of each row of S_k sum up to 1 for all $k \in \mathbb{N}_0$, then the non-stationary subdivision scheme $\{\mathcal{S}_k, k \in \mathbb{N}_0\}$ is affinely invariant in the neighborhood of extraordinary elements (see Remark 2.26).*

Let $\mathbf{f}^{(0)}$ be the vector with the initial control points defining the local portion of the mesh in the vicinity of an extraordinary element. The goal is to study the behavior of the sequence $\{\mathbf{f}^{(k+1)}, k \in \mathbb{N}_0\}$ defined in (3.4) and hence the convergence of the sequence of regular rings $\{\bar{\mathbf{r}}_{k+1}, k \in \mathbb{N}_0\}$ where $\bar{\mathbf{r}}_{k+1}^T = \mathbf{\Phi}_{k+1}^T \mathbf{f}^{(k+1)} = \mathbf{\Phi}_{k+1}^T S^{(k+1)} \mathbf{f}^{(0)}$. The key idea is to write the product matrix $S^{(k+1)}$ in terms of the level-dependent matrices $S_k, k \in \mathbb{N}_0$ and of the stationary matrix S. In particular, we consider two different matrix relations useful for our purposes.

Proposition 3.21 *Let $S^{(0)} = I$ and for all $k \in \mathbb{N}_0$ let $S^{(k+1)}$ be defined as in* (3.5)*. Then, for all $k \in \mathbb{N}_0$*

$$S^{(k+1)} = S^{k+1} + \sum_{j=0}^{k} S^{k-j}(S_j - S)S^{(j)}. \tag{3.21}$$

Proof: Using the definition of $S^{(k+1)}$ in (3.5) and assuming $\sum_{j=0}^{k-1} S^{k-j}(S_j - S)S^{(j)}$ to be $\mathbf{0}$ when $k = 0$, we can write

$$\begin{aligned}
S^{k+1} + \sum_{j=0}^{k} S^{k-j}(S_j - S)S^{(j)} &= S^{k+1} + \sum_{j=0}^{k-1} S^{k-j}(S_j - S)S^{(j)} + (S_k - S)S^{(k)} \\
&= S^{k+1} + (S_k - S)S^{(k)} + \sum_{j=0}^{k-1} S^{k-j} S_j S^{(j)} - \sum_{j=0}^{k-1} S^{k-j} S S^{(j)} \\
&= S^{k+1} + S^{(k+1)} + \sum_{j=0}^{k-1} S^{k-j} S^{(j+1)} - \sum_{j=0}^{k-1} S^{k-j+1} S^{(j)} - S S^{(k)} \\
&= S^{k+1} + S^{(k+1)} + \sum_{j=1}^{k} S^{k-j+1} S^{(j)} - \sum_{j=0}^{k} S^{k-j+1} S^{(j)} \\
&= S^{k+1} + S^{(k+1)} - S^{k+1} \\
&= S^{(k+1)}.
\end{aligned}$$

■

Proposition 3.22 *For all $k, m \in \mathbb{N}_0$*

$$S_{k+m-1} \cdot \ldots \cdot S_k = S^{m+1} + \sum_{j=0}^{m} \left(\prod_{h=1}^{j-1} S_{k+m-h} \right) (S_{k+m-j} - S) S^{m-j} \tag{3.22}$$

where $\prod_{h=1}^{j-1} S_{k+m-h}$ is assumed to be I when $j = 1$.

Proof: We can write

$$
\begin{aligned}
&S^{m+1} + \sum_{j=0}^{m} \left(\prod_{h=1}^{j-1} S_{k+m-h} \right) (S_{k+m-j} - S) S^{m-j} \\
&= S^{m+1} + \sum_{j=0}^{m-1} \left(\prod_{h=1}^{j-1} S_{k+m-h} \right) (S_{k+m-j} - S) S^{m-j} + \prod_{h=1}^{m-1} S_{k+m-h} (S_k - S) \\
&= S^{m+1} + \sum_{j=0}^{m-1} \left(\prod_{h=1}^{j-1} S_{k+m-h} \right) S_{k+m-j} S^{m-j} - \sum_{j=0}^{m-1} \left(\prod_{h=1}^{j-1} S_{k+m-h} \right) S^{m-j+1} \\
&+ \left(\prod_{h=1}^{m} S_{k+m-h} \right) - \left(\prod_{h=1}^{m-1} S_{k+m-h} \right) S \\
&= S^{m+1} + \sum_{j=0}^{m-1} \left(\prod_{h=1}^{j} S_{k+m-h} \right) S^{m-j} - \sum_{j=0}^{m} \left(\prod_{h=1}^{j-1} S_{k+m-h} \right) S^{m-j+1} + \left(\prod_{h=1}^{m} S_{k+m-h} \right) \\
&= S^{m+1} + \sum_{j=1}^{m} \left(\prod_{h=1}^{j-1} S_{k+m-h} \right) S^{m-j+1} - \sum_{j=0}^{m} \left(\prod_{h=1}^{j-1} S_{k+m-h} \right) S^{m-j+1} + \left(\prod_{h=1}^{m} S_{k+m-h} \right) \\
&= S^{m+1} - S^{m+1} + \left(\prod_{h=1}^{m} S_{k+m-h} \right) \\
&= S_{k+m-1} \cdot \ldots \cdot S_k.
\end{aligned}
$$

■

Exploiting the Jordan decomposition in Section 2.3.1, we show the boundedness of $\|S^k\|$ for all $k \in \mathbb{N}_0$, when convergence of the associated stationary subdivision scheme is assumed. Note that, here and in the sequel, we use C to refer to any generic finite positive constant.

Proposition 3.23 *If a stationary subdivision scheme $\mathcal{S}$ is convergent in correspondence to irregular regions of the mesh, then there exists a finite positive constant C such that its matrix S satisfies $\|S^k\| < C$ for all $k \in \mathbb{N}_0$.*

Proof: We use the Jordan decomposition of S^k to write

$$\|S^k\| = \|X J^k X^{-1}\| \leq \|X\| \|J^k\| \|X^{-1}\| \leq C \|J^k\|$$

with C such that $\|X\| \|X^{-1}\| \leq C$. We consider

$$\|J^k\| = \max_{r=0,\ldots,\overline{r}} \left(\sum_{\ell=0}^{\ell_r} |\lambda_r^{k,\ell}| \right) = \max \left\{ \sum_{\ell=0}^{\ell_0} |\lambda_0^{k,\ell}|, \max_{r=1,\ldots,\overline{r}} \left(\sum_{\ell=0}^{\ell_r} |\lambda_r^{k,\ell}| \right) \right\}.$$

Since $\mathcal{S}$ is convergent, the largest eigenvalue of S is $\lambda_0 = 1$ with multiplicity 1 (see Theorem 2.25). Thus $\sum_{\ell=0}^{\ell_0} |\lambda_0^{k,\ell}| = |\lambda_0^k| = 1$. It follows that,

$$\|J^k\| = \max \left\{ 1, \max_{r=1,\ldots,\overline{r}} \left(\sum_{\ell=0}^{\ell_r} |\lambda_r^{k,\ell}| \right) \right\}.$$

Since the terms $\lambda_r^{k,\ell}$, for $r = 1, \ldots, \overline{r}$, decay to zero as $k \to +\infty$ (see Remark 2.24), and hence they are limited for all $k \in \mathbb{N}_0$, the summand $\sum_{\ell=0}^{\ell_r} |\lambda_r^{k,\ell}|$ is limited too for all $k \in \mathbb{N}_0$. Thus $\|S^k\| < C$ for all $k \in \mathbb{N}_0$. ■

The result in the next proposition aims at identifying the crucial assumption to be required on the sequence $\|S_k - S\|$, $k \in \mathbb{N}_0$ to prove in Theorem 3.25 the convergence of the non-stationary subdivision scheme in the vicinity of an extraordinary element.

Proposition 3.24 *Let $\{\mathcal{S}_k, k \in \mathbb{N}_0\}$ be a non-stationary subdivision scheme whose action in correspondence to irregular regions of the mesh is described by the matrix sequence $\{S_k, k \in \mathbb{N}_0\}$. Moreover, let $\mathcal{S}$ be a stationary subdivision scheme that is identified by the subdivision matrix S in correspondence to irregular regions. If*

$$\lim_{k \to +\infty} \frac{\|S_{k+1} - S\|}{\|S_k - S\|} < |\lambda_1|, \tag{3.23}$$

where λ_1 denotes the subdominant eigenvalue of S verifying $1 = \lambda_0 > |\lambda_1| \geq |\lambda_i|$, $i = 2, \ldots, \overline{r}$, then

(a) $\lim_{k \to +\infty} \|S_k - S\| = 0$*;*

(b) there exists a finite positive constant C such that $\|S_{k+m-1} \cdots S_k\| < C$ for all $k, m \in \mathbb{N}_0$.

Proof: (a) let us consider the series $\sum_{k=0}^{+\infty} \|S_k - S\|$. It converges since hypothesis (3.23) verifies the ratio criterion. As a consequence $\lim_{k \to +\infty} \|S_k - S\| = 0$.
(b) from Proposition 3.22 we get that, for all $k, m \in \mathbb{N}_0$,

$$\|S_{k+m-1} \cdot \ldots \cdot S_k\| \leq \|S^{m+1}\| + \sum_{j=0}^{m} \left(\prod_{h=1}^{j-1} \|S_{k+m-h}\| \right) \|S_{k+m-j} - S\| \|S^{m-j}\|.$$

Proposition 3.23 implies that there exists $0 < C < +\infty$ such that $\|S^{m+1}\| < C$ for all $m \in \mathbb{N}_0$ and $\|S^{m-j}\| < C$ for all $m \geq j \geq 0$. Moreover, from case (a) we also know that $\|S_{k+m-j} - S\| < C$ for all $k \in \mathbb{N}_0$, $m \geq j \geq 0$. Therefore, for all $k \in \mathbb{N}_0$,

$$\|S_k\| \leq \|S_k - S\| + \|S\| \leq C,$$

and the claimed result follows straightforwardly. ■

We are now able to provide sufficient conditions to show the convergence of a non-stationary subdivision scheme in correspondence to irregular regions of the mesh.

Theorem 3.25 *Let $\{\mathcal{S}_k, k \in \mathbb{N}_0\}$ be a non-stationary subdivision scheme whose action in correspondence to irregular regions of the mesh is described by the matrix sequence $\{S_k, k \in \mathbb{N}_0\}$. Moreover, let $\mathcal{S}$ be a stationary subdivision scheme that is identified by the subdivision matrix S in correspondence to irregular regions. If*

(i) $\mathcal{S}$ is convergent in correspondence to both regular and irregular regions of the mesh,

(ii) $\{\mathcal{S}_k, k \in \mathbb{N}_0\}$ is asymptotically equivalent to $\mathcal{S}$ in correspondence to regular regions of the mesh,

(iii) $\{S_k, k \geq 1\}$ and S satisfy

$$\lim_{k \to +\infty} \frac{\|S_{k+1} - S\|}{\|S_k - S\|} < |\lambda_1|,$$

with λ_1 the subdominant eigenvalue of S verifying $1 = \lambda_0 > |\lambda_1| \geq |\lambda_i|$, $i = 2, \ldots, \overline{r}$,

then, for all bounded initial data $\mathbf{f}^{(0)}$*, the non-stationary subdivision scheme* $\{\mathcal{S}_k, k \in \mathbb{N}_0\}$ *is convergent also in correspondence to irregular regions of the mesh. In particular,*

$$\lim_{k\to+\infty} \overline{\mathbf{r}}_{k+1} = \mathbf{q}_0 + \boldsymbol{\beta}_0,$$

where

- $\mathbf{q}_0^T = \tilde{\boldsymbol{x}}_0^T \mathbf{f}^{(0)}$ *with* $\tilde{\boldsymbol{x}}_0^T = \boldsymbol{e}_1^T X^{-1}$ *such that* $\tilde{\boldsymbol{x}}_0^T S = \lambda_0 \tilde{\boldsymbol{x}}_0^T$,
- $\boldsymbol{\beta}_0 \in \mathbb{R}^3$ *such that* $\lim_{k\to+\infty} \mathbf{y}_k = \boldsymbol{x}_0 \boldsymbol{\beta}_0^T$ *for* $\mathbf{y}_k := \sum_{j=0}^{k} S^{k-j}(S_j - S)S^{(j)}\mathbf{f}^{(0)}$*, and* $\boldsymbol{x}_0$ *such that* $S\boldsymbol{x}_0 = \lambda_0 \boldsymbol{x}_0$.

Proof: Let $s \in \mathbb{N}_0$. From the definition of $\mathbf{y}_k$ we can write

$$\|\mathbf{y}_{k+s} - \mathbf{y}_k\| \le \sum_{j=0}^{k} \|(S^{k+s-j} - S^{k-j})(S_j - S)S^{(j)}\mathbf{f}^{(0)}\| + \sum_{j=k+1}^{k+s} \|S^{k+s-j}(S_j - S)S^{(j)}\mathbf{f}^{(0)}\|. \quad (3.24)$$

Therefore, recalling the boundedness of the initial data as well as the results in Proposition 3.23 and 3.24(b), we can write

$$\|\mathbf{y}_{k+s} - \mathbf{y}_k\| \le C \left(\sum_{j=0}^{k} \|S^{k+s-j} - S^{k-j}\| \|S_j - S\| + \sum_{j=k+1}^{k+s} \|S_j - S\| \right). \quad (3.25)$$

Now, to bound the first summand in (3.25) we exploit the Jordan decomposition of S^{k+s-j} and S^{k-j} as

$$\|S^{k+s-j} - S^{k-j}\| = \|X(J^{k+s-j} - J^{k-j})X^{-1}\| \le C\|J^{k+s-j} - J^{k-j}\| \quad (3.26)$$

for a finite constant $C > 0$ such that $\|X\|\|X^{-1}\| \le C$. Moreover, recalling that $\lambda_0 = 1$ is unique in view of the hypothesis of convergence of $\mathcal{S}$, we have

$$\begin{aligned} \|J^{k+s-j} - J^{k-j}\| &= \max_{r=0,\dots,\overline{r}} \left\{ \sum_{\ell=0}^{\ell_r} |\lambda_r^{k+s-j,\ell} - \lambda_r^{k-j,\ell}| \right\} = \max_{r=1,\dots,\overline{r}} \left\{ \sum_{\ell=0}^{\ell_r} |\lambda_r^{k+s-j,\ell} - \lambda_r^{k-j,\ell}| \right\} \\ &\le \max_{r=1,\dots,\overline{r}} \left\{ \sum_{\ell=0}^{\ell_r} |\lambda_r^{k+s-j,\ell}| + |\lambda_r^{k-j,\ell}| \right\} \end{aligned} \quad (3.27)$$

Now, for all $r = 1, \dots, \overline{r}$, let $L_r := \arg\max_{\ell=0,\dots,\ell_r} \left\{ |\lambda_r^{k+s-j,\ell}| + |\lambda_r^{k-j,\ell}| \right\}$, thus

$$\max_{r=1,\dots,\overline{r}} \left\{ \sum_{\ell=0}^{\ell_r} |\lambda_r^{k+s-j,\ell} - \lambda_r^{k-j,\ell}| \right\} \le \max_{r=1,\dots,\overline{r}} \left\{ (\ell_r + 1)(|\lambda_r^{k+s-j,L_r}| + |\lambda_r^{k-j,L_r}|) \right\}$$

and denoting with $\hat{r} = \arg\max_{r=1,\dots,\overline{r}} \left\{ (\ell_r + 1)(|\lambda_r^{k+s-j,L_r}| + |\lambda_r^{k-j,L_r}| \right\}$, we find

$$\max_{r=1,\dots,\overline{r}} \left\{ \sum_{\ell=0}^{\ell_r} |\lambda_r^{k+s-j,\ell} - \lambda_r^{k-j,\ell}| \right\} \le (\ell_{\hat{r}} + 1)(|\lambda_{\hat{r}}^{k+s-j,L_{\hat{r}}}| + |\lambda_{\hat{r}}^{k-j,L_{\hat{r}}}|).$$

Recalling the definition of $\lambda_r^{k,\ell}$ in (2.28) we have

$$\max_{r=1,\dots,\overline{r}} \left\{ \sum_{\ell=0}^{\ell_r} |\lambda_r^{k+s-j,\ell} - \lambda_r^{k-j,\ell}| \right\} \leq (\ell_{\hat{r}}+1) \left(|\lambda_{\hat{r}}^{k+s-j-L_{\hat{r}}}| \binom{k+s-j}{L_{\hat{r}}} + |\lambda_{\hat{r}}^{k-j-L_{\hat{r}}}| \binom{k-j}{L_{\hat{r}}} \right).$$

Since $|\lambda_{\hat{r}}| \leq |\lambda_1| < 1$ and $\binom{k+s-j}{L_{\hat{r}}} < \binom{k+s}{L_{\hat{r}}}$ as well as $\binom{k-j}{L_{\hat{r}}} < \binom{k+s}{L_{\hat{r}}}$, for all $k, j, s \geq 1$, we arrive at

$$\max_{r=1,\dots,\overline{r}} \left\{ \sum_{\ell=0}^{\ell_r} |\lambda_r^{k+s-j,\ell} - \lambda_r^{k-j,\ell}| \right\} \leq 2(L_{\hat{r}}+1)|\lambda_1^{k-j-L_{\hat{r}}}| \binom{k+s}{L_{\hat{r}}}. \tag{3.28}$$

Combining (3.27) and (3.28) with (3.26), we have that

$$\sum_{j=0}^{k} \|S^{k+s-j} - S^{k-j}\| \|S_j - S\| \leq C|\lambda_1^{k-L_{\hat{r}}}| \binom{k+s}{L_{\hat{r}}} \sum_{j=0}^{k} |\lambda_1^{-j}| \|S_j - S\|,$$

Using the ratio criterion and exploiting hypothesis (iii) it is easy to see that $\sum_{j=0}^{k} |\lambda_1^{-j}| \|S_j - S\|$ is convergent as $k \to +\infty$. In fact

$$\lim_{j\to+\infty} \frac{|\lambda_1^{-j-1}| \ \|S_{j+1} - S\|}{|\lambda_1^{-j}| \ \|S_j - S\|} = \lim_{j\to+\infty} \frac{\|S_{j+1} - S\|}{|\lambda_1| \ \|S_j - S\|} < 1.$$

Thus, $\sum_{j=0}^{k} \|S^{k+s-j} - S^{k-j}\| \|S_j - S\| \leq C|\lambda_1^{k-L_{\hat{r}}}| \binom{k+s}{L_{\hat{r}}} \leq C|\lambda_1^{k}| \binom{k+s}{L_{\hat{r}}}$.
For the second summand in (3.25) we start by applying the following reasoning. Exploiting assumption (iii) we can write that, for all $\epsilon > 0$, there exists k_ϵ such that

$$\|S_{k+1} - S\| < |\lambda_1| \ \|S_k - S\|, \quad \text{for all} \quad k \geq k_\epsilon. \tag{3.29}$$

Now, we consider

$$\sum_{j=k+1}^{k+s} \|S_j - S\| = \sum_{m=0}^{s-1} \|S_{k+m+1} - S\|$$

and exploiting (3.29) we have

$$\|S_{k+m+1} - S\| < |\lambda_1| \|S_{k+m} - S\| < |\lambda_1^2| \|S_{k+m-1} - S\| < \ldots < |\lambda_1^{m+1}| \|S_k - S\|,$$

for all $k \geq k_\epsilon$. Thus

$$\sum_{j=k+1}^{k+s} \|S_j - S\| = \sum_{m=0}^{s-1} \|S_{k+m+1} - S\| < \sum_{m=0}^{s-1} |\lambda_1^{m+1}| \|S_k - S\|$$

where $\sum_{m=0}^{s-1} |\lambda_1^{m+1}| < C$ for any $s \geq 1$ due to the assumption $0 < |\lambda_1| < 1$.
As a consequence, combining the two above results, we arrive at claiming that, for k sufficiently large,

$$\|\mathbf{y}_{k+s} - \mathbf{y}_k\| < C \left(|\lambda_1^k| \binom{k+s}{L_{\hat{r}}} + \|S_k - S\| \right).$$

In light of the fact that by assumption (iii) $0 < |\lambda_1| < 1$, we have that both $|\lambda_1^k|$ and $|\lambda_1^k|\binom{k+s}{L_{\hat{r}}}$ converges to 0 as $k \to +\infty$. Exploiting also Proposition 3.24 (a), we can finally conclude that, for all $\epsilon > 0$, there exists k_ϵ such that

$$\|\mathbf{y}_{k+s} - \mathbf{y}_k\| < \epsilon, \qquad \text{for all } k \geq k_\epsilon,\ s \geq 1.$$

There follows that $\{\mathbf{y}_k, k \geq 1\}$ is convergent as $k \to +\infty$. Exploiting the basis of generalized eigenvectors, its limit $\mathbf{y}$ can be written as

$$\mathbf{y} = \boldsymbol{x}_0\boldsymbol{\beta}_0^T + \sum_{r=1}^{\overline{r}} \sum_{\ell=0}^{\ell_r} \boldsymbol{x}_r^\ell \boldsymbol{\beta}_{r,\ell}^T,$$

for certain coefficients $\boldsymbol{\beta}_0, \boldsymbol{\beta}_{r,\ell} \in \mathbb{R}^3$, $r = 1, \ldots, \overline{r},\ \ell = 0, \ldots, \ell_r$. To find the explicit expression of $\mathbf{y}$, we consider

$$\|S\mathbf{y} - \mathbf{y}\| \leq \|S\mathbf{y} - S\mathbf{y}_k\| + \|S\mathbf{y}_k - \mathbf{y}_{k+1}\| + \|\mathbf{y}_{k+1} - \mathbf{y}\|. \tag{3.30}$$

In particular,

$$\begin{aligned} \|S\mathbf{y}_k - \mathbf{y}_{k+1}\| &= \left\| S \sum_{j=0}^{k} S^{k-j}(S_j - S)S^{(j)}\mathbf{f}^{(0)} - \sum_{j=0}^{k+1} S^{k+1-j}(S_j - S)S^{(j)}\mathbf{f}^{(0)} \right\| \\ &= \|(S_{k+1} - S)S^{(k)}\mathbf{f}^{(0)}\| \end{aligned}$$

and thus, replacing the last equality in (3.30), we obtain

$$\|S\mathbf{y} - \mathbf{y}\| \leq \|S\|\|\mathbf{y} - \mathbf{y}_k\| + \|S_{k+1} - S\|\|S^{(k)}\|\|\mathbf{f}^{(0)}\| + \|\mathbf{y}_{k+1} - \mathbf{y}\|.$$

Therefore, using again Propositions 3.23 and 3.24, together with the convergence of $\{\mathbf{y}_k, k \in \mathbb{N}_0\}$, we obtain that the right hand side of the last inequality tends to 0 as $k \to +\infty$. This implies that, as $k \to +\infty$, $S\mathbf{y} = \mathbf{y}$, i.e. the columns of $\mathbf{y}$ lies in the eigenspace corresponding to the right eigenvector of S associated to the eigenvalue $\lambda_0 = 1$ and therefore $\mathbf{y}$ must be of the form $\mathbf{y} = \boldsymbol{x}_0\boldsymbol{\beta}_0^T$ with $\boldsymbol{x}_0 = [1, ..., 1]^T$. Exploiting Proposition 3.21 and the fact that $\mathbf{f}^{(k+1)} = S_k\mathbf{f}^{(k)} = ... = S^{(k+1)}\mathbf{f}^{(0)}$, we can finally write

$$\mathbf{f}^{(k+1)} = S^{(k+1)}\mathbf{f}^{(0)} = \left(S^{k+1} + \sum_{j=0}^{k} S^{k-j}(S_j - S)S^{(j)} \right) \mathbf{f}^{(0)} = S^{k+1}\mathbf{f}^{(0)} + \mathbf{y}_k.$$

From the last observation we have that $\mathbf{y}_k$ converges to $\mathbf{y} = \boldsymbol{x}_0\boldsymbol{\beta}_0^T$ as $k \to +\infty$, thus

$$\lim_{k\to+\infty} \mathbf{f}^{(k+1)} = \lim_{k\to+\infty} S^{k+1}\mathbf{f}^{(0)} + \boldsymbol{x}_0\boldsymbol{\beta}_0^T. \tag{3.31}$$

As a consequence, to prove the convergence of the sequence $\{\mathbf{f}^{(k+1)}, k \in \mathbb{N}_0\}$ we only need to show the behavior of the term $S^{k+1}\mathbf{f}^{(0)}$ as $k \to +\infty$. Using the Jordan decomposition of S^{k+1} (see Section 2.3.1) we can write $S^{k+1}\mathbf{f}^{(0)} = XJ^{k+1}X^{-1}\mathbf{f}^{(0)}$. Hence, introducing the notation $\mathbf{q} := X^{-1}\mathbf{f}^{(0)}$ and recalling the fact that $\lambda_0 = 1$ is unique and $|\lambda_r| < 1$, $\forall r = 1, \ldots, \overline{r}$, we have

$$\lim_{k\to+\infty} S^{k+1}\mathbf{f}^{(0)} = \lim_{k\to+\infty} XJ^{k+1}\mathbf{q} = X\left(\lim_{k\to+\infty} J^{k+1}\right)\mathbf{q} = X\begin{pmatrix} 1 & \cdots & 0 & 0 \\ 0 & 0 & \cdots & 0 \\ \vdots & \ddots & \ddots & \vdots \\ 0 & \cdots & \cdots & 0 \end{pmatrix}\mathbf{q} = \boldsymbol{x}_0\mathbf{q}_0^T, \tag{3.32}$$

with $\mathbf{q}_0^T = \tilde{\boldsymbol{x}}_0^T \mathbf{f}^{(0)}$. Replacing (3.32) in (3.31), we thus get

$$\lim_{k\to+\infty} \mathbf{f}^{(k+1)} = \boldsymbol{x}_0(\mathbf{q}_0 + \boldsymbol{\beta}_0)^T.$$

As a consequence, taking into consideration assumption (ii) and Remark 3.13 we can write

$$\lim_{k\to+\infty} \overline{\mathbf{r}}_{k+1}^T = \lim_{k\to+\infty} \boldsymbol{\Phi}_{k+1}^T \mathbf{f}^{(k+1)} = \boldsymbol{\Phi}^T \boldsymbol{x}_0(\mathbf{q}_0 + \boldsymbol{\beta}_0)^T,$$

and, in view of Remark 2.21, we conclude that

$$\lim_{k\to+\infty} \overline{\mathbf{r}}_{k+1} = \mathbf{q}_0 + \boldsymbol{\beta}_0.$$

■

Chapter 4

Families of stationary and non-stationary univariate subdivision schemes

Most of the univariate ($s = 1$) subdivision schemes proposed in literature are binary and stationary since these characteristics make it easier to study the mathematical properties of the limit curve, although they seriously limit the applications of the scheme. In fact, it is already well-known that passing from stationary to non-stationary schemes we can gain tension control and conics reproduction (see e.g. [9]), while passing from binary to ternary subdivision we can improve the smoothness order of the basic limit function without dramatically increasing its support width (see [9, 72]).
In this chapter, we do not present new subdivision schemes, but we show some generalizations of existent schemes in order to provide a complete framework and to extend their use to more applications.

4.1 A combined ternary 4-point scheme

In this section we study a 3-parameter combined ternary 4-point subdivision scheme which provides a unifying framework for several independent proposals of stationary ternary schemes appeared in the literature. For such a scheme we completely characterize the regions of C^2 and C^3 convergence, that is the sets of parameters that fulfill the necessary and sufficient conditions for C^2 and C^3 convergence, respectively.
As recalled in Section 1.2, in general subdivision schemes are classified as interpolatory or approximating, depending if the obtained limit shape passes or not through all the points of the given initial set. However, there also exists a class of parameter-dependent subdivision schemes, called combined subdivision schemes, that according to the specific values assumed by the parameters, can be regarded either as a member of the approximating group or of the interpolatory one. A combined subdivision scheme of arity m is indeed characterized by a parameter-dependent symbol $\mathrm{a}(z)$, $z \in \mathbb{C}\backslash\{0\}$, that satisfies the odd-symmetry property $\mathrm{a}(z) = \mathrm{a}(z^{-1})$ for all choices of the free parameters, while it verifies the interpolation property in (2.11) only for some special choices of the free parameters. When passing from an approximating scheme to an interpolating one, the maximum and minimum power of z in

the symbol $\mathrm{a}(z)$ remain unchanged; only the coefficients of $\mathrm{a}(z)$ assume different values. This means that, differently from the so-called primal pseudo-spline schemes (which also blend approximating schemes with interpolatory ones [25]), the combined subdivision schemes pass from the approximating to the interpolatory form without modifying the length of the subdivision mask associated with $\mathrm{a}(z)$. Although combined subdivision schemes of any arity can be constructed, here we focus our attention on combined subdivision schemes of arity 3 and, in particular, on combined ternary 4-point schemes. This choice is motivated by the fact that the literature on ternary 4-point subdivision schemes is extremely fragmentary and thus there is a special need of a unifying framework. In particular, we want to show that the numerous independent proposals appeared in the last fifteen years [71, 72, 66, 109, 67, 116], can indeed be regarded as special instances of a unique combined ternary 4-point scheme.

4.1.1 Construction of the ternary combined subdivision scheme

We start by considering the refinement rules of the ternary quadratic B-spline scheme

$$\begin{cases} \tilde{f}_{3i}^{(k+1)} &= \frac{1}{9} f_{i-1}^{(k)} + \frac{7}{9} f_i^{(k)} + \frac{1}{9} f_{i+1}^{(k)}, \\ \tilde{f}_{3i+1}^{(k+1)} &= \frac{2}{3} f_i^{(k)} + \frac{1}{3} f_{i+1}^{(k)}, \\ \tilde{f}_{3i+2}^{(k+1)} &= \frac{1}{3} f_i^{(k)} + \frac{2}{3} f_{i+1}^{(k)}, \end{cases} \tag{4.1}$$

and we define the displacement factor

$$\Delta f_i^{(k)} := -(f_{i-1}^{(k)} - 2f_i^{(k)} + f_{i+1}^{(k)}).$$

Moving the points $\tilde{\mathbf{f}}^{(k+1)}$ provided by the ternary quadratic B-spline scheme in (4.1) to new positions according to the displacements $\alpha\Delta f_i^{(k)}$, $-\beta\Delta f_i^{(k)} - \gamma\Delta f_{i+1}^{(k)}$ and $-\gamma\Delta f_i^{(k)} - \beta\Delta f_{i+1}^{(k)}$, respectively, we obtain the refinement rules

$$\begin{cases} f_{3i}^{(k+1)} &= \tilde{f}_{3i}^{(k+1)} + \alpha\Delta f_i^{(k)}, \\ f_{3i+1}^{(k+1)} &= \tilde{f}_{3i+1}^{(k+1)} - \beta\Delta f_i^{(k)} - \gamma\Delta f_{i+1}^{(k)}, \\ f_{3i+2}^{(k+1)} &= \tilde{f}_{3i+2}^{(k+1)} - \gamma\Delta f_i^{(k)} - \beta\Delta f_{i+1}^{(k)}. \end{cases} \tag{4.2}$$

In this way, the refined data sequence $\mathbf{f}^{(k+1)}$ is explicitly defined by

$$\begin{cases} f_{3i}^{(k+1)} &= (\frac{1}{9} - \alpha) f_{i-1}^{(k)} + (\frac{7}{9} + 2\alpha) f_i^{(k)} + (\frac{1}{9} - \alpha) f_{i+1}^{(k)}, \\ f_{3i+1}^{(k+1)} &= \beta f_{i-1}^{(k)} + (\frac{2}{3} + \gamma - 2\beta) f_i^{(k)} + (\frac{1}{3} + \beta - 2\gamma) f_{i+1}^{(k)} + \gamma f_{i+2}^{(k)}, \\ f_{3i+2}^{(k+1)} &= \gamma f_{i-1}^{(k)} + (\frac{1}{3} + \beta - 2\gamma) f_i^{(k)} + (\frac{2}{3} + \gamma - 2\beta) f_{i+1}^{(k)} + \beta f_{i+2}^{(k)}, \end{cases} \tag{4.3}$$

and thus, when $\alpha = \frac{1}{9}$, the rule associated to the new point $f_{3i}^{(k+1)}$ reduces to $f_{3i}^{(k+1)} = f_i^{(k)}$, i.e. the interpolatory rule. As a consequence, the ternary subdivision scheme defined in (4.3) is a combined ternary 4-point scheme.

Remark 4.1 *When $\gamma = 0$, the combined 4-point scheme defined in* (4.3) *reduces to a combined 3-point scheme and, when $\beta = \gamma = 0$, to a combined 2-point scheme.*

In terms of Laurent polynomials, denoting by

$$\tilde{\mathrm{a}}(z) = \frac{(1+z+z^2)^3}{9z^3}$$

the subdivision symbol of the ternary quadratic B-spline scheme, and by

$$\tilde{\mathrm{a}}_0(z) = \frac{1}{9}z^{-3} + \frac{7}{9} + \frac{1}{9}z^3, \qquad \tilde{\mathrm{a}}_1(z) = \frac{1}{3}z^{-2} + \frac{2}{3}z, \qquad \tilde{\mathrm{a}}_2(z) = \frac{2}{3}z^{-1} + \frac{1}{3}z^2,$$

its sub-symbols, we can write the subdivision sub-symbols $\mathrm{a}_{(\alpha,\beta,\gamma),j}(z), j = 0, 1, 2$, associated to the three sub-rules of the scheme in (4.2), as

$$\begin{aligned}
\mathrm{a}_{(\alpha,\beta,\gamma),0}(z) &= \tilde{\mathrm{a}}_0(z) + 9(1-\tilde{\mathrm{a}}_0(z))\alpha, \\
\mathrm{a}_{(\alpha,\beta,\gamma),1}(z) &= \tilde{\mathrm{a}}_1(z) + 9(1-\tilde{\mathrm{a}}_0(z))(-\gamma z^{-2} - \beta z), \\
\mathrm{a}_{(\alpha,\beta,\gamma),2}(z) &= \tilde{\mathrm{a}}_2(z) + 9(1-\tilde{\mathrm{a}}_0(z))(-\beta z^{-1} - \gamma z^2).
\end{aligned}$$

Therefore, the symbol of the subdivision scheme in (4.2) is

$$\begin{aligned}
\mathrm{a}_{\alpha,\beta,\gamma}(z) &= \mathrm{a}_{(\alpha,\beta,\gamma),0}(z) + \mathrm{a}_{(\alpha,\beta,\gamma),1}(z) + \mathrm{a}_{(\alpha,\beta,\gamma),2}(z) \\
&= \tilde{\mathrm{a}}(z) + 9(1-\tilde{\mathrm{a}}_0(z))(-\gamma z^{-2} - \beta z^{-1} + \alpha - \beta z - \gamma z^2) \\
&= \left(\frac{1+z+z^2}{3z}\right)^2 b_{\alpha,\beta,\gamma}(z),
\end{aligned} \tag{4.4}$$

with

$$\begin{aligned}
b_{\alpha,\beta,\gamma}(z) = {} & 9\gamma z^{-3} - 9(2\gamma-\beta)z^{-2} - (9\alpha + 18\beta - 9\gamma - 1)z^{-1} + (18\alpha + 18\beta + 1) \\
& - (9\alpha + 18\beta - 9\gamma - 1)z - 9(2\gamma-\beta)z^2 + 9\gamma z^3.
\end{aligned}$$

As can be easily expected, the choice of the three parameters α, β, γ strongly influences the shape of the limit curves, as illustrated in Figure 4.1. In particular, α controls the interpolation property: for $\alpha = \frac{1}{9}$ the limit curve interpolates the vertices of the starting polyline; if α is larger than $\frac{1}{9}$ the limit curve lies outside the starting polyline; conversely, if α is smaller than $\frac{1}{9}$, the limit curve is inside the starting polyline and the closer α is to $\frac{1}{9}$ the more the limit curve is attracted towards the vertices of $\mathbf{f}^{(0)}$ (Fig. 4.1(a)). On the other hand, β and γ are tension parameters: varying their values the limit curve stays closer or farther to the starting polyline edges. Thus, as well as allowing the user to obtain a family of curves interpolating the vertices of the given polyline (Fig. 4.1(b)-(c)), by choosing in a suitable way the three parameters, the combined scheme allows the user to design also curves that progressively move from the inside to the outside of the control polyline (Fig. 4.1(d)). The combined scheme with symbol in (4.4) also generalizes many ternary schemes appeared in the literature. Precisely, fixing the free parameters α, β, γ as specified below, the combined scheme reduces to these known ternary schemes:

- The approximating linear, quadratic, cubic and quartic B-spline scheme if (α, β, γ) is respectively $(\frac{1}{9}, 0, 0)$, $(0, 0, 0)$, $(-\frac{1}{27}, \frac{1}{27}, 0)$ and $(-\frac{2}{27}, \frac{5}{81}, \frac{1}{81})$;
- The 2-point, 3-point and 4-point scheme in [66, 67] if (α, β, γ) is respectively $\left(\frac{1}{9} - \frac{1}{9}\theta, 0, 0\right)$, $(-\frac{\theta}{27}, \frac{\theta}{27}, 0)$ and $(-\frac{1}{27} - \frac{1}{27}\theta, \frac{1}{27} + \frac{2}{81}\theta, \frac{\theta}{81})$ with θ a free parameter;

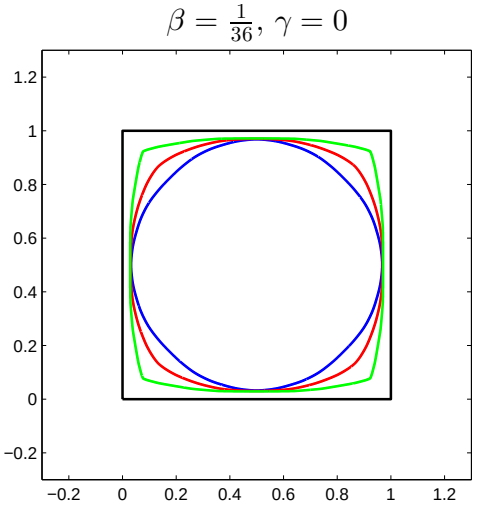

(a) From inner to outer line: $\alpha = -\frac{1}{18}, 0, \frac{1}{18}$.

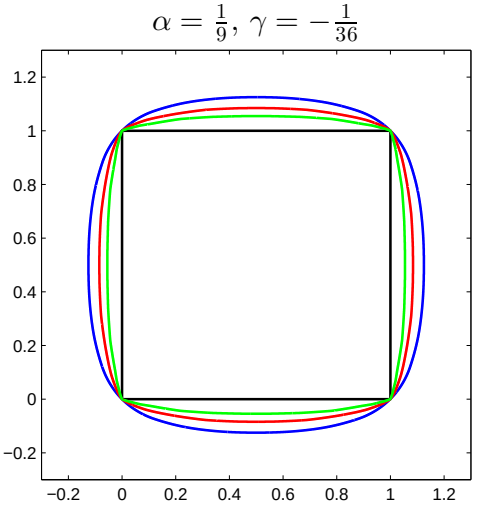

(b) From inner to outer line: $\beta = -\frac{1}{42}, -\frac{1}{20}, -\frac{1}{12}$.

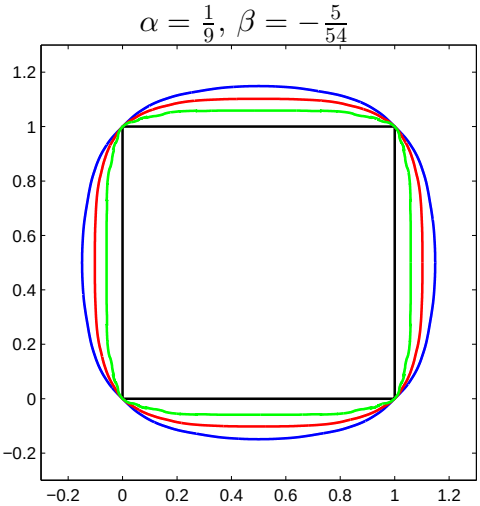

(c) From inner to outer line: $\gamma = \frac{1}{27}, 0, -\frac{1}{27}$.

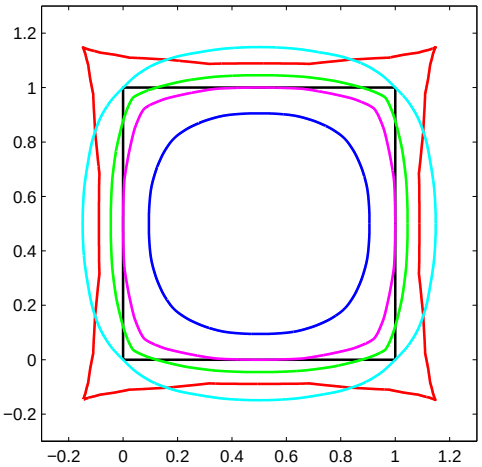

(d) From inner to outer line: $(\alpha, \beta, \gamma) = (-\frac{1}{18}, \frac{1}{20}, \frac{1}{27}), (\frac{1}{20}, 0, 0), (\frac{1}{12}, -\frac{1}{54}, -\frac{1}{42}), (\frac{1}{9}, -\frac{5}{54}, -\frac{1}{27}), (\frac{1}{5}, -\frac{1}{18}, -\frac{1}{30})$.

Figure 4.1: Limit curves obtained by the combined subdivision scheme in (4.3) varying the free parameters α, β, γ.

- The interpolating 3-point scheme in [71] if $(\alpha, \beta, \gamma) = \left(\frac{1}{9}, \mu - \frac{1}{3}, 0\right)$ with μ a free parameter;
- The combined 3-point scheme in [116] if $(\alpha, \beta, \gamma) = \left(\frac{1}{9} - \omega, -\frac{1}{18}, 0\right)$ with ω a free parameter;
- The interpolating 4-point scheme in [72] if $(\alpha, \beta, \gamma) = \left(\frac{1}{9}, -\frac{1}{18} - \frac{1}{6}\nu, -\frac{1}{18} + \frac{1}{6}\nu\right)$ with ν a free parameter;
- The combined 4-point scheme in [109] if $(\alpha, \beta, \gamma) = \left(\frac{1}{9} - \frac{4}{27}\lambda, \frac{1}{27} - \frac{1}{54}(1 - \lambda)(5 +\right.$

$3\eta)$, $-\frac{1}{18}(1-\lambda)(1-\eta)\Big)$ with λ, η free parameters.

In the following section we analyze how the choice of the free parameters α, β, γ influences the C^r convergence of the combined subdivision scheme in (4.4).

4.1.2 C^r convergence of the combined subdivision scheme

As recalled in Proposition 2.16, a necessary condition for C^r convergence is given by the fulfillment of the sum rules of order $r+1$, which means that the univariate ternary schemes having symbol $\mathrm{a}_{\alpha,\beta,\gamma}(z)$, can be written as

$$D^\ell \mathrm{a}_{\alpha,\beta,\gamma}(e^{\frac{2}{3}\pi}) = D^\ell \mathrm{a}_{\alpha,\beta,\gamma}(e^{\frac{4}{3}\pi}) = 0, \quad \text{for all } \ell = 0, \dots, r, \tag{4.5}$$

(see Definition (2.8)).

Proposition 4.2 *The combined ternary subdivision scheme with symbol* $\mathrm{a}_{\alpha,\beta,\gamma}(z)$ *in* (4.4) *satisfies*

- *sum rules of order* 2 *for all* $(\alpha, \beta, \gamma) \in \mathbb{R}^3$*;*
- *sum rules of order* 3 *for all* $(\alpha, \beta, \gamma) \in \mathcal{G}_2 := \{(\alpha, \beta, \gamma) \in \mathbb{R}^3 \ : \ \alpha = -\beta - \gamma\}$*;*
- *sum rules of order* 4 *for all* $(\alpha, \beta, \gamma) \in \mathcal{G}_3 := \Big\{(\alpha, \beta, \gamma) \in \mathbb{R}^3 \ : \ \beta = 2\gamma + \frac{1}{27}, \ \alpha = -\beta - \gamma\Big\}$*;*
- *sum rules of order* 5 *for* $(\alpha, \beta, \gamma) = (-\frac{2}{27}, \frac{5}{81}, \frac{1}{81})$.

Proof: It is easy to see that the symbol $\mathrm{a}_{\alpha,\beta,\gamma}(z)$ in (4.4) satisfies

$$D^\ell \mathrm{a}_{\alpha,\beta,\gamma}(e^{\frac{2}{3}\pi}) = D^\ell \mathrm{a}_{\alpha,\beta,\gamma}(e^{\frac{4}{3}\pi}) = 0, \quad \text{for } \ell = 0, 1,$$

for all $\alpha, \beta, \gamma \in \mathbb{R}$. Moreover, requiring $\alpha = -\beta - \gamma$, the symbol in (4.4) becomes

$$\mathrm{a}_{-\beta-\gamma,\beta,\gamma}(z) = \left(\frac{1+z+z^2}{3z}\right)^3 (27\gamma + 27\beta z - 81\gamma z - 54\beta z^2 + 27\beta z^3 + 108\gamma z^2 - 81\gamma z^3 + 27\gamma z^4 + 3z^2),$$

and it satisfies

$$D^\ell \mathrm{a}_{-\beta-\gamma,\beta,\gamma}(e^{\frac{2}{3}\pi}) = D^\ell \mathrm{a}_{-\beta-\gamma,\beta,\gamma}(e^{\frac{4}{3}\pi}) = 0, \quad \text{for } \ell = 0, 1, 2.$$

In addiction, requiring also $\beta = 2\gamma + \frac{1}{27}$, we obtain the symbol

$$\mathrm{a}_{-\beta-\gamma,2\gamma+\frac{1}{27},\gamma}(z) = \left(\frac{1+z+z^2}{3z}\right)^4 (81\gamma + (3 - 162\gamma)z + 81\gamma z^2),$$

which verifies

$$D^\ell \mathrm{a}_{-\beta-\gamma,2\gamma+\frac{1}{27},\gamma}(e^{\frac{2}{3}\pi}) = D^\ell \mathrm{a}_{-\beta-\gamma,2\gamma+\frac{1}{27},\gamma}(e^{\frac{4}{3}\pi}) = 0, \quad \text{for } \ell = 0, 1, 2, 3.$$

Finally, imposing $\alpha = -\frac{2}{27}, \beta = \frac{5}{81}, \gamma = \frac{1}{81}$, the symbol becomes

$$\mathrm{a}_{-\frac{2}{27},\frac{5}{81},\frac{1}{81}}(z) = 3\left(\frac{1+z+z^2}{3z}\right)^5,$$

from which we have

$$D^\ell \mathrm{a}_{-\frac{2}{27},\frac{5}{81},\frac{1}{81}}(e^{\frac{2}{3}\pi}) = D^\ell \mathrm{a}_{-\frac{2}{27},\frac{5}{81},\frac{1}{81}}(e^{\frac{4}{3}\pi}) = 0, \quad \text{for } \ell = 0,1,2,3,4.$$

■

The conditions provided by Proposition 4.2 are just necessary conditions for C^r continuity, $r = 1,2,3,4$. To find sufficient and necessary conditions, we exploit the joint spectral radius technique explained in Section 2.2.1. In particular, we look for the conditions that have to be satisfied by the parameters of the combined subdivision scheme with symbol in (4.4) to produce limit curves of class C^2 and C^3.

Proposition 4.3 *The combined subdivision scheme with symbol in* (4.4) *produces* C^2 *limit curves if and only if* $(\alpha,\beta,\gamma) \in \mathcal{C}_2$ *where*

$$\mathcal{C}_2 := \left\{(\alpha,\beta,\gamma) \in \mathbb{R}^3,\ -\tfrac{1}{18} < \gamma < \tfrac{1}{9},\ \max\left(2\gamma, 4\gamma - \tfrac{1}{9}\right) < \beta < \min\left(4\gamma + \tfrac{1}{9}, 2\gamma + \tfrac{1}{9}\right),\ \alpha = -\beta - \gamma, \right\}. \tag{4.6}$$

Proof: In view of Proposition 2.16, the combined subdivision scheme is C^2 convergent if and only if it satisfies sum rules of order 3 and the joint spectral radius ρ of the subdivision matrices associated with the 3-rd order difference scheme is in $[1,3)$. From Proposition 4.2 we already know that the subdivision scheme satisfies sum rules of order 3 for all $(\alpha,\beta,\gamma) \in \mathcal{G}_2$. Thus, to identify the complete region of C^2 convergence, the region $\mathcal{G}_2$ has to be made narrower in such a way that $\rho \in [1,3)$. For the computation of ρ, we consider the 3-rd order difference scheme having mask $\mathbf{b}^{[3]} = \{\mathrm{b}_2^{[3]}, \mathrm{b}_1^{[3]}, \mathrm{b}_0^{[3]}, \mathrm{b}_1^{[3]}, \mathrm{b}_2^{[3]}\}$ where

$$\mathrm{b}_0^{[3]} = 108\gamma - 54\beta + 3, \quad \mathrm{b}_1^{[3]} = 27\beta - 81\gamma, \quad \mathrm{b}_2^{[3]} = 27\gamma.$$

The associated matrices $B_\epsilon^{[3]}$, $\epsilon = 0,1,2$, are of the form

$$B_0^{[3]} = \begin{pmatrix} \mathrm{b}_2^{[3]} & \mathrm{b}_1^{[3]} & 0 & 0 \\ 0 & \mathrm{b}_0^{[3]} & 0 & 0 \\ 0 & \mathrm{b}_1^{[3]} & \mathrm{b}_2^{[3]} & 0 \\ 0 & \mathrm{b}_2^{[3]} & \mathrm{b}_1^{[3]} & 0 \end{pmatrix}, \quad B_1^{[3]} = \begin{pmatrix} 0 & \mathrm{b}_0^{[3]} & 0 & 0 \\ 0 & \mathrm{b}_1^{[3]} & \mathrm{b}_2^{[3]} & 0 \\ 0 & \mathrm{b}_2^{[3]} & \mathrm{b}_1^{[3]} & 0 \\ 0 & 0 & \mathrm{b}_0^{[3]} & 0 \end{pmatrix}, \quad B_2^{[3]} = \begin{pmatrix} 0 & \mathrm{b}_1^{[3]} & \mathrm{b}_2^{[3]} & 0 \\ 0 & \mathrm{b}_2^{[3]} & \mathrm{b}_1^{[3]} & 0 \\ 0 & 0 & \mathrm{b}_0^{[3]} & 0 \\ 0 & 0 & \mathrm{b}_1^{[3]} & \mathrm{b}_2^{[3]} \end{pmatrix}.$$

As a consequence,

$$\|B_0^{[3]}\| = \|B_1^{[3]}\| = \|B_2^{[3]}\| = \max\{|\mathrm{b}_0^{[3]}|, |\mathrm{b}_1^{[3]}| + |\mathrm{b}_2^{[3]}|\}$$
$$\rho(B_0^{[3]}) = \rho(B_2^{[3]}) = \max\{|\mathrm{b}_0^{[3]}|, |\mathrm{b}_2^{[3]}|\}, \quad \rho(B_1^{[3]}) = \max\{|\mathrm{b}_1^{[3]} + \mathrm{b}_2^{[3]}|, |\mathrm{b}_1^{[3]} - \mathrm{b}_2^{[3]}|\}.$$

For all $\beta,\gamma \in \mathbb{R}$, $\max\{|\mathrm{b}_1^{[3]} + \mathrm{b}_2^{[3]}|, |\mathrm{b}_1^{[3]} - \mathrm{b}_2^{[3]}|\} = |\mathrm{b}_1^{[3]}| + |\mathrm{b}_2^{[3]}|$. Thus,

$$\max\{\|B_0^{[3]}\|, \|B_1^{[3]}\|, \|B_2^{[3]}\|\} = \max\{|\mathrm{b}_0^{[3]}|, |\mathrm{b}_1^{[3]}| + |\mathrm{b}_2^{[3]}|\} = \max\{\rho(B_0^{[3]}), \rho(B_1^{[3]}), \rho(B_2^{[3]})\},$$

from which follows that $\rho = \max\{|\mathrm{b}_0^{[3]}|, |\mathrm{b}_1^{[3]}| + |\mathrm{b}_2^{[3]}|\}$. At this point it is not difficult to see that $1 \le \rho < 3$ if and only if

$$\left(-\frac{1}{18} < \gamma \le 0 \ \wedge\ 2\gamma < \beta < \frac{36\gamma+1}{9}\right) \quad \vee \quad \left(0 < \gamma \le \frac{1}{18} \ \wedge\ 2\gamma < \beta < \frac{18\gamma+1}{9}\right)$$
$$\vee \quad \left(\frac{1}{18} < \gamma < \frac{1}{9} \ \wedge\ \frac{36\gamma-1}{9} < \beta < \frac{18\gamma+1}{9}\right).$$

Therefore, the combined subdivision scheme is C^2 convergent if and only if (α, β, γ) belongs to the subregion of $\mathcal{G}_2$ that we denoted by $\mathcal{C}_2$ in (4.6). ■

Figure 4.2 shows all possible choices of the free parameters for which the combined scheme in (4.3) is C^2.

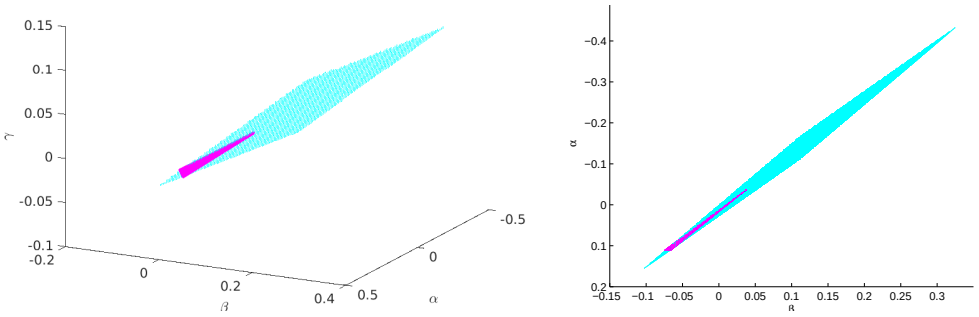

Figure 4.2: The region $\mathcal{C}_2$ (cyan) that guarantees C^2 continuity for the scheme in (4.3) compared to the region in (4.7) (magenta) that was found in [109]: 3D view (left) and top view (right).

Remark 4.4 *The result of Proposition 4.3 provides a great improvement of [109, Theorem 1]. In fact, the parameters constraints given in [109] to guarantee C^2 convergence of the combined scheme, i.e. $(0 \leq \lambda \leq 1) \wedge (\frac{1}{5} < \eta < \frac{1}{3})$, coincide with the subset of $\mathcal{C}_2$ (see Figure 4.2) defined by*

$$\left\{(\alpha, \beta, \gamma) \in \mathbb{R}^3 \ : \ -\frac{2}{45} < \gamma < 0, \ \max\left(3\gamma + \frac{1}{27}, -\gamma - \frac{1}{9}\right) < \beta < \frac{7}{3}\gamma + \frac{1}{27}, \ \alpha = -\beta - \gamma\right\}. \tag{4.7}$$

An additional improvement of our combined ternary scheme over the one proposed in [109] is given by the fact that, if selecting α, β, γ in a suitable way, we can also obtain limit curves of class C^3, as proved in the following.

Proposition 4.5 *The combined subdivision scheme with symbol in* (4.4) *produces C^3 limit curves if and only if $(\alpha, \beta, \gamma) \in \mathcal{C}_3$ where*

$$\mathcal{C}_3 := \left\{(\alpha, \beta, \gamma) \in \mathbb{R}^3 \ : \ 0 < \gamma < \frac{1}{27}, \ \beta = 2\gamma + \frac{1}{27}, \ \alpha = -\beta - \gamma\right\}. \tag{4.8}$$

Proof: In view of Proposition 2.16, the combined subdivision scheme is C^3 convergent if and only if it satisfies sum rules of order 4 and the joint spectral radius ρ of the subdivision matrices associated with the 4-th order difference scheme is in $[1, 3)$. From Proposition 4.2 we already know that the subdivision scheme satisfies sum rules of order 4 for all $(\alpha, \beta, \gamma) \in \mathcal{G}_3$. Thus, to identify the complete region of C^3 convergence, the region $\mathcal{G}_3$ has to be made narrower in such a way that $\rho \in [1, 3)$. For the computation of ρ, we consider the 4-th order

difference scheme having mask $\mathbf{b}^{[4]} = \{81\gamma, 3(1-54\gamma), 81\gamma\}$. The associated matrices $B_\epsilon^{[4]}$, $\epsilon = 0, 1, 2$, are of the form

$$B_0^{[4]} = \begin{pmatrix} 81\gamma & 0 \\ 0 & 81\gamma \end{pmatrix}, \quad B_1^{[4]} = \begin{pmatrix} 0 & 81\gamma \\ 0 & 3(1-54\gamma) \end{pmatrix}, \quad B_2^{[4]} = \begin{pmatrix} 0 & 3(1-54\gamma) \\ 0 & 81\gamma \end{pmatrix}.$$

There follows that

$$\|B_0^{[4]}\| = \rho(B_0^{[4]}) = 81|\gamma|, \quad \|B_1^{[4]}\| = \|B_2^{[4]}\| = \max\{81|\gamma|, 3|1-54\gamma|\},$$
$$\rho(B_1^{[4]}) = 3|1-54\gamma|, \quad \rho(B_2^{[4]}) = 81|\gamma|.$$

As a consequence,

$$\max\{\rho(B_0^{[4]}), \rho(B_1^{[4]}), \rho(B_2^{[4]})\} = \max\{81|\gamma|, 3|1-54\gamma|\} = \max\{\|B_0^{[4]}\|, \|B_1^{[4]}\|, \|B_2^{[4]}\|\},$$

and thus $\rho = \max\{81|\gamma|, 3|1-54\gamma|\}$. It is therefore very easy to see that $1 \leq \rho < 3$ if and only if $0 < \gamma < \frac{1}{27}$. Hence, the combined subdivision scheme is C^3 convergent if and only if (α, β, γ) belongs to the subregion of $\mathcal{G}_3$ that we denoted by $\mathcal{C}_3$ in (4.8). ■

Remark 4.6 *Denoting by* $\mathcal{R}_2 := \left\{(\alpha, \beta, \gamma) \in \mathbb{R}^3 \ : \ \beta = -\gamma - \frac{1}{9}, \ \alpha = \frac{1}{9}\right\}$ *the subregion of* $\mathcal{G}_2$ *where the interpolation condition* $\alpha = \frac{1}{9}$ *is satisfied, we obtain that the complete set of parameters that allow the user to define an interpolatory limit curve of class* C^2*, is*

$$\mathcal{I}_2 := \mathcal{R}_2 \cap \mathcal{C}_2 = \left\{(\alpha, \beta, \gamma) \in \mathbb{R}^3 \ : \ -\frac{2}{45} < \gamma < -\frac{1}{27}, \ \beta = -\gamma - \frac{1}{9}, \ \alpha = \frac{1}{9}\right\}. \tag{4.9}$$

$\mathcal{I}_2$ provides exactly the same range found in [72]. Following a similar reasoning, we can see that the combined ternary 4-point scheme with rules in (4.3) *can not provide C^3 interpolating limit curves. In fact, the parameter setting* $(\alpha, \beta, \gamma) = (\frac{1}{9}, -\frac{5}{81}, -\frac{4}{81})$*, obtained by considering the subregion $\mathcal{R}_3$ of $\mathcal{G}_3$ where the interpolation condition* $\alpha = \frac{1}{9}$ *is satisfied, does not lie in $\mathcal{C}_3$, and so* $\mathcal{R}_3 \cap \mathcal{C}_3 = \emptyset$*. Indeed, for* $(\alpha, \beta, \gamma) \in \mathcal{C}_3$*, the symbol in* (4.4) *assumes the non-interpolatory form*

$$\mathrm{a}_{\alpha,\beta,\gamma}(z) = \left(\frac{z^2 + z + 1}{3z}\right)^4 \left(81\gamma z^{-1} + 3(1-54\gamma) + 81\gamma z\right),$$

with $\gamma \in \left(0, \frac{1}{27}\right)$*. There follows that, for all values of* $\gamma \in (0, \frac{1}{54})$*, the combined ternary 4-point scheme contains as a special subcase the class of C^3 GP ripplets with dilation* 3 *[66, 67].*

Figure 4.3-left shows the shapes of the regions $\mathcal{C}_2$, $\mathcal{C}_3$ and $\mathcal{G}_3$. Figure 4.3-right shows the result highlighted in Remark 4.6.

4.1.3 Positive and negative aspects of combined ternary 4-point scheme

The combined ternary 4-point scheme with symbol in (4.4) is able to produce approximating or interpolatory limit curves with high regularity, but it is not able to reach approximation order 4. In fact, let us consider the C^2 interpolatory counterpart of the combined ternary

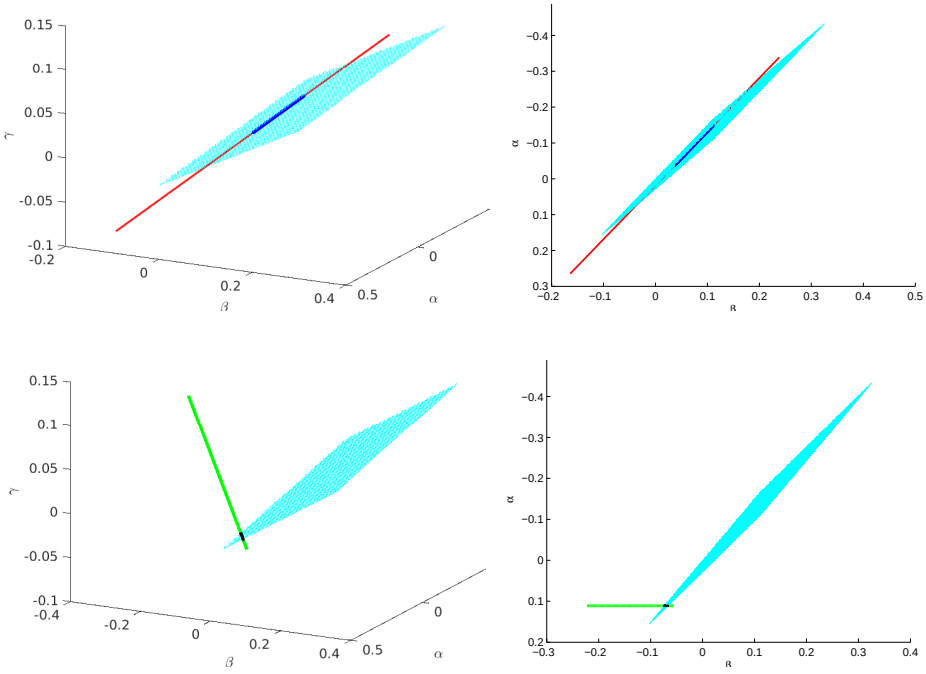

Figure 4.3: Top: the regions $\mathcal{C}_2$ (cyan) and $\mathcal{C}_3$ (blue) together with the region $\mathcal{G}_3$ (red): 3D view (left) and top view (right). Bottom: the regions $\mathcal{C}_2$ (cyan), $\mathcal{R}_2$ (green) and $\mathcal{I}_2$ (black): 3D view (left) and top view (right).

4-point scheme, i.e. we choose $(\alpha, \beta, \gamma) \in \mathcal{I}_2$ in (4.9). The scheme satisfies sum rules of order 3 (see Proposition 4.2), which means that it generates the polynomial space Π_2^1 (see Proposition 2.7). It follows from the interpolation condition and Corollary 2.12 that the scheme also reproduces Π_2^1 and thus, from Proposition 2.10, it has only approximation order 3. We can generalize this reasoning in the following proposition.

Proposition 4.7 *A ternary subdivision scheme defined by refinement rules involving at most 4 points can not produce limit curves with the properties of interpolation, C^2 regularity and approximation order 4.*

Proof: Let us consider a generic subdivision mask of a ternary 4-point scheme, that is

$$\mathbf{a} = [\mathrm{a}_0, \mathrm{a}_1, \mathrm{a}_2, \mathrm{a}_3, \mathrm{a}_4, \mathrm{a}_5, \mathrm{a}_6, \mathrm{a}_7, \mathrm{a}_8, \mathrm{a}_9, \mathrm{a}_{10}, \mathrm{a}_{11}, \mathrm{a}_{12}].$$

We first impose the conditions of interpolation and symmetry

$$\mathbf{a} = [0, \mathrm{a}_1, \mathrm{a}_2, 0, \mathrm{a}_4, \mathrm{a}_5, 1, \mathrm{a}_5, \mathrm{a}_4, 0, \mathrm{a}_2, \mathrm{a}_1, 0].$$

Then, we require the necessary condition for convergence, i.e. the coefficients of the mask sum up to 3, which gives $\mathrm{a}_5 = \frac{1}{2} - \mathrm{a}_1 - \mathrm{a}_2 - \mathrm{a}_4$ and thus

$$\mathbf{a} = \left[0, \mathrm{a}_1, \mathrm{a}_2, 0, \mathrm{a}_4, \frac{1}{2} - \mathrm{a}_1 - \mathrm{a}_2 - \mathrm{a}_4, 1, \frac{1}{2} - \mathrm{a}_1 - \mathrm{a}_2 - \mathrm{a}_4, \mathrm{a}_4, 0, \mathrm{a}_2, \mathrm{a}_1, 0\right].$$

A subdivision scheme with this mask generates and reproduces constants. To require the generation and reproduction of a space of dimension 3, we need to impose two additional conditions which determine, for example, the values of a_4 and a_2. It remains only one free parameter a_1 that could be used to enlarge by one the space of generated and reproduced functions, thus incrementing the approximation order, or to gain C^2 continuity. Thus, a ternary 4-point subdivision scheme can not achieve the properties of interpolation, C^2 regularity and approximation order 4. ■

The existing proposals of ternary interpolatory 4-point schemes either satisfy the properties of C^2 regularity (see [72]) or guarantee approximation order 4 (see [9]). To gain the properties of interpolation, C^2 regularity and approximation order 4 we need to consider a ternary subdivision scheme whose rules involve at least 5 points. We study this kind of schemes in the following section.

4.2 A piecewise uniform interpolatory ternary 5-point scheme

Another important property often required in many applications is the preservation in the limit curves of the convexity of the initial control points. Linear subdivision schemes that are only C^1 cannot preserve convexity in general, thus the class of C^2 subdivision schemes is considered of remarkable importance in the design of application oriented algorithms since it contains the subclass of convexity preserving subdivision schemes. The topic of convexity preservation in subdivision has been subject of extensive studies as proven by the publication of several papers dealing with such a problem (see, e.g., [2, 3, 4, 11, 55, 69, 86, 87, 88, 129, 130]). In particular, Kuijt and van Damme were the first to investigate the convexity-preserving properties of linear interpolatory schemes. Together with Dyn and Levin, in [55] they derived a set of conditions dependent on the initial data, that the parameter of the interpolating 4-point binary scheme presented in [58] has to satisfy to preserve convexity. Then, many years later, after the introduction of the C^2 interpolating 4-point ternary subdivision scheme [72], Cai derived the conditions that the free parameter of such scheme and the vertices of the initial polyline have to satisfy to preserve convexity [11]. However, the ternary 4-point scheme in [72] has only approximation order 3. As proven in Proposition 4.7, to gain approximation order 4 we need to consider ternary subdivision schemes defined by at least five points. In this section, we study the ternary 5-point subdivision scheme recently proposed in [136] and we propose a non-stationary generalization that allows for the reproduction of conic sections.

4.2.1 The interpolatory ternary 5-point subdivision scheme

Given the polyline $\mathbf{f}^{(0)} = \{f_i^{(0)} \in \mathbb{R}^2,\, i \in \mathbb{Z}\}$, the interpolatory 5-point ternary subdivision scheme recursively applies the refinement rules

$$\begin{cases} f_{3i-1}^{(k+1)} &= (w-\frac{4}{81})f_{i-2}^{(k)} + (-4w+\frac{10}{27})f_{i-1}^{(k)} + (6w+\frac{20}{27})f_i^{(k)} + (-4w-\frac{5}{81})f_{i+1}^{(k)} + wf_{i+2}^{(k)}, \\ f_{3i}^{(k+1)} &= f_i^{(k)}, \\ f_{3i+1}^{(k+1)} &= wf_{i-2}^{(k)} + (-4w-\frac{5}{81})f_{i-1}^{(k)} + (6w+\frac{20}{27})f_i^{(k)} + (-4w+\frac{10}{27})f_{i+1}^{(k)} + (w-\frac{4}{81})f_{i+2}^{(k)}, \end{cases} \tag{4.10}$$

where $w \in (\frac{1}{324}, \frac{1}{162})$ to achieve the construction of C^2 limit curves (see [136, Section 3.C]). From the refinement rules in (4.10) we can easily write the mask of the subdivision scheme

as

$$\begin{aligned} T_{5,w} = \quad & \Big[w,\, 0,\, w-\frac{4}{81},\, -4w-\frac{5}{81},\, 0,\, -4w+\frac{10}{27},\, 6w+\frac{20}{27},\, 1,\\ & 6w+\frac{20}{27},\, -4w+\frac{10}{27},\, 0,\, -4w-\frac{5}{81},\, w-\frac{4}{81},\, 0,\, w\Big], \end{aligned} \tag{4.11}$$

and hence the associated subdivision symbol is

$$\begin{aligned} T_{5,w}(z) = \quad & \frac{(z^2+z+1)^4}{27z^7}\bigg(27wz^6-108wz^5+\left(189w-\frac{4}{3}\right)z^4+\left(\frac{11}{3}-216w\right)z^3\\ & +\left(189w-\frac{4}{3}\right)z^2-108wz+27w\bigg). \end{aligned} \tag{4.12}$$

Proposition 4.8 *The ternary interpolatory 5-point subdivision scheme with symbol in* (4.12) *reproduces polynomials up to degree 3 with respect to the parametrization* $\{\mathbf{T}^{(k)}, k \in \mathbb{N}_0\}$ *in* (2.6) *with* $\tau = 0$ *for any choice of* $w \in \mathbb{R}$ *that guarantees the convergence.*

Proof: It is easy to see that for any $w \in \mathbb{R}$,

$$D^\ell T_{5,w}(e^{\frac{2\pi \mathrm{i}}{3}}) = D^\ell T_{5,w}(e^{\frac{4\pi \mathrm{i}}{3}}) = 0, \quad \forall\, \ell = 0, \ldots, 3,$$

thus recalling Proposition 2.7, the ternary interpolatory 5-point subdivision scheme with symbol in (4.12) generates Π_3^1. Moreover, since the scheme is interpolatory, from Corollary 2.12 we also have the reproduction of Π_3^1. ■

From Proposition 2.10, it also follows that the ternary interpolatory 5-point subdivision scheme with symbol in (4.12) has approximation order 4.
Following the procedure shown in [136, Section 3.C], the expression of the subdivision symbol $T_{5,w}(z)$ can be also rewritten in terms of Lagrange fundamental polynomials for interpolation. Precisely, we denote by $\mathcal{L}^0_{j,[m,m+d]}(x)$, $m \in \mathbb{Z}, d \in \mathbb{N}$, the j-th Lagrange fundamental polynomial of the space $\Pi_d^1 := span\{1, x, \ldots, x^d\}$, defined by the nodes $m, m+1, \ldots, m+d$, that is

$$\mathcal{L}^0_{j,[m,m+d]}(x) := \prod_{\substack{i=m \\ i\neq j}}^{m+d} \frac{x-i}{j-i}, \quad j = m, \ldots, m+d. \tag{4.13}$$

In particular, we consider

$$\begin{aligned} &\mathcal{L}^0_{-2,[-2,1]}(x) := -\tfrac{(x+1)x(x-1)}{6}, && \mathcal{L}^0_{-1,[-1,2]}(x) := -\tfrac{x(x-1)(x-2)}{6},\\ &\mathcal{L}^0_{-1,[-2,1]}(x) := \tfrac{(x+2)x(x-1)}{2}, && \mathcal{L}^0_{0,[-1,2]}(x) := \tfrac{(x+1)(x-1)(x-2)}{2},\\ &\mathcal{L}^0_{0,[-2,1]}(x) := -\tfrac{(x+2)(x+1)(x-1)}{2}, \quad \text{and} && \mathcal{L}^0_{1,[-1,2]}(x) := -\tfrac{x(x+1)(x-2)}{2},\\ &\mathcal{L}^0_{1,[-2,1]}(x) := \tfrac{(x+2)(x+1)x}{6}, && \mathcal{L}^0_{2,[-1,2]}(x) := \tfrac{x(x-1)(x+1)}{6}, \end{aligned} \tag{4.14}$$

i.e. the Lagrange fundamental polynomials of the space Π_3^1 defined by the nodes $-2,-1,0,1$ and $-1,0,1,2$, respectively, and

$$\begin{aligned}
\mathcal{L}^0_{-2,[-2,2]}(x) &:= -\tfrac{x(x-1)(x-2)(x+1)}{24},\\
\mathcal{L}^0_{-1,[-2,2]}(x) &:= -\tfrac{x(x-1)(x-2)(x+2)}{6},\\
\mathcal{L}^0_{0,[-2,2]}(x) &:= \tfrac{(x-1)(x-2)(x+2)(x+1)}{4},\\
\mathcal{L}^0_{1,[-2,2]}(x) &:= -\tfrac{x(x-2)(x+2)(x+1)}{6},\\
\mathcal{L}^0_{2,[-2,2]}(x) &:= \tfrac{x(x-1)(x+2)(x+1)}{24},
\end{aligned} \tag{4.15}$$

denoting the Lagrange fundamental polynomials of the space Π_4^1 corresponding to the nodes $-2,-1,0,1,2$. We rewrite the subdivision symbol $T_{5,w}(z)$ as

$$T_{5,w}(z) = T_{5,0}(z) + w\,N(z), \qquad w \in \mathbb{R}, \tag{4.16}$$

with

$$T_{5,0}(z) = \frac{(z^2+z+1)^4}{27z^4}\left(-\frac{4}{3}z + \frac{11}{3} - \frac{4}{3}z^{-1}\right) \quad \text{and} \quad N(z) = z^{-7}(z^2+1)(z^3-1)^4. \tag{4.17}$$

The Laurent polynomial $T_{5,0}(z)$ in (4.17) can thus be rewritten in the form

$$T_{5,0}(z) = z^{-1}\left(\sum_{j=-2}^{1}\mathcal{L}^0_{j,[-2,1]}\left(-\frac{1}{3}\right)z^{-3j}\right) + 1 + z\left(\sum_{j=-1}^{2}\mathcal{L}^0_{j,[-1,2]}\left(\frac{1}{3}\right)z^{-3j}\right). \tag{4.18}$$

Moreover, in light of the fact that all functions in Π_3^1 satisfy $D^4\cdot = 0$, we can also write

$$N(z) = (z^{-1}+z)\sum_{j=-2}^{2} h_j\, z^{3j} \quad \text{with} \quad h_j = D^4\mathcal{L}^0_{j,[-2,2]} = (-1)^j\binom{4}{j+2}, \quad j=-2,\dots,2. \tag{4.19}$$

Summarizing, the interpolatory ternary 5-point scheme is able to produce limit curves of class C^2 and to reproduce Π_3^1, thus gaining approximation order 4. The property of convexity preservation is analyzed in the following.

Convexity preservation of the interpolatory ternary 5-point subdivision scheme

First of all, we recall that a subdivision scheme is said to satisfy the property of strict convexity preservation if, starting from a strictly convex control polyline, the limit curves produced by the scheme preserve the strict convexity of the initial data. For an interpolating subdivision scheme, the property of strict convexity preservation is achieved by simply requiring that, at each refinement level, the second-order divided differences of the scheme are all strictly positive. Namely, for a given k-th level sequence of real values $\{p_j^{(k)} \in \mathbb{R}, j \in \mathbb{Z}\}$ placed at regularly spaced parameter values $x_j^{(k)} = \frac{j}{3^k}$, $j \in \mathbb{Z}$, we denote by

$$d_j^{(k)} := \frac{1}{x_{j+1}^{(k)} - x_{j-1}^{(k)}}\left(\frac{p_{j+1}^{(k)} - p_j^{(k)}}{x_{j+1}^{(k)} - x_j^{(k)}} - \frac{p_j^{(k)} - p_{j-1}^{(k)}}{x_j^{(k)} - x_{j-1}^{(k)}}\right) = \frac{3^{2k}}{2}\,(p_{j-1}^{(k)} - 2p_j^{(k)} + p_{j+1}^{(k)}), \tag{4.20}$$

the k-th level second-order divided differences of the scheme, and we require that

$$d_j^{(k)} > 0, \quad \forall j \in \mathbb{Z},\ \forall k \in \mathbb{N}_0 := \mathbb{N} \cup \{0\}. \tag{4.21}$$

To guarantee the fulfillment of (4.21), suitable constraints on the initial control points $\mathbf{f}^{(0)}$ have to be assumed. In fact, without any constraints on the initial control points, the property of strict convexity preservation does not hold. To provide a counterexample of this fact, we can consider the strictly convex 2D control polyline defined by the vertices

$$f_{i-2}^{(0)} = (1, 0.9826), \quad f_{i-1}^{(0)} = (1.1, 0.491), \quad f_i^{(0)} = (2.01, 0.28),$$
$$f_{i+1}^{(0)} = (3, 0.1486), \quad f_{i+2}^{(0)} = (4.8, 0.3927),$$

see Figure 4.4. If for the two sequences {1, 1.1, 2.01, 3, 4.8} and {0.9826, 0.491, 0.28, 0.1486, 0.3927} (obtained by considering the components of the 2D points separately) we compute the second-order divided differences $d_j^{(0)}$, $j = i-1, i, i+1$, using the formulas in (4.20), we find that in both cases $d_{i-1}^{(0)}, d_i^{(0)}, d_{i+1}^{(0)}$ are strictly positive. However, after applying the refinement rules in (4.10) with $w = \frac{1}{200}$ (such that $w \in (\frac{1}{324}, \frac{1}{162})$) we get

$$f_{3i-2}^{(1)} = (1.3427, 0.3921), \quad f_{3i-1}^{(1)} = (1.669, 0.334), \quad f_{3i}^{(1)} = (2.01, 0.28),$$
$$f_{3i+1}^{(1)} = (2.3024, 0.2152), \quad f_{3i+2}^{(1)} = (2.5903, 0.1595).$$

Thus, when using the refined sequence {1.3427, 1.669, 2.01, 2.3024, 2.5903}, given by the first components of the obtained 2D points, $d_{3i}^{(1)}$ and $d_{3i+1}^{(1)}$ are not positive anymore, and also $d_{3i}^{(1)} < 0$ when using the refined sequence {0.3921, 0.334, 0.28, 0.2152, 0.1595} given by the second components.

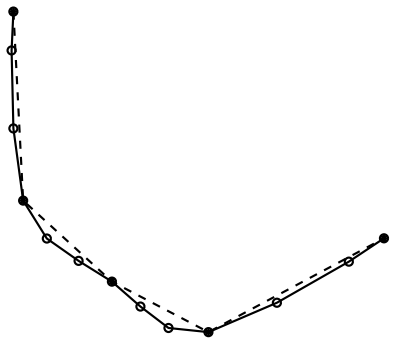

Figure 4.4: The given strictly convex control polyline $\mathbf{f}^{(0)}$ (dotted line) and the not strictly convex control polyline $\mathbf{f}^{(1)}$ obtained after one application of the subdivision rules in (4.10) with $w = \frac{1}{200}$ (solid line).

The problem of identifying under which constraints on the configuration of the initial data, a set of refinement rules with a free parameter w can achieve the property of strict convexity preservation, has been already faced by several authors (see, e.g., [11, 129]). The general idea pursued in these papers consists in investigating the existence of a constant $\lambda > 1$ (which

depends on the selected value of the free parameter w) such that, if assuming $d_i^{(0)} > 0$ for all $i \in \mathbb{Z}$, it is verified that

$$\max_i \left\{ \frac{d_{i+1}^{(0)}}{d_i^{(0)}}, \frac{d_i^{(0)}}{d_{i+1}^{(0)}} \right\} < \lambda.$$

Moreover, the selected value of λ has to guarantee also that, for all $k \in \mathbb{N}$,

$$d_i^{(k)} > 0, \quad \forall\, i \in \mathbb{Z} \qquad \text{and} \qquad \max_i \left\{ \frac{d_{i+1}^{(k)}}{d_i^{(k)}}, \frac{d_i^{(k)}}{d_{i+1}^{(k)}} \right\} < \lambda.$$

Instead of using the condition $\max_i \left\{ \frac{d_{i+1}^{(0)}}{d_i^{(0)}}, \frac{d_i^{(0)}}{d_{i+1}^{(0)}} \right\} < \lambda$, in [100, Theorem 5.1] Mustafa et al. proposed to use a different constraint, which unfortunately turns out to be not correct. In fact, after introducing the notation $p_i^{(0)} := \frac{d_{i+1}^{(0)}}{d_i^{(0)}}$ and $q_i^{(0)} := \frac{d_i^{(0)}}{d_{i+1}^{(0)}} = \frac{1}{p_i^{(0)}}$ with $d_i^{(0)}$ and $d_{i+1}^{(0)}$ defined according to (4.20), they require the initial data to satisfy the condition $r^{(0)} := \min_i \{p_i^{(0)}, q_i^{(0)}\} > \lambda$, which is totally nonsense. To understand why it is incorrect, let us denote by $\bar{i}$ the index for which this minimum is realized and suppose that $r^{(0)} = p_{\bar{i}}^{(0)} > \lambda > 1$. Thus $q_{\bar{i}}^{(0)} = \frac{1}{p_{\bar{i}}^{(0)}} < 1$. It follows that $q_{\bar{i}}^{(0)} < p_{\bar{i}}^{(0)}$, which is in contradiction with $r^{(0)} = \min_i \{p_i^{(0)}, q_i^{(0)}\} = p_{\bar{i}}^{(0)}$.

To derive a correct condition that can guarantee the convexity preservation property of the interpolating 5-point ternary scheme in (4.10), we start writing the refinement rules for the second-order divided difference scheme as

$$\begin{cases} d_{3i-1}^{(k+1)} &= a_1 d_{i-2}^{(k)} + a_4 d_{i-1}^{(k)} + a_5 d_i^{(k)} + a_2 d_{i+1}^{(k)}, \\ d_{3i}^{(k+1)} &= a_3 d_{i-1}^{(k)} + a_6 d_i^{(k)} + a_3 d_{i+1}^{(k)}, \\ d_{3i+1}^{(k+1)} &= a_2 d_{i-1}^{(k)} + a_5 d_i^{(k)} + a_4 d_{i+1}^{(k)} + a_1 d_{i+2}^{(k)}, \end{cases} \tag{4.22}$$

where

$$\begin{array}{llllll} a_1 = 9w, & a_2 = -18w, & a_3 = 18w - \frac{4}{9}, \\ a_4 = \frac{1}{3} - 36w, & a_5 = \frac{2}{3} + 45w, & a_6 = \frac{17}{9} - 36w. \end{array} \tag{4.23}$$

Exploiting (4.22), we can reformulate the conditions yielding the preservation of strict convexity as $d_{3i-1}^{(k+1)}, d_{3i}^{(k+1)}, d_{3i+1}^{(k+1)} > 0$ provided that $d_i^{(k)} > 0$ for all $i \in \mathbb{Z}$. Thus, we proceed by proving the following result.

Proposition 4.9 *Let* $p_i^{(k)} := \frac{d_{i+1}^{(k)}}{d_i^{(k)}}$, $q_i^{(k)} := \frac{d_i^{(k)}}{d_{i+1}^{(k)}} = \frac{1}{p_i^{(k)}}$ *and* $r^{(k)} := \max_i \{p_i^{(k)}, q_i^{(k)}\}$. *If the initial polyline is strictly convex, i.e.* $d_j^{(0)} > 0$ *for all* j, *then for all* $w \in \left(\frac{1}{324}, \frac{1}{162}\right)$ *and* $r^{(0)} < \lambda := -\frac{405w+6}{243w-8}$, *the ternary interpolatory 5-point scheme with refinement rules in* (4.10) *preserves the convexity of the given data.*

To simplify the proof of Proposition 4.9 as much as possible, we first introduce two auxiliary lemmas in which we provide some inequalities that will be used to show the fulfillment of condition (4.21). The proofs of these lemmas are skipped since quite straightforward.

Lemma 4.10 *For all* $w \in \left(\frac{1}{324}, \frac{1}{162}\right)$ *the coefficients in* (4.23) *satisfy the inequalities*

$$a_1 > 0, \quad a_2 < 0, \quad a_3 < 0, \quad a_4 > 0, \quad a_5 > 0, \quad a_6 > 0.$$

Lemma 4.11 *Let* a_i, $i = 1, ..., 6$ *denote the coefficients defined in* (4.23) *and* λ *the value in Proposition 4.9. Assuming* $w \in \left(\frac{1}{324}, \frac{1}{162}\right)$ *it follows immediately that* $\lambda \in (1, \frac{17}{13})$. *Moreover, for all* $w \in \left(\frac{1}{324}, \frac{1}{162}\right)$ *the inequalities*

(i) $a_6 + 2a_3\lambda > 0$;
(ii) $\frac{a_1}{\lambda^2} + \frac{a_4}{\lambda} + a_5 + a_2\lambda > 0$;
(iii) $\frac{a_1+a_5}{\lambda} + a_4 + a_2\lambda^2 > 0$;
(iv) $a_3 - a_2\lambda < 0$;
(v) $\frac{2a_3-a_1}{\lambda} + a_6 - a_4 - a_2 - a_5\lambda < 0$;
(vi) $a_2 - a_3\lambda > 0$;
(vii) $a_4 + (a_1 - a_5)\lambda - a_2\lambda^2 < 0$;
$(viii)$ $\frac{a_2+a_4}{\lambda} - (a_2 + a_4)\lambda < 0$;
(ix) $\frac{a_2}{\lambda} - (a_1 - a_5) - a_4\lambda > 0$;
(x) $a_5 + (a_2 - a_6)\lambda - a_3\lambda^2 < 0$;
(xi) $\frac{a_3}{\lambda} - (a_2 - a_6) - a_5\lambda > 0$;
(xii) $a_3 - a_1 - a_4\lambda < 0$;
$(xiii)$ $a_4 + a_1\lambda - a_3\lambda > 0$;
(xiv) $a_2 - a_1\lambda < 0$;
(xv) $a_1 - a_2\lambda > 0$

are also fulfilled.

Proof of Proposition 4.9 We start by observing that, from the definition of $p_i^{(k)}, q_i^{(k)}$ and $r_i^{(k)}$, we immediately have $r^{(0)} < \lambda$ and $r^{(0)} > \frac{1}{\lambda}$ as well as $p_i^{(0)}, q_i^{(0)} < \lambda$ and $-p_i^{(0)}, -q_i^{(0)} < -\frac{1}{\lambda}$. Then, we continue by showing via mathematical induction that, for all $k \in \mathbb{N}$, $d_i^{(k)} > 0$ for all $i \in \mathbb{Z}$ and $r^{(k)} < \lambda$. Therefore, assuming $d_i^{(k)} > 0$ for all $i \in \mathbb{Z}$ and $r^{(k)} < \lambda$, the proof consists in showing that $d_{3i+j}^{(k+1)} > 0$ for $j = 0, 1, 2$ and $r^{(k+1)} < \lambda$, namely $p_{3i+j}^{(k+1)}, q_{3i+j}^{(k+1)} < \lambda$ for $j = 0, 1, 2$.
Exploiting the inequalities $-p_i^{(k)}, -q_i^{(k)} > -\lambda$, in view of Lemma 4.10 and Lemma 4.11 (i), from (4.22) we obtain

$$d_{3i}^{(k+1)} = d_i^{(k)} \left(a_6 - a_3(-q_{i-1}^{(k)} - p_i^{(k)})\right) > d_i^{(k)}(a_6 + 2a_3\lambda) > 0.$$

Analogously, from (4.22) and Lemma 4.11 (ii) we also get

$$d_{3i+1}^{(k+1)} = d_i^{(k)} \left(-a_2(-q_{i-1}^{(k)}) + a_5 + a_4 p_i^{(k)} + a_1 p_i^{(k)} p_{i+1}^{(k)}\right) > d_i^{(k)} \left(\frac{a_1}{\lambda^2} + \frac{a_4}{\lambda} + a_5 + a_2\lambda\right) > 0,$$

and, additionally, using condition (iii) the first equation in (4.22) yields

$$d_{3i+2}^{(k+1)} = d_i^{(k)} \left(a_1 q_{i-1}^{(k)} + a_4 + a_5 p_i^{(k)} + a_2 p_i^{(k)} p_{i+1}^{(k)}\right) > d_i^{(k)} \left(\frac{a_1 + a_5}{\lambda} + a_4 + a_2\lambda^2\right) > 0.$$

Now we prove that $r^{(k+1)} < \lambda$. Since

$$\begin{aligned} d_{3i}^{(k+1)} - \lambda d_{3i+1}^{(k+1)} &= d_i^{(k)} \left(a_3 q_{i-1}^{(k)} + a_6 + a_3 p_i^{(k)} - a_2\lambda q_{i-1}^{(k)} - a_5\lambda - a_4\lambda p_i^{(k)} + a_1\lambda p_i^{(k)}(-p_{i+1}^{(k)})\right) \\ &< d_i^{(k)} \left(a_6 - a_5\lambda - (a_3 - a_2\lambda)(-q_{i-1}^{(k)}) - (a_3 - a_1 - a_4\lambda)(-p_i^{(k)})\right) \\ &< d_i^{(k)} \left(\tfrac{2a_3-a_1}{\lambda} + a_6 - a_4 - a_2 - a_5\lambda\right), \end{aligned}$$

then, in view of Lemma 4.10 and Lemma 4.11 (iv),(v),(xii) we have $d_{3i}^{(k+1)} - \lambda d_{3i+1}^{(k+1)} < 0$, i.e. $q_{3i}^{(k+1)} < \lambda$. In a similar way, considering Lemma 4.10 and Lemma 4.11 (vi),$(xiii)$, we get

$$\begin{aligned} d_{3i+1}^{(k+1)} - \lambda d_{3i}^{(k+1)} &= d_i^{(k)} \left(a_2 q_{i-1}^{(k)} + a_5 + a_4 p_i^{(k)} + a_1 p_i^{(k)} p_{i+1}^{(k)} - a_3 \lambda q_{i-1}^{(k)} - a_6 \lambda - a_3 \lambda p_i^{(k)} \right) \\ &< d_i^{(k)} \left(a_5 - a_6 \lambda + (a_2 - a_3 \lambda) q_{i-1}^{(k)} + (a_4 + a_1 \lambda - a_3 \lambda) p_i^{(k)} \right) \\ &< d_i^{(k)} \left(a_5 + (a_2 + a_4 - a_6) \lambda + (a_1 - 2a_3) \lambda^2 \right) \\ &= d_i^{(k)} \tfrac{1}{9} (\lambda - 1) \left((8 - 243w) \lambda - 405w - 6 \right) = 0 \end{aligned}$$

due to the definition of λ. Thus $d_{3i+1}^{(k+1)} - \lambda d_{3i}^{(k+1)} < 0$, i.e. $p_{3i}^{(k+1)} < \lambda$.
Moreover, using Lemma 4.10 and Lemma 4.11 (vii),$(viii)$,(xiv), we obtain

$$\begin{aligned} d_{3i+1}^{(k+1)} - \lambda d_{3i+2}^{(k+1)} &= d_i^{(k)} (a_2 q_{i-1}^{(k)} + a_5 + a_4 p_i^{(k)} + a_1 p_i^{(k)} p_{i+1}^{(k)} - a_1 \lambda q_{i-1}^{(k)} - a_4 \lambda - a_5 \lambda p_i^{(k)} \\ &- a_2 \lambda p_i^{(k)} p_{i+1}^{(k)}) \\ &< d_i^{(k)} (a_5 - a_4 \lambda - (a_2 - a_1 \lambda)(-q_{i-1}^{(k)}) - (a_4 + a_1 \lambda - a_5 \lambda \\ &- a_2 \lambda^2)(-p_i^{(k)})) \\ &< d_i^{(k)} \left(\tfrac{a_2}{\lambda} + \tfrac{a_4}{\lambda} - a_2 \lambda - a_4 \lambda \right), \end{aligned}$$

hence $d_{3i+1}^{(k+1)} - \lambda d_{3i+2}^{(k+1)} < 0$, i.e. $q_{3i+1}^{(k+1)} < \lambda$.
Analogously, considering Lemma 4.10 and Lemma 4.11 $(viii)$,(ix),(xv), we have

$$\begin{aligned} d_{3i+2}^{(k+1)} - \lambda d_{3i+1}^{(k+1)} &= d_i^{(k)} \Big(a_1 q_{i-1}^{(k)} + a_4 + a_5 p_i^{(k)} - a_2 p_i^{(k)} (-p_{i+1}^{(k)}) - a_2 \lambda q_{i-1}^{(k)} - a_5 \lambda - a_4 \lambda p_i^{(k)} \\ &+ a_1 \lambda p_i^{(k)} (-p_{i+1}^{(k)}) \Big) \\ &< d_i^{(k)} \left(a_4 - a_5 \lambda + (a_1 - a_2 \lambda) q_{i-1}^{(k)} + (\tfrac{a_2}{\lambda} - a_1 + a_5 - a_4 \lambda) p_i^{(k)} \right) \\ &< d_i^{(k)} \left(a_2 + a_4 - a_2 \lambda^2 - a_4 \lambda^2 \right), \end{aligned}$$

so $d_{3i+2}^{(k+1)} - \lambda d_{3i+1}^{(k+1)} < 0$, i.e. $p_{3i+1}^{(k+1)} < \lambda$.
Finally, using Lemma 4.10 as well as Lemma 4.11 (vi) and (x), we can write

$$\begin{aligned} d_{3i+2}^{(k+1)} - \lambda d_{3i+3}^{(k+1)} &= d_i^{(k)} \left(a_1 q_{i-1}^{(k)} + a_4 + a_5 p_i^{(k)} + a_2 p_i^{(k)} p_{i+1}^{(k)} - a_3 \lambda - a_6 \lambda p_i^{(k)} - a_3 \lambda p_i^{(k)} p_{i+1}^{(k)} \right) \\ &< d_i^{(k)} \left(a_4 + (a_1 - a_3) \lambda + (a_5 - a_6 \lambda) p_i^{(k)} + (a_2 - a_3 \lambda) p_i^{(k)} p_{i+1}^{(k)} \right) \\ &< d_i^{(k)} \left(a_4 + (a_1 - a_3) \lambda - (a_5 - a_6 \lambda + a_2 \lambda - a_3 \lambda^2)(-p_i^{(k)}) \right) \\ &< d_i^{(k)} \left(\tfrac{a_5}{\lambda} + a_2 + a_4 - a_6 + (a_1 - 2a_3) \lambda \right) \\ &= d_i^{(k)} \tfrac{1}{\lambda} \tfrac{1}{9} (\lambda - 1) \left((8 - 243w) \lambda - 405w - 6 \right) = 0 \end{aligned}$$

due to the definition of λ. Hence, the latter yields $d_{3i+2}^{(k+1)} - \lambda d_{3i+3}^{(k+1)} < 0$, i.e. $q_{3i+2}^{(k+1)} < \lambda$.
To conclude the proof we consider Lemma 4.10 together with Lemma 4.11 (iv),(v) and (xi), from which we obtain

$$\begin{aligned} d_{3i+3}^{(k+1)} - \lambda d_{3i+2}^{(k+1)} &= d_i^{(k)} \left(a_3 + a_6 p_i^{(k)} + a_3 p_i^{(k)} p_{i+1}^{(k)} - a_1 \lambda q_{i-1}^{(k)} - a_4 \lambda - a_5 \lambda p_i^{(k)} - a_2 \lambda p_i^{(k)} p_{i+1}^{(k)} \right) \\ &< d_i^{(k)} \left(a_3 - a_1 - a_4 \lambda + (a_6 - a_5 \lambda) p_i^{(k)} - (a_3 - a_2 \lambda) p_i^{(k)} (-p_{i+1}^{(k)}) \right) \\ &< d_i^{(k)} \left(a_3 - a_1 - a_4 \lambda + (\tfrac{a_3}{\lambda} - a_2 + a_6 - a_5 \lambda) p_i^{(k)} \right) \\ &< d_i^{(k)} \left(2a_3 - a_1 + (a_6 - a_4 - a_2) \lambda - a_5 \lambda^2 \right), \end{aligned}$$

so that $d_{3i+3}^{(k+1)} - \lambda d_{3i+2}^{(k+1)} < 0$, i.e. $p_{3i+2}^{(k+1)} < \lambda$. ■

Figure 4.5 shows C^2 limit curves obtained for different values of $w \in \left(\frac{1}{324}, \frac{1}{162}\right)$, when applying the ternary interpolatory 5-point scheme to initial convex control polylines satisfying the condition in Proposition 4.9.

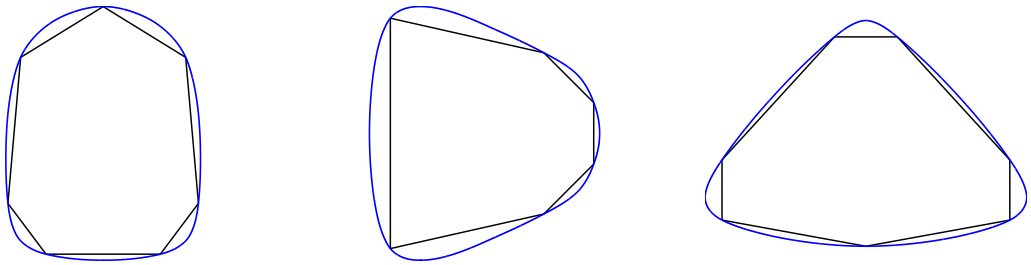

Figure 4.5: C^2 limit curves obtained by applying the ternary interpolatory 5-point scheme in (4.10) with $w = \frac{5}{867}$ (left), $w = \frac{3}{500}$ (center), $w = \frac{1}{200}$ (right), to initial convex data that satisfy the condition in Proposition 4.9.

4.2.2 A non-stationary extension of the interpolatory 5-point ternary subdivision scheme

As already recalled, the use of non-stationary refinement rules let us gain a tension control parameter and the capability of reproducing not only polynomials but also exponential polynomials, that is conic sections. To this purpose, in this section we propose a non-stationary generalization of the interpolating 5-point ternary subdivision scheme in (4.10).

To construct the symbol of the non-stationary interpolatory ternary 5-point scheme we follow the same procedure shown for its stationary counterpart (see equations (4.18)-(4.19)). First, when replacing Π_d^1 by the space of exponential polynomials $\mathcal{W}_{d-2}^1$ in (3.9) represented by

$$\mathcal{W}_{d-2}^1 = span\{1, x, \ldots, x^{d-2}, e^{tx}, e^{-tx}\}, \qquad t \in \left[0, \frac{3}{2}\pi\right) \cup \mathrm{i}\mathbb{R}^+,$$

we denote by $\mathcal{L}_{j,[m,m+d]}^t(x)$, $j = m, \ldots, m+d$, the exponential polynomial of the form

$$\mathcal{L}_{j,[m,m+d]}^t(x) := \sum_{i=0}^{d-2} \beta_{j,i}^t \, x^i + \beta_{j,d-1}^t \, e^{tx} + \beta_{j,d}^t \, e^{-tx}, \tag{4.24}$$

whose unknown coefficients $\beta_{j,i}^t$, $i = 0, ..., d$ are uniquely determined to satisfy the $d+1$ conditions

$$\mathcal{L}_{j,[m,m+d]}^t(i) = \delta_{j,i}$$

with $\delta_{j,i}$ denoting the Kronecker delta. It is worth emphasizing that, for all $m \in \mathbb{Z}$ and $d \in \mathbb{N}$, the exponential polynomial $\mathcal{L}_{j,[m,m+d]}^t(x)$ converges to the degree-d polynomial $\mathcal{L}_{j,[m,m+d]}^0(x)$

when $t \to 0$.
In particular, we consider

$$\begin{aligned}
\mathcal{L}^t_{-2,[-2,1]}(x) &:= -\frac{e^{t(2+x)} - e^{t(2-x)} - x\, e^t(e^{2t}-1)}{(e^t-1)^3\,(e^t+1)},\\
\mathcal{L}^t_{-1,[-2,1]}(x) &:= -\frac{x\,(e^{2t}+e^t+1)+e^t}{(e^t-1)^2} + \frac{e^{t(2+x)}\,(e^t+2) - e^{t(2-x)}(e^{-t}+2)}{(e^t-1)^3\,(e^t+1)},\\
\mathcal{L}^t_{0,[-2,1]}(x) &:= \frac{x\,(e^{2t}+e^t+1)+e^{2t}+1}{(e^t-1)^2} + \frac{e^{t(1-x)}(e^t+2) - e^{t(3+x)}(e^{-t}+2)}{(e^t-1)^3\,(e^t+1)},\\
\mathcal{L}^t_{1,[-2,1]}(x) &:= \frac{e^{t(3+x)} - e^{t(1-x)} - (1+x)\,e^t\,(e^{2t}-1)}{(e^t-1)^3\,(e^t+1)},
\end{aligned} \tag{4.25}$$

and

$$\begin{aligned}
\mathcal{L}^t_{-1,[-1,2]}(x) &:= -\frac{e^{t(1+x)} - e^{t(3-x)} + (1-x)\,e^t(e^{2t}-1)}{(e^t-1)^3(e^t+1)},\\
\mathcal{L}^t_{0,[-1,2]}(x) &:= -\frac{x\,(e^{2t}+e^t+1) - e^{2t} - 1}{(e^t-1)^2} + \frac{e^{t(1+x)}(e^t+2) - e^{t(3-x)}(e^{-t}+2)}{(e^t-1)^3(e^t+1)},\\
\mathcal{L}^t_{1,[-1,2]}(x) &:= \frac{x\,(e^{2t}+e^t+1) - e^t}{(e^t-1)^2} + \frac{e^{t(2-x)}(e^t+2) - e^{t(2+x)}(e^{-t}+2)}{(e^t-1)^3(e^t+1)},\\
\mathcal{L}^t_{2,[-1,2]}(x) &:= \frac{e^{t(2+x)} - e^{t(2-x)} - xe^t(e^{2t}-1)}{(e^t-1)^3(e^t+1)},
\end{aligned} \tag{4.26}$$

i.e. the fundamental polynomials related to the exponential space $\mathcal{W}_1^1$ defined by the nodes $-2,-1,0,1$ and $-1,0,1,2$, respectively, and

$$\begin{aligned}
\mathcal{L}^t_{-2,[-2,2]}(x) &:= \frac{x(1-x)e^t}{2(e^t-1)^2} + \frac{(e^{tx}-1)(e^{2t}-e^{t(3-x)})}{(e^t-1)^4(e^t+1)},\\
\mathcal{L}^t_{-1,[-2,2]}(x) &:= \frac{x(x(e^t+1)^2-(e^{2t}+1))}{2(e^t-1)^2} + \frac{e^{2t}(e^{-tx}-1)(e^{tx}(e^t+3)-3e^t-1)}{(e^t-1)^4(e^t+1)},\\
\mathcal{L}^t_{0,[-2,2]}(x) &:= \frac{(1-x^2)(e^{2t}+e^t+1)}{(e^t-1)^2} + \frac{3e^{2t}(e^{tx}+e^{-tx}-e^t-e^{-t})}{(e^t-1)^4},\\
\mathcal{L}^t_{1,[-2,2]}(x) &:= \frac{x(x(e^t+1)^2+(e^{2t}+1))}{2(e^t-1)^2} + \frac{e^{3t}(e^{-tx}-1)(e^{tx}(e^{-t}+3)-3e^{-t}-1)}{(e^t-1)^4(e^t+1)},\\
\mathcal{L}^t_{2,[-2,2]}(x) &:= -\frac{x(1+x)e^t}{2(e^t-1)^2} + \frac{(e^{tx}-1)(e^{3t}-e^{t(2-x)})}{(e^t-1)^4(e^t+1)},
\end{aligned} \tag{4.27}$$

that is the fundamental polynomials associated to the exponential space $\mathcal{W}_2^1$ defined by the nodes $-2,-1,0,1,2$.
Thus, we set

$$T^{(k)}_{5,0}(z) := z^{-1}\left(\sum_{j=-2}^{1}\mathcal{L}^{3^{-k}t}_{j,[-2,1]}\left(-\frac{1}{3}\right)z^{-3j}\right) + 1 + z\left(\sum_{j=-1}^{2}\mathcal{L}^{3^{-k}t}_{j,[-1,2]}\left(\frac{1}{3}\right)z^{-3j}\right), \tag{4.28}$$

and since all functions in $\mathcal{W}_1^1$ satisfy the differential equation $D^4\cdot - t^2D^2\cdot = 0$, we define

$$N^{(k)}(z) := (z^{-1}+z)\sum_{j=-2}^{2} h_j^{(k)}\, z^{3j} \quad \text{with} \quad h_j^{(k)} = D^4\mathcal{L}^{3^{-k}t}_{j,[-2,2]} - (3^{-k}t)^2\, D^2\mathcal{L}^{3^{-k}t}_{j,[-2,2]},\ j=-2,\dots,2. \tag{4.29}$$

At this point, following again the same approach used in the stationary case, we construct the k-th level symbol $T^{(k)}_{5,w^{(k)}}(z)$ as

$$T^{(k)}_{5,w^{(k)}}(z) = T^{(k)}_{5,0}(z) + w^{(k)}N^{(k)}(z), \qquad w^{(k)} \in \mathbb{R}. \tag{4.30}$$

Introducing the notation

$$v^{(k)} = \frac{1}{2}\left(e^{\mathrm{i}\frac{t}{3^{k+1}}} + e^{-\mathrm{i}\frac{t}{3^{k+1}}}\right), \quad t \in \left[0, \frac{3}{2}\pi\right) \cup \mathrm{i}\mathbb{R}^{+},$$

as in (3.11) we can conveniently rewrite (4.28) as

$$\begin{array}{rl} T^{(k)}_{5,0}(z) & = -\frac{(z^2+z+1)^2}{3(2v^{(k)}+1)^3(2v^{(k)}-1)z^5}\Big((2v^{(k)}+2)z^2 + (-4(v^{(k)})^2 - 4v^{(k)} - 3)z \\ & +(2v^{(k)}+2)\Big)\Big(z^4 + 2v^{(k)}z^3 + (4(v^{(k)})^2 - 1)z^2 + 2v^{(k)}z + 1\Big) \end{array} \tag{4.31}$$

and the term $w^{(k)}N^{(k)}(z)$ as

$$w^{(k)}N^{(k)}(z) = w^{(k)}\left(\frac{3^{-k}t}{e^{\frac{3^{-k}t}{2}} - e^{-\frac{3^{-k}t}{2}}}\right)^2 z^{-7}(z^2+1)\left(z^6 - 2v^{(k)}(4(v^{(k)})^2 - 3)z^3 + 1\right)(z^3-1)^2.$$

Incorporating $\left(\frac{3^{-k}t}{e^{\frac{3^{-k}t}{2}} - e^{-\frac{3^{-k}t}{2}}}\right)^2$ in the free parameter $w^{(k)}$, we finally obtain

$$w^{(k)}N^{(k)}(z) = w^{(k)}z^{-7}(z^2+1)\left(z^6 - 2v^{(k)}(4(v^{(k)})^2 - 3)z^3 + 1\right)(z^3-1)^2, \tag{4.32}$$

so that $T^{(k)}_{5,w^{(k)}}(z)$ is nothing but the sum of the Laurent polynomials in (4.31) and (4.32). Now, expanding $T^{(k)}_{5,w^{(k)}}(z)$ with respect to z, we find the unknown entries

$$\begin{array}{rcl} c_1^{(k)} & = & w^{(k)}, \\ c_3^{(k)} & = & w^{(k)} - \dfrac{2(v^{(k)}+1)}{3(2v^{(k)}-1)(2v^{(k)}+1)^3}, \\ c_4^{(k)} & = & -2w^{(k)}\left(4(v^{(k)})^3 - 3v^{(k)} + 1\right) - \dfrac{4v^{(k)}+1}{3(2v^{(k)}-1)(2v^{(k)}+1)^3}, \\ c_6^{(k)} & = & -2w^{(k)}\left(4(v^{(k)})^3 - 3v^{(k)} + 1\right) + \dfrac{1}{(2v^{(k)}-1)(2v^{(k)}+1)^3} + \dfrac{1}{3}, \\ c_7^{(k)} & = & 2w^{(k)}\left(8(v^{(k)})^3 - 6v^{(k)} + 1\right) + \dfrac{2v^{(k)}}{(2v^{(k)}-1)(2v^{(k)}+1)^3} + \dfrac{2}{3}, \end{array} \tag{4.33}$$

of the k-th level mask

$$\mathbf{T}^{(k)}_{5,w^{(k)}} = [c_1^{(k)}, 0, c_3^{(k)}, c_4^{(k)}, 0, c_6^{(k)}, c_7^{(k)}, 1, c_7^{(k)}, c_6^{(k)}, 0, c_4^{(k)}, c_3^{(k)}, 0, c_1^{(k)}], \tag{4.34}$$

and hence the refinement rules of the interpolating 5-point ternary non-stationary subdivision scheme

$$\left\{\begin{array}{rcl} f_{3i-1}^{(k+1)} & = & c_3^{(k)}p_{i-2}^{(k)} + c_6^{(k)}f_{i-1}^{(k)} + c_7^{(k)}f_i^{(k)} + c_4^{(k)}f_{i+1}^{(k)} + c_1^{(k)}f_{i+2}^{(k)}, \\ f_{3i}^{(k+1)} & = & p_i^{(k)}, \\ f_{3i+1}^{(k+1)} & = & c_1^{(k)}f_{i-2}^{(k)} + c_4^{(k)}f_{i-1}^{(k)} + c_7^{(k)}f_i^{(k)} + c_6^{(k)}f_{i+1}^{(k)} + c_3^{(k)}f_{i+2}^{(k)}. \end{array}\right. \tag{4.35}$$

Remark 4.12 *Observe that, when* $k \to +\infty$*, then from* (3.16) $v^{(k)} \to 1$ *and the Laurent polynomials* $T_{5,0}^{(k)}(z)$ *in* (4.31) *and* $N^{(k)}(z)$ *in* (4.32) *converge to their stationary counterparts in* (4.17)*. As a consequence, under the conditions* $v^{(k)} = 1$ *and* $w^{(k)} = w$*, the* k*-th level symbol* $T_{5,w^{(k)}}^{(k)}(z)$ *reduces to the stationary symbol* $T_{5,w}(z)$*, and the associated subdivision rules in* (4.35) *are brought back to the stationary ones in* (4.10)*.*

4.2.3 Properties of the non-stationary interpolatory 5-point ternary scheme

When investigating the support width of the basic limit function of the subdivision scheme with symbols $\{T_{5,w^{(k)}}^{(k)}(z),\ k \in \mathbb{N}_0\}$, the setting of the parameter t defining $\{v^{(k)} \in \mathbb{R}^+, k \in \mathbb{N}_0\}$ is not crucial. In fact, we must simply select $\{v^{(k)} \in \mathbb{R}^+, k \in \mathbb{N}_0\}$ and $\{w^{(k)} \in \mathbb{R} \setminus \{0\}, k \in \mathbb{N}_0\}$ such that convergence is guaranteed. Hence, the next result is obtained.

Proposition 4.13 *Let* ϕ *be the basic limit function of the subdivision scheme with* k*-th level symbol* $T_{5,w^{(k)}}^{(k)}(z)$ *in* (4.30)*. Then* ϕ *has support* $[-\frac{7}{2}, \frac{7}{2}]$ *for any choice of* $\{v^{(k)} \in \mathbb{R}^+, k \in \mathbb{N}_0\}$ *and* $\{w^{(k)} \in \mathbb{R} \setminus \{0\}, k \in \mathbb{N}_0\}$ *that guarantees convergence.*

Proof: Let $\mathbf{f}^{(0)} := \{\delta_{i,0},\ i \in \mathbb{Z}\}$, and for all $k \in \mathbb{N}_0$ define by $\phi^{(k)}$ the piecewise linear function interpolating the data $\mathbf{f}^{(k)}$, generated by the subdivision scheme, at the parameter values $3^{-k}\mathbb{Z}$. We first prove that $\phi^{(k)}$ has support $[-\xi^{(k)}, \xi^{(k)}]$ with $\xi^{(k)} = 1 + \frac{5}{2}\left(1 - 3^{-k}\right)$. We proceed by induction on k. For $k = 0$, the support of $\phi^{(0)}$ is trivially $[-1, 1]$, which verifies the given statement. Now, we show that the fulfillment of the given statement for an arbitrary level k implies its validity for the next level too. Indeed, assume that at the k-th iteration the support of $\phi^{(k)}$ is $[-\xi^{(k)}, \xi^{(k)}]$ with $\xi^{(k)} = 1 + \frac{5}{2}\left(1 - 3^{-k}\right)$. Then the last control point of $\mathbf{f}^{(k)}$ with non-zero y-coordinate is placed at $x_0 = \xi^{(k)} - 3^{-k}$. To find the parameter value of the last control point of $\mathbf{f}^{(k+1)}$ with non-zero y-coordinate, we need to apply to x_0 and its four following points (which have zero y-coordinate and are placed at $x_1 = \xi^{(k)},\ x_2 = \xi^{(k)} + 3^{-k},\ x_3 = \xi^{(k)} + 2\,3^{-k},\ x_4 = \xi^{(k)} + 3\,3^{-k}$), the third formula in (4.35). This yields

$$c_1^{(k)} x_0 + c_4^{(k)} x_1 + c_7^{(k)} x_2 + c_6^{(k)} x_3 + c_3^{(k)} x_4 = 1 + \frac{5}{2}(1 - 3^{-k-1}) - 3^{-k-1},$$

and thus the support of $\phi^{(k+1)}$ is exactly $[-\xi^{(k+1)}, \xi^{(k+1)}]$ with $\xi^{(k+1)} = 1 + \frac{5}{2}\left(1 - 3^{-k-1}\right)$, so concluding the induction proof. Finally, under the hypothesis of convergence, the basic limit function $\phi := \lim_{k\to\infty} \phi^{(k)}$ exists and its support is given by $\lim_{k\to\infty}[-\xi^{(k)}, \xi^{(k)}] = \left[-\frac{7}{2}, \frac{7}{2}\right]$. ■

The same results could be obtained using the method proposed in [44].

Differently, a correct setting of the parameter t, and hence of the sequences $\{v^{(k)} \in \mathbb{R}^+, k \in \mathbb{N}_0\}$ and $\{w^{(k)} \in \mathbb{R} \setminus \{0\}, k \in \mathbb{N}_0\}$ is required to achieve high smoothness order and reproduction of conic sections, i.e. reproduction of the space of exponential polynomials in $\mathcal{W}_1^1$.

Smoothness analysis

Since we are not interested in limit curves that are only C^0 continuous, we do not explicitly specify which choices of the parameter sequence $\{w^{(k)} \in \mathbb{R},\, k \in \mathbb{N}_0\}$ can ensure the convergence of the subdivision scheme defined in (4.35), but we directly point out which parameter setting can yield its C^2-convergence. First of all we observe that, when $w^{(k)} = 0$, then the k-th level symbol $T^{(k)}_{5,w^{(k)}}(z)$ in (4.30) reduces to the k-th level symbol $T^{(k)}_{5,0}(z)$ in (4.31). The latter coincides with the subdivision symbol of the non-stationary ternary interpolatory 4-point scheme in [9], which is of class C^1 for any sequence $\{v^{(k)} \in \mathbb{R}^+,\, k \in \mathbb{N}_0\}$ (see [9, Proposition 10]). Hence the parameter setting $\{w^{(k)} = 0,\, k \in \mathbb{N}_0\}$ does not yield C^2 continuity. The following proposition provides the conditions to be satisfied by the parameter sequence $\{w^{(k)} \in \mathbb{R}\backslash\{0\},\, k \in \mathbb{N}_0\}$ such that the non-stationary ternary interpolatory 5-point scheme defined in (4.35) indeed produces C^2 limit curves.

Proposition 4.14 *Let $v^{(0)} \in \mathbb{R}^+$ and $v^{(k)}$ be defined as in* (3.15) *for any $k \in \mathbb{N}$. Moreover, assume that $w^{(k)}$ converges to $w \in \left(\frac{1}{324}, \frac{1}{162}\right)$ with the rate $O(3^{-2k})$ as $k \to \infty$. Then the ternary interpolatory 5-point scheme with symbols $\{T^{(k)}_{5,w^{(k)}}(z),\, k \in \mathbb{N}_0\}$ produces limit curves of class C^2.*

Proof: Recalling property (3.16) and in view of the assumption on $w^{(k)}$, the k-th level symbol $T^{(k)}_{5,w^{(k)}}(z)$ is such that

$$\lim_{k\to+\infty} T^{(k)}_{5,w^{(k)}}(z) = T_{5,w}(z),$$

with $T_{5,w}(z)$ the symbol in (4.12). Thus, according to Definition 3.16, the non-stationary subdivision scheme with symbols $\{T^{(k)}_{5,w^{(k)}}(z),\, k \in \mathbb{N}_0\}$ is asymptotically similar to the stationary scheme defined by the symbol $T_{5,w}(z)$. Since the basic limit function of the stationary scheme is stable and C^2 for all $w \in \left(\frac{1}{324}, \frac{1}{162}\right)$ (see Section 4.2.1), if we could show that the non-stationary scheme satisfies the so-called approximate sum rules of order 3 (see Definition 3.15), i.e.

$$\begin{aligned} &(a)\ \sum_{k=0}^{\infty} \mu_k < \infty \quad \text{with} \quad \mu_k := \left|T^{(k)}_{5,w^{(k)}}(1) - 3\right|, \\ &(b)\ \sum_{k=0}^{\infty} 3^{2k}\,\delta_k < \infty \quad \text{with} \quad \delta_k := \max_{\ell=0,1,2} \max_{\epsilon\in\left\{e^{\frac{2\pi\mathrm{i}}{3}}, e^{\frac{4\pi\mathrm{i}}{3}}\right\}} 3^{-ks} \left|D^{\ell} T^{(k)}_{5,w^{(k)}}(\epsilon)\right|, \end{aligned} \tag{4.36}$$

the claim would follow from Proposition 3.17. Since $T^{(k)}_{5,w^{(k)}}(1) = 3$, condition (a) is trivially verified. Moreover, since

$$T^{(k)}_{5,w^{(k)}}(\epsilon) = D^1 T^{(k)}_{5,w^{(k)}}(\epsilon) = 0 \qquad \text{for} \quad \epsilon \in \{e^{\frac{2\pi\mathrm{i}}{3}}, e^{\frac{4\pi\mathrm{i}}{3}}\}$$

and

$$\max_{\epsilon\in\left\{e^{\frac{2\pi\mathrm{i}}{3}}, e^{\frac{4\pi\mathrm{i}}{3}}\right\}} \left|D^2 T^{(k)}_{5,w^{(k)}}(\epsilon)\right| = \max_{\epsilon\in\left\{e^{\frac{2\pi\mathrm{i}}{3}}, e^{\frac{4\pi\mathrm{i}}{3}}\right\}} \left|(1+\epsilon)\,(v^{(k)} - 1)\, f(v^{(k)}, w^{(k)})\right|$$

with

$$f(v^{(k)}, w^{(k)}) := \frac{4\big(4(v^{(k)})^2 + 6v^{(k)} + 5\big)}{(2v^{(k)} - 1)(2v^{(k)} + 1)^2} - 36w^{(k)}(2v^{(k)} + 1)^2,$$

in order to prove condition (b) we simply have to show that

$$\max_{\epsilon\in\left\{e^{\frac{2\pi\mathrm{i}}{3}},e^{\frac{4\pi\mathrm{i}}{3}}\right\}} |1+\epsilon| \sum_{k=0}^{\infty} \left|(v^{(k)}-1)\, f(v^{(k)}, w^{(k)})\right| < \infty.$$

The convergence of this series easily follows from (3.16) and the assumption on $w^{(k)}$, so proving the fulfillment of approximate sum rules of order 3 and thus of the claimed result. ■

Figure 4.6 shows different C^2 limit curves that have been obtained modifying the initial parameter $v^{(0)}$ in the admissible range $\mathbb{R}^+$ and choosing the parameter sequence $\{w^{(k)} \in \mathbb{R}^+\backslash\{0\},\, k \in \mathbb{N}_0\}$ in the respect of the assumptions of Proposition 4.14. As we can see, $v^{(0)}$ plays the role of a tension parameter since, as far as its value increases, the limit curve stays closer and closer to the initial control polyline.

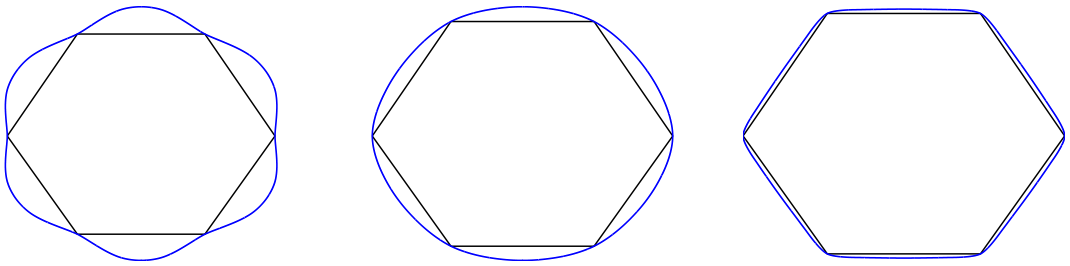

Figure 4.6: C^2 limit curves obtained by applying the non-stationary ternary interpolatory 5-point scheme with k-th level symbol in (4.30) when setting $w^{(k)} = \frac{1}{32(8(v^{(k)})^3-2v^{(k)}+2)}$ and choosing $v^{(0)} = 0.8$ (left), $v^{(0)} = 1$ (center), $v^{(0)} = 3$ (right).

Reproduction of conic sections

We conclude this section by investigating the reproduction properties of the C^2 non-stationary ternary interpolatory 5-point scheme.

Proposition 4.15 *For all* $\{w^{(k)} \in \mathbb{R}\backslash\{0\},\, k \in \mathbb{N}_0\}$ *satisfying the assumption in Proposition 4.14, the* C^2 *non-stationary ternary interpolatory 5-point scheme with* k*-th level symbol in* (4.30) *reproduces* $\mathcal{W}_1^1$ *with respect to the parametrization* $\{\mathbf{T}^{(k)}, k \in \mathbb{N}_0\}$ *in* (2.6) *with* $\tau = 0$.

Proof: Since $T^{(k)}_{5,w^{(k)}}(z)$ is such that

$$T^{(k)}_{5,w^{(k)}}(\epsilon) = D^1 T^{(k)}_{5,w^{(k)}}(\epsilon) = 0 \quad \text{for} \quad \epsilon \in \left\{e^{\frac{2\pi\mathrm{i}}{3}},\, e^{\frac{4\pi\mathrm{i}}{3}}\right\},$$

in view of Proposition 2.7 it is easily shown that the space Π_1^1 is generated for any choice of $w^{(k)}$ as in Proposition 4.14. Moreover, since

$$T^{(k)}_{5,w^{(k)}}(\epsilon\, e^{\pm\frac{t}{3^{k+1}}}) = 0, \quad \text{for} \quad \epsilon \in \left\{e^{\frac{2\pi\mathrm{i}}{3}},\, e^{\frac{4\pi\mathrm{i}}{3}}\right\},$$

then from Proposition 3.6 the space $\{e^{tx}, e^{-tx}\}$ is generated for any choice of $w^{(k)}$ as in Proposition 4.14. Thus the whole space $\mathcal{W}_1^1$ is generated. There follows that, being the scheme interpolatory, the space $\mathcal{W}_1^1$ is also reproduced with respect to the parametrization $\{\mathbf{T}^{(k)}, k \in \mathbb{N}_0\}$ in (2.6) with $\tau = 0$ (see Corollary 2.12). ■

Remark 4.16 *Note that, if the initial data are of the form $(j, f(j))$, $j \in \mathbb{Z}$ with $f \in \mathcal{W}_1^1$, then in order to reproduce the function f in the limit, we need to choose t respectively as:*

- *$t = s$ with $s \in \left(0, \frac{3}{2}\pi\right)$, if $f \in span\{1, x, e^{\mathrm{i}sx}, e^{-\mathrm{i}sx}\}$;*
- *$t = 0$, if $f \in span\{1, x, x^2, x^3\}$;*
- *$t = \mathrm{i}s$ with $s \in \mathbb{R}^+$, if $f \in span\{1, x, e^{sx}, e^{-sx}\}$.*

Thus, accordingly, the initial parameter $v^{(0)}$ has to be defined as in (3.14).

Corollary 4.17 *In consequence of Proposition 4.15 and in view of Proposition 3.18, we immediately have that the non-stationary ternary 5-point interpolatory subdivision scheme has approximation order 4.*

4.2.4 Combining convexity preservation with conic reproduction

As already recalled in Section 4.1.3, in literature we cannot find examples of ternary interpolatory 4-point schemes satisfying at the same time the properties of C^2 regularity, convexity preservation and reproduction of a 4-dimensional space of exponential polynomials. Thus, our new proposal provides a great improvement over the 4-point schemes in the literature since, by means of refinement rules involving only one additional point, it is able to design limit curves that fulfill all the above three properties. Precisely, in the previous section we have seen that, when the parameter sequence $\{w^{(k)} \in \mathbb{R}^+\backslash\{0\}, k \in \mathbb{N}_0\}$ is defined as in Proposition 4.14, then the limit curve is C^2 for any arbitrary initial polyline. Furthermore, the subdivision scheme can

- reproduce conics whenever the value of t identifying the parameter sequence $\{v^{(k)} \in \mathbb{R}^+, k \in \mathbb{N}_0\}$ is properly set and the vertices of the initial polyline $\mathbf{f}^{(0)}$ are points on a conic section corresponding to equally-spaced parameter values (see Proposition 4.15);
- preserve the convexity of the given data whenever the constant parameter sequences $\{v^{(k)} = 1, k \in \mathbb{N}_0\}$ and $\{w^{(k)} = w \in \left(\frac{1}{324}, \frac{1}{162}\right), k \in \mathbb{N}_0\}$ are used and the initial polyline satisfies the assumptions in Proposition 4.9.

The goal of this section is the construction of a piecewise-uniform subdivision algorithm that allows the user to generate a C^2 continuous limit curve including arcs of conic sections as well as locally convex pieces that preserve the convexity of the corresponding portion of initial control polyline.
In the following, we first focus on how to construct a limit curve that contains an alternation of curve pieces generated by the rules in (4.35) with different choices of the parameters $\{v^{(k)} \in \mathbb{R}^+, k \in \mathbb{N}_0\}$ and $\{w^{(k)} \in \mathbb{R}^+\backslash\{0\}, k \in \mathbb{N}_0\}$. Then, we show that the limit curve obtained via this piecewise-uniform scheme is C^2 everywhere, that is also in the region in

which the convexity preserving rules and the conic reproducing rules overlap. Finally, we show some examples of C^2 limit curves obtained by the piecewise-uniform scheme, that both contain curve pieces reproducing conic sections and curve pieces that preserve the convexity of the initial data.

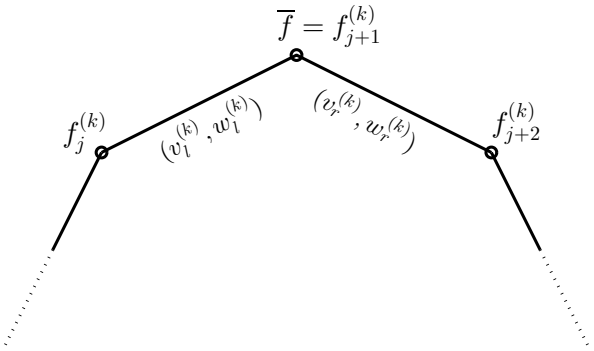

Figure 4.7: Configuration of parameter pairs around the contact point $\overline{f}$ at the k-th refinement step.

For the sake of conciseness, in the following we denote by $\mathcal{T}^{(k)}$ the C^2 ternary interpolatory 5-point scheme with symbols $\{T^{(k)}_{5,w^{(k)}}(z),\ k \in \mathbb{N}_0\}$ satisfying the assumptions of Proposition 4.14. Moreover, we denote the parameter sequences $\{v^{(k)} \in \mathbb{R}^+,\, k \in \mathbb{N}_0\}$ and $\{w^{(k)} \in \mathbb{R}^+\backslash\{0\},\, k \in \mathbb{N}_0\}$ needed for its construction by $V^{(k)}$ and $W^{(k)}$, respectively. Given an initial control polyline, we study the problem of including in the limit curve an alternation of curve pieces obtained using schemes $\mathcal{T}^{(k)}$ defined by different choices of the parameters $V^{(k)}$ and $W^{(k)}$. For this purpose, we associate to each edge of the initial control polyline a different scheme $\mathcal{T}^{(k)}$ and we suppose that edge to be refined using such scheme for all the subdivision steps. As a consequence, the resulting subdivision method belongs to the class of *piecewise-uniform* schemes since, essentially, it consists in using two different refinements to the left and to the right hand side of a contact point. Since all the schemes that are applied locally have a finite support, each contact point is influenced only by the schemes applied in its neighborhood. So we can generalize the previously proposed (uniform) subdivision scheme to the situation described in Figure 4.7. More precisely, we assume that on the left hand side of the contact point $\overline{f}$ the subdivision scheme denoted by $\mathcal{T}_l^{(k)}$, identified by the parameter sequences $V_l^{(k)} := \{v_l^{(k)},\, k \in \mathbb{N}_0\}$ and $W_l^{(k)} := \{w_l^{(k)},\, k \in \mathbb{N}_0\}$, is applied, while on its right hand side the subdivision scheme $\mathcal{T}_r^{(k)}$, identified by the parameter sequences $V_r^{(k)} := \{v_r^{(k)},\, k \in \mathbb{N}_0\}$ and $W_r^{(k)} := \{w_r^{(k)},\, k \in \mathbb{N}_0\}$, is used.
Denoted by $\mathcal{T}_{\overline{f}}^{(k)}$ the combined scheme, we are interested in determining the smoothness of the limit curves it produces. To this end we can limit ourselves to analyze the behaviour of the two schemes $\mathcal{T}_l^{(k)}$ and $\mathcal{T}_r^{(k)}$ in the region around the contact point $\overline{f}$. Since both schemes

are separately C^2, away from the contact point $\overline{f}$ the limit curves are clearly C^2. Therefore, we need to study the regularity of $\mathcal{T}_{\overline{f}}^{(k)}$ only in the region where they overlap. To formalize the application of the combined scheme $\mathcal{T}_{\overline{f}}^{(k)}$ in the neighborhood of the contact point $\overline{f}$, it is convenient to write the bi-infinite subdivision matrix

$$S_{\overline{f}}^{(k)} = \begin{pmatrix} \cdot & \cdot & \cdot & \cdot & \cdot & \cdot & \cdot & \cdot & \cdot \\ \cdot & 0 & 0 & 1 & 0 & 0 & 0 & 0 & \cdot \\ \cdot & c_{1,l}^{(k)} & c_{4,l}^{(k)} & c_{7,l}^{(k)} & c_{6,l}^{(k)} & c_{3,l}^{(k)} & 0 & 0 & \cdot \\ \cdot & 0 & c_{3,l}^{(k)} & c_{6,l}^{(k)} & c_{7,l}^{(k)} & c_{4,l}^{(k)} & c_{1,l}^{(k)} & 0 & \cdot \\ \cdot & 0 & 0 & 0 & 1 & 0 & 0 & 0 & \cdot \\ \cdot & 0 & c_{1,r}^{(k)} & c_{4,r}^{(k)} & c_{7,r}^{(k)} & c_{6,r}^{(k)} & c_{3,r}^{(k)} & 0 & \cdot \\ \cdot & 0 & 0 & c_{3,r}^{(k)} & c_{6,r}^{(k)} & c_{7,r}^{(k)} & c_{4,r}^{(k)} & c_{1,r}^{(k)} & \cdot \\ \cdot & 0 & 0 & 0 & 0 & 1 & 0 & 0 & \cdot \\ \cdot & \cdot & \cdot & \cdot & \cdot & \cdot & \cdot & \cdot & \cdot \end{pmatrix} \tag{4.37}$$

where for $i = 1, 3, 4, 6, 7$, the coefficients $c_{i,l}^{(k)}$ and $c_{i,r}^{(k)}$ are the ones in (4.33) with parameters $v_l^{(k)}, w_l^{(k)}$ and $v_r^{(k)}, w_r^{(k)}$, respectively. Let $S^\infty := \lim_{k\to\infty} S_{\overline{f}}^{(k)}$ denote the stationary counterpart of the matrix $S_{\overline{f}}^{(k)}$, and observe that $\lim_{k\to\infty} \mathcal{T}_l^{(k)} = \lim_{k\to\infty} \mathcal{T}_r^{(k)} = \lim_{k\to\infty} \mathcal{T}_{\overline{f}}^{(k)} =: \mathcal{T}^\infty$, with $\mathcal{T}^\infty$ denoting the stationary scheme related to the subdivision matrix S^∞, which, as previously recalled, is C^2 for $w \in \left(\frac{1}{324}, \frac{1}{162}\right)$ (see Section 4.2.1). To prove Proposition 4.19, regarding C^2 continuity of the limit curves in the overlapping regions of $\mathcal{T}_l^{(k)}$ and $\mathcal{T}_r^{(k)}$, we exploit the following result which is a straightforward generalization of [56, Theorem 8] to the m-ary case.

Proposition 4.18 *Let $\{\mathcal{S}_{\mathbf{a}^{(k)}}, k \in \mathbb{N}_0\}$ be a non-stationary subdivision scheme of arity $m \in \mathbb{N}$, $m \geq 2$, and $\mathcal{S}_{\mathbf{a}}$ a stationary subdivision scheme of the same arity and support width. If $\mathcal{S}_{\mathbf{a}}$ is of class C^r and if $\sum_{k=0}^{\infty} m^{\ell k} \|\mathcal{S}_{\mathbf{a}^{(k)}} - \mathcal{S}_{\mathbf{a}}\| < \infty$ for $\ell = 0, 1, \ldots, r$, then the non-stationary scheme $\{\mathcal{S}_{\mathbf{a}^{(k)}}, k \in \mathbb{N}_0\}$ is also of class C^r.*

Hence, C^2-smoothness of the piecewise-uniform scheme can be proved as follows.

Proposition 4.19 *The combined subdivision scheme $\mathcal{T}_{\overline{f}}^{(k)}$ generates C^2 continuous limit curves in the region where $\mathcal{T}_l^{(k)}$ and $\mathcal{T}_r^{(k)}$ overlap.*

Proof: To prove the claim it is sufficient to show that $\mathcal{T}_{\overline{f}}^{(k)}$ and $\mathcal{T}^\infty$ are asymptotically equivalent of order 2, namely, in view of Proposition 4.18, they satisfy $\sum_{k=0}^{\infty} 3^{\ell k} ||\mathcal{T}_{\overline{f}}^{(k)} - \mathcal{T}^\infty|| < \infty$ for $\ell = 0, 1, 2$, which means that the associated subdivision matrices also satisfy $\sum_{k=0}^{\infty} 3^{\ell k} ||S_{\overline{f}}^{(k)} - S^\infty|| < \infty$ for $\ell = 0, 1, 2$. Since $S_{\overline{f}}^{(k)}$ is built from the rows of $S_l^{(k)}$, $S_r^{(k)}$ and the subdivision schemes $\mathcal{T}_l^{(k)}$, $\mathcal{T}_r^{(k)}$ are independently known to be C^2, it is easy to show that

$$\sum_{k=0}^{\infty} 3^{\ell k} ||S_{\overline{f}}^{(k)} - S^\infty|| \leq \max\left\{ \sum_{k=0}^{\infty} 3^{\ell k} ||S_l^{(k)} - S^\infty||, \sum_{k=0}^{\infty} 3^{\ell k} ||S_r^{(k)} - S^\infty|| \right\} < \infty$$

for all $\ell = 0, 1, 2$, from which the claim is obtained. ■

We conclude this section pointing out that the proposed piecewise-uniform subdivision algorithm allows the user to generate a C^2 continuous limit curve including arcs of conic sections as well as locally convex pieces that preserve the convexity of the corresponding portion of initial control polyline.
Precisely, let $n > 6$ and assume that the initial polyline is such that the vertices from $f_j^{(0)}$ to $f_{j+n}^{(0)}$ are points on a conic arc corresponding to equally-spaced parameter values. If

$$f_\ell^{(0)} = \begin{cases} \text{(i)} & (a\cos(\ell t), b\sin(\ell t)), & t \in \left(0, \frac{3}{2}\pi\right) \\ \text{(ii)} & (\ell, \ell^2), & \\ \text{(iii)} & (a\cosh(\ell t), b\sinh(\ell t)), & t \in \mathbb{R}^+ \end{cases} \qquad \ell = j, \dots, j+n$$

$$\text{and} \qquad v_\ell^{(0)} = \begin{cases} \text{(i)} & \cos(\frac{t}{3}), & t \in \left(0, \frac{3}{2}\pi\right) \\ \text{(ii)} & 1, & \\ \text{(iii)} & \cosh(\frac{t}{3}), & t \in \mathbb{R}^+ \end{cases} \qquad \ell = j, \dots, j+n-1,$$

then when setting the parameters $w_\ell^{(k)}$, $\ell = j, \dots, j+n-1$ according to the condition in Proposition 4.14, the portion of limit curve confined between the vertices $f_{j+3}^{(0)}$ and $f_{j+n-3}^{(0)}$ exactly coincides with the conic arc from which they have been sampled, and the adjacent pieces join C^2 continuously.
In a similar way, if the portion of initial control polyline between $f_j^{(0)}$ and $f_{j+n}^{(0)}$ is locally convex and satisfies conditions in Proposition 4.9, then provided that, for all $\ell = j, \dots, j+n-1$, $v_\ell^{(0)} = 1$ and $w_\ell^{(k)}$ fulfills the assumptions of Proposition 4.9, the obtained limit curve is strictly convex between $f_{j+3}^{(0)}$ and $f_{j+n-3}^{(0)}$, and joins C^2 continuously to the neighboring pieces.

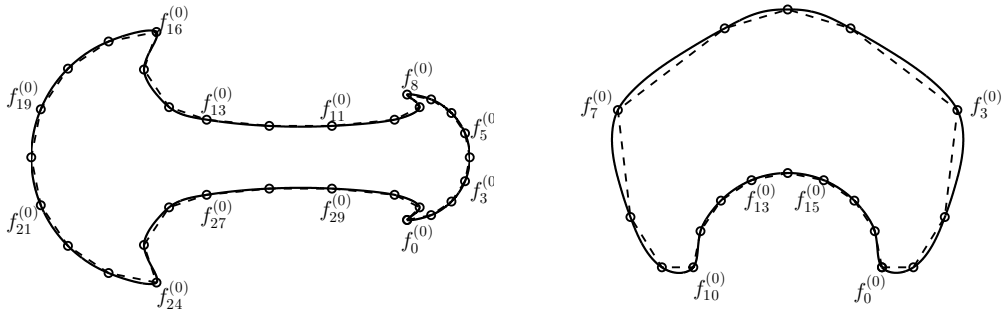

(a) (b)

Figure 4.8: Examples of application of the C^2 piecewise-uniform subdivision scheme.

Figure 4.8 shows some application examples of the proposed piecewise-uniform subdivision algorithm in order to generate C^2 continuous limit curves including arcs of conic sections as well as pieces that preserve the convexity of the corresponding portion of initial control polyline. In case (a), the parameter $v_\ell^{(0)}$, $\ell = 0, \dots, 31$ to be associated to the ℓ-th edge of the control polyline is defined as

$$\begin{aligned} &[v_0^{(0)}, \dots, v_7^{(0)}, v_8^{(0)}, \dots, v_{15}^{(0)}, v_{16}^{(0)}, \dots, v_{23}^{(0)}, v_{24}^{(0)}, \dots, v_{31}^{(0)}] = \\ &= [\cos\left(\tfrac{\pi}{24}\right), \dots, \cos\left(\tfrac{\pi}{24}\right), 1, \dots, 1, \cos\left(\tfrac{\pi}{24}\right), \dots, \cos\left(\tfrac{\pi}{24}\right), 1, \dots, 1], \end{aligned}$$

and the shape parameter vectors for the successive refinement levels are simply obtained via the recursive formula (3.15). In contrast, the smoothness parameter $w_\ell^{(k)}$ to be associated with the ℓ-th edge of the control polyline is given by $w_\ell^{(k)} = \frac{1}{10(2(v_\ell^{(k)})^3+3v_\ell^{(k)}+12)}$.
In a similar way, in case (b) the initial shape parameter vector is chosen as

$$[v_0^{(0)}, \ldots, v_8^{(0)}, v_9^{(0)}, \ldots, v_{16}^{(0)}, v_{17}^{(0)}] = \left[1, \ldots, 1, \cos\left(\frac{\pi}{24}\right), \ldots, \cos\left(\frac{\pi}{24}\right), 1\right],$$

$v_\ell^{(k)}$ is again defined from the corresponding $v_\ell^{(0)}$ via recurrence (3.15) and $w_\ell^{(k)} = \frac{1}{7((v_\ell^{(k)})^3+20(v_\ell^{(k)})^2-v_\ell^{(k)}+5)}$.

Concerning Figure 4.8 (a), the initial control polyline is locally convex from $f_8^{(0)}$ to $f_{16}^{(0)}$ as well as from $f_{24}^{(0)}$ to $f_{32}^{(0)} \equiv f_0^{(0)}$; thus, from $f_{11}^{(0)}$ to $f_{13}^{(0)}$ and from $f_{27}^{(0)}$ to $f_{29}^{(0)}$ the limit curve preserves the convexity of the given data. Differently, the initial control points from $f_0^{(0)}$ to $f_8^{(0)}$ and from $f_{16}^{(0)}$ to $f_{24}^{(0)}$ are uniform samples of the circle of radius 1 and 2, respectively; hence the limit curve reproduces the corresponding circle arc between $f_3^{(0)}$ and $f_5^{(0)}$ as well as between $f_{19}^{(0)}$ and $f_{21}^{(0)}$.
As to Figure 4.8 (b), from $f_0^{(0)}$ to $f_{10}^{(0)}$ the initial control polyline is locally convex, thus from $f_3^{(0)}$ to $f_7^{(0)}$ the limit curve is convex too. Conversely, from $f_{10}^{(0)}$ to $f_{18}^{(0)} \equiv f_0^{(0)}$ the initial control points are equally-spaced samples of the circle of radius 1.5; thus from $f_{13}^{(0)}$ to $f_{15}^{(0)}$ the limit curve coincides with an arc of such circle.

4.3 Families of non-stationary subdivision schemes reproducing conic sections

In the previous section, we have seen the usefulness of non-stationary subdivision schemes to design limit curves able to reproduce not only polynomials but also exponential polynomials. This property, together with interpolation and arbitrarily high smoothness, is considered wished tool both in geometric modeling and image segmentation. As to the latter, we recall that one of the most used tools for efficient image segmentation are active contours (snakes), i.e. 2D curves evolving through the image, capable of perfectly outlining elliptic objects and offering user-friendly models, versatile enough to provide a close smooth approximation of any closed polyline in the plane [37] (see also Section 6).
In the stationary context, many fundamental families of subdivision schemes have been proposed and studied during the years (e.g. [42, 74, 90]), which are able to produce limit curves with high smoothness and to generate or reproduce polynomials. However, non-stationary extensions of these schemes have never been proposed, thus limiting their application.
Among these families of stationary subdivision schemes, there is the Lane-Riesenfeld algorithm [90] which defines the symbols associated to the family of B-spline schemes of order ℓ, with $\ell \in \mathbb{N}$. In literature, the use of these symbols as 'building blocks' to define both interpolatory schemes [27] and subdivision schemes with enhanced reproduction capabilities [74] has been recently shown. In fact, Conti and Romani observed that ℓ-point (with ℓ even) Dubuc-Deslauriers schemes [42] are characterized by a symbol containing the factor $\frac{(z+1)^\ell}{2^{\ell-1}}$, while Hormann and Sabin noticed that the same factor (with $\ell \in \mathbb{N}$) is also contained in the

symbol of the family of subdivision schemes with cubic precision. Moreover, in [39] it has been also recently illustrated that the first member of the Lane-Riesenfeld's family and that of the Hormann-Sabin's family can be combined together to give rise to a recursive formula defining the interpolatory $2n$-point Dubuc-Deslauriers schemes for all $n \geq 3$.
These observations prompted us to propose a non-stationary generalization of these fundamental classes. First, we show a level-dependent extension of the Lane-Riesenfeld algorithm, aimed at providing the symbols of normalized exponential B-splines. These symbols, together with a non-stationary version of Hormann-Sabin's kernels, are successively used as 'building blocks' to define a family of alternating primal/dual subdivision schemes reproducing conics. The first member of the resulting family, combined with the first one of the novel Lane-Riesenfeld's family, is shown to originate a three-term recurrence formula defining the symbols of the non-stationary interpolatory $2n$-point schemes reproducing the space $\mathcal{W}_{2n-3} = span\{1, x, ..., x^{2n-3}, e^{tx}, e^{-tx}\}$, where $t \in [0, \pi) \cup \mathrm{i}\mathbb{R}^+$ and $n \in \mathbb{N}$, $n \geq 3$.
In the following, we start with a review of known results in the stationary setting, then we propose non-stationary generalizations and we analyze the support width, generation and reproduction capabilities and smoothness properties of the new non-stationary families.

4.3.1 The stationary setting: review of known results

Lane-Riesenfeld algorithm

Refine-and-Smooth algorithms are characterized by a refine step which introduces new points on the initial control polyline, and a following smoothing step, which modifies the obtained points using simple local averaging rules. More smoothing steps provide limit curves of wider support as well as of higher smoothness [13]. One of the simplest Refine-and-Smooth algorithms is the well-known Lane-Riesenfeld algorithm, which generates polynomial uniform B-splines of degree $(n+1)$ for all $n \in \mathbb{N}_0$ [90]. We remind that this algorithm is defined using a smoothing operator described by a symbol of the form

$$S(z) = \frac{z+1}{2},$$

and a refine operator

$$R(z) = 1 + S(z^2)z^{-1} = \frac{(z+1)^2}{2z},$$

which is well-known to reproduce Π_1^1 [13].
The Lane-Riesenfeld algorithm is obtained by applying the smoothing operator S n times, after one application of the refine operator R. This mechanism provides the symbol

$$A_n(z) = z^{-\lceil \frac{n}{2} \rceil} \Big(S(z)\Big)^n R(z) = \frac{(z+1)^{n+2}}{2^{n+1} z^{\lceil \frac{n}{2} \rceil + 1}}, \qquad n \in \mathbb{N}_0, \tag{4.38}$$

which is indeed the symbol of the degree-$(n+1)$ polynomial B-spline. We notice that the schemes defined by the symbol in (4.38) generate $\Pi_{n+1}^1 = span\{1, x, x^2, \ldots, x^{n+1}\}$, but reproduce only Π_1^1.

Hormann-Sabin's family

In order to increase the degree of polynomial reproduction of B-spline schemes from one to three, the family of stationary subdivision schemes with cubic precision, hereinafter denoted

by $\{F_n(z)\}_{n\geq 2}$, was proposed by Hormann and Sabin [74]. Its symbol can be written as

$$\begin{gathered} F_n(z) = A_n(z)\, K_n(z), \qquad n \in \mathbb{N}\backslash\{1\}, \\ \text{where} \quad A_n(z) = \frac{(z+1)^{n+2}}{2^{n+1} z^{\left\lceil \frac{n}{2} \right\rceil + 1}} \quad \text{and} \quad K_n(z) = -\frac{n+2}{8z} + \frac{n+6}{4} - \frac{n+2}{8} z. \end{gathered} \tag{4.39}$$

Thus this family is defined by using a convolution of the symbol of the Lane-Riesenfeld's family with some degree-2 polynomials, that they called *kernels*, tailored to increase the degree of polynomial reproduction of B-spline schemes from one to three.
We remind that the scheme with symbol $F_1(z)$ is the dual three-point scheme which reproduces quadratics but not cubics, and hence it is not considered a member of the family. On the other hand, $F_2(z)$, $F_3(z)$ and $F_4(z)$ are respectively the symbols of the Dubuc-Deslauriers interpolatory four-point scheme, the dual four-point scheme and a relaxation of the interpolatory four-point scheme (see [74]).

The family of interpolatory $2n$-point Dubuc-Deslauriers schemes

The interpolatory $2n$-point ($n \in \mathbb{N}$, $n \geq 1$) Dubuc-Deslauriers scheme [42] is identified by the symbol (see e.g. [27, 62])

$$I_{2n}(z) = A_{2n-2}(z) \sum_{\ell=0}^{n-1} (-1)^\ell\, 2^{-2\ell} \binom{n-1+\ell}{\ell} \frac{(1-z)^{2\ell}}{z^\ell} \tag{4.40}$$

where

$$A_{2n-2}(z) = \frac{(z+1)^{2n}}{2^{2n-1} z^n},$$

which satisfies the interpolatory condition $I_{2n}(z) + I_{2n}(-z) = 2$ and reproduces Π^1_{2n-1}.
In [39] it was recently proven that for all $n \in \mathbb{N}$, $n \geq 2$ the subdivision schemes with symbols $\{I_{2n}(z)\}_{n\geq 2}$ satisfy the two-term recurrence relation

$$I_{2n}(z) = I_{2n-2}(z) + \frac{(-1)^{n-1}}{2^{4(n-1)}} \binom{2n-3}{n-1} \left(z - \frac{1}{z}\right)^{2n-2} \left(z + \frac{1}{z}\right), \tag{4.41}$$

starting from

$$I_2(z) = A_0(z) = \frac{(z+1)^2}{2z},$$

which is also the first member of the Lane-Riesenfeld's family $\{A_{2n-2}(z)\}_{n\geq 1}$.
From (4.41) the following three-term recurrence relation

$$I_{2n}(z) = I_{2n-2}(z) - \beta_n \left(z - \frac{1}{z}\right)^2 \Big(I_{2n-2}(z) - I_{2n-4}(z)\Big) \qquad \text{where} \quad \beta_n = \frac{2n-3}{8(n-1)}, \tag{4.42}$$

defining the symbols of all interpolatory $2n$-point Dubuc-Deslauriers schemes with $n \geq 3$, can be also easily worked out [39]. The last recurrence is clearly based on the knowledge of the first member of the Lane-Riesenfeld's family, $I_2(z)$, and the first one in Hormann-Sabin's family, i.e.,

$$I_4(z) = F_2(z) = (z+1)^4 \frac{(-z^2 + 4z - 1)}{16 z^3}.$$

4.3.2 A non-stationary Lane-Riesenfeld algorithm

In the stationary setting we looked for a Refine-and-Smooth algorithm capable of defining the symbols of degree-$(n+1)$ polynomial B-splines for all $n \in \mathbb{N}_0$, and we observed that all the resulting schemes are featured by reproduction of Π_1^1. Here, instead of Π_1^1, we consider the 2-dimensional space

$$span\{e^{tx},\, e^{-tx}\}, \qquad \text{with} \quad t \in [0,\pi) \cup \mathrm{i}\mathbb{R}^+. \tag{4.43}$$

Following the stationary case, we define the k-th level symbols of the smoothing and refine operators as follows.

Definition 4.20 *Let $v^{(k)}$ be as in* (3.11)*. For all $k \in \mathbb{N}_0$ we define*

$$S^{(k)}(z) := \frac{z+1}{2v^{(k)}}, \tag{4.44}$$

and

$$R^{(k)}(z) = 1 + \frac{v^{(k+1)}}{v^{(k)}} S^{(k)}(z^2) z^{-1}$$

to be the k-th level symbols of the smoothing and refine operators, respectively.

Lemma 4.21 *The refine operator in Definition 4.20, explicity described by the k-th level symbol*

$$R^{(k)}(z) := \frac{z + 2v^{(k)} + z^{-1}}{2v^{(k)}}, \tag{4.45}$$

reproduces the 2-dimensional space in (4.43)*.*

Proof: Since $R^{(k)}(z)$ fulfils the conditions

$$R^{(k)}(-e^{\frac{t}{2^{k+1}}}) = 0, \quad R^{(k)}(-e^{-\frac{t}{2^{k+1}}}) = 0, \quad R^{(k)}(e^{\frac{t}{2^{k+1}}}) = 2, \quad R^{(k)}(e^{-\frac{t}{2^{k+1}}}) = 2,$$

then, in view of Proposition 3.7, it reproduces reproduces the 2-dimensional space in (4.43) with respect to the parametrization $\{\mathbf{T}^{(k)}, k \in \mathbb{N}_0\}$ in (2.6) with $\tau = 0$. ■

The non-stationary Lane-Riesenfeld algorithm, obtained by one application of the refine operator and n successive applications of smoothing operator, is thus performed by the k-th level symbol

$$A_n^{(k)}(z) = z^{-\lceil \frac{n}{2} \rceil} \left(S^{(k)}(z)\right)^n R^{(k)}(z) = \frac{(z+1)^n \left(z + 2v^{(k)} + z^{-1}\right)}{2v^{(k)} \left(2(v^{(k)}+1)\right)^{\frac{n}{2}} z^{\lceil \frac{n}{2} \rceil}}, \quad n \in \mathbb{N}_0, \tag{4.46}$$

where $v^{(k)}$ is the level-dependent parameter in (3.11).

Proposition 4.22 *For all $n \in \mathbb{N}_0$ the subdivision scheme related to the symbols $\{A_n^{(k)}(z), k \in \mathbb{N}_0\}$ generates $\mathcal{W}_{n-1}^1 = span\{1, x, \ldots, x^{n-1}, e^{tx}, e^{-tx}\}$ and reproduces the 2-dimensional subspace $span\{e^{tx}, e^{-tx}\}$ with $t \in [0,\pi) \cup \mathrm{i}\mathbb{R}^+$.*

Proof: We start by observing that, $\forall n \in \mathbb{N}_0$, $A_n^{(k)}(-e^{\pm\frac{t}{2^{k+1}}}) = 0$ and, whenever $n \geq 1$, $D^\ell A_n^{(k)}(-1) = 0$ for all $\ell = 0, \ldots, n-1$. Thus, recalling conditions in Proposition 3.6, the generation of the space $\mathcal{W}_{n-1}^1$ is proven. Moreover, we notice that $S^{(k)}(e^{\pm\frac{t}{2^{k+1}}}) = e^{\pm\frac{t}{2^{k+1}}}$, while from Lemma 4.21 we have $R^{(k)}(e^{\pm\frac{t}{2^{k+1}}}) = 2$. Thus the condition $A_n^{(k)}(e^{\pm\frac{t}{2^{k+1}}}) = 2(e^{\pm\frac{t}{2^{k+1}}})^\tau$ with

$$\tau = \begin{cases} 0 & \text{if } n \text{ even}, \\ -\frac{1}{2} & \text{of } n \text{ odd}, \end{cases} \tag{4.47}$$

are satisfied, too. Hence reproduction of $\{e^{tx}, e^{-tx}\}$ is guaranteed for all values of $n \in \mathbb{N}_0$. ■

Remark 4.23 *Note that, when $v^{(0)} = 1$, $A_n^{(k)}(z)$ reduces to the symbol of the degree-$(n+1)$ polynomial B-spline in* (4.38)*, namely, the non-stationary Lane-Riesenfeld algorithm in* (4.46) *gets back to its stationary counterpart.*

We conclude by observing that the proposed non-stationary extension of the Lane-Riesenfeld algorithm offers an alternative definition of the symbols of normalized exponential B-splines recently introduced in [76, 77].

4.3.3 A family of alternating primal/dual subdivision schemes reproducing conics

We consider the space of exponential polynomials

$$\mathcal{W}_1^1 = span\{1, x, e^{tx}, e^{-tx}\}, \qquad t \in [0, \pi) \cup \mathrm{i}\mathbb{R}^+. \tag{4.48}$$

Using the symbols of the non-stationary extension of the Lane-Riesenfeld's family we can define a family of non-stationary subdivision schemes reproducing $\mathcal{W}_1^1$, as shown in the following proposition.

Proposition 4.24 *Let $v^{(k)}$ be defined as in* (3.11)*. The family of non-stationary subdivision schemes with k-level symbol*

$$F_n^{(k)}(z) = A_n^{(k)}(z)\, K_n^{(k)}(z), \tag{4.49}$$

with $A_n^{(k)}(z)$ in (4.46) *and*

$$K_n^{(k)}(z) = u_n^{(k)} z + (1 - 2u_n^{(k)} v^{(k)}) + u_n^{(k)} z^{-1}, \qquad u_n^{(k)} = \frac{1}{2(v^{(k)} - 1)} - v^{(k)} \frac{\left(\frac{v^{(k)}+1}{2}\right)^{\frac{n}{2}}}{(v^{(k)})^2 - 1},$$

reproduces the space $\mathcal{W}_1^1$ in (4.48) *for all $n \in \mathbb{N}\backslash\{1\}$, with respect to the parametrization $\{\mathbf{T}^{(k)}, k \in \mathbb{N}_0\}$ in* (2.6) *with τ in* (4.47)*.*

Proof: Recalling Proposition 3.6 it can be easily verified that conditions for generation of $\mathcal{W}_1$ are fulfilled for all $n \in \mathbb{N}\backslash\{1\}$. Moreover, for all $n \in \mathbb{N}\backslash\{1\}$

$$F_n^{(k)}(1) = 2, \quad D^1 F_n^{(k)}(1) = 2\tau, \quad F_n^{(k)}(e^{\frac{t}{2^{k+1}}}) = 2(e^{\frac{t}{2^{k+1}}})^\tau, \quad F_n^{(k)}(e^{-\frac{t}{2^{k+1}}}) = 2(e^{-\frac{t}{2^{k+1}}})^\tau,$$

with τ in (4.47), thus proving the claim using Proposition 3.7. ■

Lemma 4.25 *For all $n \in \mathbb{N}\backslash\{1\}$ and for all $v^{(0)} \in \mathbb{R}^+$, the parameter $u_n^{(k)}$ in Proposition 4.24 verifies*

$$\lim_{k\to+\infty} u_n^{(k)} = -\frac{n}{8} - \frac{1}{4}.$$

Proof: The claimed result follows from (3.16) and de l'Hôpital's theorem. ■

Corollary 4.26 *For all $n \in \mathbb{N}\backslash\{1\}$ and for all $v^{(0)} \in \mathbb{R}^+$, the symbol in* (4.49) *is such that*

$$\lim_{k\to+\infty} F_n^{(k)}(z) = F_n(z), \tag{4.50}$$

with $F_n(z)$ in (4.39)*. Thus, the non-stationary subdivision scheme with k-level symbol $F_n^{(k)}(z)$ is asymptotically similar to the stationary scheme with symbol $F_n(z)$.*

Proof: The claimed result follows from (3.16) and Lemma 4.25. ■

Proposition 4.27 *Let ϕ_n be the basic limit function of the non-stationary subdivision scheme with k-level symbol $F_n^{(k)}(z)$, $n \in \mathbb{N}\backslash\{1\}$ in* (4.49)*. Then the support of ϕ_n is $\mathcal{J}_n = \left[-\frac{n+4}{2}, \frac{n+4}{2}\right]$.*

Proof: By definition, the basic limit function ϕ_n is obtained as the limit function of the non-stationary subdivision scheme with k-level symbol $F_n^{(k)}(z)$, when applied to the initial data $f_i^{(0)} = \delta_{i,0}$, $i \in \mathbb{Z}$. Thus, introducing the notation $\mathcal{I}^{(k)} = \{\frac{i}{2^k} \,|\, i \in \mathbb{Z}\}$, we have that, at the initial level $k = 0$, the restriction of the basic limit function ϕ_n to $\mathcal{I}^{(0)}$ vanishes everywhere except at $i = 0$. Then, by equation (4.49) we get that, at refinement step $k = 1$, the restriction of the basic limit function ϕ_n to $\mathcal{I}^{(1)}$ vanishes outside the interval $\mathcal{J}_n^{(1)} = [-\frac{n+4}{4}, \frac{n+4}{4}] \subset \mathcal{J}_n$ and, at each successive step $k > 1$, the width of the interval $\mathcal{J}_n^{(k)}$, where the restriction of ϕ_n to $\mathcal{I}^{(k)}$ does not vanish, is obtained by extending the left and right hand side of $\mathcal{J}_n^{(k-1)}$ by a factor of $\frac{n+4}{2}\frac{1}{2^k}$. Hence, at the N-th subdivision step, the restriction of the basic limit function ϕ_n to $\mathcal{I}^{(N)}$ vanishes outside the interval

$$\begin{aligned}\mathcal{J}_n^{(N)} &= \left[-\frac{n+4}{4} - \sum_{k=2}^{N} \frac{n+4}{2}\frac{1}{2^k}, \frac{n+4}{4} + \sum_{k=2}^{N} \frac{n+4}{2}\frac{1}{2^k}\right] \\ &= \left[-\frac{n+4}{2}\left(1 - \frac{1}{2^N}\right), \frac{n+4}{2}\left(1 - \frac{1}{2^N}\right)\right]\end{aligned}$$

and from the inequality $\left(1 - \frac{1}{2^N}\right) < 1$, it follows $\mathcal{J}_n^{(N)} \subset \mathcal{J}_n$ for all $N \in \mathbb{N}$. Since the support $\mathcal{J}_n$ of the basic limit function ϕ_n is given by $\lim_{N\to+\infty} \mathcal{J}_n^{(N)}$, the thesis follows straightforwardly. ■

In Figure 4.9 we plot the basic limit function ϕ_n obtained when varying the value of $n \in \mathbb{N}\backslash\{1\}$ and of the initial tension parameter $v^{(0)} \in \mathbb{R}^+$. Note that the x-axis has been reduced to $[-4, 4]$ even if the supports of ϕ_8 and ϕ_{18} are larger.

The following proposition analyzes the smoothness properties of the new family of non-stationary subdivision schemes.

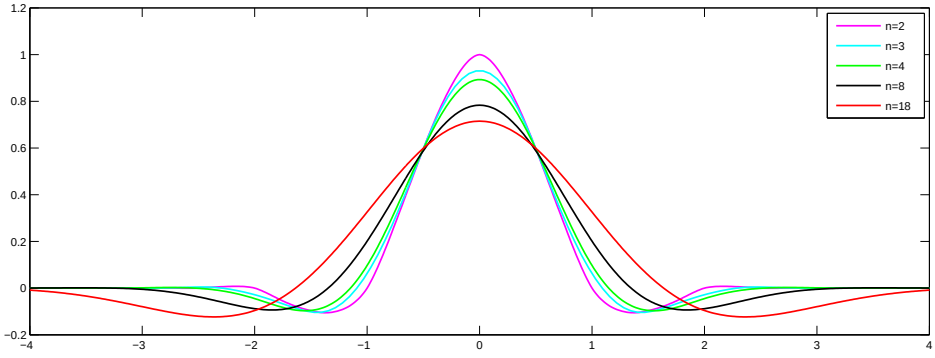

(a) $v^{(0)} = 0.1$

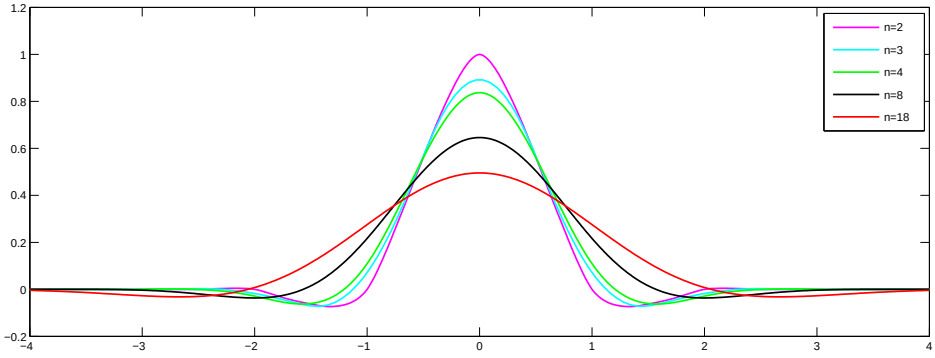

(b) $v^{(0)} = 1$

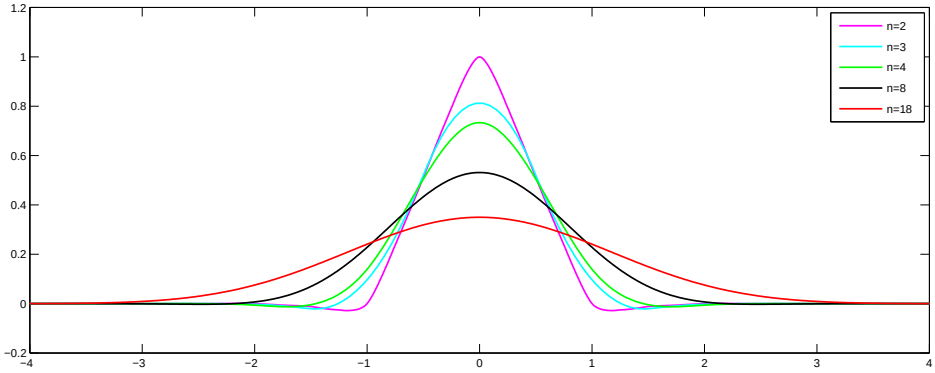

(c) $v^{(0)} = 15$

Figure 4.9: Basic limit function of the subdivision scheme having symbol $F_n^{(k)}(z)$ with $n = 2, 3, 4, 8, 18$ and $v^{(0)} = 0.1$ (a), 1 (b), 15 (c). In each picture the function with the highest peak at 0 corresponds to $n = 2$, and as n increases, the height of the peak decreases.

Proposition 4.28 *The family of non-stationary subdivision schemes with k-level symbols*

$\{F_n^{(k)}(z)\}_{n\geq 2}$ in (4.49) has the same integer smoothness as the family described by the stationary symbols $\{F_n(z)\}_{n\geq 2}$ in (4.39).

Proof: From (4.50) we have that, for all $n \in \mathbb{N}\setminus\{1\}$, the non-stationary scheme related to the k-level symbol $F_n^{(k)}(z)$ is asymptotically similar to the stationary scheme with symbol $F_n(z)$. Moreover, $F_n^{(k)}(z)$ satisfies approximate sum rules of order n. In fact, according to Definition 3.15, $F_n^{(k)}(1) = 2$ and, since from (4.46) we also have $D^\ell A_n^{(k)}(-1) = 0$ for all $\ell = 0,\dots,n-1$, we thus obtain

$$\max_{\ell=0,\dots,n-1}\left|D^\ell F_n^{(k)}(-1)\right| = 0, \qquad \forall k\in\mathbb{N}_0,\ n\in\mathbb{N}\setminus\{1\}.$$

Hence, recalling that for all values of $n \in \mathbb{N}\setminus\{1\}$ the integer smoothness of the subdivision scheme with symbol $F_n(z)$ is not greater than C^{n-1} [74, Theorem 1], in view of Corollary 3.17 the proof is concluded. ■

For the sake of completeness, we close this section by showing the refinement rules of the subdivision scheme with k-level symbol $F_1^{(k)}(z)$ (that we have excluded from the family since it does not reproduce $\mathcal{W}_1^1$) and the first three members of $\{F_n^{(k)}(z)\}_{n\geq 2}$ corresponding to $n = 2, 3, 4$, in order to connect them to existing results from the literature.

- $n = 1$: the non-stationary dual 3-point scheme. The subdivision scheme with k-level symbol $F_1^{(k)}(z)$ reproduces only $\mathcal{W}_0^1 = \{1, e^{tx}, e^{-tx}\}$. In fact

$$F_1^{(k)}(-1) = 0, \quad F_1^{(k)}(-e^{\frac{t}{2^{k+1}}}) = 0, \quad F_1^{(k)}(-e^{-\frac{t}{2^{k+1}}}) = 0,$$
$$F_1^{(k)}(1) = 2, \quad F_1^{(k)}(e^{\frac{t}{2^{k+1}}}) = 2(e^{\frac{t}{2^{k+1}}})^{-\frac{1}{2}}, \quad F_1^{(k)}(e^{-\frac{t}{2^{k+1}}}) = 2(e^{-\frac{t}{2^{k+1}}})^{-\frac{1}{2}},$$

  but

$$D^1F_1^{(k)}(-1) = \frac{4}{\left(e^{\frac{t}{2^{k+1}}}+e^{-\frac{t}{2^{k+1}}}\right)\left(e^{\frac{\frac{t}{2^{k+1}}}{2}}+e^{-\frac{\frac{t}{2^{k+1}}}{2}}\right)} - 1 \neq 0, \quad \text{for all} \quad t\neq 0.$$

  The subdivision rules of this scheme are

$$\begin{cases} f_{2i}^{(k+1)} &= \frac{1}{8v^{(k+1)}v^{(k)}((v^{(k)})^2-1)}\Big(\left((v^{(k)}+1)(2v^{(k)}-1)-2v^{(k)}v^{(k+1)}\right)f_{i-1}^{(k)} \\ &+ \left(4v^{(k)}(2(v^{(k)})^2-1)v^{(k+1)}-2v^{(k)}(v^{(k)}+1)\right)f_i^{(k)} \\ &+ \left(v^{(k)}+1-2v^{(k)}v^{(k+1)}\right)f_{i+1}^{(k)}\Big), \\ f_{2i+1}^{(k+1)} &= \frac{1}{8v^{(k+1)}v^{(k)}((v^{(k)})^2-1)}\Big(\left(v^{(k)}+1-2v^{(k)}v^{(k+1)}\right)f_{i-1}^{(k)} \\ &+ \left(4v^{(k)}(2(v^{(k)})^2-1)v^{(k+1)}-2v^{(k)}(v^{(k)}+1)\right)f_i^{(k)} \\ &+ \left((v^{(k)}+1)(2v^{(k)}-1)-2v^{(k)}v^{(k+1)}\right)f_{i+1}^{(k)}\Big). \end{cases}$$

- $n = 2$: the interpolatory 4-point scheme reproducing conics. The subdivision scheme with k-level symbol $F_2^{(k)}(z)$ coincides with the scheme proposed in [8], having refinement rules

$$\begin{cases} f_{2i}^{(k+1)} &= f_i^{(k)}, \\ f_{2i+1}^{(k+1)} &= \frac{1}{8v^{(k)}(v^{(k)}+1)}\left(-f_{i-1}^{(k)} + (2v^{(k)}+1)^2 f_i^{(k)} + (2v^{(k)}+1)^2 f_{i+1}^{(k)} - f_{i+2}^{(k)}\right). \end{cases}$$

- $n = 3$: the dual 4-point scheme reproducing conics. $F_3^{(k)}(z)$ is the k-level symbol associated to the subdivision scheme with refinement rules

$$\begin{cases} f_{2i}^{(k+1)} &= \frac{1}{32v^{(k)}((v^{(k)})^2-1)(v^{(k+1)})^3}\left(\left(2(v^{(k)})^2 + 3v^{(k)} + 1 - 6v^{(k)}(v^{(k+1)})^3\right) f_{i-1}^{(k)}\right. \\ &+ \left((12(v^{(k)})^2 - 7)v^{(k)}(v^{(k)}+1)v^{(k+1)} - 4(v^{(k)})^2 - 5v^{(k)} - 1\right) f_i^{(k)} \\ &+ \left(2(v^{(k)})^2 + v^{(k)} - 1 + 2(4(v^{(k)})^2 - 5)v^{(k)}(v^{(k+1)})^3\right) f_{i+1}^{(k)} \\ &+ \left.(v^{(k)}+1)(1 - v^{(k)}v^{(k+1)}) f_{i+2}^{(k)}\right), \\ f_{2i+1}^{(k+1)} &= \frac{1}{32v^{(k)}((v^{(k)})^2-1)(v^{(k+1)})^3}\left((v^{(k)}+1)(1 - v^{(k)}v^{(k+1)}) f_{i-1}^{(k)}\right. \\ &+ \left(2(v^{(k)})^2 + v^{(k)} - 1 + 2(4(v^{(k)})^2 - 5)v^{(k)}(v^{(k+1)})^3\right) f_i^{(k)} \\ &+ \left((12(v^{(k)})^2 - 7)v^{(k)}(v^{(k)}+1)v^{(k+1)} - 4(v^{(k)})^2 - 5v^{(k)} - 1\right) f_{i+1}^{(k)} \\ &+ \left.\left(2(v^{(k)})^2 + 3v^{(k)} + 1 - 6v^{(k)}(v^{(k+1)})^3\right) f_{i+2}^{(k)}\right), \end{cases}$$

  which has been recently proposed in [21].

- $n = 4$: a relaxation of the interpolatory 4-point scheme reproducing conics. The subdivision rules of the non-stationary scheme with k-level symbol $F_4^{(k)}(z)$ are

$$\begin{cases} f_{2i}^{(k+1)} &= \frac{1}{32v^{(k)}(v^{(k)}+1)^2}\left(-(2+v^{(k)}) f_{i-2}^{(k)} + \left(4(v^{(k)})^2(2+v^{(k)})\right) f_{i-1}^{(k)}\right. \\ &+ 2\left(12(v^{(k)})^3 + 24(v^{(k)})^2 + 17v^{(k)} + 2\right) f_i^{(k)} \\ &+ \left.\left(4(v^{(k)})^2(2+v^{(k)})\right) f_{i+1}^{(k)} - (2+v^{(k)}) f_{i+2}^{k}\right), \\ f_{2i+1}^{(k+1)} &= \frac{1}{8v^{(k)}(v^{(k)}+1)}\left(-f_{i-1}^{(k)} + (2v^{(k)}+1)^2 f_i^{(k)} + (2v^{(k)}+1)^2 f_{i+1}^{k} - f_{i+2}^{(k)}\right). \end{cases}$$

  Thus, it can be interpreted as a relaxation of the interpolatory 4-point scheme in [8], since they share the same odd-point rule.

Remark 4.29 *It is interesting to observe that all members of the family $\{F_n^{(k)}(z)\}_{n\geq 2}$ corresponding to odd values of n, being dual, are characterized by k-level refinement rules involving the parameters $v^{(k)}$ and $v^{(k+1)} = \sqrt{\frac{v^{(k)}+1}{2}}$. This is a direct consequence of the definition of $A_n^{(k)}(z)$ with n odd.*

4.3.4 A family of non-stationary interpolatory $2n$-point schemes

In this section we introduce a non-stationary variant of equation (4.41) and we show that it provides an explicit formula for the definition of a family of non-stationary interpolatory $2n$-point schemes featured by conic precision.

Proposition 4.30 *Let $I_{2n-2}(z)$ denote the Laurent polynomial of the $(2n-2)$-point Dubuc-Deslauriers scheme in (4.40). Let also $v^{(k)}$ be as in (3.11) and define the space*

$$\mathcal{W}^1_{2n-3} = span\{1,\, x,\, x^2,\, ...,\, x^{2n-3},\, e^{tx},\, e^{-tx}\}, \quad t \in [0,\pi) \cup \mathrm{i}\mathbb{R}^+.$$

For all $n \in \mathbb{N}$, $n \geq 2$, the non-stationary subdivision scheme with k-level symbol

$$I^{(k)}_{2n}(z) = I_{2n-2}(z) + (-1)^{n-1}\, \frac{\gamma^{(k)}_{n-2}}{2^{3(n-1)} v^{(k)} (v^{(k)}+1)^{n-1}} \left(z - \frac{1}{z}\right)^{2n-2} \left(z + \frac{1}{z}\right) \tag{4.51}$$

where

$$\gamma^{(k)}_{n-2} = \sum_{\ell=0}^{n-2} 2^{-\ell} \binom{n-2+\ell}{\ell} (v^{(k)}+1)^{\ell}, \tag{4.52}$$

is interpolatory and reproduces $\mathcal{W}^1_{2n-3}$.

Proof: To simplify notation, we define the Laurent polynomial

$$G^{(k)}_n(z) := (-1)^{n-1}\, \frac{\gamma^{(k)}_{n-2}}{2^{3(n-1)} v^{(k)} (v^{(k)}+1)^{n-1}} \left(z - \frac{1}{z}\right)^{2n-2} \left(z + \frac{1}{z}\right), \tag{4.53}$$

such that $I^{(k)}_{2n}(z)$ can be simply written as $I^{(k)}_{2n}(z) = I_{2n-2}(z) + G^{(k)}_n(z)$. Since $G^{(k)}_n(z)$ verifies $G^{(k)}_n(z) + G^{(k)}_n(-z) = 0$ and $I_{2n-2}(z)$ fulfills the interpolatory condition in (2.11) $I_{2n-2}(z) + I_{2n-2}(-z) = 2$, it clearly follows that $I^{(k)}_{2n}(z) + I^{(k)}_{2n}(-z) = 2$ and hence the non-stationary $2n$-point scheme is also interpolatory.
Moreover, from the polynomial reproduction properties of the $(2n-2)$-point interpolatory Dubuc-Deslauriers scheme we know that

$$D^{\ell} I_{2n-2}(-1) = 0, \qquad \ell = 0, \ldots, 2n-3.$$

Taking into account that the symbol $I_{2n-2}(z)$ also satisfies

$$\begin{aligned} I_{2n-2}(-e^{\frac{t}{2^{k+1}}}) &= I_{2n-2}(-e^{-\frac{t}{2^{k+1}}}) \\ &= \frac{(-1)^{n-1}}{2^{2n-3}} \frac{(e^{\frac{t}{2^{k+1}}}-1)^{2n-2}}{(e^{\frac{t}{2^{k+1}}})^{n-1}} \sum_{\ell=0}^{n-2} 2^{-2\ell} \binom{n-2+\ell}{\ell} \frac{(e^{\frac{t}{2^{k+1}}}+1)^{2\ell}}{(e^{\frac{t}{2^{k+1}}})^{\ell}}, \end{aligned}$$

while the Laurent polynomial $G^{(k)}_n(z)$ in (4.53) is such that

$$D^{\ell} G^{(k)}_n(-1) = 0, \qquad \ell = 0, \ldots, 2n-3,$$

and

$$G^{(k)}_n(-e^{\frac{t}{2^{k+1}}}) = G^{(k)}_n(-e^{-\frac{t}{2^{k+1}}}) = \frac{(-1)^{n}}{2^{2n-3}} \frac{(e^{\frac{t}{2^{k+1}}}-1)^{2n-2}}{(e^{\frac{t}{2^{k+1}}})^{n-1}} \sum_{\ell=0}^{n-2} 2^{-2\ell} \binom{n-2+\ell}{\ell} \frac{(e^{\frac{t}{2^{k+1}}}+1)^{2\ell}}{(e^{\frac{t}{2^{k+1}}})^{\ell}},$$

we can conclude that

$$\begin{aligned} D^\ell I_{2n}^{(k)}(-1) &= 0, \qquad \ell = 0, \ldots, 2n-3, \\ I_{2n}^{(k)}(-e^{\frac{t}{2^{k+1}}}) &= 0, \\ I_{2n}^{(k)}(-e^{-\frac{t}{2^{k+1}}}) &= 0. \end{aligned}$$

Therefore, in view of Proposition 3.6, the scheme with k-level symbol in (4.51) generates $\mathcal{W}_{2n-3}$ for all $n \in \mathbb{N}$, $n \geq 2$, and thus, being interpolatory, it also reproduces $\mathcal{W}_{2n-3}^1$. ■

Remark 4.31 *Since* $\gamma_{n-2}^{(k)}$ *in* (4.52) *verifies* $\lim_{k\to\infty} \gamma_{n-2}^{(k)} = \binom{2n-3}{n-1}$*, the family of non-stationary interpolatory* $2n$*-point schemes with* k*-level symbol* (4.51) *is asymptotically similar to the family of* $2n$*-point interpolatory Dubuc-Deslauriers schemes with symbol in* (4.41)*.*

Proposition 4.32 *For all* $n \in \mathbb{N}$ *the non-stationary subdivision scheme with* k*-level symbol* $I_{2n}^{(k)}(z)$ *has the same integer smoothness as the stationary* $2n$*-point interpolatory Dubuc-Deslauriers scheme with symbol* $I_{2n}(z)$*.*

Proof: From [42], for all $n \in \mathbb{N}$ the stationary $2n$-point Dubuc-Deslauriers scheme is C^r continuous with $r \leq n-1$, and from Remark 4.31 the non-stationary scheme with k-level symbol $I_{2n}^{(k)}(z)$ is asymptotically similar to $I_{2n}(z)$. Moreover, $I_{2n}^{(k)}(z)$ satisfies the approximate sum rules of order n. In fact, $I_{2n}^{(k)}(1) = 2$ for all $n \in \mathbb{N}$ and $k \in \mathbb{N}_0$ and since, in view of Proposition 4.30 $I_{2n}^{(k)}(z)$ generates Π_{2n-3}^1, we have that

$$\max_{\ell=0,\ldots,n-1} \left| D^\ell I_{2n}^{(k)}(-1) \right| = 0 \quad \text{for all } n \in \mathbb{N},\ k \in \mathbb{N}_0.$$

Thus, from Corollary 3.17, the claim is proven. ■

As seen in the stationary case, we conclude the section by showing that the first member of the non-stationary Lane-Riesenfeld's family, $A_0^{(k)}(z)$, and that of the corresponding Hormann-Sabin's family, $F_2^{(k)}(z)$, can be used as building blocks to obtain the family of non-stationary interpolatory $2n$-point schemes with k-level symbols $\{I_{2n}^{(k)}(z)\}_{n\geq 2}$ by means of two- and three-term recurrence relations.

Lemma 4.33 *For all* $n \in \mathbb{N}$*,* $n \geq 3$*, the factors* $\gamma_{n-2}^{(k)}$ *in* (4.52) *and*

$$\gamma_{n-3}^{(k)} = \sum_{\ell=0}^{n-3} 2^{-\ell} \binom{n-3+\ell}{\ell} (v^{(k)}+1)^\ell, \tag{4.54}$$

satisfy the relation

$$\gamma_{n-3}^{(k)} = \frac{1-v^{(k)}}{2}\, \gamma_{n-2}^{(k)} + v^{(k)} \left(\frac{v^{(k)}+1}{2}\right)^{n-2} \binom{2n-5}{n-2}.$$

Proof: After rewriting $\gamma_{n-3}^{(k)}$ in the following equivalent form,

$$\gamma_{n-3}^{(k)} = \sum_{\ell=0}^{n-2} 2^{-\ell} \binom{n-3+\ell}{\ell} (v^{(k)}+1)^{\ell} - 2^{-(n-2)} \binom{2n-5}{n-2} (v^{(k)}+1)^{n-2},$$

by using the well-known relation $\binom{n-2+\ell}{\ell} = \binom{n-3+\ell}{\ell} + \binom{n-3+\ell}{\ell-1}$ on binomial coefficients, we get

$$\begin{aligned}
\gamma_{n-3}^{(k)} &= \sum_{\ell=0}^{n-2} 2^{-\ell} \binom{n-2+\ell}{\ell} (v^{(k)}+1)^{\ell} - \frac{v^{(k)}+1}{2} \sum_{\ell=0}^{n-3} 2^{-\ell} \binom{n-2+\ell}{\ell} (v^{(k)}+1)^{\ell} \\
&- 2^{-(n-2)} \binom{2n-5}{n-2} (v^{(k)}+1)^{n-2} \\
&= \gamma_{n-2}^{(k)} - \frac{v^{(k)}+1}{2} \left(\gamma_{n-2}^{(k)} - 2^{-(n-2)} \binom{2n-4}{n-2} (v^{(k)}+1)^{n-2} \right) \\
&- 2^{-(n-2)} \binom{2n-5}{n-2} (v^{(k)}+1)^{n-2} \\
&= \frac{1-v^{(k)}}{2} \gamma_{n-2}^{(k)} + 2^{-(n-2)} (v^{(k)}+1)^{n-2} \left(\frac{v^{(k)}+1}{2} \binom{2n-4}{n-2} - \binom{2n-5}{n-2} \right).
\end{aligned}$$

Finally, using the fact that $\frac{1}{2}\binom{2n-4}{n-2} = \binom{2n-5}{n-2}$, the claimed result is obtained. ■

Proposition 4.34 *Let $v^{(k)}$ be as in (3.11) and $I_2^{(k)}(z) = A_0^{(k)}(z) = \frac{z^2+2v^{(k)}z+1}{2v^{(k)}z}$. For all $n \in \mathbb{N}$, $n \geq 2$, the non-stationary subdivision scheme with k-level symbol $I_{2n}^{(k)}(z)$ in (4.51) satisfies the two-term recurrence relation*

$$\begin{aligned}
I_{2n}^{(k)}(z) &= I_{2n-2}^{(k)}(z) \\
&+ (-1)^{n-1} \left(z - \frac{1}{z}\right)^{2n-4} \left(z + \frac{1}{z}\right) \left(z^2 - (4(v^{(k)})^2 - 2) + \frac{1}{z^2}\right) \frac{\gamma_{n-2}^{(k)}}{2^{3(n-1)} v^{(k)} (v^{(k)}+1)^{n-1}},
\end{aligned} \tag{4.55}$$

where $\gamma_{n-2}^{(k)}$ is defined as in (4.52).

Proof: From equations (4.40) and (4.51) we obtain

$$I_{2n}^{(k)}(z) - I_{2n-2}^{(k)}(z) = \frac{(-1)^{n-2}}{2^{4(n-2)}} \binom{2n-5}{n-2} \left(z - \frac{1}{z}\right)^{2n-4} \left(z + \frac{1}{z}\right) + G_n^{(k)}(z) - G_{n-1}^{(k)}(z),$$

with $G_n^{(k)}(z)$ in (4.53). Introducing the explicit expression of $G_n^{(k)}(z) - G_{n-1}^{(k)}(z)$ and simplifying the result, we have that

$$\begin{aligned}
I_{2n}^{(k)}(z) - I_{2n-2}^{(k)}(z) &= \frac{(-1)^{n-1}}{2^{3(n-1)}} \left(z - \frac{1}{z}\right)^{2n-4} \left(z + \frac{1}{z}\right) \left(- \frac{1}{2^{n-5}} \binom{2n-5}{n-2} \right. \\
&\left. + \frac{\gamma_{n-2}^{(k)}}{v^{(k)}(v^{(k)}+1)^{n-1}} \left(z - \frac{1}{z}\right)^2 + \frac{8\gamma_{n-3}^{(k)}}{v^{(k)}(v^{(k)}+1)^{n-2}} \right).
\end{aligned}$$

Finally, using Lemma 4.33, we can write

$$\frac{8\gamma_{n-3}^{(k)}}{v^{(k)}(v^{(k)}+1)^{n-2}} = \frac{4(1-v^{(k)})}{v^{(k)}(v^{(k)}+1)^{n-2}}\,\gamma_{n-2}^{(k)} + \frac{1}{2^{n-5}}\binom{2n-5}{n-2},$$

and hence the claim is obtained. ■

The following corollary is a straightforward consequence of the result in Proposition 4.34.

Corollary 4.35 *Let*

$$I_2^{(k)}(z) = A_0^{(k)}(z) = \frac{z^2+2v^{(k)}z+1}{2v^{(k)}z},$$

and

$$I_4^{(k)}(z) = F_2^{(k)}(z) = \frac{(z+1)^2(z^2+2v^{(k)}z+1)(-z^2+2(v^{(k)}+1)z-1)}{8v^{(k)}(v^{(k)}+1)z^3}.$$

For all $n \in \mathbb{N}$, $n \geq 3$, the symbol $I_{2n}^{(k)}(z)$ of Proposition 4.34 satisfies the three-term recurrence relation

$$I_{2n}^{(k)}(z) = I_{2n-2}^{(k)}(z) - \frac{(z^2-1)^2}{8(v^{(k)}+1)z^2}\,\frac{\gamma_{n-2}^{(k)}}{\gamma_{n-3}^{(k)}}\left(I_{2n-2}^{(k)}(z) - I_{2n-4}^{(k)}(z)\right),$$

with $\gamma_{n-2}^{(k)}$ in (4.52) and $\gamma_{n-3}^{(k)}$ in (4.54).

Remark 4.36 *The subdivision scheme with symbol $I_6^{(k)}(z)$, obtained from the family $\{I_{2n}^{(k)}(z)\}_{n\geq 1}$ when setting $n = 3$, coincides with the interpolatory 6-point scheme proposed in [119, Section 4.1].*

Chapter 5

Smoothness analysis near extraordinary elements

Univariate stationary subdivision schemes could be easily generalized to the bivariate setting, defining subdivision surfaces on regular meshes. However, stationary bivariate subdivision schemes defined only on regular meshes can not be used in many applications. In fact in order to design surfaces of general topology, it is necessary to introduce irregular vertices and faces in the initial control mesh, together with special valence-dependent refinement rules. Moreover, to design particular shapes such as spheres, ellipsoids, cylinders and tori, it is necessary to pass from stationary to non-stationary rules.
In this chapter, we focus on stationary subdivision schemes applied on arbitrary manifold topology meshes. Since in this case the limit surface and its properties are known away from a finite number of points corresponding to the extraordinary elements, the analysis of the subdivision scheme is concentrated at these points. Moreover, we pay particular attention to the special refinement rules that have to be applied near an extraordinary element in order to obtain C^1 limit surfaces with bounded curvature and optimal shrinkage.
In the first following section, we show how to choose the weights of the extraordinary stencils in case of an interpolatory subdivision scheme based on quadrilateral meshes. We also propose a choice for these weights which improves the schemes in [84, 93, 39]. The second section is devoted to the description of a new general computational strategy based on the block diagonalization of subdivision matrices via unitary transforms associated with the block-Fourier matrix that could be used to choose the weights of the extraordinary stencils for any kind of stationary subdivision schemes. We apply this method to define new extraordinary weights for binary and ternary Loop's scheme [96, 97] defined on triangular meshes.

5.1 A quad-based interpolatory subdivision scheme

This section deals with interpolatory subdivision schemes generalizing the tensor-product version of the Dubuc-Deslauriers 4-point scheme to quadrilateral meshes of arbitrary manifold topology. Among these schemes, we can find proposals featured by edge-point rules that, near an extraordinary vertex of valence n, either involve $2n + 2$ vertices from the coarser mesh or only a subset of $n + 2$ of them. The existing schemes falling into the first group (see [84, 92, 94]), besides more computationally expensive, are C^1 smooth with unbounded curvature at extraordinary points. Among these schemes there is also the well-known Kobbelt's

scheme already recalled in Section 2.4.5. As a matter of fact, dealing with refinement rules of larger size not only increases the computational costs for generating the limit surface, but remarkably complicates the tuning of the weights appearing in the affine combination such that bounded curvature at extraordinary points is hardly satisfied. In light of this, we believe strategic to restrict our attention to the subclass of interpolatory subdivision schemes for closed quadrilateral meshes that compute

(i) new edge-points near extraordinary vertices of valence n by means of an affine combination of $n+2$ vertices from the coarser mesh;

(ii) new face-points near extraordinary vertices of valence n by means of an affine combination of $2n+8$ vertices from the coarser mesh.

Due to requirement (i), the rule for positioning a new vertex on an edge relies only on edge adjacent vertices and not on face adjacent vertices (see Figure 5.2). This assumption not only allows the algorithm to reduce the computational costs for generating the limit surface, but reveals that the subdivision scheme can also be thought of as a subdivision scheme for curve networks [123]. To the best of our knowledge, the only existing interpolatory subdivision schemes with the property that the position of new edge points is determined exclusively by edge adjacent vertices, are the ones proposed by Schaefer-Warren [123], Li-Ma-Bao [93] and Deng-Ma [39]. All such schemes have been shown independently by their authors to be suitable for generating limit surfaces that are globally C^1 continuous, but while the two most recent ones (namely [39, 93]) have also both principal curvatures bounded at extraordinary points, this is not the case for their precursor in [123]. The aim consists in identifying which constraints are required to be fulfill by the weights appearing in the above stencils in order to get closed limit surfaces that are C^1 continuous at extraordinary points, have both principal curvatures bounded and at least one of them nonzero.

5.1.1 Edge-point and face-point rules

We consider an interpolatory subdivision scheme on quadrilateral meshes generalizing the tensor-product of the 4-point Dubuc–Deslauriers scheme [42, 49]. This means that, when the mesh is regular, that is each vertex has valence $n=4$, the rule for computing the edge-point E_4 is nothing but the 4-point scheme applied to the vertices P_{-1}, P_1, P_0, P_5 (see Figure 5.1), i.e.

$$E_4 = -\frac{1}{16}P_{-1} + \frac{9}{16}P_1 + \frac{9}{16}P_0 - \frac{1}{16}P_5, \tag{5.1}$$

while the rule for computing the face-point F_4 is exactly the tensor-product of the edge-point rule, namely

$$\begin{aligned} F_4 &= \frac{1}{256}(P_{-3}+P_{-8}+P_{-6}+P_6) + \frac{81}{256}(P_0+P_1+P_2+P_3) \\ &- \frac{9}{256}(P_{-1}+P_{-2}+P_{-4}+P_{-5}+P_4+P_5+P_7+P_8). \end{aligned} \tag{5.2}$$

On the other hand, for meshes of arbitrary manifold topology, special edge-point and face-point rules are defined in the vicinity of extraordinary vertices of valence $n \neq 4$. Here, we study subdivision schemes that apply an $(n+2)$-point and a $(2n+8)$-point stencil respectively for computing edge- and face-points in the neighborhood of an extraordinary vertex

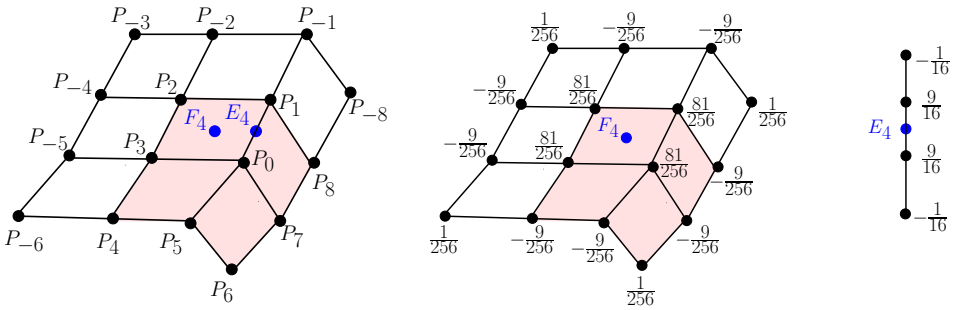

Figure 5.1: Edge-point and face-point rules for regular regions.

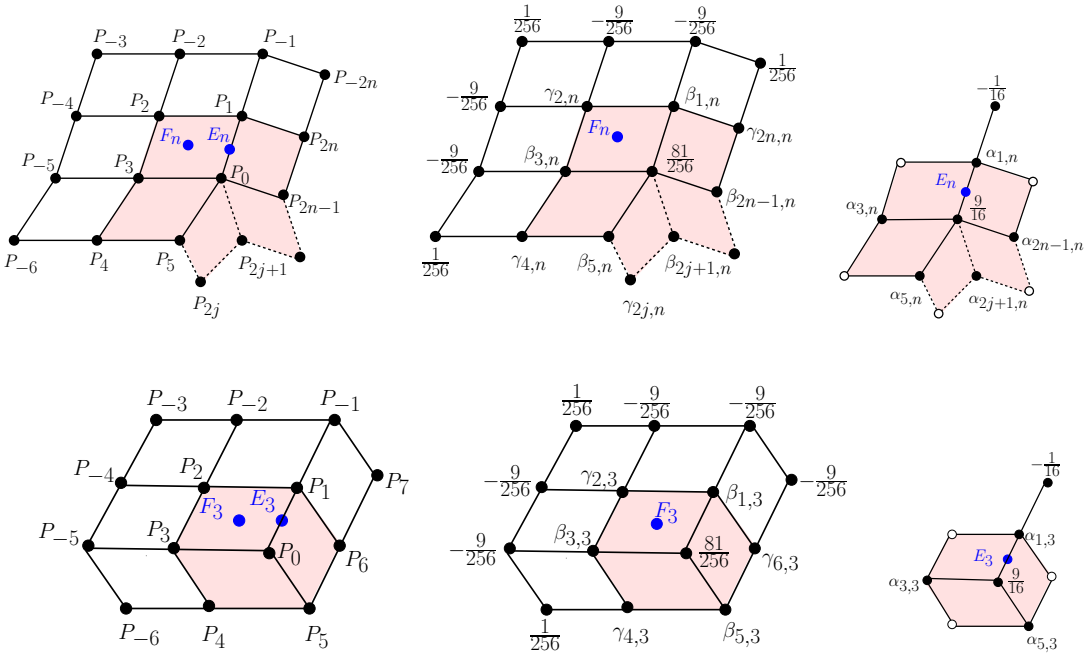

Figure 5.2: Edge-point and face-point rules in the neighborhood of extraordinary vertices of valence $n \geq 5$ (top) and $n = 3$ (bottom).

of valence $n \neq 4$ (see Figure 5.2). More precisely, the edge-point rule used in presence of an extraordinary vertex P_0 of valence $n = 3$ is

$$E_3 = -\frac{1}{16}P_{-1} + \frac{9}{16}P_0 + \alpha_{1,3}P_1 + \alpha_{3,3}P_3 + \alpha_{5,3}P_5, \tag{5.3}$$

with $\alpha_{1,3}, \alpha_{3,3}, \alpha_{5,3} \in \mathbb{R}$, while the general edge-point rule to be used when P_0 has valence $n \geq 5$ reads as

$$E_n = -\frac{1}{16}P_{-1} + \frac{9}{16}P_0 + \sum_{j=1}^{n} \alpha_{2j-1,n}P_{2j-1} \tag{5.4}$$

with $\alpha_{2j-1,n} \in \mathbb{R}$ for all $j = 1, \ldots, n$. Thus for all $n \neq 4$ the edge-point rule is defined by an affine combination involving P_{-1}, P_0 and all vertices connected to P_0 by an edge. Analogously, for the face-point rule we consider an affine combination of the four vertices

identifying the face of insertion (i.e., P_0, P_1, P_2, P_3) plus the first ring of vertices around it. In formulas, the face-point rule for the case $n = 3$ is given by

$$\begin{aligned} F_3 &= \frac{1}{256}(P_{-3} + P_{-6} + P_7) + \frac{81}{256}P_0 - \frac{9}{256}(P_{-1} + P_{-2} + P_{-4} + P_{-5}) \\ &+ \beta_{1,3}P_1 + \beta_{3,3}P_3 + \beta_{5,3}P_5 + \gamma_{2,3}P_2 + \gamma_{4,3}P_4 + \gamma_{6,3}P_6, \end{aligned} \tag{5.5}$$

with $\beta_{1,3}, \beta_{3,3}, \beta_{5,3} \in \mathbb{R}$ and $\gamma_{2,3}, \gamma_{4,3}, \gamma_{6,3} \in \mathbb{R}$, while for the general case $n \geq 5$ it reads as

$$\begin{aligned} F_n &= \frac{1}{256}(P_{-3} + P_{-6} + P_{-2n}) + \frac{81}{256}P_0 - \frac{9}{256}(P_{-1} + P_{-2} + P_{-4} + P_{-5}) \\ &+ \sum_{j=1}^{n} \beta_{2j-1,n}P_{2j-1} + \sum_{j=1}^{n} \gamma_{2j,n}P_{2j} \end{aligned} \tag{5.6}$$

with $\beta_{2j-1,n}, \gamma_{2j,n} \in \mathbb{R}$ for all $j = 1, \ldots, n$. In order to guarantee the symmetry of the scheme and a good visual quality of the limit surface we require the above coefficients to be such that

$$\begin{aligned} &|\alpha_{1,n}| > |\alpha_{2j-1,n}|, \quad j = 2, \ldots, n, \\ &|\beta_{1,n}| = |\beta_{3,n}| > |\beta_{5,n}| = |\beta_{2n-1,n}| > |\beta_{2j-1,n}|, \quad j = 4, \ldots, n-1, \\ &|\gamma_{2,n}| > |\gamma_{4,n}| = |\gamma_{2n,n}| > |\gamma_{2j,n}|, \quad j = 3, \ldots, n-1. \end{aligned}$$

Taking into account that the regular rules in (5.1) - (5.2) are well-known to generate C^1 limit surfaces (see [42, 49]), the goal of this work is to identify the conditions that the free parameters involved in the extraordinary rules have to satisfy in order to guarantee C^1 smoothness also at extraordinary points. To this end, we start by considering the necessary conditions for convergence, inferred by the requirement that the weights of the edge- and face-point stencils sum up to 1 [112].

Condition 1.a *For all $n \neq 4$ the necessary conditions for convergence can be shortly written as*

$$A_0^n = \frac{1}{2} \qquad \textit{and} \qquad B_0^n + C_0^n = \frac{13}{16},$$

by introducing the auxiliary notation

$$A_0^n := \sum_{j=1}^{n} \alpha_{2j-1,n}, \qquad B_0^n := \sum_{j=1}^{n} \beta_{2j-1,n}, \qquad C_0^n := \sum_{j=1}^{n} \gamma_{2j,n}. \tag{5.7}$$

5.1.2 The local subdivision matrix

By ordering the points as explained in Order 2 (see Section 2.3), the subdivision rules in (5.1)-(5.2) and (5.4)-(5.6) allow one to construct a local subdivision matrix $\tilde{S} \in \mathbb{R}^{(6n+1)\times(6n+1)}$ of the form in (2.21) where we consider $p = 6$ points in each sector. In particular, $\tilde{a} = 0$, $\tilde{\mathbf{b}} = \mathbf{0}$, $\tilde{\mathbf{c}} = \left(\frac{9}{16}, \frac{81}{256}, 0, 0, 0, 0\right)^T$ and the blocks are

$$\tilde{M}_0 = \begin{pmatrix} \alpha_{1,n} & 0 & -\frac{1}{16} & 0 & 0 & 0 \\ \beta_{1,n} & \gamma_{2,n} & -\frac{9}{256} & -\frac{9}{256} & \frac{1}{256} & -\frac{9}{256} \\ 1 & 0 & 0 & 0 & 0 & 0 \\ \frac{9}{16} & \frac{9}{16} & 0 & 0 & 0 & -\frac{1}{16} \\ 0 & 1 & 0 & 0 & 0 & 0 \\ 0 & \frac{9}{16} & 0 & -\frac{1}{16} & 0 & 0 \end{pmatrix}, \qquad \tilde{M}_1 = \begin{pmatrix} \alpha_{3,n} & 0 & 0 & 0 & 0 & 0 \\ \beta_{3,n} & \gamma_{4,n} & -\frac{9}{256} & \frac{1}{256} & 0 & 0 \\ 0 & 0 & 0 & 0 & 0 & 0 \\ 0 & 0 & 0 & 0 & 0 & 0 \\ 0 & 0 & 0 & 0 & 0 & 0 \\ \frac{9}{16} & -\frac{1}{16} & 0 & 0 & 0 & 0 \end{pmatrix},$$

$$\tilde{M}_i = \begin{pmatrix} \alpha_{2i+1,n} & 0 & 0 & 0 & 0 & 0 \\ \beta_{2i+1,n} & \gamma_{2i+2,n} & 0 & 0 & 0 & 0 \\ 0 & 0 & 0 & 0 & 0 & 0 \\ 0 & 0 & 0 & 0 & 0 & 0 \\ 0 & 0 & 0 & 0 & 0 & 0 \\ 0 & 0 & 0 & 0 & 0 & 0 \end{pmatrix}, \; i = 2, \ldots, n-2, \quad \tilde{M}_{n-1} = \begin{pmatrix} \alpha_{2n-1,n} & 0 & 0 & 0 & 0 & 0 \\ \beta_{2n-1,n} & \gamma_{2n,n} & 0 & 0 & 0 & \frac{1}{256} \\ 0 & 0 & 0 & 0 & 0 & 0 \\ 0 & -\frac{1}{16} & 0 & 0 & 0 & 0 \\ 0 & 0 & 0 & 0 & 0 & 0 \\ 0 & 0 & 0 & 0 & 0 & 0 \end{pmatrix}.$$

$\tilde{S}$ thus provides a compact representation of a single refinement step restricted to the vertices within the 2-ring of an extraordinary vertex P_0 of valence $n \geq 5$. Using the trasformation in (2.22), we denote

$$M_j := \begin{pmatrix} \frac{1}{n} & \mathbf{0} \\ \frac{\mathbf{c}}{n} & \tilde{M}_j \end{pmatrix} \in \mathbb{R}^{7\times 7}, \quad j = 0, \ldots, n-1,$$

we construct the $n \times n$ block-circulant matrix

$$S = \left(\begin{array}{c|c|c|c|c} M_0 & M_1 & \cdots & M_{n-2} & M_{n-1} \\ \hline M_{n-1} & M_0 & M_1 & \cdots & M_{n-2} \\ \hline M_{n-2} & \ddots & \ddots & \ddots & \vdots \\ \hline \vdots & \ddots & \ddots & \ddots & M_1 \\ \hline M_1 & \cdots & M_{n-2} & M_{n-1} & M_0 \end{array}\right), \tag{5.8}$$

and applying a discrete Fourier transform explained in Method 2 (see Section 2.3) to the blocks M_j, $j = 0, \ldots, n-1$, we obtain the blocks

$$\hat{S}_\nu = \sum_{j=0}^{n-1} M_j \omega^{j\nu}, \quad \nu = 0, \ldots, n-1 \quad \text{with} \quad \omega = e^{\frac{2\pi \mathrm{i}}{n}},$$

defining the block-diagonal matrix

$$\hat{S} = \left(\begin{array}{c|c|c|c|c} \hat{S}_0 & 0 & \cdots & 0 & 0 \\ \hline 0 & \hat{S}_1 & 0 & \cdots & 0 \\ \hline \vdots & \ddots & \ddots & \ddots & \vdots \\ \hline 0 & \cdots & 0 & \hat{S}_{n-2} & 0 \\ \hline 0 & \cdots & 0 & 0 & \hat{S}_{n-1} \end{array}\right) \in \mathbb{R}^{7n\times 7n},$$

for which $n-1$ eigenvalues are zero and all the others are exactly the eigenvalues of $\tilde{S}$. For each rotational frequency component $\nu = 0, \ldots, n-1$ the general block $\hat{S}_\nu \in \mathbb{R}^{7\times 7}$ is of the form

$$\hat{S}_\nu = \begin{pmatrix} w^n_{0,\nu} & 0 & 0 & 0 & 0 & 0 & 0 \\ w^n_{1,\nu} & A^n_\nu & 0 & -\frac{1}{16} & 0 & 0 & 0 \\ w^n_{2,\nu} & B^n_\nu & C^n_\nu & -\frac{9+9\omega^\nu}{256} & \frac{-9+\omega^v}{256} & \frac{1}{256} & \frac{-9+\omega^{(n-1)\nu}}{256} \\ 0 & 1 & 0 & 0 & 0 & 0 & 0 \\ 0 & \frac{9}{16} & \frac{9-\omega^{(n-1)\nu}}{16} & 0 & 0 & 0 & -\frac{1}{16} \\ 0 & 0 & 1 & 0 & 0 & 0 & 0 \\ 0 & \frac{9}{16}\omega^\nu & \frac{9-\omega^\nu}{16} & 0 & -\frac{1}{16} & 0 & 0 \end{pmatrix}, \tag{5.9}$$

where

$$A_\nu^n := \sum_{j=1}^{n} \alpha_{2j-1,n}\, \omega^{(j-1)\nu}, \qquad B_\nu^n := \sum_{j=1}^{n} \beta_{2j-1,n}\, \omega^{(j-1)\nu}, \qquad C_\nu^n := \sum_{j=1}^{n} \gamma_{2j,n}\, \omega^{(j-1)\nu}, \tag{5.10}$$

and

$$w_{0,\nu}^n := \frac{1}{n}\sum_{j=0}^{n-1} \omega^{j\nu} = \delta_{\nu,0}, \quad w_{1,\nu}^n := \frac{1}{n}\sum_{j=0}^{n-1} \frac{9}{16}\omega^{j\nu} = \frac{9}{16}\delta_{\nu,0}, \quad w_{2,\nu}^n := \frac{1}{n}\sum_{j=0}^{n-1} \frac{81}{256}\omega^{j\nu} = \frac{81}{256}\delta_{\nu,0}, \tag{5.11}$$

with $\delta_{\nu,0}$ denoting the Kronecker delta function.

Remark 5.1 *Definition* (5.10) *implies that* $A_\nu^n, B_\nu^n, C_\nu^n \in \mathbb{C}$ *for* $\nu \neq 0$. *Indeed, we will show in Section 5.1.3 that choosing* $A_\nu^n, C_\nu^n \in \mathbb{R}$ *for all* $\nu = 0, \dots, n-1$ *we can obtain a local subdivision matrix* S *with the desired spectrum.*

Now, let λ_j^ν, $j = 0, \dots, 6$ denote the eigenvalues of the matrix $\hat{S}_\nu$ in (5.9). Furthermore, as recalled in Definition 2.30, whenever μ is an eigenvalue of $\hat{S}_\nu$, we call ν the Fourier index of μ and we write $\mathcal{F}(\mu) = \nu$.
The complete spectrum of the local subdivision matrix $\hat{S}$ could be written as

$$\Lambda^{[n]} = \bigcup_{\nu=0}^{n-1} \{\lambda_0^\nu,\, \lambda_1^\nu,\, \lambda_2^\nu,\, \lambda_3^\nu,\, \lambda_4^\nu,\, \lambda_5^\nu,\, \lambda_6^\nu\}.$$

Let $\mathbf{I}_n$ denote the $n \times n$ identity matrix. To work out the explicit expressions of the eigenvalues of each block $\hat{S}_\nu$ we have to compute the roots of the characteristic polynomial $\det(\hat{S}_\nu - \lambda\, \mathbf{I}_7)$. Using Laplace Expansion Theorem we can write

$$\det(\hat{S}_\nu - \lambda\, \mathbf{I}_7) = \Big(w_{0,\nu}^n - \lambda\Big) \cdot \det(\hat{M}_\nu - \lambda\, \mathbf{I}_6), \tag{5.12}$$

where $\hat{M}_\nu$ is the 6×6 sub-matrix of $\hat{S}_\nu$ given by

$$\hat{M}_\nu = \begin{pmatrix} A_\nu^n & 0 & -\frac{1}{16} & 0 & 0 & 0 \\ B_\nu^n & C_\nu^n & -\frac{9+9\omega^\nu}{256} & \frac{-9+\omega^v}{256} & \frac{1}{256} & \frac{-9+\omega^{(n-1)\nu}}{256} \\ 1 & 0 & 0 & 0 & 0 & 0 \\ \frac{9}{16} & \frac{9-\omega^{(n-1)\nu}}{16} & 0 & 0 & 0 & -\frac{1}{16} \\ 0 & 1 & 0 & 0 & 0 & 0 \\ \frac{9}{16}\omega^\nu & \frac{9-\omega^\nu}{16} & 0 & -\frac{1}{16} & 0 & 0 \end{pmatrix}. \tag{5.13}$$

As a straightforward consequence of the factorization in (5.12) we have that the eigenvalue of the real matrix $\hat{S}_0$ that firstly emerges is $\lambda_0^0 = w_{0,0}^n = 1$. Thus $\mathcal{F}(1) = 0$. In contrast, for $\nu = 1, \dots, n-1$, we find $\lambda_0^\nu = w_{0,\nu}^n = 0$, so obtaining all $n-1$ zero eigenvalues of $\hat{S}$. To compute the remaining eigenvalues of the matrix $\hat{S}_\nu$ (i.e. λ_j^ν, $j = 1, \dots, 6$ in our notation), we have to compute the eigenvalues of its submatrix $\hat{M}_\nu$, i.e. the roots of the characteristic polynomial $\det(\hat{M}_\nu - \lambda \mathbf{I}_6)$. For this purpose we consider the permutation matrix

$$\mathbf{P}_{2,3} = \begin{pmatrix} 1 & 0 & 0 & 0 & 0 & 0 \\ 0 & 0 & 1 & 0 & 0 & 0 \\ 0 & 1 & 0 & 0 & 0 & 0 \\ 0 & 0 & 0 & 1 & 0 & 0 \\ 0 & 0 & 0 & 0 & 1 & 0 \\ 0 & 0 & 0 & 0 & 0 & 1 \end{pmatrix},$$

and observe that, applying $\mathbf{P}_{2,3}$ to the left and to the right of $\hat{M}_\nu$, we get the block-triangular matrix

$$\overline{M}_\nu = \mathbf{P}_{2,3}\hat{M}_\nu\mathbf{P}_{2,3} = \left(\begin{array}{c|c} \mathbf{K}_1 & \mathbf{O} \\ \hline \mathbf{K}_2 & \mathbf{K}_3 \end{array}\right), \tag{5.14}$$

where $\mathbf{O}$ is the 2×2 null matrix, $\mathbf{K}_1 \in \mathbb{R}^{2\times 2}, \mathbf{K}_2 \in \mathbb{R}^{4\times 2}$ and $\mathbf{K}_3 \in \mathbb{R}^{4\times 4}$. Hence, the roots of the characteristic polynomial of $\hat{M}_\nu$ can be more easily found by computing the roots of the characteristic polynomial of $\overline{M}_\nu$ since the latter can be conveniently factorized as

$$\det(\overline{M}_\nu - \lambda\mathbf{I}_6) = \det(\mathbf{K}_1 - \lambda\mathbf{I}_2)\cdot\det(\mathbf{K}_3 - \lambda\mathbf{I}_4).$$

The six eigenvalues of $\overline{M}_\nu$ are indeed the two roots of

$$\det(\mathbf{K}_1 - \lambda\mathbf{I}_2) = \lambda^2 - A_\nu^n\lambda + \tfrac{1}{16},$$

and the four roots of

$$\det(\mathbf{K}_3 - \lambda\mathbf{I}_4) = \lambda^4 - C_\nu^n\lambda^3 + g_\nu\lambda^2 + h_\nu\lambda + \tfrac{1}{2^{16}},$$

where

$$g_\nu := -\frac{3(3\omega^{2\nu} - 22\omega^\nu + 3)}{2^{11}\omega^\nu} = -\frac{3}{2^{10}}\Big(3\cos\left(\frac{2\pi\nu}{n}\right) - 11\Big)$$

and

$$\begin{aligned} h_\nu &:= \frac{-1 + 18\omega^\nu + 256C_\nu^n\omega^{2\nu} - 162\omega^{2\nu} + 18\omega^{3\nu} - \omega^{4\nu}}{2^{16}\omega^{2\nu}} \\ &= \frac{1}{2^{15}}\Big(128C_\nu^n - 80 + 18\cos\left(\frac{2\pi\nu}{n}\right) - 2\cos^2\left(\frac{2\pi\nu}{n}\right)\Big). \end{aligned}$$

Computing the roots of the quadratic polynomial we find

$$\lambda_1^\nu = \frac{2A_\nu^n + \sqrt{4(A_\nu^n)^2 - 1}}{4}, \qquad \lambda_2^\nu = \frac{2A_\nu^n - \sqrt{4(A_\nu^n)^2 - 1}}{4}, \tag{5.15}$$

while computing those of the quartic one we get

$$\begin{aligned} \lambda_3^\nu &= \frac{C_\nu^n}{4} - S_\nu + \frac{1}{2}\sqrt{-4S_\nu^2 - 2R_\nu + \frac{T_\nu}{S_\nu}}, & \lambda_4^\nu &= \frac{C_\nu^n}{4} - S_\nu - \frac{1}{2}\sqrt{-4S_\nu^2 - 2R_\nu + \frac{T_\nu}{S_\nu}}, \\ \lambda_5^\nu &= \frac{C_\nu^n}{4} + S_\nu + \frac{1}{2}\sqrt{-4S_\nu^2 - 2R_\nu - \frac{T_\nu}{S_\nu}}, & \lambda_6^\nu &= \frac{C_\nu^n}{4} + S_\nu - \frac{1}{2}\sqrt{-4S_\nu^2 - 2R_\nu - \frac{T_\nu}{S_\nu}}, \end{aligned} \tag{5.16}$$

where

$$\begin{aligned} R_\nu &= \frac{8g_\nu - 3(C_\nu^n)^2}{8}, & T_\nu &= \frac{-(C_\nu^n)^3 + 4C_\nu^n g_\nu + 8h_\nu}{8}, \\ \Delta_{\nu,0} &= g_\nu^2 + 3C_\nu^n h_\nu + \frac{3}{2^{14}}, & \Delta_{\nu,1} &= 2g_\nu^3 + 9C_\nu^n g_\nu h_\nu + \frac{27}{2^{16}}(C_\nu^n)^2 + 27h_\nu^2 - \frac{9}{2^{13}}g_\nu, \\ Q_\nu &= \sqrt[3]{\frac{\Delta_{\nu,1} + \sqrt{\Delta_{\nu,1}^2 - 4\Delta_{\nu,0}^3}}{2}}, & S_\nu &= \frac{1}{2}\sqrt{-\frac{2}{3}R_\nu + \frac{1}{3}\left(Q_\nu + \frac{\Delta_{\nu,0}}{Q_\nu}\right)}. \end{aligned}$$

Note that since the blocks $\hat{S}_\nu$, $\nu = 1,\dots,n-1$ come in complex conjugate pairs, i.e. $\hat{S}_{n-\nu} = (\hat{S}_\nu)^*$, $\nu = 1,\dots,n-1$, then λ_j^ν is eigenvalue of $\hat{S}_\nu$ if and only if λ_j^ν is eigenvalue of $\tilde{S}_{n-\nu}$, i.e. $\mathcal{F}(\lambda_j^\nu) = \{\nu,\, n-\nu\}$, $\nu = 1,\dots,n-1$.

5.1.3 Constraints

The eigenvalues and eigenvectors of the subdivision matrix S could be exploited to find some constraints that the stencil weights has to satisfy in order to obtain limit surfaces with the desired properties.

Constraints inferred from eigenvalues analysis

As previously observed in Section 5.1.2, 1 is an eigenvalue of the local subdivision matrix S and $\mathcal{F}(1) = 0$. Moreover, in view of Condition 1.a, $\boldsymbol{x}_0 = \mathbf{1}$ is the associated eigenvector. Thus, provided that all remaining eigenvalues of S are smaller than 1, the subdivision scheme will be convergent. In the following we identify the constraints to be imposed on the weights of the extraordinary rules such that this can happen. Moreover, we also require the necessary conditions for C^1 continuity, boundedness curvature and optimal shrinkage explained in Section 2.3 and summarized in Table 2.1. Since the considered scheme is binary, the optimal shrinkage is obtained setting $\lambda = \frac{1}{2}$.
As previously emphasized, since $\hat{S}_{n-1} = (\hat{S}_1)^*$, to identify the conditions regarding the sub-dominant eigenvalue we can simply focus on the case $\nu = 1$. Thus, we select $\nu = 1$ and observe that, if setting $A_1^n = \frac{5}{8}$, from the eigenvalues expressions in (5.15) we can easily get

$$\lambda_1^1 = \frac{2A_1^n + \sqrt{4(A_1^n)^2 - 1}}{4} = \frac{1}{2},$$

as desired, and also

$$\lambda_2^1 = \frac{2A_1^n - \sqrt{4(A_1^n)^2 - 1}}{4} = \frac{1}{8}.$$

Hence, analogously, the setting of $A_{n-1}^n = \frac{5}{8}$ will provide $\lambda_1^{n-1} = \frac{1}{2}$ and $\lambda_2^{n-1} = \frac{1}{8}$.

Condition 2.a *The constraint*

$$A_1^n = A_{n-1}^n = \frac{5}{8}, \qquad \textit{for all } n \geq 5,$$

guarantees the existence of the sub-dominant eigenvalue $\lambda = \frac{1}{2}$ *with Fourier index* $\mathcal{F}(\lambda) = \{1, n-1\}$.

Next, we consider $\nu = 0, 2, \ldots, n-2$ and observe that, if setting $A_\nu^n = \frac{1}{2}$, then from equation (5.15) we obtain

$$\lambda_1^\nu = \frac{2A_\nu^n + \sqrt{4(A_\nu^n)^2 - 1}}{4} = \frac{1}{4}, \quad \nu = 0, 2, \ldots, n-2$$

as well as

$$\lambda_2^\nu = \frac{2A_\nu^n - \sqrt{4(A_\nu^n)^2 - 1}}{4} = \frac{1}{4}, \quad \nu = 0, 2, \ldots, n-2.$$

Condition 3.a *The constraint*

$$A_\nu^n = \frac{1}{2}, \qquad \textit{for all } \nu = 0, 2, \ldots, n-2 \quad \textit{and} \quad n \geq 5,$$

guarantees the existence of the subsub-dominant eigenvalue $\eta = \frac{1}{4}$ *with multiplicity* $m(\eta) = 2n - 4$ *and Fourier index* $\mathcal{F}(\eta) \supseteq \{0, 2, n-2\}$.

Finally, we have to find an additional condition that can guarantee that all other eigenvalues $\lambda_3^\nu, \lambda_4^\nu, \lambda_5^\nu, \lambda_6^\nu$ are such that $|\lambda_j^\nu| \leq \frac{1}{4}$ for all $j = 3,4,5,6$ and $\nu = 0,1,\ldots,n-1$. Since the explicit expressions of these eigenvalues exclusively depend on C_ν^n, as shown in equation (5.16), to achieve our objective we assume C_ν^n to be a function within the family of real functions

$$\begin{aligned} f_{\nu,\sigma}^n : [-1,1] &\to \mathbb{R} \\ \cos\left(\frac{2\pi\nu}{n}\right) &\mapsto \frac{25}{64} - \sigma\Big(1+\cos\left(\frac{2\pi\nu}{n}\right)\Big), \end{aligned} \tag{5.17}$$

whose members are identified by a specific choice of σ.

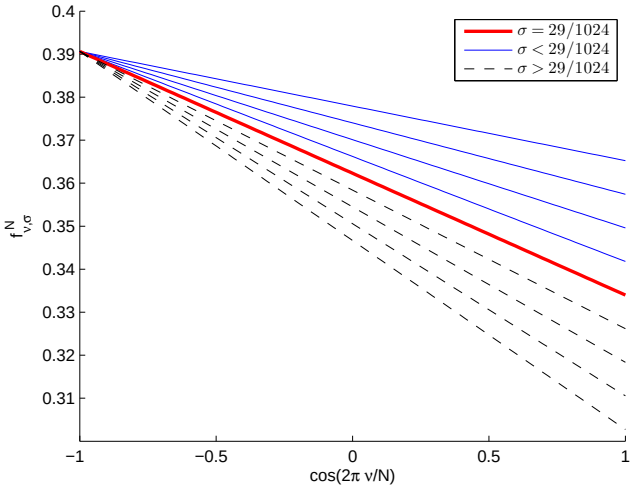

Figure 5.3: The family of functions f_{ν,σ_i}^n with $\sigma_i = \frac{13+4i}{2^{10}}$, $i = 0,1,\ldots,8$. The solid thicker (red) curve identifies $f_{\nu,\frac{29}{2^{10}}}^n$.

Figure 5.3 shows the behavior of the family members $f_{\nu,\sigma}^n$ for different values of σ. Plotting also the behaviour of the eigenvalues $\lambda_3^\nu, \lambda_4^\nu, \lambda_5^\nu, \lambda_6^\nu$, $\nu = 0,1,\ldots,n-1$, obtained with $C_\nu^n = f_{\nu,\sigma}^n$, $\sigma \in [\frac{13}{2^{10}}, \frac{45}{2^{10}}]$ (see Figure 5.4), we can observe that $|\lambda_3^\nu|, |\lambda_4^\nu|, |\lambda_6^\nu|$ are always smaller than $\frac{1}{4}$, while $|\lambda_5^\nu|$ is not greater than $\frac{1}{4}$ only if $C_\nu^n = f_{\nu,\sigma}^n$ with $\sigma \geq \frac{29}{2^{10}}$. Moreover, we notice that $\lambda_5^\nu = \frac{1}{4}$ whenever $\nu = \frac{n}{2}$ since $C_{\frac{n}{2}}^n = f_{\frac{n}{2},\sigma}^n = \frac{25}{64}$ for all $\sigma \geq \frac{29}{2^{10}}$.

Condition 4.a *Let $\nu \in \{0,1,\ldots,n-1\}$. Setting*

$$C_\nu^n = \frac{25}{64} - \sigma\Big(1+\cos\left(\frac{2\pi\nu}{n}\right)\Big) \quad \textit{with} \quad \sigma \geq \frac{29}{2^{10}}, \tag{5.18}$$

we obtain

$$|\lambda_3^\nu| < \frac{1}{4}, \quad |\lambda_4^\nu| < \frac{1}{4}, \quad |\lambda_5^\nu| < \frac{1}{4}, \quad |\lambda_6^\nu| < \frac{1}{4}, \quad \textit{if } \nu \neq \frac{n}{2}$$

and

$$|\lambda_3^\nu| < \frac{1}{4}, \quad |\lambda_4^\nu| < \frac{1}{4}, \quad \lambda_5^\nu = \frac{1}{4}, \quad |\lambda_6^\nu| < \frac{1}{4}, \quad \textit{if } \nu = \frac{n}{2}.$$

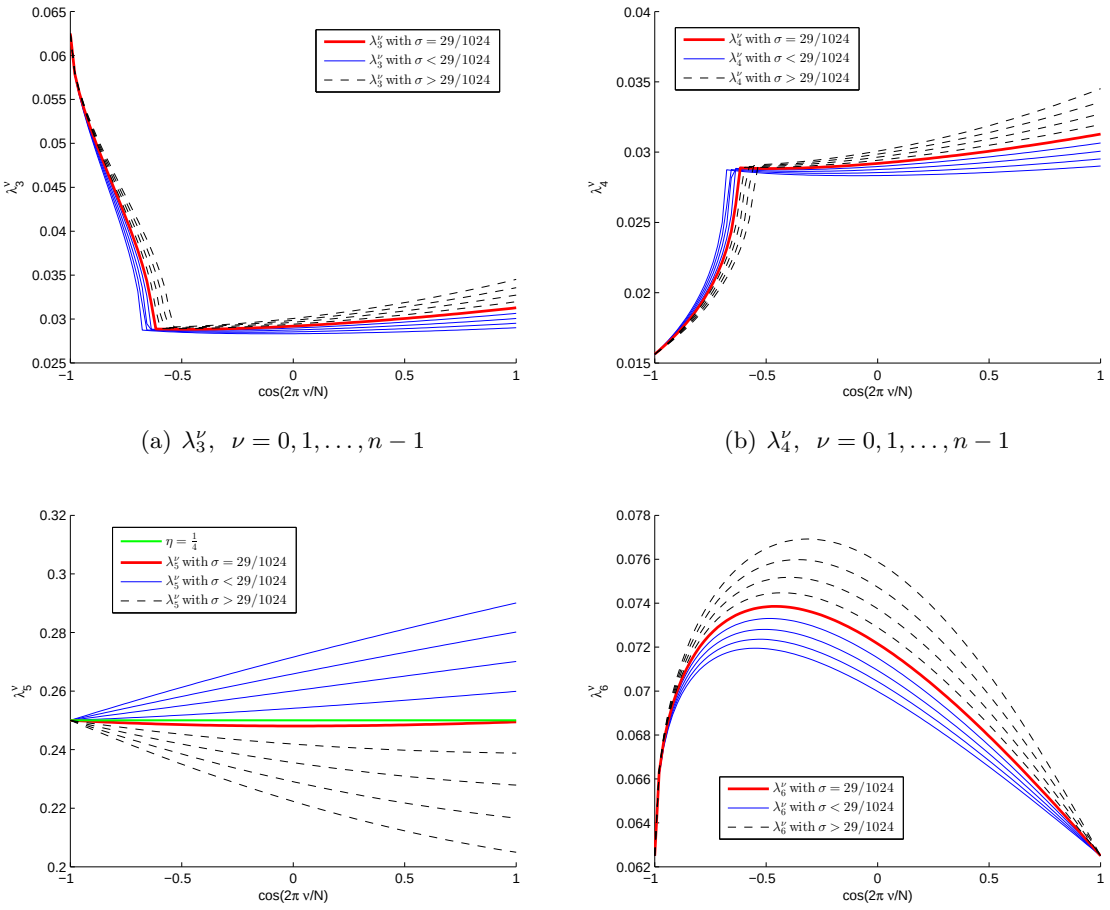

(a) λ_3^ν, $\nu = 0, 1, \ldots, n-1$

(b) λ_4^ν, $\nu = 0, 1, \ldots, n-1$

(c) λ_5^ν, $\nu = 0, 1, \ldots, n-1$

(d) λ_6^ν, $\nu = 0, 1, \ldots, n-1$

Figure 5.4: Behavior of eigenvalues $\lambda_3^\nu, \lambda_4^\nu, \lambda_5^\nu, \lambda_6^\nu$, $\nu = 0, 1, \ldots, n-1$ when $C_\nu^n = f_{\nu,\sigma_i}^n$ and $\sigma_i = \frac{13+4i}{2^{10}}$, $i = 0, 1, \ldots, 8$.

Remark 5.2 *Conditions 3.a and 4.a imply that the subsub-dominant eigenvalue* $\eta = \frac{1}{4}$ *has multiplicity*

$$m(\eta) = \begin{cases} 2n-4, & \text{if } n \text{ odd,} \\ 2n-3, & \text{if } n \text{ even.} \end{cases}$$

Remark 5.3 *To guarantee that the local subdivision matrix* S *has the desired spectrum, we have no conditions on* B_ν^n*. Looking at equations* (5.13)-(5.14) *this can be easily understood. In fact,* B_ν^n *appears only in the block* $\mathbf{K}_2$ *which has no influence on the characteristic polynomial and thus on the computation of the eigenvalues of* $\overline{M}_\nu$*.*

All the constraints inferred from the eigenvalues analysis are summarized in Table 5.1.

1.	$\sum_{j=1}^{n} \alpha_{2j-1,n} = \frac{1}{2}$ for $n \neq 4$, $\sum_{j=1}^{n} (\beta_{2j-1,n} + \gamma_{2j,n}) = \frac{13}{16}$ for $n \neq 4$
2.	$\sum_{j=1}^{n} \alpha_{2j-1,n}\, \omega^{(j-1)\nu} = \frac{5}{8}$ for $n \neq 4$, $\nu = 1, n-1$
3.	$\sum_{j=1}^{n} \alpha_{2j-1,n}\, \omega^{(j-1)\nu} = \frac{1}{2}$ for $n \geq 5$, $\nu = 0, 2, \ldots, n-2$
4.	$\sum_{j=1}^{n} \gamma_{2j,n}\, \omega^{(j-1)\nu} = \frac{25}{64} - \sigma\left(1 + \cos\left(\frac{2\pi\nu}{n}\right)\right)$ with $\sigma \geq \frac{29}{2^{10}}$ for $n \neq 4$, $\nu = 0, 1, \ldots, n-1$

Table 5.1: Summary of the conditions required on the coefficients $\alpha_{2j-1,n}$, $\beta_{2j-1,n}$, $\gamma_{2j,n}$, $j = 1, \ldots, n$ for all valences $n \neq 4$.

Constraints inferred from eigenvectors analysis

If an interpolatory subdivision scheme with extraordinary stencils in Figure 5.2 fulfills Conditions 1.a, 2.a, 3.a, 4.a, then it is convergent and satisfies the necessary conditions to achieve also C^1 continuity and bounded curvature at extraordinary points of valence $n \geq 5$. The achievement of C^1 continuity is subject only to the additional fulfillment of the condition regarding the regularity of the characteristic map $\mathbf{\Psi}$. In fact, since we already proved that the Fourier indices of the subdominant eigenvalue λ are $1, n-1$, once the regularity has been proven the injectivity follows immediately (see Remark 2.31). As recalled in Section 2.3, the characteristic map is a special parametrization that allows one to express the limit surface around an extraordinary vertex as a differentiable function of two variables. Such parametrization depends not only on the mesh connectivity, but also on the weights defining the extraordinary rules, and can be obtained as the planar limit surface generated by the so-called characteristic mesh, i.e. the control mesh provided by the eigenvectors $\boldsymbol{x}_1$, $\boldsymbol{x}_2$ corresponding to the sub-dominant eigenvalue $\lambda := \lambda_1 = \lambda_2$ [7, 112, 117, 138]. This planar limit surface is made by a ring of regular surface patches of the tensor-product interpolatory Dubuc-Deslauriers 4-point scheme, and the characteristic mesh contains the control points for the definition of such patches. By the property of rotational symmetry around the extraordinary vertex, the characteristic mesh can be conveniently decomposed into n segments. By normalizing the eigenvectors $\boldsymbol{x}_1$, $\boldsymbol{x}_2$ such that the characteristic mesh is centered at $(0, 0)$ and the furthest corner in the first segment is at $(1, 0)$ of the global (x, y)-coordinate system (see Figure 5.5), we can obtain the so-called normalized characteristic mesh. Exploiting the results presented by Deng-Ma in [39, Appendix A], we here show a standard procedure which allows one to verify if a bivariate interpolatory subdivision scheme defined by the extraordinary stencils in Figure 5.2 and satisfying Conditions 1.a, 2.a, 3.a, 4.a, has a regular characteristic map, and is thus of class C^1. Before showing the pseudo-code of the procedure, we underline the fact that the eigenvectors $\boldsymbol{x}_1$ and $\boldsymbol{x}_2$, used to define the characteristic mesh, must be computed from a local subdivision matrix $\tilde{S} \in \mathbb{R}^{(42n+1)\times(42n+1)}$. This is due to the fact that, in the univariate case, for the Dubuc-Deslauriers interpolatory 4-point scheme, a limit curve segment between two consecutive vertices is defined by a set of 6 vertices. For the class of schemes here considered, a limit surface patch bounded by 4 vertices defining a quadrilateral face is thus identified by a set of 6×6 vertices, being a tensor-product surface patch of the Dubuc-Deslauriers interpolatory 4-point scheme (see Figure 5.5).

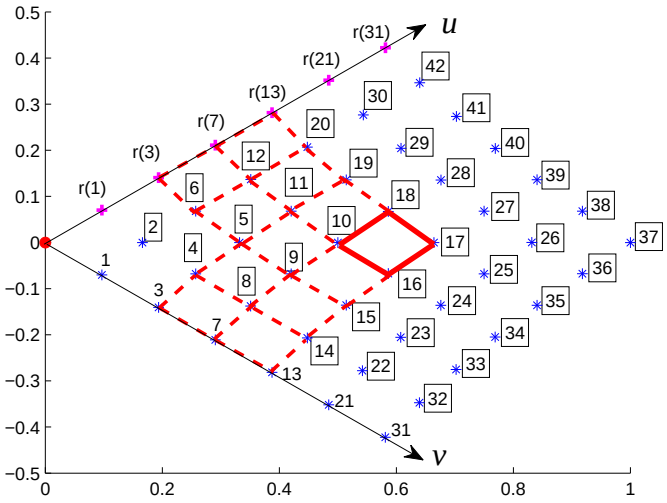

Figure 5.5: First segment of the normalized characteristic mesh: entries of the 7×6 matrix $\mathbf{V}$ (marked by *) and entries of the first row of $\mathbf{V}$ rotated counterclockwise by $\frac{2\pi}{n}$ (marked by +).

Algorithm 1 *Pseudo code for verifying the regularity of the characteristic map.*

1. *Compute the subdivision matrix* $\tilde{S} \in \mathbb{R}^{(42n+1)\times(42n+1)}$, *where each block* $\tilde{M}_\ell \in \mathbb{R}^{42\times 42}$ *for* $\ell = 0, 1, \ldots, n-1$.

2. *Following the reasoning in Section 5.1.2, compute the* 43×43 *block* $\hat{S}_1$ *and consider its* 42×42 *sub-matrix* $\overline{M}_1$.

3. *Compute the subdominant eigenvector of* $\overline{M}_1$, *that is the eigenvector* $\mathbf{v} \in \mathbb{C}^{42}$ *related to the eigenvalue* $\lambda = \frac{1}{2}$.

4. *Re-order the entries* $v_k, k = 1, \ldots 42$ *of* $\mathbf{v}$ *defining a matrix* $\mathbf{V} \in \mathbb{C}^{7\times 6}$ *of the form*

$$(\mathrm{V}_{i,j})_{\substack{1\le i\le 7\\ 1\le j\le 6}} = \begin{pmatrix} v_1 & v_3 & v_7 & v_{13} & v_{21} & v_{31} \\ v_2 & v_4 & v_8 & v_{14} & v_{22} & v_{32} \\ v_6 & v_5 & v_9 & v_{15} & v_{23} & v_{33} \\ v_{12} & v_{11} & v_{10} & v_{16} & v_{24} & v_{34} \\ v_{20} & v_{19} & v_{18} & v_{17} & v_{25} & v_{35} \\ v_{30} & v_{29} & v_{28} & v_{27} & v_{26} & v_{36} \\ v_{42} & v_{41} & v_{40} & v_{39} & v_{38} & v_{37} \end{pmatrix}.$$

5. *Denoting by* $\boldsymbol{x} := \mathcal{R}(\mathbf{V})$ *and* $\mathbf{y} := \mathcal{I}(\mathbf{V})$ *the real and imaginary part of* $\mathbf{V}$, *respectively, define the* x *and* y *coordinates of the points marked by * in Figure 5.5. notice that they all depend on* B_1^n *and* C_1^n.

6. *Rotating rows and columns of* $\mathbf{V}$ *clockwise and counterclockwise by* $\frac{2\pi}{n}$, *construct all the* 6×6 *sets of control points defining the 12 surface patches bounded by the vertices of the quadrilateral faces highlighted in Figure 5.5.*

7. *For the surface patch bounded by the four vertices*

$$\big(\mathcal{R}(\mathrm{V}_{i,j}),\mathcal{I}(\mathrm{V}_{i,j})\big),\big(\mathcal{R}(\mathrm{V}_{i,j+1}),\mathcal{I}(\mathrm{V}_{i,j+1})\big),\big(\mathcal{R}(\mathrm{V}_{i+1,j}),\mathcal{I}(\mathrm{V}_{i+1,j})\big),\big(\mathcal{R}(\mathrm{V}_{i+1,j+1}),\mathcal{I}(\mathrm{V}_{i+1,j+1})\big),$$

let $\big(\mathcal{R}(\mathrm{V}_{m,n})=x_{m,n},\mathcal{I}(\mathrm{V}_{m,n})=y_{m,n}\big)$, $m=i-2,\dots,i+3$, $n=j-2,\dots,j+3$ *identify its* 6×6 *set of control points. Then compute*

$$\begin{aligned} c^x_m &= \max\nolimits_{n=j-1,\dots,j+2}\{|2x_{m,n}-x_{m,n-1}-x_{m,n+1}|\}, \quad m=i-2,\dots,i+3,\\ \Delta^x_m &= \max\{x_{m+1,j}-x_{m,j},\, x_{m+1,j+1}-x_{m,j+1}\}, \quad m=i-2,\dots,i+2,\\ \delta^x_m &= \min\{x_{m+1,j}-x_{m,j},\, x_{m+1,j+1}-x_{m,j+1}\}, \quad m=i-2,\dots,i+2, \end{aligned} \tag{5.19}$$

and verify the fulfillment of

Condition 5.a

$$(i)\quad \frac{(c^x_{m+1}+c^x_m)}{\delta^x_m}<4 \qquad \forall\, m=i-2,\dots,i+2,$$

$$(ii)\quad \frac{1}{K}\le\frac{4\delta^x_{m+1}-(c^x_{m+2}+c^x_{m+1})}{4\Delta^x_m+(c^x_{m+1}+c^x_m)}\le K \qquad \forall\, m=i-2,\dots,i+1,$$

$$(iii)\quad \frac{1}{K}\le\frac{4\Delta^x_{m+1}+(c^x_{m+2}+c^x_{m+1})}{4\delta^x_m-(c^x_{m+1}+c^x_m)}\le K \qquad \forall\, m=i-2,\dots,i+1,$$

with $K=3+2\sqrt{2}$.

Remark 5.4 *Conditions 5.a.(i),5.a.(ii),5.a.(iii), together with Conditions 1.a, 2.a, 3.a, 4.a, have been proven by Deng-Ma [39] to guarantee the positivity of the x and y components of the first derivative of a surface patch along the u direction, and thus, in view of [112, Theorem 5.25] provide sufficient conditions for the regularity of the characteristic map.*

8. *Compute the values in* (5.19) *for the y-coordinates and check if Condition 5.a is satisfied.*

9. *Repeat steps 7, 8 for all the 12 surface patches contained in the first sector of the normalized characteristic map.*

10. *If for all such patches Condition 5.a is verified for both x- and y-coordinates, then the characteristic map is regular. Conversely, if a patch does not satisfy these equations, subdivide it into four subpatches and check Condition 5.a for both x- and y-coordinates of each subpatch. If Condition 5.a is not satisfied within a predefined number of refinement steps (say 10), then no proof of regularity of the characteristic map is available.*

Extraordinary vertices of valence $n=3$

The analysis conducted for the case $n\ge 5$ can be exploited also for the special case $n=3$, just introducing the following changes when formulating Conditions 1.a, 2.a, 3.a and 4.a.

Condition 1.b *The constraints* $A^3_0=\frac{1}{2}$, $B^3_0+C^3_0=\frac{13}{16}$ *imply that* $\lambda_0=1$ *with* $\mathcal{F}(1)=0$ *and* $\boldsymbol{x}_0=\mathbf{1}$.

Condition 2.b *The constraints* $A_1^3 = A_2^3 = \frac{5}{8}$ *imply that* $\lambda := \lambda_1 = \lambda_2 = \frac{1}{2}$ *with* $\mathcal{F}(\lambda) = \{1, 2\}$.

Condition 3.b *The constraint* $A_0^3 = \frac{1}{2}$ *yields* $\eta := \lambda_3 = \frac{1}{4}$ *with* $\mathcal{F}(\eta) = \{0\}$.

Remark 5.5 *We thus point out that, when* $n = 3$*, the limit surface is not* L^2*-hyperbolic because both* 2 *and* $n-2$ *do not belong to the Fourier indices of the subsub-dominant eigenvalue* $\frac{1}{4}$ *[112].*

Condition 4.b *The constraint* $C_\nu^3 = \frac{25}{64} - \sigma(1 + \cos(\frac{2\pi\nu}{n}))$ *with* $\sigma \geq \frac{29}{2^{10}}$ *for all* $\nu \in \{0, 1, 2\}$ *guarantees that* $|\lambda_i| < \frac{1}{4}$ *for all* $i \geq 4$.

Finally, to check the regularity of the characteristic map, and thus the C^1 continuity of the scheme in the neighborhood of an extraordinary point of valence $n = 3$, we can again use Algorithm 1.

5.1.4 Numerical examples: special weights settings

In this section, we consider interpolatory subdivision schemes from the literature which fall into the general class studied in this section. Such schemes are featured by

(i) the regular rules in (5.1)-(5.2), obtained from the tensor-product of the Dubuc-Deslauriers interpolatory 4-point scheme [42, 49];

(ii) the extraordinary rules in (5.4)-(5.6) and (5.3)-(5.5) for the cases $n \geq 5$ and $n = 3$, respectively.

Moreover, they satisfy the constraints appearing in Conditions 1.a, 2.a, 3.a, 4.a and 5.a for any $n \neq 4$, and thus guarantee convergence, C^1 continuity and boundedness of principal curvatures at extraordinary vertices. We thus exclude from our discussion the proposal in [123] since, although fulfilling requirements (i)-(ii), it fails to satisfy boundedness of curvature.

Li-Ma-Bao's subdivision scheme

The weights $\alpha_{2j-1,n}, \beta_{2j-1,n}, \gamma_{2j,n}$, $j = 1, \ldots, n$ for the extraordinary rules proposed by Li-Ma-Bao [93] are shown in Tables 5.2 and 5.3 for the cases $n \geq 5$ and $n = 3$, respectively. For such weights setting we prove that the constraints in Conditions 1.a, 2.a, 3.a, 4.a are all satisfied for any $n \neq 4$.

Proposition 5.6 *Li-Ma-Bao's subdivision scheme satisfies the constraints in Condition 1.a for all* $n \geq 5$.

Proof: From Table 5.2 we have that

$$A_0^n = \sum_{j=1}^{n} \alpha_{2j-1,n} = \frac{1}{2} + \frac{1}{4n} + \frac{1}{4n} \sum_{j=2}^{n} \cos\left(\frac{2\pi(j-1)}{n}\right).$$

Since $\sum_{j=2}^{n} \cos\left(\frac{2\pi(j-1)}{n}\right) = -1$ for all $n \geq 5$, then $A_0^n = \frac{1}{2}$. In order to compute B_0^n, we observe that

$$\frac{3}{32n} \sum_{j=1}^{n} \left(1 + \cos\left(\frac{2\pi(j-1)}{n}\right) + \sin\left(\frac{2\pi(j-1)}{n}\right) + \cos\left(\frac{2\pi(j-2)}{n}\right) - \sin\left(\frac{2\pi(j-2)}{n}\right)\right) = \frac{3}{32},$$

$\alpha_{1,n}$	$\frac{1}{2}+\frac{1}{4n}$
$\alpha_{2j-1,n}, \quad j=2,\dots,n$	$\frac{1}{4n}\cos\left(\frac{2\pi(j-1)}{n}\right)$
$\beta_{1,n}=\beta_{3,n}$	$\frac{63}{256}+\frac{3}{32n}\left(2+\cos\left(\frac{2\pi}{n}\right)+\sin\left(\frac{2\pi}{n}\right)\right)$
$\beta_{5,n}=\beta_{2n-1,n}$	$-\frac{3}{256}+\frac{3}{32n}\left(1+\cos\left(\frac{4\pi}{n}\right)+\sin\left(\frac{4\pi}{n}\right)\right.$ $\left.+\cos\left(\frac{2\pi}{n}\right)-\sin\left(\frac{2\pi}{n}\right)\right)$
$\beta_{2j-1,n}$ $j=4,\dots,n-1$	$\frac{3}{32n}\left(1+\cos\left(\frac{2\pi(j-1)}{n}\right)+\sin\left(\frac{2\pi(j-1)}{n}\right)\right.$ $\left.+\cos\left(\frac{2\pi(j-2)}{n}\right)-\sin\left(\frac{2\pi(j-2)}{n}\right)\right)$
$\gamma_{2,n}$	$\frac{11}{32}-\frac{7}{64n}$
$\gamma_{4,n}=\gamma_{2n,n}$	$-\frac{3}{128}-\frac{1}{64n}\left(3+4\cos\left(\frac{2\pi}{n}\right)\right)$
$\gamma_{2j,n}, \quad j=3,\dots,n-1$	$-\frac{1}{64n}\left(3+4\cos\left(\frac{2\pi(j-1)}{n}\right)\right)$

Table 5.2: Weights proposed by Li-Ma-Bao for the edge- and face-point rule around extraordinary vertices of valence $n \geq 5$.

$\alpha_{1,3}=\frac{7}{12}$	$\alpha_{3,3}=\alpha_{5,3}=-\frac{1}{24}$
$\beta_{1,3}=\beta_{3,3}=\frac{75}{256}+\frac{\sqrt{3}}{64}$	$\beta_{5,3}=-\frac{3}{128}-\frac{\sqrt{3}}{32}$
$\gamma_{2,3}=\frac{59}{192}$	$\gamma_{4,3}=\gamma_{6,3}=-\frac{11}{384}$

Table 5.3: Weights proposed by Li-Ma-Bao for the edge- and face-point rule around extraordinary vertices of valence $n = 3$.

for all $n \geq 5$, and the latter yields $B_0^n = \frac{3}{32} + 2 \cdot \frac{63}{256} + 2 \cdot \left(-\frac{3}{256}\right) = \frac{9}{16}$. In a similar way we can compute C_0^n by noticing that

$$-\frac{1}{64n}\sum_{j=1}^{n}\left(3+4\cos\left(\frac{2\pi(j-1)}{n}\right)\right) = -\frac{3}{64}, \quad \forall n \geq 5,$$

which yields $C_0^n = -\frac{3}{64} + \frac{11}{32} + 2 \cdot \left(-\frac{3}{128}\right) = \frac{1}{4}$. Hence $B_0^n + C_0^n = \frac{13}{16}$. ■

For the following propositions we recall that $\omega = e^{\frac{2\pi \mathrm{i}}{n}} = \cos\left(\frac{2\pi}{n}\right) + \mathrm{i}\sin\left(\frac{2\pi}{n}\right)$.

Proposition 5.7 *Li-Ma-Bao's subdivision scheme satisfies the constraints in Condition 2.a for all $n \geq 5$.*

Proof: Since

$$\frac{1}{4n}\sum_{j=1}^{n}\cos\left(\frac{2\pi(j-1)}{n}\right)\omega^{(j-1)} = \frac{1}{8}, \qquad \forall n \geq 5,$$

thus $A_1^n = \frac{1}{8} + \frac{1}{2} = \frac{5}{8}$ for all $n \geq 5$. Analogously we can also prove that $A_{n-1}^n = \frac{5}{8}$ for all $n \geq 5$. ■

Proposition 5.8 *Li-Ma-Bao's subdivision scheme satisfies the constraints in Condition 3.a for all $n \geq 5$.*

Proof: In Proposition 5.6 we have already proven that $A_0^n = \frac{1}{2}$. Thus, we have to prove the claim for $\nu = 2, \ldots, n-2$ only. Since for all $n \geq 5$ and $\nu = 2, \ldots, n-2$

$$\frac{1}{4n} \sum_{j=1}^{n} \cos\left(\frac{2\pi(j-1)}{n}\right) \omega^{(j-1)\nu} = 0,$$

then $A_\nu^n = \frac{1}{2}$ for all $n \geq 5$ and $\nu = 2, \ldots, n-2$. ■

Proposition 5.9 *Li-Ma-Bao's subdivision scheme satisfies the constraints in Condition 4.a for all $n \geq 5$.*

Proof: Using the coefficients in Table 5.2 we can compute C_ν^n for all $\nu = 0, \ldots, n-1$.

- If $\nu = 0$, then $C_0^n = \frac{1}{4}$ as it was already shown in Proposition 5.6.
- If $\nu = 1$, we observe that for all $n \geq 5$

  $$-\frac{1}{64n} \sum_{j=1}^{n} \left(3 + 4\cos\left(\frac{2\pi(j-1)}{n}\right)\right) \omega^{(j-1)} = -\frac{1}{32},$$

  so that

  $$C_1^n = \frac{5}{16} - \frac{3}{128}\left(\omega + \omega^{n-1}\right) \qquad \forall n \geq 5.$$

  Analogously, we can also show that $C_{n-1}^n = \frac{5}{16} - \frac{3}{128}\left(\omega + \omega^{n-1}\right)$, for all $n \geq 5$.
- If $\nu = 2, \ldots, n-2$, we notice that for all $n \geq 5$

  $$-\frac{1}{64n} \sum_{j=1}^{n} \left(3 + 4\cos\left(\frac{2\pi(j-1)}{n}\right)\right) \omega^{(j-1)\nu} = 0,$$

  thus yielding

  $$C_\nu^n = \frac{11}{32} - \frac{3}{128}\left(\omega^\nu + \omega^{(n-1)\nu}\right) \qquad \forall n \geq 5 \text{ and } \nu = 2, \ldots, n-2.$$

Finally, re-writing the above results in the compact form

$$C_\nu^n = \begin{cases} \frac{1}{4} & \text{if} \quad \nu = 0; \\ \frac{23}{64} - \frac{3}{64}\left(1 + \cos\left(\frac{2\pi}{n}\right)\right) & \text{if} \quad \nu = 1, n-1; \\ \frac{25}{64} - \frac{3}{64}\left(1 + \cos\left(\frac{2\pi\nu}{n}\right)\right) & \text{if} \quad \nu = 2, \ldots, n-2; \end{cases}$$

we get

$$C_\nu^n = \begin{cases} f^n_{0,\frac{9}{128}} & \text{if} \quad \nu = 0; \\ f^n_{1,\frac{3}{64}+\frac{1}{32(1+\cos(\frac{2\pi}{n}))}} & \text{if} \quad \nu = 1, n-1; \\ f^n_{\nu,\frac{3}{64}} & \text{if} \quad \nu = 2, \ldots, n-2. \end{cases}$$

Since $\frac{9}{128} > \frac{29}{2^{10}}$, $\frac{3}{64} > \frac{29}{2^{10}}$ and $\frac{3}{64} + \frac{1}{32(1+\cos(\frac{2\pi}{n}))} > \frac{3}{64} > \frac{29}{2^{10}}$, then for all $0 \leq \nu \leq n-1$ the constraints in Condition 4.a are satisfied. ■

Remark 5.10 *From Table 5.3 we obtain that, when $n = 3$, Li-Ma-Bao's scheme satisfies the constraints in Conditions 1.b and 3.b since $A_0^3 = \frac{1}{2}$ and $B_0^3 = \frac{9}{16}$, $C_0^3 = \frac{1}{4}$, so providing $B_0^3 + C_0^3 = \frac{13}{16}$. Additionally, since $A_1^3 = A_2^3 = \frac{7}{12} - \frac{1}{12}\cos\left(\frac{2\pi}{3}\right) = \frac{5}{8}$, the constraints in Condition 2.b are also fulfilled. Furthermore, since $C_0^3 = \frac{1}{4} = f^3_{0,\frac{9}{128}}$ and $C_1^3 = C_2^3 = \frac{43}{128} = f^3_{1,\frac{7}{64}}$ with $\frac{9}{128} > \frac{29}{2^{10}}$ and $\frac{7}{64} > \frac{29}{2^{10}}$, thus the constraints in Condition 4.b are satisfied too for all $0 \le \nu \le 2$.*

Finally, using Algorithm 1, we checked that Li-Ma-Bao's scheme also satisfies Condition 5.a for all $3 \le n \le 50$ after 7 refinement steps, thus showing convergence, C^1 smoothness and boundedness of principal curvatures at extraordinary points with these valences.

Deng-Ma's subdivision scheme

For the subdivision scheme recently proposed by Deng-Ma [39], the weights defining the edge-point and the face-point stencil are shown in Tables 5.4 and 5.5 for $n \ge 5$ and $n = 3$. As already shown for Li-Ma-Bao's subdivision scheme, we now prove that also the coefficients defining the extraordinary rules of Deng-Ma's scheme satisfy the constraints in Conditions 1.a, 2.a, 3.a and 4.a.

$\alpha_{1,n}$	$\frac{1}{2} + \frac{1}{4n}$
$\alpha_{2j-1,n}, \quad j = 2, \dots, n$	$\frac{1}{4n}\cos\left(\frac{2\pi(j-1)}{n}\right)$
$\beta_{1,n} = \beta_{3,n}$	$\frac{153}{512} + \frac{9}{128n}\left(1 + \cos\left(\frac{2\pi}{n}\right)\right)$
$\beta_{5,n} = \beta_{2n-1,n}$	$-\frac{9}{512} + \frac{9}{128n}\left(\cos\left(\frac{4\pi}{n}\right) + \cos\left(\frac{2\pi}{n}\right)\right)$
$\beta_{2j-1,n}, \quad j = 4, \dots, n-1$	$\frac{9}{128n}\left(\cos\left(\frac{2\pi(j-1)}{n}\right) + \cos\left(\frac{2\pi(j-2)}{n}\right)\right)$
$\gamma_{2,n}$	$\frac{81}{256}$
$\gamma_{4,n} = \gamma_{2n,n}$	$-\frac{9}{256}$
$\gamma_{6,n} = \gamma_{2n-2,n}$	$\frac{1}{512}$
$\gamma_{2j,n}, \quad j = 4, \dots, n-2$	0

Table 5.4: Weights proposed by Deng-Ma for the edge- and face-point rule around extraordinary vertices of valence $n \ge 5$.

Remark 5.11 *Comparing Tables 5.2 and 5.4, we notice that the coefficients $\alpha_{2j-1,n}$, $j = 1, \dots, n$ are the same for both schemes. Thus, Propositions 5.7 and 5.8 immediately yield that Deng-Ma's subdivision scheme satisfies the constraints in Condition 2.a and Condition 3.a.*

Proposition 5.12 *Deng-Ma's subdivision scheme satisfies the constraints in Condition 1.a for all $n \ge 5$.*

$\alpha_{1,3} = \frac{7}{12}$	$\alpha_{3,3} = \alpha_{5,3} = -\frac{1}{24}$
$\beta_{1,3} = \beta_{3,3} = \frac{159}{512}$	$\beta_{5,3} = -\frac{15}{256}$
$\gamma_{2,3} = \frac{81}{256}$	$\gamma_{4,3} = \gamma_{6,3} = -\frac{17}{512}$

Table 5.5: Weights proposed by Deng-Ma for the edge- and face-point rule around extraordinary vertices of valence $n = 3$.

Proof: From Remark 5.11 we have that $A_0^n = \frac{1}{2}$. Now, in order to compute B_0^n we observe that, for all $n \geq 5$,

$$\frac{9}{128n} \sum_{j=1}^{n} \left(\cos\left(\frac{2\pi(j-1)}{n} \right) + \cos\left(\frac{2\pi(j-2)}{n} \right) \right) = 0,$$

so that $B_0^n = 2 \cdot \frac{153}{512} + 2 \cdot \left(-\frac{9}{512} \right) = \frac{9}{16}$. Additionally, from Table 5.4 we have that $C_0^n = \frac{1}{4}$ so obtaining $B_0^n + C_0^n = \frac{13}{16}$. ■

Proposition 5.13 *Deng-Ma's subdivision scheme satisfies the constraints in Condition 4.a for all $n \geq 5$.*

Proof: From Table 5.4 we find that, for all $n \geq 5$ and $\nu = 0, \ldots, n-1$,

$$C_\nu^n = \frac{81}{256} - \frac{9}{128} \cos\left(\frac{2\pi\nu}{n} \right) + \frac{1}{256} \cos\left(\frac{4\pi\nu}{n} \right) = f^n_{\nu, \frac{10 - \cos\left(\frac{2\pi\nu}{n}\right)}{128}},$$

with

$$\frac{10 - \cos\left(\frac{2\pi\nu}{n} \right)}{128} > \frac{29}{2^{10}}.$$

Then the constraints in Condition 4.a are fulfilled. ■

Remark 5.14 *From Table 5.5 we immediately find that $A_0^3 = \frac{1}{2}$, $B_0^3 = \frac{9}{16}$, $C_0^3 = \frac{1}{4}$, so that $B_0^3 + C_0^3 = \frac{13}{16}$. Hence Deng-Ma's subdivision scheme satisfies the constraints in Condition 1.b and 3.b Additionally, since $A_1^3 = A_2^3 = \frac{7}{12} - \frac{1}{12} \cos\left(\frac{2\pi}{3} \right) = \frac{5}{8}$, the constraints in Condition 2.b are also fulfilled. Furthermore, by the fact that $C_0^3 = \frac{1}{4} = f^3_{0, \frac{9}{128}}$, $C_1^3 = C_2^3 = \frac{179}{512} = f^3_{1, \frac{21}{256}}$ and $\frac{9}{128} > \frac{29}{2^{10}}$ as well as $\frac{21}{256} > \frac{29}{2^{10}}$, thus the constraints in Condition 4.b are satisfied too.*

Finally, we conclude by observing that, using Algorithm 1, Deng-Ma's scheme also satisfies Condition 5.a for all $3 \leq n \leq 50$ with 8 refinement steps, and thus guarantees convergence, C^1 continuity and boundedness of principal curvatures at extraordinary points with these valences.

$\alpha_{1,n}$	$\frac{1}{2}+\frac{1}{4n}$
$\alpha_{2j-1,n},\ \ j=2,\dots,n$	$\frac{1}{4n}\cos\left(\frac{2\pi(j-1)}{n}\right)$
$\beta_{1,n}=\beta_{3,n}$	$\frac{81}{256}$
$\beta_{5,n}=\beta_{2n-1,n}$	$\frac{n-38}{512(n-2)}$
$\beta_{2j-1,n},\ \ j=4,\dots,n-1$	$\frac{9}{128(n-2)}$
$\gamma_{2,n}$	$\frac{81}{256}$
$\gamma_{4,n}=\gamma_{2n,n}$	$-\frac{9}{256}$
$\gamma_{2j,n},\quad j=3,\dots,n-1$	0

Table 5.6: New weights proposal for the edge- and face-point rule around extraordinary vertices of valence $n \geq 5$.

A new scheme with simplified face-point stencils

The goal of this part is to show how easily new interpolatory C^1 subdivision schemes with bounded curvature at extraordinary points can be designed by suitably choosing the weights $\alpha_{2j-1,n}$, $\beta_{2j-1,n}$, $\gamma_{2j,n}$, $j=1,\dots,n$ such that all the constraints previously found are fulfilled. Keeping the regular rules in (5.1)-(5.2) and the choice of $\alpha_{2j-1,n}$, $j=1,\dots,n$ for all $n\neq 4$ as in Li-Ma-Bao's and Deng-Ma's proposal, we focus our attention on the selection of the weights appearing in the face-point rule only. Our idea is to simplify the expressions of the coefficients used in the above proposals and to reduce the number of vertices involved. To this purpose we choose the weights for the face-point stencil as follows

- if $n=3$, we set

$$\beta_{1,3}=\beta_{3,3}=\frac{79}{256},\quad \beta_{5,3}=-\frac{19}{256},\qquad \gamma_{2,3}=\frac{85}{256},\quad \gamma_{4,3}=\gamma_{6,3}=-\frac{1}{32}, \tag{5.20}$$

- if $n\geq 5$ we choose

$$\begin{gathered}\beta_{1,n}=\beta_{3,n}=\frac{81}{256},\quad \beta_{5,n}=\beta_{2n-1,n}=\frac{n-38}{512(n-2)},\\ \beta_{2j-1,n}=-\frac{9}{128(n-2)},\ j=4,\dots,n-1\\ \gamma_{2,n}=\frac{81}{256},\quad \gamma_{4,n}=\gamma_{2n,n}=-\frac{9}{256},\quad \gamma_{2j,n}=0,\quad j=3,\dots,n-1.\end{gathered} \tag{5.21}$$

All the new weights are summarized in Tables 5.6 and 5.7.
Regarding the new choice of the coefficients $\beta_{2j-1,n}$, $j=1,\dots,n$ we observe that they have a simpler expression than those proposed by Li-Ma-Bao and Deng-Ma. Moreover, the coefficients $\gamma_{2j,n}$, $j=1,\dots,n$ are independent of the valence n and only 3 of them are non-zero. Thus the choice in (5.20) - (5.21) is computationally cheaper since we simplify the expressions of $\beta_{2j-1,n}$ and $\gamma_{2j,n}$, and reduce the number of vertices involved in the face-point rule definition.

$\alpha_{1,3} = \frac{7}{12}$	$\alpha_{3,3} = \alpha_{5,3} = -\frac{1}{24}$
$\beta_{1,3} = \beta_{3,3} = \frac{79}{256}$	$\beta_{5,3} = -\frac{19}{256}$
$\gamma_{2,3} = \frac{85}{256}$	$\gamma_{4,3} = \gamma_{6,3} = -\frac{1}{32}$

Table 5.7: New weights proposal for the edge- and face-point rule around extraordinary vertices of valence $n = 3$.

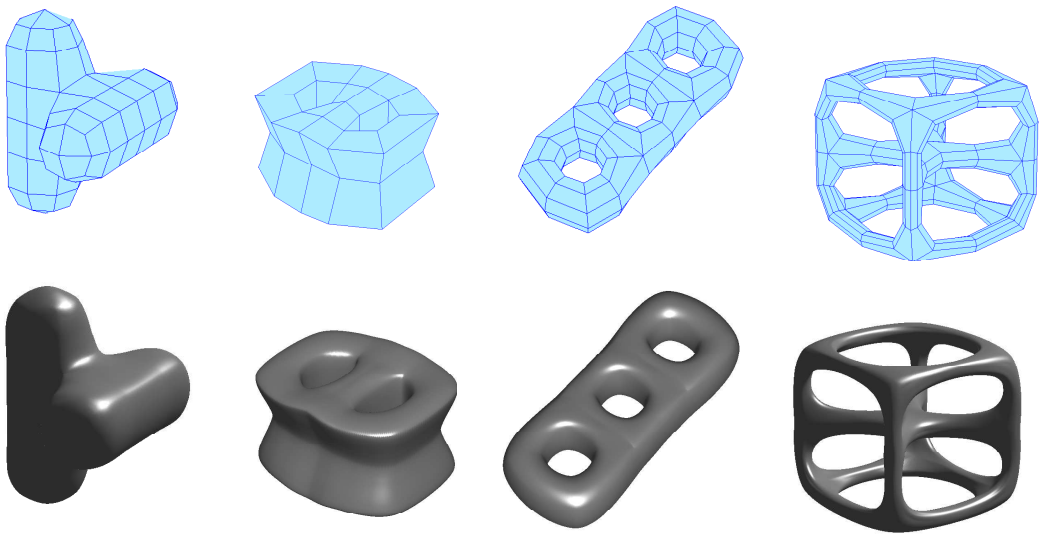

Figure 5.6: Limit surfaces obtained by the new subdivision scheme with weights in Tables 5.6 and 5.7, after 6 steps of refinement.

In the following we show that the new weights fulfill all the necessary conditions required for C^1 continuity and bounded curvature at extraordinary vertices of valence $n = 3$ and $n \geq 5$.

Proposition 5.15 *The interpolatory subdivision scheme with coefficients in Tables 5.6 and 5.7 satisfies Conditions 1.b, 2.b, 3.b, 4.b for valence $n = 3$ and Conditions 1.a, 2.a, 3.a, 4.a for valence $n \geq 5$.*

Proof: Since we keep the same $\alpha_{2j-1,n}$ $j = 1, \ldots, n$ proposed by Li-Ma-Bao and Deng-Ma, from Remarks 5.10 and 5.14 we immediately have that for $n = 3$ Conditions 2.b and 3.b are verified and, in the same way, from Propositions 5.7 and 5.8 we have that for $n \geq 5$ Conditions 2.a and 3.a are fulfilled. Additionally, we can easily see that $B_0^3 + C_0^3 = \frac{13}{16}$, thus satisfying Condition 1.b. For $n \geq 5$ we notice that

$$\sum_{j=2}^{n-1} \left(-\frac{9}{128(n-2)} \right) = -\frac{9}{128}.$$

It easily follows that $B_0^n = \frac{145}{256}$ and, since $C_0^n = \frac{63}{256}$, we have $B_0^n + C_0^n = \frac{13}{16}$ and Condition 1.a is verified. Furthermore, by the fact that, for $n = 3$, $C_0^3 = \frac{69}{256} = f^3_{0,\frac{31}{512}}$ and $C_1^3 = C_2^3 = \frac{93}{256} =$

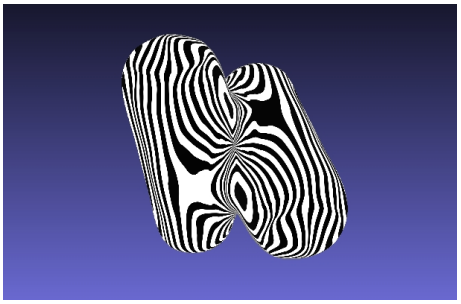

(a) Li-Ma-Bao's limit surface

(b) Closeup view of (a)

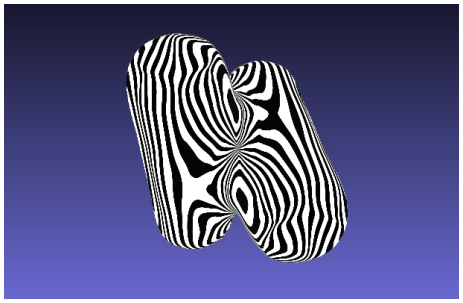

(c) Deng-Ma's limit surface

(d) Closeup view of (c)

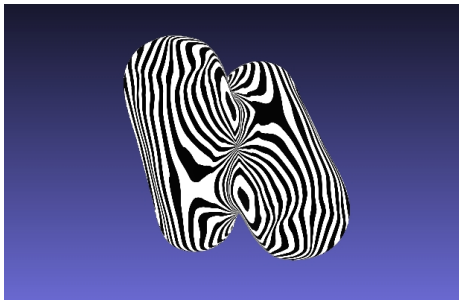

(e) new scheme limit surface

(f) Closeup view of (e)

Figure 5.7: C^1 limit surfaces (obtained after 6 steps of refinement) displayed with reflection lines with closeup views at extraordinary vertices of valence 3 and 6.

$f^3_{1,\frac{7}{128}}$ where $\frac{31}{512} > \frac{29}{2^{10}}$ as well as $\frac{7}{128} > \frac{29}{2^{10}}$, Condition 4.b is satisfied too. In a similar way, we find

$$C^n_\nu = \frac{81}{256} - \frac{9}{128}\cos\left(\frac{2\pi\nu}{n}\right) = f^n_{\nu,\frac{9}{128}+\frac{1}{256\cos\left(\frac{2\pi\nu}{n}\right)}}$$

and since $\frac{9}{128}+\frac{1}{256\cos\left(\frac{2\pi\nu}{n}\right)} > \frac{29}{2^{10}}$ for all $0 \le \nu \le n-1$, then for all $0 \le \nu \le n-1$ Condition 4.a is fulfilled. ■

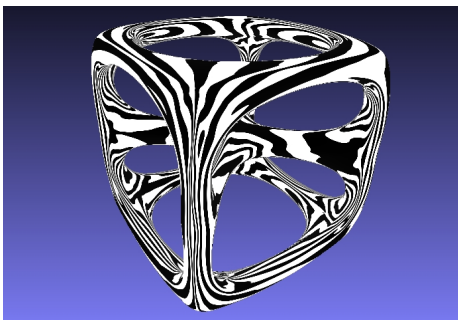

(a) Li-Ma-Bao's limit surface

(b) Closeup view of (a)

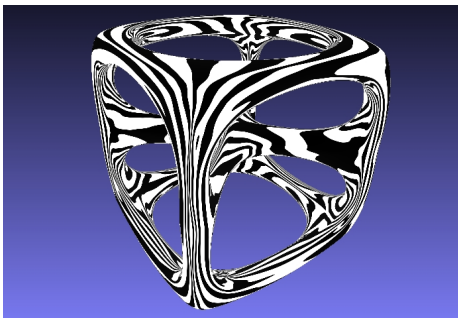

(c) Deng-Ma's limit surface

(d) Closeup view of (c)

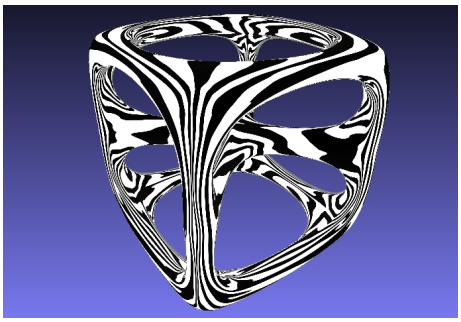

(e) new scheme limit surface

(f) Closeup view of (e)

Figure 5.8: C^1 limit surfaces (obtained after 6 steps of refinement) displayed with reflection lines with closeup views at extraordinary vertices of valence 6.

Finally, using Algorithm 1, we have verified that the new interpolatory subdivision scheme satisfies Condition 5.a for all $3 \leq n \leq 50$ after 9 refinement steps, and thus guarantees convergence, C^1 continuity and boundedness of principal curvatures at extraordinary points with these valences.
In Figure 5.6 we show four examples of initial control meshes refined by using the new interpolatory subdivision scheme. In Figures 5.7 and 5.8 we compare the limit surfaces obtained by the new extraordinary rules with the ones obtained via Li-Ma-Bao's and Deng-Ma's proposals. Analyzing the behavior of the reflection lines it turns out that the new

scheme produces limit surfaces of the same quality as Deng-Ma's and Li-Ma-Bao's schemes, but at a reduced computational cost.

5.2 A general computational approach to determine bounds of extraordinary rule weights

As already shown in Section 2.3, the structure of the subdivision matrix depends on the way with which we label the old and the new vertices around the central vertex or face. We recall that usually we can choose between two kinds of ordering, which determine two different techniques for the spectral analysis of the subdivision matrix. In particular,

Order 1. Primal scheme: ordering the vertices outwards from the central vertex, that is on successive rings with increasing radial distance, yields a matrix S that, discarded the first row and column, is a $p \times p$ block-matrix where each block, of size $n \times n$, is circulant;
Dual scheme: ordering the vertices outwards from one of the vertices of the central face, that is on successive rings with increasing radial distance, yields a matrix S that is a $p \times p$ block-matrix where each block, of size $n \times n$, is circulant;

Order 2. Primal scheme: ordering the vertices starting from the central vertex and outwards within each sector, before moving on to the next, and labeling compatibly within the sectors, gives a matrix S that, discarded the first row and column, is a $n \times n$ block-circulant matrix with blocks of size $p \times p$;
Dual scheme: ordering the vertices starting from one of the vertices of the central face and outwards within each sector, before moving on to the next, and labeling compatibly within the sectors, gives a matrix S that is a $n \times n$ block-circulant matrix with blocks of size $p \times p$.

Given these ordering, two different methods have been proposed for the eigen-analysis

Method 1. Originally presented by Doo and Sabin [48] and successively exploited by Ball and Storry [7] and by Zorin [137], it applies a similarity transform to S given by the matrix $\left[\begin{array}{c|c} 1 & 0 \\ \hline 0 & I_p \otimes F_n \end{array}\right]$ for primal schemes, and $I_p \otimes F_n$ for dual schemes, with I_p denoting the identity matrix of size p and F_n the Fourier matrix $F_n = \frac{1}{\sqrt{n}} \left[\mathrm{e}^{-\frac{2\pi \mathrm{i} j \ell}{n}} \right]_{j,\ell=0}^{n-1}$. Then, once a matrix with diagonal blocks is obtained, a permutation is applied to finally reduce the local subdivision matrix into a block-diagonal matrix containing one block of size $(p+1) \times (p+1)$ and $n-1$ blocks each of size $p \times p$ for primal schemes, or n blocks each of size $p \times p$ for dual schemes.

Method 2. Introduced by Peters and Reif [112], if the scheme is primal, it artificially extends each block of size $p \times p$ by one row and one column such that the local subdivision matrix assumes a standard block-circulant structure, and then diagonalizes it by applying the block-Fourier matrix $F_n \otimes I_{p+1}$, while if the scheme is dual the extension is not necessary and a diagonalization is obtained by applying the block-Fourier matrix $F_n \otimes I_p$.

We observe that, from a computational viewpoint, Method 2 offers the advantage of requiring the spectral analysis of matrices whose size does not change with the valence n. However, if the considered scheme is primal, this method generates $n-1$ eigenvalues "in surplus" that are not necessary to investigate the properties of the subdivision scheme, as we have seen in Section 5.1. For dual schemes the problem of generating useless zero eigenvalues does not exist since it is due to the formula in (2.22) with transform the hybrid block-circulant matrix $\tilde{S}$ into a block-circulant matrix S, which is a characteristic of primal subdivision schemes (see equations in (2.21)- (2.22)). Therefore, in this section we construct the primal subdivision matrix $\tilde{S}$ ordering the points as explained in Order 2, but, following the strategy used in [126], we study the eigenproperties of $\tilde{S}$ by applying a block-diagonalization via the unitary matrix

$$\tilde{F}_n = \left[\begin{array}{c|c} 1 & 0 \\ \hline 0 & F_n \otimes I_p \end{array}\right],$$

which avoid the generation of useless zero eigenvalues. In this way, the block-diagonal matrix

$$\tilde{F}_n \tilde{S} \tilde{F}_n^* = \begin{bmatrix} \tilde{S}_0 & 0 & \cdots & \cdots & 0 \\ 0 & \hat{S}_1 & \ddots & & \vdots \\ \vdots & \ddots & \hat{S}_2 & \ddots & \vdots \\ \vdots & & \ddots & \ddots & 0 \\ 0 & \cdots & \cdots & 0 & \hat{S}_{n-1} \end{bmatrix}, \tag{5.22}$$

with one block $\tilde{S}_0$ of size $(p+1)\times(p+1)$ and $n-1$ blocks $\hat{S}_\nu$, $\nu = 1,\ldots,n-1$, of size $p \times p$, is directly obtained, so that the eigenproperties of $\tilde{S}$ can be read from the spectrum of the n blocks.

5.2.1 Block-circulant and hybrid block-circulant algebras

In this section we sketch the main properties of the famous block-circulant algebra, introducing then the so-called hybrid block-circulant algebra, useful for the spectral study of subdivision matrices of primal subdivision schemes. Block-circulants form an algebra and represent a subspace of block-Toeplitz used for their approximation in numerical methods such as multigrid methods, preconditioned Krylov methods and combination of them: for the algebraic properties of such algebra see [33]; for the numerical techniques related to these structures see [80]. In particular such matrices are encountered in signal/image processing (see the problem of signal reconstruction with missing data [36]), in Markov chain problems (see [10] and references therein), in the approximation of vector partial differential equations (PDEs) as the elasticity problem (see [47]), or of scalar PDEs by standard Finite Element methods [64]. To confirm their pervasive nature, these structures arise in the context of our approximation problems as described below.
A matrix A of size pn is called block-circulant if its entries $a_j \in \mathbb{C}^{p\times p}$, $j = 0,\ldots,n-1$, obey

the rule $A = [a_{(s-r) \bmod n}]_{r,s=0}^{n-1}$, that is

$$A = \begin{bmatrix} a_0 & a_1 & \cdots & a_{n-2} & a_{n-1} \\ a_{n-1} & a_0 & a_1 & \ddots & a_{n-2} \\ a_{n-2} & a_{n-1} & \ddots & \ddots & \vdots \\ \vdots & \ddots & \ddots & \ddots & a_1 \\ a_1 & \cdots & a_{n-2} & a_{n-1} & a_0 \end{bmatrix}.$$

Thus, the following spectral decomposition holds

$$A = (F_n^* \otimes I_p) D_n (F_n \otimes I_p),$$

where $\otimes$ is the Kronecker product of matrices, F_n^* is the conjugate transpose of F_n, and

$$D_n = \operatorname{diag}(\sqrt{n} F_n^* \mathbf{a}),$$

is a block-diagonal matrix with $\mathbf{a} = [a_0, a_1, \ldots, a_{n-1}]^T$ denoting the first block-row of the matrix A.

Remark 5.16 *Usually, the block-circulant matrix is defined with* $\mathbf{a} = [a_0, a_1, \ldots, a_{n-1}]$ *as the first block-column instead of the first block-row. Here we use this formulation to meet the notations used in the context of subdivision schemes.*

If we embed the block-circulant matrix A in a structure with this form

$$\tilde{A} = \left[\begin{array}{c|ccc} u & \mathbf{v}^T & \cdots & \mathbf{v}^T \\ \hline \mathbf{w} & & & \\ \vdots & & A & \\ \mathbf{w} & & & \end{array}\right],$$

with $u \in \mathbb{C}$ and $\mathbf{v}, \mathbf{w} \in \mathbb{C}^{p \times 1}$ so that $\tilde{A} \in \mathbb{C}^{(pn+1)\times(pn+1)}$, we can construct a new algebra of matrices, the so called hybrid block-circulant algebra, such that

$$\tilde{A} = \tilde{F}_n^* \tilde{D}_n \tilde{F}_n,$$

where

$$\tilde{F}_n = \left[\begin{array}{c|c} 1 & 0 \\ \hline 0 & F_n \otimes I_p \end{array}\right] \quad \text{and} \quad \tilde{D}_n = \left[\begin{array}{c|ccc} u & \sqrt{n}\mathbf{v}^T & 0 & 0 \\ \hline \sqrt{n}\mathbf{w} & & & \\ 0 & & D_n & \\ 0 & & & \end{array}\right].$$

5.2.2 Spectral properties of the subdivision matrix and limit surface characteristics

Primal subdivision schemes are characterized by a local subdivision matrix $\tilde{S} \in \mathbb{R}^{(pn+1)\times(pn+1)}$ of the form shown in (2.21), which belongs to the hybrid block-circulant matrix algebra

described in Section 5.2.1. As a consequence, it satisfies

$$\tilde{F}_n \tilde{S} \tilde{F}_n^* = \left[\begin{array}{c|ccccc} a & \sqrt{n}\mathbf{b}^T & 0 & \cdots & 0 & 0 \\ \hline \sqrt{n}\mathbf{c} & \hat{S}_0 & 0 & \cdots & 0 & 0 \\ 0 & 0 & \hat{S}_1 & 0 & \ddots & 0 \\ 0 & 0 & 0 & \ddots & \ddots & \vdots \\ \vdots & \vdots & \ddots & \ddots & \ddots & 0 \\ 0 & 0 & \cdots & 0 & 0 & \hat{S}_{n-1} \end{array}\right], \tag{5.23}$$

where the blocks $\hat{S}_\nu$, $\nu = 0, \ldots, n-1$, are obtained by the blocks $\tilde{M}_j$, $j = 0, \ldots, n-1$, in (2.21) applying a discrete Fourier transform

$$\hat{S}_\nu = \sum_{j=0}^{n-1} \omega^{j\nu} \tilde{M}_j, \qquad \nu = 0, 1, \ldots, n-1,$$

where $\omega = e^{\mathrm{i}\frac{2\pi}{n}}$. Denoting with $\tilde{S}_0$ the $(p+1) \times (p+1)$ block

$$\tilde{S}_0 = \left[\begin{array}{cc} a & \sqrt{n}\mathbf{b}^T \\ \sqrt{n}\mathbf{c} & \hat{S}_0 \end{array}\right],$$

we can rewrite the matrix in (5.23) as in (5.22).
It is well-known that, to guarantee that the subdivision surface will lie within the convex hull of the control mesh, all the entries of $\tilde{S}$ have to be in $[0, 1]$, i.e. all the weights appearing in the subdivision rules have to be in such interval. Moreover, Table 2.1 summarizes all the necessary conditions required on the eigenvalues of $\tilde{S}$ in order to obtain a limit surface that is convergent and tangent plane continuous, with bounded curvature and optimal shrinkage at the extraordinary vertices.

Remark 5.17 *The conditions summarized in Table 2.1 are not sufficient to guarantee the generation of C^1 continuous limit surfaces. In fact, they do not take into account the behavior of the characteristic map $\mathbf{\Psi}$. Additionally requiring that this map is regular and injective, we can indeed guarantee that the limit surface produced by the subdivision scheme will be C^1 with bounded curvature, convex hull property and optimal shrinkage [112]. However, as also previously done in [65, 96], here we focus our attention on the spectral properties of the subdivision matrix that are essential to obtain C^1 limit surfaces with bounded curvature, convex hull property and optimal shrinkage effect.*

5.2.3 Computing bounds for extraordinary rule weights

Exploiting all the notions recalled in the previous sections, we now define a computational strategy to find the weights of extraordinary stencils in order to obtain limit surfaces with the desired characteristics. We proceed as follows

- we consider the refinement rules of a primal subdivision scheme which depend on some free parameters;
- from these rules, we construct the subdivision matrix $\tilde{S}$ as in (2.21);

- using the discrete Fourier transform, we build a similar block-diagonal matrix as in (5.23);

- we compute the eigenvalues of each block and we impose on them the necessary conditions for convergence, tangent plane continuity and boundedness of curvature summarized in Table 2.1;

- we set $\lambda = \frac{1}{m}$ to guarantee also the optimal shrinkage;

- we find the ranges in which the free parameters defining the subdivision rules could vary;

- if we want to ensure also the convex hull property, we require that the range of variability of each parameter is contained in $[0, 1]$.

In the following, we apply this general strategy to two examples of primal subdivision schemes for triangular meshes, both improving the well-known Loop's subdivision scheme [95].

In 1987 C. Loop proposed a binary subdivision scheme for triangular meshes, capable of producing a limit surface that is C^2 continuous everywhere except at the extraordinary points where it is only C^1. Although Loop's limit surface satisfies the convex hull property, neither boundedness of curvature nor optimal shrinkage are achieved [95]. The vertex-point and edge-point stencils of this scheme are shown in Figure 2.5, and the corresponding subdivision rules read as

$$\begin{aligned} V &= \delta P_0 + \sum_{i=1}^{n} \left(\frac{1-\delta}{n} P_i \right), \qquad \text{with} \qquad \delta = \left(\frac{3}{8} + \frac{1}{4} \cos\left(\frac{2\pi}{N} \right) \right)^2 + \frac{3}{8}, \\ E &= \frac{3}{8}(P_0 + P_1) + \frac{1}{8}(P_2 + P_n), \end{aligned} \tag{5.24}$$

where P_0 denotes the central (extraordinary) vertex, P_1 the vertex on its right hand side and P_i, $i = 2, \ldots, n$ all the remaining ones ordered counterclockwise. We notice that, while the vertex-point rule depends on the valence n of the extraordinary vertex, the edge-point rule is not influenced by n.
During the years different improvements of original Loop's subdivision scheme have been proposed to gain boundedness of curvature at extraordinary vertices. The goal has been reached by considering either a larger edge-point stencil [65, 96] or a suitable transformation of the subdivision rules into the ternary setting [97]. The resulting innovative schemes in [96, 97] propose vertex-point and edge-point stencils where the weights assume a specific appropriate value in order to produce a limit surface of class C^1 and with bounded curvature at extraordinary vertices. However, the property of optimal shrinkage is never reached except for the regular case $n = 6$. The goal of this section is to consider the stencils of modified binary Loop's scheme as well as of ternary Loop's scheme, and to apply our theoretical results in order to determine in which ranges the stencil weights could vary to achieve not only the boundedness of curvature and the convex hull property, but also the optimal shrinkage property at extraordinary vertices of valence $n \geq 5, n \neq 6$.

Binary Loop's scheme: 1-ring rules

In [96], new rules of binary Loop's scheme near an extraordinary vertex of valence $n \neq 6$ have been proposed, which are described by the stencils in Figure 5.9. The coefficients $\delta, \alpha, \beta_j,\ j = 0, \ldots, n-1$ chosen by the author satisfy the necessary conditions for convex hull, tangent plane continuity and boundedness of curvature at extraordinary vertices, but not the optimal shrinkage, i.e. the version of Loop's scheme in [96] satisfies requirements (i)-(iv) of Table 2.1, but not condition (v).

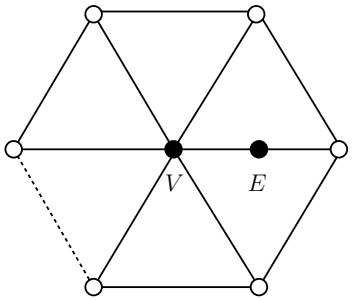

(a) New Loop's scheme

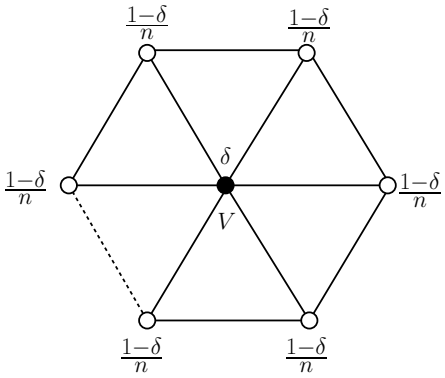

(b) New Loop's vertex-point stencil

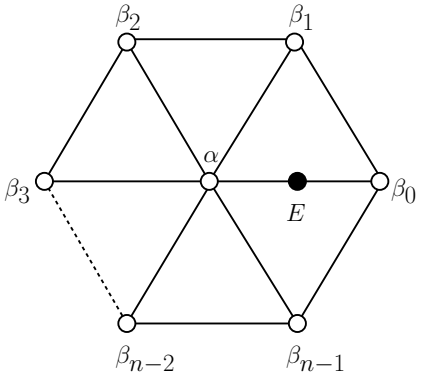

(c) New Loop's edge-point stencil

Figure 5.9: Stencils for the vertex-point rule and the edge-point rule of new Loop's subdivision scheme at vertices of valence n.

Comparing the extraordinary stencils of the bounded curvature version of Loop's scheme in Figure 5.9 with the original ones in Figure 2.5, we notice that the vertex-point rule has the same structure, while the edge-point rule of the new version of Loop's scheme involves a higher number of points than the original one and depends on the valence of the extraordinary vertex. Moreover, we notice that binary Loop's scheme is a 1-ring scheme, since both the vertex-rule and the edge-rule require just the contribution of the points that are on the first ring around the extraordinary vertex.
In the following, we show the main steps to find new weights for the extraordinary stencils in Figure 5.9 in order to satisfy not only the properties of convex hull, tangent plane continuity and boundedness of curvature, but also optimal shrinkage. Since we have a binary scheme,

the arity is $m = 2$, so condition (v) is satisfied by setting $\lambda = \frac{1}{2}$.
First of all, we notice that for the symmetry of the scheme we have

$$\beta_j = \beta_{n-j}, \quad j = 1, \dots, n-1, \tag{5.25}$$

and

$$\beta_{\lfloor \frac{n}{2} \rfloor} = \begin{cases} \dfrac{1}{2}\left(1 - \alpha - \beta_0 - 2\displaystyle\sum_{j=1}^{\lfloor \frac{n}{2} \rfloor - 1} \beta_j\right), & \text{if } n \text{ odd}, \\ 1 - \alpha - \beta_0 - 2\displaystyle\sum_{j=1}^{\frac{n}{2}-1} \beta_j, & \text{if } n \text{ even}, \end{cases} \quad \Rightarrow \quad \sum_{j=0}^{n-1} \beta_j = 1 - \alpha. \tag{5.26}$$

Then, we construct the subdivision matrix $\tilde{S}$ of the form in (2.21) with blocks $M_i \in \mathbb{R}^{p \times p}$, $i = 0, \dots, n-1$. Since Loop's scheme has 1-ring rules, from (2.18) we simply have $p = 1$. Thus $\tilde{S}$ is a hybrid circulant matrix of the form

$$\tilde{S} = \left[\begin{array}{c|ccccc} \delta & \frac{1-\delta}{n} & \frac{1-\delta}{n} & \dots & \frac{1-\delta}{n} & \frac{1-\delta}{n} \\ \hline \alpha & \beta_0 & \beta_1 & \cdots & \beta_{n-2} & \beta_{n-1} \\ \alpha & \beta_{n-1} & \beta_0 & \beta_1 & \ddots & \beta_{n-2} \\ \alpha & \beta_{n-2} & \beta_{n-1} & \ddots & \ddots & \vdots \\ \vdots & \vdots & \ddots & \ddots & \ddots & \beta_1 \\ \alpha & \beta_1 & \cdots & \beta_{n-2} & \beta_{n-1} & \beta_0 \end{array}\right].$$

Then, we apply the discrete Fourier transform obtaining

$$\hat{S}_\nu = \sum_{j=0}^{n-1} \beta_j \omega^{j\nu}, \quad \nu = 1, \dots, n-1, \qquad \text{and} \qquad \tilde{S}_0 = \begin{pmatrix} \delta & \frac{1-\delta}{\sqrt{n}} \\ \sqrt{n}\alpha & \sum_{j=0}^{n-1} \beta_j \end{pmatrix}. \tag{5.27}$$

Since $p = 1$ we have $\hat{S}_\nu = \lambda_0^\nu$ and, in particular,

$$\lambda_0^\nu = \sum_{j=0}^{n-1} \beta_j \omega^{j\nu}, \quad \nu = 1, \dots, n-1, \tag{5.28}$$

while for $\tilde{S}_0$, thanks to (5.26), we find $\lambda_0^0 = 1$, $\lambda_1^0 = \delta - \alpha$.

Remark 5.18 *Since for $j = 1, \dots, n-1$ we have $\omega^{j\nu} + \omega^{(n-j)\nu} = \omega^{j(n-\nu)} + \omega^{(n-j)(n-\nu)}$ and, for n even, $\omega^{\frac{n}{2}\nu} = \omega^{\frac{n}{2}(N-\nu)}$, from (5.25) and (5.28) it holds*

$$\lambda_0^\nu = \lambda_0^{n-\nu},$$

so conditions (ii)-(iii) of Table 2.1 reduce to $\lambda_0^1 = \lambda$ and $\lambda_0^2 = \lambda^2$, respectively.

Summarizing, taking into account Remark 5.18, the condition (i) in Table 2.1 is satisfied with

$$\delta - \alpha = \frac{1}{4}, \tag{5.29}$$

the condition (ii) leads to

$$\sum_{j=0}^{n-1} \beta_j \omega^j = \frac{1}{2}, \tag{5.30}$$

and from condition (iii) has to hold

$$\sum_{j=0}^{n-1} \beta_j \omega^{2j} = \frac{1}{4}. \tag{5.31}$$

Finally, to gain also condition (iv), we have to check for which ranges of the free parameters we have $|\lambda_0^\nu| \leq \frac{1}{4}$, for $\nu = 3, \ldots, n-3$, and if the convex hull property is satisfied, i.e. all the free parameters are in $[0, 1]$.

Remark 5.19 *From (5.29) it is clear that α and δ are strictly related. If we find an expression for α, then $\delta = \frac{1}{4} + \alpha$ and, in order to ensure the convex hull property also for δ, we have to restrict the set of values for α to $\left[0, \frac{3}{4}\right]$. On the other hand, if we obtain δ, then $\alpha = \delta - \frac{1}{4}$ with $\delta \in \left[\frac{1}{4}, 1\right]$ for the convex hull property for α.*

In the following, we show the details of the computation for the cases $n = 5$ and $n = 7$ since, as already recalled in Section 2.3.3, these are considered the crucial extraordinary valences when dealing with triangular meshes.

Proposition 5.20 *Binary Loop's scheme with extraordinary stencils in Figure 5.9 satisfies the conditions (i)-(iv) in Table 2.1 and the convex hull property at an extraordinary vertex of valence $n = 5$ if*

$$\beta_1 \in \left[\frac{\sqrt{5}}{20}, \frac{\sqrt{5}+5}{40}\right] \approx [0.1118, 0.1809], \tag{5.32}$$

and

$$\alpha = \frac{\sqrt{5}+5}{8} - 5\beta_1, \quad \beta_0 = \beta_1 + \frac{15-\sqrt{5}}{40}, \quad \beta_2 = \beta_1 - \frac{\sqrt{5}}{20}, \quad \delta = \frac{\sqrt{5}+7}{8} - 5\beta_1,$$

with $\beta_3 = \beta_2$ and $\beta_4 = \beta_1$.

Proof: In case of an extraordinary vertex of valence $n = 5$, recalling the condition (5.25), the stencil weights are $\alpha, \beta_0, \beta_1, \beta_2$ and δ with

$$\beta_2 = \frac{1}{2}(1 - \alpha - \beta_0 - 2\beta_1), \tag{5.33}$$

thanks to (5.26). For $n = 5$, the expressions in (5.27) become

$$\hat{S}_\nu = \beta_0 + \beta_1(\omega^\nu + \omega^{4\nu}) + \beta_2(\omega^{2\nu} + \omega^{3\nu}) \qquad \text{and} \qquad \tilde{S}_0 = \begin{pmatrix} \delta & \frac{1-\delta}{\sqrt{5}} \\ \sqrt{5}\alpha & 1-\alpha \end{pmatrix},$$

since $\sum_{j=0}^{4}\beta_j = 1-\alpha$. Hence, from (5.30) and (5.33), we have

$$\begin{aligned}\frac{1}{2} &= \beta_0 + \beta_1(\omega+\omega^4) + \beta_2(\omega^2+\omega^3)\\ &= \frac{1}{2}(\omega^2+\omega^3) - \frac{\alpha}{2}(\omega^2+\omega^3) + \beta_0(1-\frac{1}{2}(\omega^2+\omega^3)) + \beta_1(\omega+\omega^4-(\omega^2+\omega^3))\\ &= -\frac{\sqrt{5}+1}{4} + \frac{\sqrt{5}+1}{4}\alpha + \frac{\sqrt{5}+5}{4}\beta_0 + \sqrt{5}\beta_1,\end{aligned}$$

where the last equality holds for $\omega+\omega^4 = \frac{\sqrt{5}-1}{2}$ and $\omega^2+\omega^3 = -\frac{\sqrt{5}+1}{2}$. Similarly, it holds

$$\frac{\sqrt{5}-1}{4} - \frac{\sqrt{5}-1}{4}\alpha + \frac{5-\sqrt{5}}{4}\beta_0 - \sqrt{5}\beta_1 = \frac{1}{4},$$

thanks to equation (5.31). From these relations, we find

$$\alpha = \frac{\sqrt{5}+5}{8} - 5\beta_1, \qquad \beta_0 = \beta_1 + \frac{15-\sqrt{5}}{40},$$

and, as a consequence of (5.33), $\beta_2 = \beta_1 - \frac{\sqrt{5}}{20}$. Moreover, (5.29) gives $\delta = \frac{\sqrt{5}+7}{8} - 5\beta_1$, and since there are no other eigenvalues, condition (iv) in Table 2.1 is verified too. Now we have to ensure the convex hull property for all the parameters, that is, by considering Remark 5.19,

$$\begin{aligned}\alpha \in \left[0,\frac{3}{4}\right] \quad &\Leftrightarrow \quad \beta_1 \in \left[\frac{\sqrt{5}-1}{40}, \frac{\sqrt{5}+5}{40}\right] \approx [0.0309, 0.1809],\\ \beta_0 \in [0,1] \quad &\Leftrightarrow \quad \beta_1 \in \left[\frac{\sqrt{5}-15}{40}, \frac{\sqrt{5}+25}{40}\right] \approx [-0.3191, 0.6809],\\ \beta_2 \in [0,1] \quad &\Leftrightarrow \quad \beta_1 \in \left[\frac{\sqrt{5}}{20}, \frac{\sqrt{5}+20}{20}\right] \approx [0.1118, 1.1118],\end{aligned}$$

and the intersection of these intervals (taking into account, if necessary, that also β_1 should be in $[0,1]$) gives (5.32). ■

Proposition 5.21 *Binary Loop's scheme with extraordinary stencils in Figure 5.9 satisfies the conditions (i)-(iv) in Table 2.1 and the convex hull property at an extraordinary vertex of valence $n=7$ if, setting $c_j = 2\cos\frac{j\pi}{7}$, $j=2,4,6$,*

$$\begin{aligned}\beta_1 &\in \left[\frac{4+c_2+c_4-2c_2c_6}{28c_2+8c_4-36c_6+8c_2c_4-8c_4c_6}, \frac{36+33c_2+10c_4-31c_6+6c_2c_4-20c_2c_6-7c_4c_6+3c_2c_4c_6}{196c_2+20c_4-216c_6+20c_2c_4-20c_4c_6}\right]\\ &\approx [0.1089, 0.2804],\end{aligned} \tag{5.34}$$

$$\begin{aligned}\beta_2 \in \Big[&\max\left\{\frac{1+4(c_4-c_2)\beta_1}{4(c_4-c_6)}, 0, \frac{3c_2-c_4-2c_6}{4(c_2c_6+c_2c_4-6-c_4-c_6-c_2+c_4c_6)} + \beta_1\right\},\\ &\min\left\{\frac{c_2-c_4}{4(c_2c_6+c_2c_4-6-c_4-c_6-c_2+c_4c_6)} + \beta_1, \frac{2+2c_2-3c_6+4(2-4c_2+3c_4+2c_6-c_4c_6)\beta_1}{4(2+3c_2+2c_4-4c_6-c_2c_4)}\right\}\Big],\end{aligned}$$

and

$$\alpha = \frac{1}{4(c_2 - c_6)}\left[2 + 2c_2 - 3c_6 + 4(2 - 4c_2 + 3c_4 + 2c_6 - c_4c_6)\beta_1 + \right. \tag{5.35}$$
$$\left. + 4(-2 - 3c_2 - 2c_4 + 4c_6 + c_2c_4)\beta_2\right],$$
$$\beta_0 = \frac{1}{4(c_2 - c_6)}\left[2c_2 - c_6 + 4(-2 - c_4 + c_4c_6)\beta_1 + 4(2 + c_2 - c_2c_4)\beta_2\right], \tag{5.36}$$
$$\beta_3 = \frac{1}{4(c_2 - c_6)}\left[-1 + 4(c_2 - c_4)\beta_1 + 4(c_4 - c_6)\beta_2\right], \tag{5.37}$$
$$\delta = \frac{1}{4(c_2 - c_6)}\left[2 + 3c_2 - 4c_6 + 4(2 - 4c_2 + 3c_4 + 2c_6 - c_4c_6)\beta_1 + \right. \tag{5.38}$$
$$\left. + 4(-2 - 3c_2 - 2c_4 + 4c_6 + c_2c_4)\beta_2\right],$$

with $\beta_4 = \beta_3$, $\beta_5 = \beta_2$ *and* $\beta_6 = \beta_1$.

Proof: Following the same reasoning of the previous proof, in case of an extraordinary vertex of valence $n = 7$, the stencil weights are $\alpha, \beta_0, \beta_1, \beta_2, \beta_3$ and δ with

$$\beta_3 = \frac{1}{2}(1 - \alpha - \beta_0 - 2\beta_1 - 2\beta_2). \tag{5.39}$$

If $n = 7$, the formulas in (5.27) become

$$\hat{S}_\nu = \beta_0 + \beta_1(\omega^\nu + \omega^{6\nu}) + \beta_2(\omega^{2\nu} + \omega^{5\nu}) + \beta_3(\omega^{3\nu} + \omega^{4\nu}),$$

and

$$\tilde{S}_0 = \begin{pmatrix} \delta & \frac{1-\delta}{\sqrt{7}} \\ \sqrt{7}\alpha & 1 - \alpha \end{pmatrix}.$$

From (5.30) and (5.31), exploiting (5.39), we have

$$\begin{aligned} -\frac{1}{2}c_6\alpha + \left(1 - \frac{1}{2}c_6\right)\beta_0 + (c_2 - c_6)\beta_1 + (c_4 - c_6)\beta_2 + \frac{1}{2}c_6 &= \frac{1}{2}, \\ -\frac{1}{2}c_2\alpha + \left(1 - \frac{1}{2}c_2\right)\beta_0 + (c_4 - c_2)\beta_1 + (c_6 - c_2)\beta_2 + \frac{1}{2}c_2 &= \frac{1}{4}. \end{aligned}$$

These equations give α and β_0 as in (5.35)-(5.36), and we obtain β_3 and δ in (5.37)-(5.38) as a consequence of (5.39) and (5.29), respectively. Moreover, from condition (iv) in Table 2.1, we require $|\lambda_0^3|, |\lambda_0^4| \leq \frac{1}{4}$. Since Remark 5.18 ensures that $\lambda_0^3 = \lambda_0^4$, the previous inequality is verified from (5.28) with $\nu = 3$ if

$$-\frac{1}{4} \leq \frac{4(c_2c_6 + c_2c_4 - 6 - c_4 - c_6 + c_4c_6 - c_2)(\beta_1 - \beta_2) + 2c_2 - c_6 - c_4}{4(c_2 - c_6)} \leq \frac{1}{4},$$

that is

$$\lambda_0^3 \in \left[-\frac{1}{4}, \frac{1}{4}\right] \quad \Leftrightarrow \quad \beta_2 \in \frac{[3c_2 - c_4 - 2c_6, c_2 - c_4]}{4(c_2c_6 + c_2c_4 - 6 - c_4 - c_6 - c_2 + c_4c_6)} + \beta_1. \tag{5.40}$$

Now we check the convex hull property, by remembering Remark 5.19,

$$\alpha \in \left[0, \frac{3}{4}\right] \quad \Leftrightarrow \quad \beta_2 \in \frac{[2-c_2, 2+2c_2-3c_6] + 4(2-4c_2+3c_4+2c_6-c_4c_6)\beta_1}{4(2+3c_2+2c_4-4c_6-c_2c_4)}, \tag{5.41}$$

$$\beta_0 \in [0,1] \quad \Leftrightarrow \quad \beta_2 \in \frac{[2c_2-c_6, -2c_2+3c_6] + 4(-2-c_4+c_4c_6)\beta_1}{4(c_2c_4-2-c_2)},$$

$$\beta_3 \in [0,1] \quad \Leftrightarrow \quad \beta_2 \in \frac{[1, 1+4c_2-4c_6] + 4(c_4-c_2)\beta_1}{4(c_4-c_6)}.$$

We observe that all the eligible values for β_2 in (5.41) and (5.40), for $\beta_1 \in [0,1]$, are contained in regions of the plane delimited by two parallel lines (see Figure 5.10). The intersection of such regions, taking into account that also β_2 should be in $[0,1]$ and using the notation explained in the caption of Figure 5.10, gives rise to

$$\beta_1 \in [(\beta_3)_{\mathrm{L}} \cap (\lambda_0^3)_{\mathrm{R}}, (\lambda_0^3)_{\mathrm{L}} \cap (\alpha)_{\mathrm{R}}],$$
$$\beta_2 \in [\max\{(\beta_3)_{\mathrm{L}}, 0, (\lambda_0^3)_{\mathrm{L}}\}, \min\{(\lambda_0^3)_{\mathrm{R}}, (\alpha)_{\mathrm{R}}\}],$$

which are written in full in (5.34) and (5.35). ■

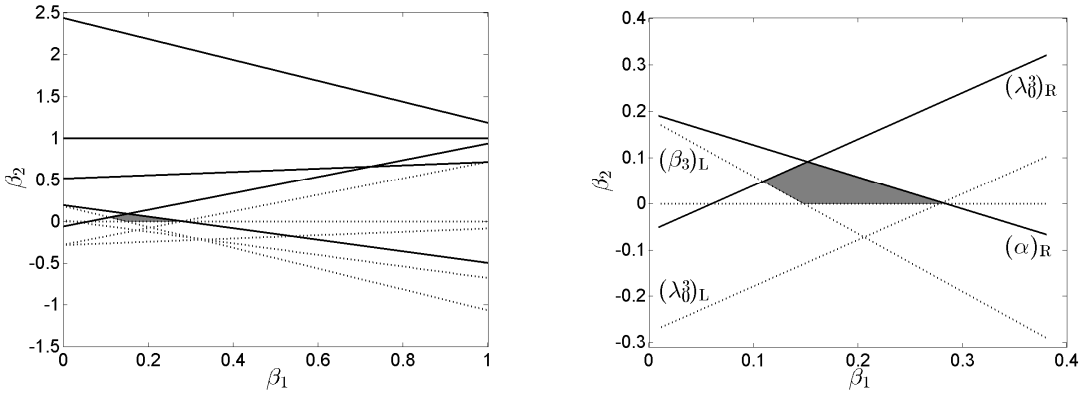

(a) (b)

Figure 5.10: (a): $(\cdots)$ lines demarcating the eligible regions from left, $(-)$ lines demarcating the eligible regions from right for β_2, given in (5.41) and (5.40), with $\beta_1 \in [0,1]$: in gray is depicted the intersection of such eligible regions. (b) Zoom of the eligibility region in (a) with indications about the involved lines: $(\theta)_{\mathrm{L}}$ and $(\theta)_{\mathrm{R}}$ are, respectively, the left and the right demarcating lines of the regions of values for β_2 related to $\theta \in \{\alpha, \beta_3, \lambda_0^3\}$.

Figure 5.11 illustrates the result of the new Loop's subdivision scheme when applied to triangle meshes containing only extraordinary vertices of valence $n = 5$ and $n = 7$ (initial data are courtesy of the authors of [1]). The free β parameters have been set accordingly to the identified bounds.

Ternary Loop's scheme: 2-ring rules

To gain the boundedness of curvature in the limit surface, another possible modification of original Loop's scheme is its ternary version, proposed in [97], whose stencils are shown in

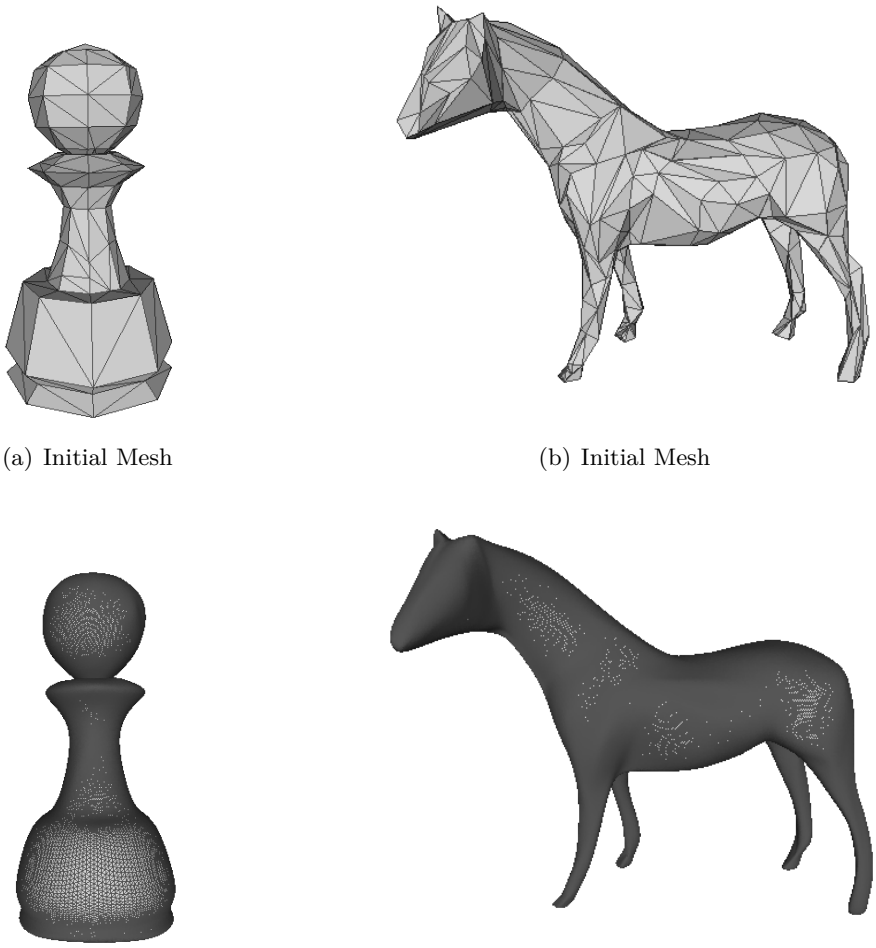

(a) Initial Mesh (b) Initial Mesh

(c) Refined Mesh (4 steps) (d) Refined Mesh (4 steps)

Figure 5.11: Refined meshes obtained from a 567-mesh using new binary Loop's scheme with parameters $\beta_1 = 0.112$ for $n = 5$, $\beta_1 = 0.14, \beta_2 = 0.02$ for $n = 7$ (left column) and $\beta_1 = 0.13$ for $n = 5$, $\beta_1 = 0.16, \beta_2 = 0.022$ for $n = 7$ (right column).

Figure 5.12. We notice that, if in the binary case the scheme is defined by 2 stencils, one for the vertex-point and one for the edge-point, the ternary variant needs 3 different stencils to define the vertex-point, the edge-point and the face-point, respectively. In the regular case, $n = 6$, the stencil weights are

$$\alpha = \frac{2}{3}, \quad \beta_0 = \frac{20}{81}, \quad \beta_1 = \beta_5 = \frac{10}{81}, \quad \beta_2 = \beta_4 = \frac{2}{81}, \quad \beta_3 = \frac{1}{81}, \quad \delta = \frac{5}{9},$$

while near extraordinary vertices the coefficients proposed in [97] are chosen to satisfy conditions (i)-(iv) in Table 2.1 and the convex hull property, but not requirement (v) regarding the optimal shrinkage effect.
We notice that the ternary Loop's scheme is a 2-ring scheme, since the vertex-point rule and the edge-point rule require just the contribution of the points on the first ring around the

extraordinary vertex, but the face-point rule involves also the points of the second ring.
In the following, we apply the discussed computational strategy to find new weights for the extraordinary stencils in Figure 5.12 in order to satisfy both the convex hull property and all requirements (i)-(v) in Table 2.1: since we have a ternary scheme, i.e. the arity is $m = 3$, condition (v) is satisfied by setting $\lambda = \frac{1}{3}$.

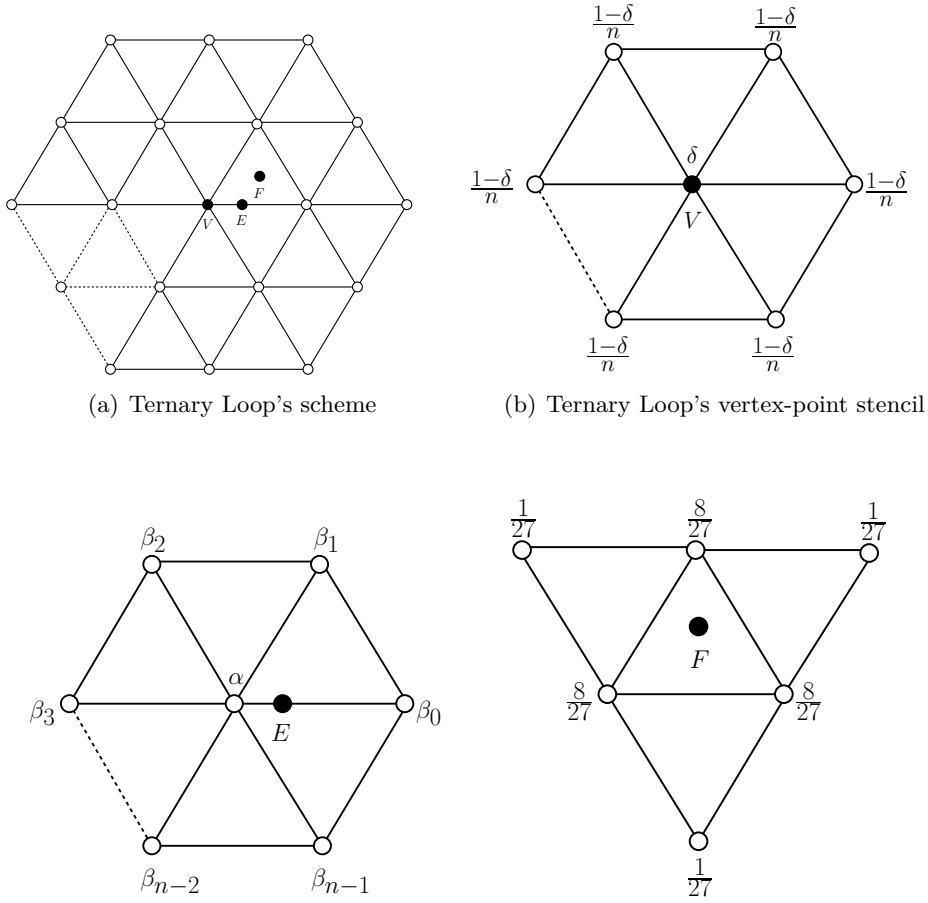

(a) Ternary Loop's scheme

(b) Ternary Loop's vertex-point stencil

(c) Ternary Loop's edge-point stencil

(d) Ternary Loop's face-point stencil

Figure 5.12: Stencils for the vertex-point rule, the edge-point rule and the face-point rule of ternary Loop's subdivision scheme at vertices of valence n.

First of all, for the symmetry of the scheme, we require (5.25) and (5.26). Then, we start by constructing the subdivision matrix $\tilde{S}$ of the form in (2.21) with blocks $M_i \in \mathbb{R}^{p\times p}$, $i = 0, \dots, n-1$. Since ternary Loop's scheme has 2-ring rules, from (2.18) we have $p = 3$. Thus $\tilde{S}$ is a block-circulant matrix as in (2.21) with $\tilde{a} = \delta$, $\tilde{\mathbf{b}} = \left[\frac{1-\delta}{n}, 0, 0\right]^T$, $\tilde{\mathbf{c}} = \left[\alpha, \frac{20}{81}, \frac{8}{27}\right]^T$,

and

$$\tilde{M}_0 = \begin{pmatrix} \beta_0 & 0 & 0 \\ \frac{4}{9} & \frac{1}{81} & \frac{2}{81} \\ \frac{8}{27} & 0 & \frac{1}{27} \end{pmatrix}, \qquad \tilde{M}_1 = \begin{pmatrix} \beta_1 & 0 & 0 \\ \frac{10}{81} & 0 & 0 \\ \frac{8}{27} & 0 & 0 \end{pmatrix}, \qquad \tilde{M}_2 = \begin{pmatrix} \beta_2 & 0 & 0 \\ 0 & 0 & 0 \\ \frac{1}{27} & 0 & 0 \end{pmatrix},$$

$$\tilde{M}_i = \begin{pmatrix} \beta_i & 0 & 0 \\ 0 & 0 & 0 \\ 0 & 0 & 0 \end{pmatrix},\ i = 3, \dots, n-2, \qquad \tilde{M}_{n-1} = \begin{pmatrix} \beta_{n-1} & 0 & 0 \\ \frac{10}{81} & 0 & \frac{2}{81} \\ \frac{1}{27} & 0 & 0 \end{pmatrix}.$$

After applying the discrete Fourier transform we get

$$\hat{S}_\nu = \begin{pmatrix} \sum_{j=0}^{n-1} \beta_j \omega^{j\nu} & 0 & 0 \\ \frac{4}{9} + \frac{10}{81}(\omega^\nu + \omega^{(n-1)\nu}) & \frac{1}{81} & \frac{2}{81}(1 + \omega^{(n-1)\nu}) \\ \frac{8}{27}(1 + \omega^\nu) + \frac{1}{27}(\omega^{2\nu} + \omega^{(n-1)\nu}) & 0 & \frac{1}{27} \end{pmatrix}, \quad \nu = 1, \dots, n-1,$$

and

$$\tilde{S}_0 = \begin{pmatrix} \delta & \frac{1-\delta}{\sqrt{n}} & 0 & 0 \\ \sqrt{n}\alpha & \sum_{j=0}^{N-1} \beta_j & 0 & 0 \\ \sqrt{n}\frac{20}{81} & \frac{56}{81} & \frac{1}{81} & \frac{4}{81} \\ \sqrt{n}\frac{8}{27} & \frac{2}{3} & 0 & \frac{1}{27} \end{pmatrix}.$$

We consider $\hat{S}_\nu, \nu = 1, \dots, n-1$, and we compute the characteristic polynomial $p_\nu(\lambda)$ which turns out to be of the form

$$p_\nu(\lambda) = \frac{1}{2187}(27\lambda - 1)(81\lambda - 1)\left(\sum_{j=0}^{n-1} \beta_j \omega^{j\nu} - \lambda\right).$$

Thus, each block $\hat{S}_\nu, \nu = 1, \dots, n-1$, has eigenvalues[1]

$$\lambda_0^\nu = \sum_{j=0}^{n-1} \beta_j \omega^{j\nu}, \quad \lambda_1^\nu = \frac{1}{27}, \quad \lambda_2^\nu = \frac{1}{81}. \tag{5.42}$$

In a similar way, we consider $\tilde{S}_0$ with characteristic polynomial

$$p_0(\lambda) = \frac{1}{2187}(\lambda - 1)(81\lambda - 1)(27\lambda - 1)(\alpha - \delta + \lambda),$$

and eigenvalues $\lambda_0^0 = 1$, $\lambda_1^0 = \delta - \alpha$, $\lambda_2^0 = \frac{1}{27}$, $\lambda_3^0 = \frac{1}{81}$. To find the admissible values of $\alpha, \beta_j, j = 0, \dots, n-1$, and δ, imposing condition (i) in Table 2.1 we find

$$\delta - \alpha = \frac{1}{9}. \tag{5.43}$$

[1]Note that for $n \geq 7$ the eigenvalue $\sum_{j=0}^{n-1} \beta_j \omega^{j\nu}$ could be smaller than $1/27$ for some ν, i.e. formally $\lambda_0^\nu < \lambda_1^\nu$, but, when the conditions in Table 2.1 are satisfied, the ordering of the remaining eigenvalues is not crucial. Since the general case $n > 7$ is not treated in detail, we decide to maintain such a notation.

Remark 5.18 is still valid for the eigenvalues λ_0^ν in (5.42), so conditions (ii)-(iii) in Table 2.1 give rise to

$$\sum_{j=0}^{n-1} \beta_j \omega^j = \frac{1}{3}, \qquad \sum_{j=0}^{n-1} \beta_j \omega^{2j} = \frac{1}{9}. \tag{5.44}$$

Since λ_2^0, λ_3^0 and $\lambda_1^\nu, \lambda_2^\nu, \nu = 1, \dots, n-1$, are equal to $\frac{1}{27}$ or $\frac{1}{81}$, to verify condition (iv) in Table 2.1, we only need to check that

$$\left| \sum_{j=0}^{n-1} \beta_j \omega^{j\nu} \right| \leq \frac{1}{9}, \qquad \text{for all } \nu = 3, \dots, n-3.$$

Finally, since we require the convex hull property, all the coefficients found have to be in $[0, 1]$.

Remark 5.22 *It is valid a consideration very similar to that in Remark 5.19. From (5.43) it is clear that α and δ are strictly related. If we find an expression for α, then $\delta = \frac{1}{9} + \alpha$ and, in order to ensure the convex hull property also for δ, we have to restrict the set of values for α to $\left[0, \frac{8}{9}\right]$. On the other hand, if we obtain δ, then $\alpha = \delta - \frac{1}{9}$ with $\delta \in \left[\frac{1}{9}, 1\right]$ for the convex hull property for α.*

In the following, we show the details of the computations for the special cases $n = 5, 7$.

Proposition 5.23 *The ternary Loop's scheme with extraordinary stencils in Figure 5.12 satisfies the conditions (i)-(iv) in Table 2.1 and the convex hull property at an extraordinary vertex of valence $n = 5$ if*

$$\beta_1 \in \left[\frac{2\sqrt{5}}{45}, \frac{7 + \sqrt{5}}{45} \right] \approx [0.0994, 0.2052], \tag{5.45}$$

and

$$\alpha = \frac{7 + \sqrt{5}}{9} - 5\beta_1, \quad \beta_0 = \beta_1 + \frac{10 - \sqrt{5}}{45}, \quad \beta_2 = \beta_1 - \frac{2\sqrt{5}}{45}, \quad \delta = \frac{8 + \sqrt{5}}{9} - 5\beta_1.$$

with $\beta_3 = \beta_2$ and $\beta_4 = \beta_1$.

Proof: We follow verbatim the proof of Proposition 5.20. The stencil weights involved in the subdivision rules in case of an extraordinary vertex of valence $n = 5$ are $\alpha, \beta_0, \beta_1, \beta_2$ and δ with

$$\beta_2 = \frac{1}{2}(1 - \alpha - \beta_0 - 2\beta_1). \tag{5.46}$$

Formulas (5.44) with (5.46) imply

$$\begin{aligned} \frac{1 + \sqrt{5}}{4}\alpha + \frac{5 + \sqrt{5}}{4}\beta_0 + \sqrt{5}\beta_1 - \frac{1 + \sqrt{5}}{4} &= \frac{1}{3}, \\ \frac{1 - \sqrt{5}}{4}\alpha + \frac{5 - \sqrt{5}}{4}\beta_0 - \sqrt{5}\beta_1 - \frac{1 - \sqrt{5}}{4} &= \frac{1}{9}, \end{aligned}$$

from which we compute

$$\alpha = \frac{7+\sqrt{5}}{9} - 5\beta_1, \qquad \beta_0 = \beta_1 + \frac{10-\sqrt{5}}{45},$$

and, as a consequence of (5.46), $\beta_2 = \beta_1 - \frac{2\sqrt{5}}{45}$. Moreover, (5.43) gives $\delta = \frac{8+\sqrt{5}}{9} - 5\beta_1$, and since for all $\nu = 0, \dots, 4$ the remaining eigenvalues are equal to $\frac{1}{27}$ or $\frac{1}{81}$, condition (iv) in Table 2.1 is verified too. now we have to ensure the convex hull property for all the parameters, that is, by considering Remark 5.22,

$$\begin{aligned}
&\alpha \in \left[0, \frac{8}{9}\right] \qquad \Leftrightarrow \qquad \beta_1 \in \left[\frac{\sqrt{5}-1}{45}, \frac{7+\sqrt{5}}{45}\right] \approx [0.0275, 0.2052],\\
&\beta_0 \in [0,1] \qquad \Leftrightarrow \qquad \beta_1 \in \left[0, \frac{35+\sqrt{5}}{45}\right] \approx [0, 0.8275],\\
&\beta_3 \in [0,1] \qquad \Leftrightarrow \qquad \beta_1 \in \left[\frac{2\sqrt{5}}{45}, 1\right] \approx [0.0994, 1],
\end{aligned}$$

and the intersection of these intervals (taking into account, if necessary, that also β_1 should be in $[0,1]$) gives (5.45). ■

Proposition 5.24 *The ternary Loop's scheme with extraordinary stencils in Figure 5.12 satisfies the conditions (i)-(iv) in Table 2.1 and the convex hull property at an extraordinary vertex of valence $n = 7$ if, setting $c_j = 2\cos\frac{j\pi}{7}$, $j = 2, 4, 6$,*

$$\begin{aligned}
\beta_1 \in &\left[\frac{2(4+c_2+c_4-2c_2c_6)}{9(7c_2+2c_4-9c_6+2c_2c_4-2c_4c_6)}, \frac{2(24+34c_2+11c_4-37c_6+6c_2c_4-13c_2c_6-7c_4c_6+2c_2c_4c_6)}{9(49c_2+5c_4-54c_6+5c_2c_4-5c_4c_6)}\right]\\
&\approx [0.0968, 0.2238],
\end{aligned} \tag{5.47}$$

$$\begin{aligned}
\beta_2 \in \Bigg[&\max\left\{\frac{2+9(c_4-c_2)\beta_1}{9(c_4-c_6)}, 0, \frac{2(2c_2-c_4-c_6)}{9(c_2c_6+c_2c_4-6-c_4-c_6-c_2+c_4c_6)} + \beta_1\right\},\\
&\min\left\{\frac{2(c_2-c_4)}{9(c_2c_6+c_2c_4-6-c_4-c_6-c_2+c_4c_6)} + \beta_1, \frac{4+6c_2-8c_6+9(2-4c_2+3c_4+2c_6-c_4c_6)\beta_1}{9(2+3c_2+2c_4-4c_6-c_2c_4)}\right\}\Bigg],
\end{aligned} \tag{5.48}$$

and

$$\begin{aligned}
\alpha = \frac{1}{9(c_2-c_6)}\,&[4 + 6c_2 - 8c_6 + 9(2 - 4c_2 + 3c_4 + 2c_6 - c_4c_6)\beta_1 + \\
&+9(-2 - 3c_2 - 2c_4 + 4c_6 + c_2c_4)\beta_2]\,,
\end{aligned} \tag{5.49}$$

$$\beta_0 = \frac{1}{9(c_2-c_6)}\,[3c_2 - c_6 + 9(-2 - c_4 + c_4c_6)\beta_1 + 9(2 + c_2 - c_2c_4)\beta_2]\,, \tag{5.50}$$

$$\beta_3 = \frac{1}{9(c_2-c_6)}\,[-2 + 9(c_2 - c_4)\beta_1 + 9(c_4 - c_6)\beta_2]\,, \tag{5.51}$$

$$\begin{aligned}
\delta = \frac{1}{9(c_2-c_6)}\,&[4 + 7c_2 - 9c_6 + 9(2 - 4c_2 + 3c_4 + 2c_6 - c_4c_6)\beta_1 + \\
&+9(-2 - 3c_2 - 2c_4 + 4c_6 + c_2c_4)\beta_2]\,,
\end{aligned} \tag{5.52}$$

with $\beta_4 = \beta_3$, $\beta_5 = \beta_2$ and $\beta_6 = \beta_1$.

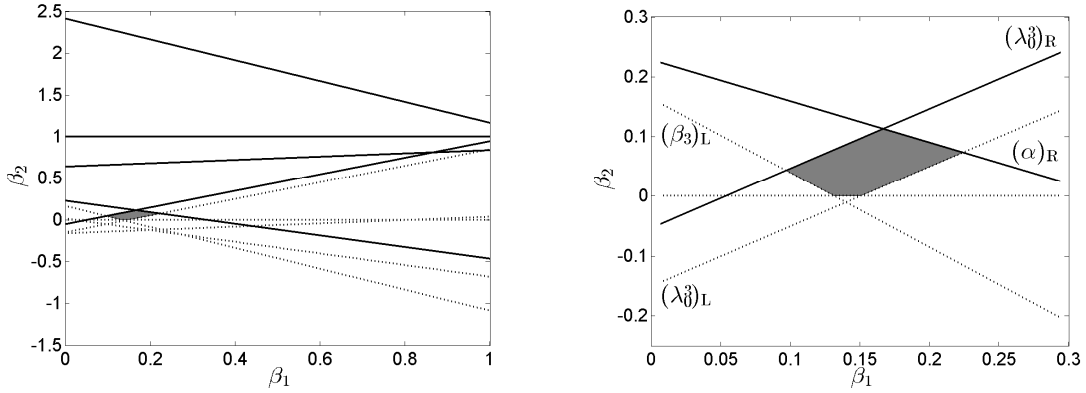

(a) (b)

Figure 5.13: (a): $(\cdots)$ lines demarcating the eligible regions from left, $(-)$ lines demarcating the eligible regions from right for β_2, given in (5.55) and (5.54), with $\beta_1 \in [0,1]$: in gray is depicted the intersection of such eligible regions. (b) Zoom of the eligibility region in (a) with indications about the involved lines: $(\theta)_{\mathrm{L}}$ and $(\theta)_{\mathrm{R}}$ are, respectively, the left and the right demarcating lines of the regions of values for β_2 related to $\theta \in \{\alpha, \beta_3, \lambda_0^3\}$.

Proof: In case of an extraordinary vertex of valence $n = 7$, the stencil weights are $\alpha, \beta_0, \beta_1, \beta_2, \beta_3$ and δ, with

$$\beta_3 = \frac{1}{2}\left(1 - \alpha - \beta_0 - 2\beta_1 - 2\beta_2\right). \tag{5.53}$$

From (5.44) and (5.53), we have

$$\begin{aligned} -\frac{1}{2}c_6\alpha + \left(1 - \frac{1}{2}c_6\right)\beta_0 + (c_2 - c_6)\beta_1 + (c_4 - c_6)\beta_2 + \frac{1}{2}c_6 &= \frac{1}{3}, \\ -\frac{1}{2}c_2\alpha + \left(1 - \frac{1}{2}c_2\right)\beta_0 + (c_4 - c_2)\beta_1 + (c_6 - c_2)\beta_2 + \frac{1}{2}c_2 &= \frac{1}{9}. \end{aligned}$$

These equations give α and β_0 as in (5.49)-(5.50), and we obtain β_3 and δ in (5.51)-(5.52) as a consequence of (5.53) and (5.43), respectively. Moreover, to verify also condition (iv) in Table 2.1, we need to check if all the other eigenvalues are not greater than $\frac{1}{9}$. Since λ_2^0, λ_3^0 and $\lambda_1^\nu, \lambda_2^\nu, \nu = 1, \ldots, 6$, are equal to $\frac{1}{27}$ or $\frac{1}{81}$, we have just to check if $|\lambda_0^3|, |\lambda_0^4| \leq \frac{1}{9}$. Since Remark 5.18 ensures that $\lambda_0^3 = \lambda_0^4$, the previous inequality is verified from (5.42) with $\nu = 3$ if

$$-\frac{1}{9} \leq \frac{9(c_2c_6 + c_2c_4 - 6 - c_4 - c_6 + c_4c_6 - c_2)(\beta_1 - \beta_2) + 3c_2 - c_6 - 2c_4}{9(c_2 - c_6)} \leq \frac{1}{9},$$

that is

$$\lambda_0^3 \in \left[-\frac{1}{9}, \frac{1}{9}\right] \quad \Leftrightarrow \quad \beta_2 \in \frac{[4c_2 - 2c_4 - 2c_6, 2c_2 - 2c_4]}{9(c_2c_6 + c_2c_4 - 6 - c_4 - c_6 - c_2 + c_4c_6)} + \beta_1. \tag{5.54}$$

now we check the convex hull property, by remembering Remark 5.22,

$$\alpha \in \left[0, \frac{8}{9}\right] \quad \Leftrightarrow \quad \beta_2 \in \frac{[4-2c_2, 4+6c_2-8c_6] + 9(2-4c_2+3c_4+2c_6-c_4c_6)\beta_1}{9(2+3c_2+2c_4-4c_6-c_2c_4)}, \tag{5.55}$$

$$\beta_0 \in [0,1] \quad \Leftrightarrow \quad \beta_2 \in \frac{[3c_2-c_6, -6c_2+8c_6] + 9(-2-c_4+c_4c_6)\beta_1}{9(c_2c_4-2-c_2)},$$

$$\beta_3 \in [0,1] \quad \Leftrightarrow \quad \beta_2 \in \frac{[2, 2+9c_2-9c_6] + 9(c_4-c_2)\beta_1}{9(c_4-c_6)}.$$

We observe that all the eligible values for β_2 in (5.55) and (5.54), for $\beta_1 \in [0,1]$, are contained in regions of the plane delimited by two parallel lines (see Figure 5.13). The intersection of such regions, taking into account that also β_2 should be in $[0,1]$ and using the notation explained in the caption of Figure 5.13, gives rise to

$$\beta_1 \in [(\beta_3)_{\mathrm{L}} \cap (\lambda_0^3)_{\mathrm{R}}, (\lambda_0^3)_{\mathrm{L}} \cap (\alpha)_{\mathrm{R}}],$$
$$\beta_2 \in [\max\{(\beta_3)_{\mathrm{L}}, 0, (\lambda_0^3)_{\mathrm{L}}\}, \min\{(\lambda_0^3)_{\mathrm{R}}, (\alpha)_{\mathrm{R}}\}],$$

which are written in full in (5.47) and (5.48). ■

Chapter 6

Subdivision schemes for biomedical imaging segmentation

As already pointed out at the beginning of Chapter 5, stationary subdivision schemes can be partially used in many applications since they can not design particular surfaces such as spheres, ellipsoids, cylinders, etc...Thus, we need to consider non-stationary subdivision schemes, which are able to generate or reproduce spaces of exponential polynomials, and thus to produce limit surfaces with these particular shapes.
The design of ellipsoids is especially important in biomedical imaging field, since very often the analyzed biological objects have an ellipsoidal shape. In fact, an important challenge in biomedical imaging is the segmentation of closed 3D structures. In the medical field the segmentation of organs, such as lung and kidney, allows one for a better 3D visualization and hence, improves preoperative preparations. In biology, microscopy images often contain hundreds of cells to be analyzed. Automatic or semi-automatic cell segmentation facilitates image analysis because manual delineation of each cell is time consuming. Active surfaces or 3D deformable models (3D generalizations of active contours) provide a convenient framework in image processing for the segmentation of volumetric biomedical images. They consist in closed flexible surfaces that evolve through a 3D volumetric image, moving from an initial position (typically specified by the user), toward the boundary of the object to be segmented. Their evolution is guided by the minimization of an appropriate energy term [75, 128], suitably defined to approximate the shape of interest. Currently, 3D deformable models are described implicitly by level sets [12] or explicitly by meshes [51, 34] and parameterizations [124]. Therefore, the explicit definition of 3D deformable models can typically rely either on a discrete (mesh-based) or a continuous (parametric) representation. Moreover, as recently shown in [38], active surfaces to be used in 3D bioimage segmentation should be affine invariant and capable of perfectly outlining ellipsoidal objects or versatile enough to provide a close approximation of any blob-like shape.
In this chapter, we provide novel explicit definitions of 3D deformable models that can combine the advantages of the discrete and the continuous representations. To achieve this objective, we propose two different subdivision-based 3D deformable models both defined on triangular meshes. The first proposal consists in an interpolatory subdivision scheme defined on regular meshes and able to reproduce exact ellipsoids starting from a mesh composed by 28 control points. The second proposal is an approximating subdivision scheme defined on arbitrary manifold topology meshes and able to produce a good approximation of an exact

ellipsoid starting from a mesh of 6 control points only. We study the advantages and the limits of both these proposals.

6.1 A non-stationary interpolatory subdivision scheme exactly reproducing ellipsoids

In this section we show and analyze a non-stationary interpolatory subdivision scheme which is affine invariant and exactly reproduces ellipsoids, thus it is useful for the definition of 3D deformable models. The construction of this non-stationary scheme is preceded by the definition and analysis of its stationary counterpart, which results to be an improvement of the Modified Butterfly scheme [73, 139] already recalled in Section 2.4.2.

6.1.1 Modified BLISS: a Modified Butterfly-Lengthened Interpolatory Subdivision Scheme

We start by recalling the main properties of the Modified Butterfly interpolatory scheme [73, 139], and then we show how we can obtain a stationary subdivision scheme on regular triangular meshes, which can improve both smoothness and accuracy of the Modified Butterfly scheme. For the sake of conciseness, hereinafter we refer to the Modified Butterfly Interpolatory Subdivision Scheme as Modified BISS, whereas we call the Modified Butterfly-Lengthened Interpolatory Subdivision Scheme, Modified BLISS.

The Modified Butterfly scheme: a short review

Since the Modified BISS is identified by the 10-point stencil in Figure 2.6 (a), the associated symbol has the following expression

$$\mathrm{a}_w(z_1,z_2)=\mathrm{a}(z_1,z_2)+w\,\frac{2}{z_1^3z_2^3}\,\mathrm{B}_{1,1,1}(z_1,z_2)(1-z_1)^2(1-z_2)^2(1-z_1z_2)^2,\qquad w\in\mathbb{R},\quad (6.1)$$

with

$$\mathrm{a}(z_1,z_2)=\frac{1}{z_1^3z_2^3}\Big(7z_1z_2\mathrm{B}_{2,2,2}(z_1,z_2)-2z_1\mathrm{B}_{1,3,3}(z_1,z_2)-2z_2\mathrm{B}_{3,1,3}(z_1,z_2)-2z_1z_2\mathrm{B}_{3,3,1}(z_1,z_2)\Big)$$

and

$$\mathrm{B}_{i,j,\ell}(z_1,z_2)=4\left(\frac{1+z_1}{2}\right)^i\left(\frac{1+z_2}{2}\right)^j\left(\frac{1+z_1z_2}{2}\right)^\ell,\qquad i,j,\ell\in\mathbb{N}_0.$$

It is known that the limit surfaces of the Modified BISS are C^1 if the free parameter w varies in the range $[-0.03,0)$ (see, e.g., [73, page 34]). To give the widest range of w for which the Modified BISS enjoys the property of cubic polynomial reproduction, in the following proposition we point out for which values of w the Modified BISS is convergent.

Proposition 6.1 *If $w\in\left(-\frac{1}{32},\frac{1}{32}\right)$, then the Modified BISS is convergent.*

Proof: In order to verify the convergence of the Modified BISS with symbol $\mathrm{a}_w(z_1,z_2)$ in (6.1), we study the contractivity of the first order difference scheme with matrix symbol

$\mathrm{b}^{[1]}(z_1, z_2)$ computed as in (2.16) with $\mathcal{Z}_1 = \{(1,0,0),(0,1,0)\}$. The associated first order difference mask $\mathbf{b}^{[1]}$ is

$$\begin{pmatrix}
\begin{pmatrix}0&0\\0&0\end{pmatrix} & \begin{pmatrix}0&0\\0&0\end{pmatrix} & \begin{pmatrix}0&0\\0&0\end{pmatrix} & \begin{pmatrix}w&0\\0&0\end{pmatrix} & \begin{pmatrix}-\frac{1}{16}&0\\0&0\end{pmatrix} & \begin{pmatrix}-w&0\\0&0\end{pmatrix} & \begin{pmatrix}0&0\\0&0\end{pmatrix}\\
\begin{pmatrix}0&0\\0&0\end{pmatrix} & \begin{pmatrix}0&0\\0&0\end{pmatrix} & \begin{pmatrix}-w-\frac{1}{16}&0\\0&0\end{pmatrix} & \begin{pmatrix}\frac{1}{16}-w&0\\0&w\end{pmatrix} & \begin{pmatrix}w+\frac{1}{16}&0\\0&w-\frac{1}{16}\end{pmatrix} & \begin{pmatrix}w-\frac{1}{16}&0\\0&-w-\frac{1}{16}\end{pmatrix} & \begin{pmatrix}0&0\\0&-w\end{pmatrix}\\
\begin{pmatrix}0&0\\0&0\end{pmatrix} & \begin{pmatrix}-w-\frac{1}{16}&0\\0&0\end{pmatrix} & \begin{pmatrix}w+\frac{3}{16}&0\\0&-w-\frac{1}{16}\end{pmatrix} & \begin{pmatrix}\frac{5}{16}&0\\0&-3w\end{pmatrix} & \begin{pmatrix}\frac{3}{16}-w&0\\0&\frac{3}{16}-w\end{pmatrix} & \begin{pmatrix}w-\frac{1}{16}&0\\0&3w+\frac{1}{16}\end{pmatrix} & \begin{pmatrix}0&0\\0&2w-\frac{1}{16}\end{pmatrix}\\
\begin{pmatrix}w&0\\0&0\end{pmatrix} & \begin{pmatrix}w&0\\0&-w-\frac{1}{16}\end{pmatrix} & \begin{pmatrix}\frac{1}{2}&0\\0&w+\frac{3}{16}\end{pmatrix} & \begin{pmatrix}\frac{1}{2}&0\\0&4w+\frac{1}{2}\end{pmatrix} & \begin{pmatrix}-w&0\\0&\frac{5}{16}\end{pmatrix} & \begin{pmatrix}-w&0\\0&-3w+\frac{1}{16}\end{pmatrix} & \begin{pmatrix}0&0\\0&-w\end{pmatrix}\\
\begin{pmatrix}-w-\frac{1}{16}&0\\0&w\end{pmatrix} & \begin{pmatrix}w+\frac{3}{16}&0\\0&3w+\frac{1}{16}\end{pmatrix} & \begin{pmatrix}\frac{5}{16}&0\\0&\frac{5}{16}\end{pmatrix} & \begin{pmatrix}\frac{3}{16}-w&0\\0&-4w+\frac{1}{2}\end{pmatrix} & \begin{pmatrix}w-\frac{1}{16}&0\\0&\frac{3}{16}-w\end{pmatrix} & \begin{pmatrix}0&0\\0&w-\frac{1}{16}\end{pmatrix} & \begin{pmatrix}0&0\\0&0\end{pmatrix}\\
\begin{pmatrix}-w-\frac{1}{16}&0\\0&-2w-\frac{1}{16}\end{pmatrix} & \begin{pmatrix}\frac{1}{16}-w&0\\0&-3w+\frac{1}{16}\end{pmatrix} & \begin{pmatrix}w+\frac{1}{16}&0\\0&w+\frac{3}{16}\end{pmatrix} & \begin{pmatrix}w-\frac{1}{16}&0\\0&3w\end{pmatrix} & \begin{pmatrix}0&0\\0&w-\frac{1}{16}\end{pmatrix} & \begin{pmatrix}0&0\\0&0\end{pmatrix} & \begin{pmatrix}0&0\\0&0\end{pmatrix}\\
\begin{pmatrix}w&0\\0&w\end{pmatrix} & \begin{pmatrix}-\frac{1}{16}&0\\0&w-\frac{1}{16}\end{pmatrix} & \begin{pmatrix}-w&0\\0&-w-\frac{1}{16}\end{pmatrix} & \begin{pmatrix}0&0\\0&-w\end{pmatrix} & \begin{pmatrix}0&0\\0&0\end{pmatrix} & \begin{pmatrix}0&0\\0&0\end{pmatrix} & \begin{pmatrix}0&0\\0&0\end{pmatrix}
\end{pmatrix}.$$

Using (2.17) with $L = 1$, we find that

$$\begin{aligned}
||S^1_{\mathbf{b}^{[1]}}|| &= \max\left\{ \left\| \begin{pmatrix} |w-\frac{1}{16}|+|w+\frac{1}{16}|+|w-\frac{3}{16}|+|w+\frac{3}{16}|+2|w|+\frac{3}{8} & 0 \\ 0 & 2|w-\frac{1}{16}|+|4w-\frac{1}{2}|+2|3w+\frac{1}{16}|+4|w| \end{pmatrix} \right\|, \right.\\
&\quad \left\| \begin{pmatrix} |w-\frac{1}{16}|+|w+\frac{1}{16}|+|w-\frac{3}{16}|+|w+\frac{3}{16}|+2|w|+\frac{3}{8} & 0 \\ 0 & 2|w+\frac{1}{16}|+2|w-\frac{3}{16}|+|2w-\frac{1}{16}|+2|w|+\frac{5}{16} \end{pmatrix} \right\|,\\
&\quad \left\| \begin{pmatrix} 4|w+\frac{1}{16}|+2|w|+\frac{1}{2} & 0 \\ 0 & 2|w-\frac{1}{16}|+2|w+\frac{3}{16}|+|2w+\frac{1}{16}|+2|w|+\frac{5}{16} \end{pmatrix} \right\|,\\
&\quad \left. \left\| \begin{pmatrix} 4|w-\frac{1}{16}|+2|w|+\frac{1}{2} & 0 \\ 0 & 2|w+\frac{1}{16}|+|4w+\frac{1}{2}|+2|3w-\frac{1}{16}|+4|w| \end{pmatrix} \right\| \right\}\\
&= \max\left\{ \left|w-\tfrac{1}{16}\right|+\left|w+\tfrac{1}{16}\right|+\left|w-\tfrac{3}{16}\right|+\left|w+\tfrac{3}{16}\right|+2|w|+\tfrac{3}{8},\quad 4\left|w-\tfrac{1}{16}\right|+2|w|+\tfrac{1}{2},\quad 4\left|w+\tfrac{1}{16}\right|+2|w|+\tfrac{1}{2}, \right.\\
&\quad 2\left|w-\tfrac{1}{16}\right|+2\left|w+\tfrac{3}{16}\right|+\left|2w+\tfrac{1}{16}\right|+2|w|+\tfrac{5}{16},\quad 2\left|w+\tfrac{1}{16}\right|+\left|4w+\tfrac{1}{2}\right|+2\left|3w-\tfrac{1}{16}\right|+4|w|,\\
&\quad \left. 2\left|w+\tfrac{1}{16}\right|+2\left|w-\tfrac{3}{16}\right|+\left|2w-\tfrac{1}{16}\right|+2|w|+\tfrac{5}{16},\quad 2\left|w-\tfrac{1}{16}\right|+\left|4w-\tfrac{1}{2}\right|+2\left|3w+\tfrac{1}{16}\right|+4|w| \right\},
\end{aligned}$$

and thus $||S_{\mathbf{b}^{[1]}}|| < 1$ if $w \in \left(-\frac{1}{32}, \frac{1}{32}\right)$. As a consequence, in view of the results recalled in Section 2.2.2, the Modified BISS converges for all $w \in \left(-\frac{1}{32}, \frac{1}{32}\right)$. ■

Proposition 6.2 *For all $w \in \left(-\frac{1}{32}, \frac{1}{32}\right)$ the Modified BISS reproduces the space Π_3^2 of bivariate polynomials of total degree at most 3 with respect to the parametrization $\{\mathbf{T}^{(k)}, k \in \mathbb{N}_0\}$ in* (2.6) *with $\boldsymbol{\tau} = 0$.*

Proof: From Proposition 2.7 we have that the Modified BISS generates Π_3^2 for all $w \in \left(-\frac{1}{32}, \frac{1}{32}\right)$. In fact, for such values of the free parameter the subdivision scheme is convergent (see Proposition 6.1) and the associated symbol satisfies $D^{(\gamma_1,\gamma_2)}\mathrm{a}_w(\epsilon_1, \epsilon_2) = 0$ for all $(\gamma_1, \gamma_2) \in \Gamma_3$ and $(\epsilon_1, \epsilon_2) \in \Xi'$. Thus, being the scheme interpolatory, reproduction of Π_3^2 with respect to the parametrization in (2.6) with $\boldsymbol{\tau} = 0$ follows straightforwardly in light of Corollary 2.12. ■

In view of Proposition 6.2, we finally get that the Modified BISS has approximation order 4 for all $w \in \left(-\frac{1}{32}, \frac{1}{32}\right)$ (see Proposition 2.10).

The Modified BLISS

We here present an extension of the Modified BISS, that we call Modified BLISS, which defines a family of quintic polynomial reproducing schemes depending on a free parameter w. The construction of such a stationary interpolatory scheme is crucial for the smoothness analysis of the non-stationary subdivision scheme presented in the following section. The edge-point stencil of the Modified BLISS is obtained by enlarging the 10-point stencil of the Modified BISS to the 16-point stencil shown in Figure 6.1, where

$$\beta_0 = 2w+\frac{9}{16}, \quad \beta_1 = -3w-\frac{1}{16}, \quad \beta_2 = w, \quad \beta_3 = \frac{3}{256}-w, \quad \beta_4 = 4w-\frac{3}{64}, \quad \beta_5 = \frac{9}{128}-6w. \tag{6.2}$$

Note that the coefficients β_0, β_1 and β_2 have been defined such that $(\beta_2, \beta_1, \beta_0, \beta_0, \beta_1, \beta_2)$ provides the odd-point stencil of the interpolatory 6-point scheme depending on a parameter (see [54, page 162]), while the coefficients β_3, β_4, and β_5 have been selected in such a way that the Modified BLISS reproduces the space Π_5^2 of bivariate polynomials of total degree at most 5 (see Proposition 6.5).

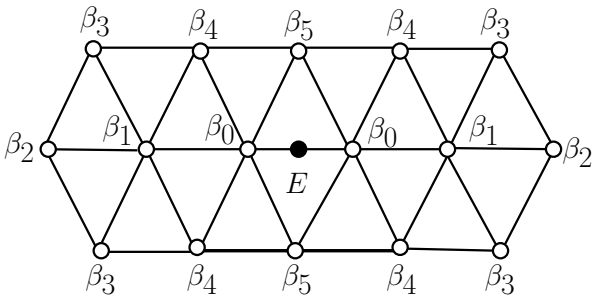

Figure 6.1: Edge-point stencil of Modified BLISS with coefficients in (6.2).

Remark 6.3 *We emphasize that, assuming $\beta_2 = w$, the remaining entries of the odd-point stencil $(\beta_2, \beta_1, \beta_0, \beta_0, \beta_1, \beta_2)$ for the univariate 6-point scheme in [54] can be worked out as*

$$\beta_1 = \frac{w}{\sigma_2}\,\sigma_1 + \left(1-\frac{w}{\sigma_2}\right)\rho_1, \qquad \beta_0 = \frac{w}{\sigma_2}\left(\frac{1}{2}-\sigma_1-\sigma_2\right) + \left(1-\frac{w}{\sigma_2}\right)\left(\frac{1}{2}-\rho_1\right),$$

where $\rho_1 = -\frac{1}{16}$ is the first entry of the odd-point stencil of the Dubuc-Deslauriers 4-point scheme, i.e. $(\rho_1, \frac{1}{2}-\rho_1, \frac{1}{2}-\rho_1, \rho_1)$, while $\sigma_2 = \frac{3}{256}$ and $\sigma_1 = -\frac{25}{256}$ are the first two entries of the odd-point stencil of the Dubuc-Deslauriers 6-point scheme given by $(\sigma_2, \sigma_1, \frac{1}{2}-\sigma_1-\sigma_2, \frac{1}{2}-\sigma_1-\sigma_2, \sigma_1, \sigma_2)$ (see [42]).

The symbol of the Modified BLISS is thus of the form

$$\mathrm{c}_w(z_1,z_2) = \frac{2}{z_1^5 z_2^5}\mathrm{B}_{1,1,1}(z_1,z_2)\,(\mathrm{r}(z_1,z_2)+w\mathrm{s}(z_1,z_2)), \tag{6.3}$$

where

$$\begin{aligned}\mathrm{r}(z_1,z_2) \;&= \tfrac{1}{\mathrm{r}_6}\Big(\mathrm{r}_1(z_1^8 z_2^6+z_2^2)+\mathrm{r}_2(z_2)(z_1^7 z_2^5+z_1 z_2^2)+\mathrm{r}_3(z_2)(z_1^6 z_2^2+z_1^2)\\ &\quad +\mathrm{r}_4(z_2)(z_1^5 z_2^2+z_1^3 z_2)+\mathrm{r}_5(z_2) z_1^4 z_2^2\Big),\end{aligned}$$

with

$$\begin{aligned}
&\mathrm{r}_1 = 3,\\
&\mathrm{r}_2(z_2) = -(z_2+1)\mathrm{r}_1,\\
&\mathrm{r}_3(z_2) = 3z_2^6 - 3z_2^5 - 10z_2^4 + 4z_2^3 - 10z_2^2 - 3z_2 + 3,\\
&\mathrm{r}_4(z_2) = -(z_2+1)(3z_2^4 - 7z_2^3 - 11z_2^2 - 7z_2 + 3),\\
&\mathrm{r}_5(z_2) = -2(5z_2^4 - 9z_2^3 - 37z_2^2 - 9z_2 + 5),\\
&\mathrm{r}_6 = 256,
\end{aligned}$$

and

$$\mathrm{s}(z_1,z_2) = \mathrm{s}_1(z_2)(z_1^8 z_2^4+1)+\mathrm{s}_2(z_2)(z_1^7 z_2^3+z_1)+\mathrm{s}_3(z_2)(z_1^6 z_2^2+z_1^2)+\mathrm{s}_4(z_2)(z_2 z_1^5+z_1^3)+\mathrm{s}_5(z_2)z_1^4,$$

with

$$\begin{aligned}
&\mathrm{s}_1(z_2) = \big(z_2^2+z_2+1\big)(z_2-1)^2,\\
&\mathrm{s}_2(z_2) = -(z_2+1)\mathrm{s}_1(z_2),\\
&\mathrm{s}_3(z_2) = z_2(z_2-1)^4,\\
&\mathrm{s}_4(z_2) = -(z_2+1)(z_2^4 - 5z_2^2 + 1)(z_2-1)^2,\\
&\mathrm{s}_5(z_2) = \big(z_2^6 + 2z_2^5 - z_2^4 - 10z_2^3 - z_2^2 + 2z_2 + 1\big)(z_2-1)^2.
\end{aligned}$$

Proposition 6.4 *If*

$$w \in \left(\frac{23}{3968} - \frac{\sqrt{3236974}}{63488}, \frac{-2189+\sqrt{12142829}}{80896}\right) \simeq (-0.0225, 0.0160), \tag{6.4}$$

then the Modified BLISS converges.

Proof: In order to verify the convergence of the Modified BLISS with symbol in (6.3), we study the contractivity of the first order difference scheme with matrix symbol $\mathrm{d}^{[1]}(z_1,z_2)$ defined as in (2.16) with $\mathcal{Z}_1 = \{(1,0,0),(0,1,0)\}$. Computing $||S^L_{\mathbf{d}^{[1]}}||$ as in (2.17) and fixing $L=1$, we find that $||S^1_{\mathbf{d}^{[1]}}|| < 1$ when $w \in \left(-\frac{3}{1024}, \frac{13}{1024}\right)$. To enlarge this range we consider $L=2$, so obtaining that $||S^2_{\mathbf{d}^{[1]}}|| < 1$ if $w \in \left(\frac{23}{3968} - \frac{\sqrt{3236974}}{63488}, \frac{-2189+\sqrt{12142829}}{80896}\right) \simeq (-0.0225, 0.0160)$. ■

Proposition 6.5 *For all w satisfying* (6.4) *the Modified BLISS reproduces the space Π_5^2 of bivariate polynomials of total degree at most 5 with respect to the parametrization $\{\mathbf{T}^{(k)}, k \in \mathbb{N}_0\}$ in* (2.6) *with $\boldsymbol{\tau} = 0$.*

Proof: From Proposition 2.7 we have that the Modified BLISS generates Π_5^2 for all w fulfilling (6.4). In fact, for such values of w the subdivision scheme is convergent (see Proposition 6.4) and the associated symbol $\mathrm{c}_w(z_1,z_2)$ satisfies $D^{(\gamma_1,\gamma_2)}\mathrm{c}_w(\epsilon_1,\epsilon_2) = 0$ for all $(\gamma_1,\gamma_2) \in \Gamma_5$ and $(\epsilon_1,\epsilon_2) \in \Xi'$. Thus, since the Modified BLISS is interpolatory, in view of Corollary 2.12 the reproduction of Π_5^2 with respect to the parametrization in (2.6) with $\boldsymbol{\tau} = 0$, follows straightforwardly. ■

Recalling the results in Proposition 2.10, Proposition 6.5 implies the following.

Corollary 6.6 *For all w satisfying* (6.4) *the Modified BLISS has approximation order 6.*

Proposition 6.7 *The limit functions produced by the Modified BLISS are of class C^1 for all*

$$w \in \left(\frac{29 - \sqrt{6673}}{4608}, \frac{121}{384(375 + \sqrt{140383})} \right) \simeq (-0.0114, 4.2032 \cdot 10^{-4}).$$

Proof: To prove that the Modified BLISS with symbol (6.3) generates C^1 limits, it suffices to check that the second order difference scheme with matrix symbol $\mathrm{d}^{[2]}(z_1, z_2)$ defined in (2.16) is such that $\|S^L_{\mathbf{d}^{[2]}}\| < \frac{1}{2}$ for some $L \in \mathbb{N}$. Fixing $L = 2$ and computing $\mathrm{d}^{[2]}(z_1, z_2)$ with $\mathcal{Z}_2 = \{(1,1,0), (1,0,1), (0,1,1)\}$, we find that $\|S^2_{\mathbf{d}^{[2]}}\| < \frac{1}{2}$ if $w \in \left(\frac{29-\sqrt{6673}}{4608}, \frac{121}{384(375+\sqrt{140383})} \right)$. Thus, for all values of w in this range, the limits of the Modified BLISS are C^1. ■

Now, to simplify the analysis of C^2 convergence, we look for a parameter $w \in \left(\frac{29-\sqrt{6673}}{4608}, \frac{121}{384(375+\sqrt{140383})} \right)$ for which the Modified BLISS symbol $\mathrm{c}_w(z_1, z_2)$ allows us to factor out the Box-spline symbol $B_{3,3,3}(z_1, z_2) = \frac{1}{128}(1 + z_1)^3(1 + z_2)^3(1 + z_1 z_2)^3$. Indeed, when $w = -\frac{3}{1024}$ we have

$$\mathrm{c}_{-\frac{3}{1024}}(z_1, z_2) = \frac{1}{z_1^5 z_2^5} B_{3,3,3}(z_1, z_2)\, m(z_1, z_2),$$

with

$$\begin{aligned} \mathrm{m}(z_1, z_2) \;=\; & -\tfrac{1}{8}(3z_1^4 z_2^4 - 9z_1^4 z_2^3 + 3z_1^4 z_2^2 - 9z_1^3 z_2^4 + 18z_1^3 z_2^3 + 18z_1^3 z_2^2 - 9z_1^3 z_2 + 3z_1^2 z_2^4 + 18z_1^2 z_2^3 \\ & -80 z_1^2 z_2^2 + 18 z_1^2 z_2 + 3z_1^2 - 9z_1 z_2^3 + 18 z_1 z_2^2 + 18 z_1 z_2 - 9z_1 + 3z_2^2 - 9z_2 + 3), \end{aligned}$$

and thus we can easily prove the following result.

Proposition 6.8 *The limit functions produced by the Modified BLISS with $w = -\frac{3}{1024}$ are of class C^2.*

Proof: To check that the Modified BLISS with $w = -\frac{3}{1024}$ produces limit functions of class C^2 we have to verify that the third order difference scheme with matrix symbol $\mathrm{d}^{[3]}(z_1, z_2)$ defined in (2.16) is such that $\|S^L_{\mathbf{d}^{[3]}}\| < \frac{1}{4}$ for some $L \in \mathbb{N}$. Working out $\mathrm{d}^{[3]}(z_1, z_2)$ with $\mathcal{Z}_3 = \{(1,1,1), (0,2,1), (2,0,1), (2,1,0)\}$ and computing $\|S^L_{\mathbf{d}^{[3]}}\|$ as shown in (2.17), we find that the required inequality is verified with $L = 4$. Thus, C^2 smoothness of the subdivision scheme with symbol $\mathrm{c}_{-\frac{3}{1024}}(z_1, z_2)$ is proven. ■

6.1.2 The non-stationary Modified BLISS

Thanks to the given preliminary results, we are now in a position to construct and analyze a non-stationary extension of the Modified BLISS. This non-stationary formulation defines a family of subdivision schemes depending on a pair of k-th level parameters denoted by $v^{(k)}$ and $w^{(k)}$, respectively. To define the parameter sequence $\{v^{(k)},\, k \in \mathbb{N}_0\}$ we choose $t \in [0, \pi) \cup \mathrm{i}\mathbb{R}^+$ and we set $v^{(0)}$ as in (3.12). Then, starting from $v^{(0)}$, we compute the successive values of the sequence $\{v^{(k)}, k \in \mathbb{N}\}$ via the recursive formula shown in (3.13). The parameter sequence $\{w^{(k)},\, k \in \mathbb{N}_0\}$ is successively defined in terms of the sequence $\{v^{(k)},\, k \in \mathbb{N}_0\}$ to increase the number of exponential polynomials reproduced by the scheme (see Propositions 6.15 and 6.17).

Construction of the parameter-dependent refinement rules

The non-stationary Modified BLISS is defined by the k-th level 16-point stencil shown in Figure 6.2, where the k-th level coefficients are of the form

$$\begin{aligned}
\beta_0^{(k)} &= 2(2(v^{(k)})^2-1)w^{(k)} + \tfrac{(2v^{(k)}+1)^2}{8v^{(k)}(v^{(k)}+1)},\\
\beta_1^{(k)} &= -(4(v^{(k)})^2-1)w^{(k)} - \tfrac{1}{8v^{(k)}(v^{(k)}+1)},\\
\beta_2^{(k)} &= w^{(k)},\\
\beta_3^{(k)} &= -(2(v^{(k)})^2-1)w^{(k)} + \tfrac{2v^{(k)}+1}{64(v^{(k)})^2(2v^{(k)}-1)(v^{(k)}+1)^2},\\
\beta_4^{(k)} &= 4(v^{(k)})^2(2(v^{(k)})^2-1)w^{(k)} - \tfrac{2v^{(k)}+1}{16(2v^{(k)}-1)(v^{(k)}+1)^2},\\
\beta_5^{(k)} &= -2(4(v^{(k)})^2-1)(2(v^{(k)})^2-1)w^{(k)} + \tfrac{(2v^{(k)}+1)^2}{32(v^{(k)})^2(v^{(k)}+1)^2}.
\end{aligned} \tag{6.5}$$

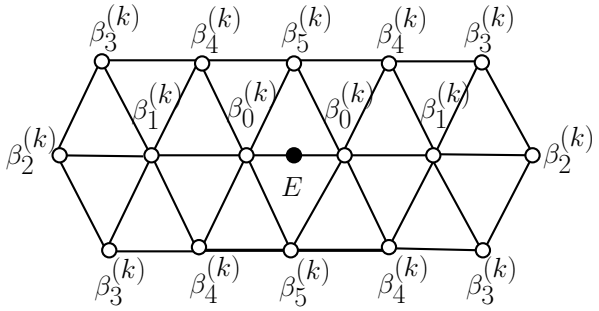

Figure 6.2: Edge-point stencil of the non-stationary Modified BLISS with coefficients in (6.5).

Mimicking the idea used in the stationary case, to work out the expressions in (6.5) we have assumed $\beta_2^{(k)} = w^{(k)}$ and we have computed the values of $\beta_0^{(k)}$, $\beta_1^{(k)}$, $\beta_3^{(k)}$, $\beta_4^{(k)}$, $\beta_5^{(k)}$ as follows. Exploiting an analogous strategy to the one described in Remark 6.3, assume $\rho_1^{(k)} = -\frac{1}{8v^{(k)}(v^{(k)}+1)}$ to be the first entry of the k-th level odd-point stencil of the non-stationary interpolatory 4-point scheme in [8], *i.e.* $(\rho_1^{(k)}, \frac{1}{2}-\rho_1^{(k)}, \frac{1}{2}-\rho_1^{(k)}, \rho_1^{(k)})$. Let also

$$\sigma_2^{(k)} = \frac{2v^{(k)}+1}{64(v^{(k)})^3(v^{(k)}+1)^2} \qquad \text{and} \qquad \sigma_1^{(k)} = -\frac{(4v^{(k)}+1)\left(4(v^{(k)})^2+2v^{(k)}-1\right)}{64(v^{(k)})^3(v^{(k)}+1)^2},$$

be the first two entries of the k-th level odd-point stencil of the non-stationary interpolatory 6-point scheme in [119, Section 4.3], namely $(\sigma_2^{(k)}, \sigma_1^{(k)}, \frac{1}{2}-\sigma_1^{(k)}-\sigma_2^{(k)}, \frac{1}{2}-\sigma_1^{(k)}-\sigma_2^{(k)}, \sigma_1^{(k)}, \sigma_2^{(k)})$. Then, if we define

$$\beta_1^{(k)} = \frac{w^{(k)}}{\sigma_2^{(k)}}\,\sigma_1^{(k)} + \left(1-\frac{w^{(k)}}{\sigma_2^{(k)}}\right)\rho_1^{(k)},$$

and

$$\beta_0^{(k)} = \frac{w^{(k)}}{\sigma_2^{(k)}}\left(\frac{1}{2}-\sigma_1^{(k)}-\sigma_2^{(k)}\right) + \left(1-\frac{w^{(k)}}{\sigma_2^{(k)}}\right)\left(\frac{1}{2}-\rho_1^{(k)}\right),$$

the vector $(\beta_2^{(k)}, \beta_1^{(k)}, \beta_0^{(k)}, \beta_0^{(k)}, \beta_1^{(k)}, \beta_2^{(k)})$ provides the k-th level odd-point stencil of a non-stationary interpolatory 6-point scheme depending on a free parameter sequence $\{w^{(k)},\, k \in \mathbb{N}_0\}$. Following again the stationary case, we determine the coefficients $\beta_3^{(k)}, \beta_4^{(k)}$ and $\beta_5^{(k)}$ by requiring the reproduction of a certain space of exponential polynomials, precisely the one specified in (3.8) (see Proposition 6.10).
The k-th level symbol of the non-stationary Modified BLISS with edge-point stencil in Figure 6.2 is

$$\mathrm{c}_{v^{(k)},w^{(k)}}(z_1,z_2) = \frac{2}{z_1^5 z_2^5}\,\mathrm{B}_{1,1,1}(z_1,z_2)\Big(\mathrm{r}^{(k)}(z_1,z_2) + w^{(k)}\mathrm{s}^{(k)}(z_1,z_2)\Big),$$

where

$$\begin{aligned}\mathrm{r}^{(k)}(z_1,z_2) &= \tfrac{1}{\mathrm{r}_6^{(k)}}\Big(\mathrm{r}_1^{(k)}(z_1^8 z_2^6 + z_2^2) + \mathrm{r}_2^{(k)}(z_2)(z_1^7 z_2^5 + z_1 z_2^2) + \mathrm{r}_3^{(k)}(z_2)(z_1^6 z_2^2 + z_1^2)\\ &\quad + \mathrm{r}_4^{(k)}(z_2)(z_1^5 z_2^2 + z_1^3 z_2) + \mathrm{r}_5^{(k)}(z_2) z_1^4 z_2^2\Big),\end{aligned}$$

with

$$\begin{aligned}\mathrm{r}_1^{(k)} &= 2v^{(k)} + 1,\\ \mathrm{r}_2^{(k)}(z_2) &= -(z_2+1)\mathrm{r}_1^{(k)},\\ \mathrm{r}_3^{(k)}(z_2) &= \mathrm{r}_1^{(k)}(z_2^6 + 1 - (z_2^5 + z_2)) - (16(v^{(k)})^3 + 8(v^{(k)})^2 - 12v^{(k)} - 2)(z_2^4 + z_2^2)\\ &\quad + (8(v^{(k)})^3 + 4(v^{(k)})^2 - 8v^{(k)})z_2^3,\\ \mathrm{r}_4^{(k)}(z_2) &= (z_2+1)\big(-r_1^{(k)}(z_2^4+1) + (8(v^{(k)})^3 + 4(v^{(k)})^2 - 6v^{(k)} + 1)(z_2^3 + z_2)\\ &\quad + (8(v^{(k)})^3 + 4(v^{(k)})^2 + 2v^{(k)} - 3)z_2^2\big),\\ \mathrm{r}_5^{(k)}(z_2) &= 2\big((-8(v^{(k)})^3 - 4(v^{(k)})^2 + 6v^{(k)} + 1)(z_2^4+1) + (8(v^{(k)})^3 + 4(v^{(k)})^2\\ &\quad - 2v^{(k)} - 1)(z_2^3 + z_2) + (32(v^{(k)})^5 + 48(v^{(k)})^4 - 24(v^{(k)})^3 - 28(v^{(k)})^2 + 6v^{(k)} + 3)z_2^2\big),\\ \mathrm{r}_6^{(k)} &= 64(v^{(k)})^2(2v^{(k)} - 1)(v^{(k)} + 1)^2,\end{aligned}$$

and

$$\begin{aligned}\mathrm{s}^{(k)}(z_1,z_2) &= \mathrm{s}_1^{(k)}(z_2)(z_1^8 z_2^4 + 1) + \mathrm{s}_2^{(k)}(z_2)(z_1^7 z_2^3 + z_1) + \mathrm{s}_3^{(k)}(z_2)(z_1^6 z_2^2 + z_1^2)\\ &\quad + \mathrm{s}_4^{(k)}(z_2)(z_2 z_1^5 + z_1^3) + \mathrm{s}_5^{(k)}(z_2) z_1^4,\end{aligned}$$

with

$$\begin{aligned}\mathrm{s}_1^{(k)}(z_2) &= (z_2^4+1) - (z_2^3 + z_2) + 2(1 - (v^{(k)})^2)z_2^2,\\ \mathrm{s}_2^{(k)}(z_2) &= -(z_2+1)\mathrm{s}_1^{(k)}(z_2),\\ \mathrm{s}_3^{(k)}(z_2) &= 2(1 - (v^{(k)})^2)(z_2^6+1) + (2(v^{(k)})^2 - 1)(z_2^5 + z_2) + 4(1 - 2(v^{(k)})^2)(z_2^4 + z_2^2)\\ &\quad + 2(4(v^{(k)})^4 - 1)z_2^3,\\ \mathrm{s}_4^{(k)}(z_2) &= (z_2+1)\Big(-(z_2^6+1) + 2(v^{(k)})^2(z_2^5 + z_2) + 2(4(v^{(k)})^4 - (v^{(k)})^2 - 1)(z_2^4 + z_2^2)\\ &\quad + 2(7(v^{(k)})^2 - 12(v^{(k)})^4)z_2^3\Big),\\ \mathrm{s}_5^{(k)}(z_2) &= (z_2^8+1) + 4(1 - 2(v^{(k)})^2)(z_2^6 + z_2^2) - 2(8(v^{(k)})^4 - 6(v^{(k)})^2 + 1)(z_2^5 + z_2^3)\\ &\quad + 6(8(v^{(k)})^4 - 6(v^{(k)})^2 + 1)z_2^4.\end{aligned}$$

Convergence and approximation order

We are interested in studying the reproduction properties and the approximation order of the non-stationary Modified BLISS. Since the subdivision scheme is parameter-dependent, in order to identify the widest choice of parameters $\{w^{(k)},\, k \in \mathbb{N}_0\}$ yielding such properties, we look for the conditions that this parameter sequence has to satisfy to guarantee convergence.

Proposition 6.9 *Let $t \in [0,\pi) \cup \mathrm{i}\mathbb{R}^+$ and $\{v^{(k)},\, k \in \mathbb{N}_0\}$ be defined as in* (3.12)-(3.13)*. For all sequences $\{w^{(k)},\, k \in \mathbb{N}_0\}$ such that*

$$\lim_{k\to+\infty} w^{(k)} = w \in \left(\frac{23}{3968} - \frac{\sqrt{3236974}}{63488}, \frac{-2189+\sqrt{12142829}}{80896}\right) \simeq (-0.0225, 0.0160), \quad (6.6)$$

the non-stationary Modified BLISS with k-th level symbol $\mathrm{c}_{v^{(k)},w^{(k)}}(z_1,z_2)$ is convergent.

Proof: Since $\lim_{k\to+\infty} v^{(k)} = 1$, if $\{w^{(k)},\, k \in \mathbb{N}_0\}$ behaves as in (6.6), then the non-stationary Modified BLISS is asympotically similar to the Modified BLISS defined by the symbol in (6.3), and the latter is convergent (see Proposition 6.4). Next, we prove that the non-stationary scheme satisfies approximate sum rules of order 1. In fact, $\mu_k = 0$ and thus we trivially have $\sum_{k=0}^{\infty} \mu_k < +\infty$. Moreover, $\mathrm{c}_{v^{(k)},w^{(k)}}(\epsilon_1,\epsilon_2) = 0$ for all $(\epsilon_1,\epsilon_2) \in \Xi'$ and thus it is also $\delta_k = 0$ which implies $\sum_{k=0}^{\infty} \delta_k < +\infty$. Hence, approximate sum rules of order 1 are satisfied and the claim follows from Proposition 3.17. ■

Once the convergence of the non-stationary Modified BLISS has been established, we can focus on the analysis of its reproduction properties. For this purpose we introduce the space of exponential polynomials $\mathcal{W}_1^2$ in (3.9), explicitly given by

$$\mathcal{W}_1^2 = \mathrm{span}\{1, x, y, e^{\pm tx}, e^{\pm ty}, e^{\pm t(x\pm y)}\}, \qquad t \in [0,\pi) \cup \mathrm{i}\mathbb{R}^+.$$

The following proposition shows that the exponential polynomial space $\mathcal{W}_1^2$ can be reproduced by the non-stationary Modified BLISS for all choices of $\{w^{(k)},\, k \in \mathbb{N}_0\}$ that guarantee convergence.

Proposition 6.10 *For all choices of $t \in [0,\pi) \cup \mathrm{i}\mathbb{R}^+$ and for all sequences $\{w^{(k)},\, k \in \mathbb{N}_0\}$ satisfying the property in* (6.6)*, the non-stationary Modified BLISS reproduces the space $\mathcal{W}_1^2$ with respect to the parametrization $\{\mathbf{T}^{(k)}, k \in \mathbb{N}_0\}$ in* (2.6) *with $\boldsymbol{\tau} = 0$.*

Proof: Let $t \in [0,\pi) \cup \mathrm{i}\mathbb{R}^+$and

$$\begin{aligned}\mathcal{V}_{k,\Theta} = \{\ & (-1,1),(1,-1),(-1,-1),(-e^{\pm\frac{t}{2^{k+1}}},1),(e^{\pm\frac{t}{2^{k+1}}},-1),(-e^{\pm\frac{t}{2^{k+1}}},-1),\\ & (-1,e^{\pm\frac{t}{2^{k+1}}}),(1,-e^{\pm\frac{t}{2^{k+1}}}),(-1,-e^{\pm\frac{t}{2^{k+1}}}),(-e^{\pm\frac{t}{2^{k+1}}},e^{\pm\frac{t}{2^{k+1}}}),\\ & (e^{\pm\frac{t}{2^{k+1}}},-e^{\pm\frac{t}{2^{k+1}}}),(-e^{\pm\frac{t}{2^{k+1}}},-e^{\pm\frac{t}{2^{k+1}}})\ \}.\end{aligned}$$

The k-th level symbol $\mathrm{c}_{v^{(k)},w^{(k)}}(z_1,z_2)$ is such that $\mathrm{c}_{v^{(k)},w^{(k)}}(\nu_1,\nu_2) = 0$ for all $(\nu_1,\nu_2) \in \mathcal{V}_{k,\Theta}$. Thus, according to Proposition 3.6, the generation of $\mathrm{span}\{1, e^{\pm tx}, e^{\pm ty}, e^{\pm t(x\pm y)}\}$ is proven for all $\{w^{(k)},\, k \in \mathbb{N}_0\}$ that guarantee convergence. Further, if we compute $D^{(1,0)}\mathrm{c}_{v^{(k)},w^{(k)}}(z_1,z_2)$ and $D^{(0,1)}\mathrm{c}_{v^{(k)},w^{(k)}}(z_1,z_2)$ we find that

$$D^{(1,0)}\mathrm{c}_{v^{(k)},w^{(k)}}(\epsilon_1,\epsilon_2) = D^{(0,1)}\mathrm{c}_{v^{(k)},w^{(k)}}(\epsilon_1,\epsilon_2) = 0, \quad \text{for all} \quad (\epsilon_1,\epsilon_2) \in \Xi'.$$

This additionally proves the generation of $\{x, y\}$. Hence we can conclude that the non-stationary Modified BLISS generates the whole space in $\mathcal{W}_1^2$ for all sequences $\{w^{(k)}, k \in \mathbb{N}_0\}$ satisfying the property in (6.6). The reproduction of this space with respect to the parametrization in (2.6) with $\boldsymbol{\tau} = 0$ follows straightforwardly from the interpolation property of the scheme, in light of Corollary 3.10. ■

Remark 6.11 *The non-stationary Modified BLISS can reproduce* Π_1^2 *as well as ellipsoids for all choices of* $\{w^{(k)}, k \in \mathbb{N}_0\}$ *that behave as in* (6.6)*. This means that the scheme satisfies the properties of affine invariance (see Remark 3.9) and ellipsoid reproduction required for the construction of subdivision-based active surfaces [38, 29]. We also point out the fact that, to achieve the property of ellipsoid reproduction, it is not necessary to handle triangular meshes with extraordinary vertices, i.e. arbitrary manifold topology meshes. In fact, an ellipsoidal shape is a* 0*-genus surface that can be obtained starting from an initial regular control mesh where the vertices lying on the first and last line are assumed to be topologically identical (so as to define the ellipsoid poles), see Figure 6.3.*

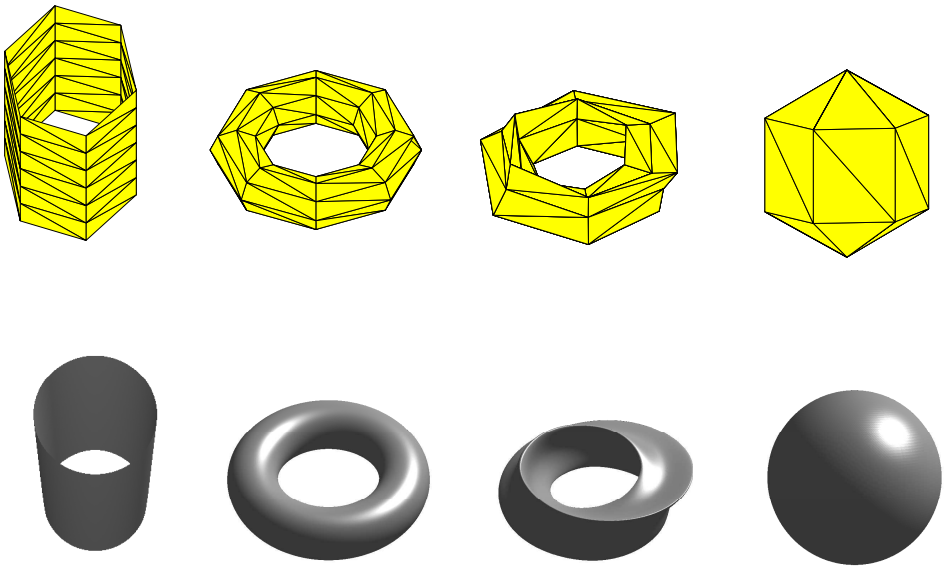

Figure 6.3: First line: initial meshes. Second line: results obtained applying 5 steps of the non-stationary Modified BLISS.

We finally focus on the approximation order of the non-stationary Modified BLISS. For this purpose, we assume that the initial data $\mathbf{f}^{(0)}$ is given as a set of discrete values of a smooth function. Precisely, denoting by $C_\infty^\sigma(\mathbb{R}^2)$, $\sigma \in \mathbb{N}$, the space of functions f whose derivatives $D^\gamma f$, $\boldsymbol{\gamma} \in \Gamma_\sigma = \{\boldsymbol{\gamma} \in \mathbb{N}_0^2 : 0 \leq \gamma_1 + \gamma_2 \leq \sigma\}$, are continuous and uniformly bounded, we define $\mathbf{f}^{(0)} := \{\mathrm{f}_{\boldsymbol{\alpha}}^{(0)} = f(2^{-k}\boldsymbol{\alpha}) : \boldsymbol{\alpha} \in \mathbb{Z}^2\}$ for some positive integer k and some function $f \in C_\infty^\sigma(\mathbb{R}^2)$.
Recalling Definition 3.3, we have that, when the non-stationary scheme $\mathcal{S}_{\mathbf{c}^{(\ell)}}$ is convergent,

its limit function obtained from the initial data $\mathbf{f}^{(0)}$ can be written as

$$\mathcal{S}_f(\boldsymbol{x}) := \sum_{\boldsymbol{\alpha}\in\mathbb{Z}^2} \phi_k(2^k\boldsymbol{x}-\boldsymbol{\alpha})\, \mathrm{f}_{\boldsymbol{\alpha}}^{(0)}.$$

The aim of this section is to investigate how the non-stationary Modified BLISS actually attains the original function f as close as possible. Specifically, we are concerned with finding the largest $\sigma \in \mathbb{N}$ such that

$$\|\mathcal{S}_f - f\|_{L_\infty(\Omega)} \le c2^{-\sigma k}$$

with a constant $c > 0$ independent of k, where Ω is a compact set in $\mathbb{R}^2$. The number σ becomes the approximation order of the non-stationary subdivision scheme $\mathcal{S}_{\mathbf{c}^{(\ell)}}$.
In what follows, we show under a suitable condition that the non-stationary Modified BLISS provides the same approximation order six as its stationary counterpart. An interesting feature is that it is required for the non-stationary Modified BLISS to reproduce ten linearly independent exponential polynomials, which is equivalent to the polynomial space Π_3^2. To do this, we denote by $\mathcal{V}_1 := \mathrm{span}\{\varphi_1, \ldots, \varphi_{10}\}$ a subspace of the exponential polynomial space $\mathcal{W}_1$, which satisfies $\dim \mathcal{V}_1 = \dim \Pi_3^2 = 10$. Then, we define the function

$$W[\varphi_1, \ldots, \varphi_{10}](\boldsymbol{x}) := \det \mathbf{W}(\boldsymbol{x})$$

where the matrix $\mathbf{W}(\boldsymbol{x})$ is given by

$$\mathbf{W}(\boldsymbol{x}) = (D^{\boldsymbol{\gamma}}\varphi_j(\boldsymbol{x}) : j = 1, \ldots, 10,\ \boldsymbol{\gamma} \in \Gamma_3), \quad \boldsymbol{x} = (x_1, x_2).$$

The function $W[\varphi_1, \ldots, \varphi_{10}](\boldsymbol{x})$ is the *Wronskian* of $\{\varphi_1, \ldots, \varphi_{10}\}$ on two dimensional case. Throughout this section, we assume that the space $\mathcal{V}_1$ is shift-invariant and $W[\varphi_1, \ldots, \varphi_{10}](\mathbf{0})$ is non-zero. Moreover, to simplify the presentation, we use the index set Γ_3 and with this notation we simply write $\{\varphi_1, \ldots, \varphi_{10}\} = \{\varphi_{\boldsymbol{\alpha}} : \boldsymbol{\alpha} \in \Gamma_3\}$.
The proof of the approximation order result will be preceded by the following preparatory lemma.

Lemma 6.12 *Suppose that* $\{w^{(k)},\ k \in \mathbb{N}_0\}$ *converges to a value* w*, that fulfills* (6.4)*, with the rate* $O(2^{-2k})$ *as* $k \to +\infty$*. Let* ϕ *be the basic limit function of the stationary Modified BLISS with parameter* w*. Then* $\|\phi_k - \phi\|_\infty \le c2^{-2k}$ *for some constant* $c > 0$*.*

Proof: From the definition of $v^{(k)}$ it is immediate to see that $|1 - v^{(k)}| = O(2^{-2k})$ as $k \to +\infty$ for all choices of $t \in [0, \pi) \cup \mathrm{i}\mathbb{R}^+$. Since $\lim_{k\to+\infty} w^{(k)} = w$ with the rate $O(2^{-2k})$ and w satisfies (6.4), then, by construction, the mask of the non-stationary Modified BLISS converges to the mask of the corresponding stationary scheme with the rate $O(2^{-2k})$ as $k \to +\infty$. As a consequence, $\|\phi_k - \phi\|_\infty = O(2^{-2k})$ (see also the proof of [56, Lemma 15]). ■

Theorem 6.13 *Suppose that the non-stationary Modified BLISS reproduces the space* $\mathcal{W}_1^2$ *and let* $\mathcal{V}_1 = \mathrm{span}\{\varphi_1, \ldots, \varphi_{10}\}$ *be a subspace of* $\mathcal{W}_1^2$ *so that* $W[\varphi_1, \ldots, \varphi_{10}](\boldsymbol{x})$ *is non-zero. Assume further that, as* $k \to +\infty$*, the parameter* $w^{(k)}$ *converges to a value* w *which satisfies* (6.4) *with the rate* $O(2^{-2k})$*. If the given initial data is of the form* $\mathbf{f}^{(0)} := \{\mathrm{f}_{\mathbf{i}}^{(0)} = f(2^{-k}\mathbf{i}) : \mathbf{i} \in \mathbb{Z}^2\}$ *with* $k \in \mathbb{N}$ *and* $f \in C_\infty^6(\mathbb{R}^2)$*, then for any compact set* Ω *in* $\mathbb{R}^2$*, we have*

$$\|\mathcal{S}_f - f\|_{L_\infty(\Omega)} \le c\, 2^{-6k},$$

with a constant $c > 0$ *depending on* f *but not on* k*.*

Proof: Let $\boldsymbol{x}$ be an arbitrary fixed point in Ω. Since the space $\mathcal{V}_1$ is shift invariant, the shifts $\varphi_{\boldsymbol{\alpha}}(\cdot - \boldsymbol{x})$, $\boldsymbol{\alpha} \in \Gamma_3$, also belong to $\mathcal{V}_1$. Then, it will be useful for our proof to define the function

$$\psi := \psi_{\boldsymbol{x}} := \sum_{\boldsymbol{\alpha}\in\Gamma_3} \mathrm{c}_{\boldsymbol{\alpha}} \varphi_{\boldsymbol{\alpha}}(\cdot - \boldsymbol{x}),$$

which depends on $\boldsymbol{x}$, so that ψ equals f at $\boldsymbol{x}$ (not on Ω) in the sense that $D^{\boldsymbol{\gamma}}\psi(\boldsymbol{x}) = D^{\boldsymbol{\gamma}} f(\boldsymbol{x})$, $\gamma \in \Gamma_3$. In other words, the coefficient vector $\bar{\mathbf{c}} := (\mathrm{c}_{\boldsymbol{\alpha}} : \boldsymbol{\alpha} \in \Gamma_3)$ is obtained by solving the linear system

$$\sum_{\boldsymbol{\alpha}\in\Gamma_3} \mathrm{c}_{\boldsymbol{\alpha}} D^{\boldsymbol{\gamma}} \varphi_{\boldsymbol{\alpha}}(0) = D^{\boldsymbol{\gamma}} f(\boldsymbol{x}), \quad \forall \boldsymbol{\gamma} \in \Gamma_3. \tag{6.7}$$

This condition can be written in matrix form as $\mathbf{W}(\mathbf{0}) \cdot \bar{\mathbf{c}}^T = \bar{\mathbf{f}}(\boldsymbol{x})^T$ with $\bar{\mathbf{f}}(\boldsymbol{x}) := (D^{\boldsymbol{\gamma}} f(\boldsymbol{x}) : \boldsymbol{\gamma} \in \Gamma_3)$. The non-singularity of the matrix, i.e. , $\det \mathbf{W}(\mathbf{0}) \neq 0$, guarantees the existence of the unique solution of this linear system, implying that $\|\bar{\mathbf{c}}\| \leq \|\mathbf{W}(\mathbf{0})^{-1}\| \|f\|_{L_\infty(\Omega)}$. Further, since $\mathcal{S}_{\mathbf{c}^{(\ell)}}$ reproduces functions in $\mathcal{V}_1$ and ψ belongs to $\mathcal{V}_1$, it is obvious that

$$\psi = \sum_{\mathbf{i}\in\mathbb{Z}^2} \phi_k(2^k \cdot - \mathbf{i})\, \psi(\mathbf{i}2^{-k}).$$

With this setting, we estimate the difference $f(\boldsymbol{x}) - \mathcal{S}_f(\boldsymbol{x})$ for a given fixed point $\boldsymbol{x} \in \Omega$. To this end, we first note from (6.7) that $\psi(\boldsymbol{x}) = f(\boldsymbol{x})$. Then it follows that

$$f(\boldsymbol{x}) - \mathcal{S}_f(\boldsymbol{x}) = \psi(\boldsymbol{x}) - \sum_{\mathbf{i}\in\mathbb{Z}^2} \phi_k(2^k\boldsymbol{x} - \mathbf{i}) f(\mathbf{i}2^{-k}) = \sum_{\mathbf{i}\in\mathbb{Z}^2} \phi_k(2^k\boldsymbol{x} - \mathbf{i})(\psi(\mathbf{i}2^{-k}) - f(\mathbf{i}2^{-k})).$$

Now, we use a finite Taylor expansion of a bivariate function with remainder. For a positive integer m, let T_g^m be the Taylor expansion up to degree m of a function g around $\boldsymbol{x}$ defined by

$$T_g^m = \sum_{\boldsymbol{\gamma}\in\Gamma_m} (\cdot - \boldsymbol{x})^{\boldsymbol{\gamma}} D^{\boldsymbol{\gamma}} g(\boldsymbol{x})/\boldsymbol{\gamma}!,$$

where $\boldsymbol{x}^{\boldsymbol{\gamma}} = x_1^{\gamma_1}\, x_2^{\gamma_2}$ and $\boldsymbol{\gamma}! = \gamma_1!\gamma_2!$, and let R_g^m be its remainder, that is,

$$R_g^m(\mathbf{s}) = \sum_{0\leq\gamma_1+\gamma_2=m+1} (\mathbf{s} - \boldsymbol{x})^{\boldsymbol{\gamma}} D^{\boldsymbol{\gamma}} g(\boldsymbol{\xi})/\boldsymbol{\gamma}!,$$

for some $\boldsymbol{\xi}$ between $\boldsymbol{x}$ and $\mathbf{s}$. Now, we first consider the case $m = 3$ for the functions ψ and f. Due to the condition $D^{\boldsymbol{\gamma}}\psi(\boldsymbol{x}) = D^{\boldsymbol{\gamma}} f(\boldsymbol{x})$ for all $\boldsymbol{\gamma} \in \Gamma_3$, it is immediate that $T_\psi^3(\mathbf{i}2^{-k}) = T_f^3(\mathbf{i}2^{-k})$ for all $\mathbf{i} \in \mathbb{Z}^2$. Therefore, introducing the notation

$$\bar{\Gamma}_{4,5} := \{\boldsymbol{\gamma} \in \mathbb{N}_0^2 : \gamma_1 + \gamma_2 = 4 \text{ or } 5\},$$

we have

$$\begin{aligned} f(\boldsymbol{x}) - \mathcal{S}_f(\boldsymbol{x}) = &\sum_{\mathbf{i}\in\mathbb{Z}^2} \phi_k(2^k\boldsymbol{x} - \mathbf{i}) \sum_{\boldsymbol{\gamma}\in\bar{\Gamma}_{4,5}} (\mathbf{i}2^{-k} - \boldsymbol{x})^{\boldsymbol{\gamma}} D^{\boldsymbol{\gamma}}(\psi - f)(\boldsymbol{x})/\boldsymbol{\gamma}! \\ &+ \sum_{\mathbf{i}\in\mathbb{Z}^2} \phi_k(2^k\boldsymbol{x} - \mathbf{i})(R_\psi^5(\mathbf{i}2^{-k}) - R_f^5(\mathbf{i}2^{-k})). \end{aligned} \tag{6.8}$$

Letting ϕ be the basic limit function of the stationary Modified BLISS $\mathcal{S}_{\mathbf{c}}$ reproducing polynomials in Π_5^2, *i.e.*, $\phi = S_{\mathbf{c}}^{\infty}\boldsymbol{\delta}$ with $\boldsymbol{\delta} = \{\delta_{\mathbf{i},\mathbf{0}} : \mathbf{i},\mathbf{0} \in \mathbb{Z}^2\}$, we find from Lemma 6.12 that $\|\phi_k - \phi\|_\infty \leq c2^{-2k}$. Moreover, using the polynomial reproducing property (up to degree five) of the basic limit function ϕ, we obtain

$$\sum_{\mathbf{i}\in\mathbb{Z}^2} \phi(2^k\boldsymbol{x} - \mathbf{i})(\mathbf{i}2^{-k} - \boldsymbol{x})^{\boldsymbol{\gamma}} = 0, \quad \forall \mathbf{i} \in \bar{\Gamma}_{4,5}. \tag{6.9}$$

Now, let $\Omega_{\boldsymbol{x}} := \{\mathbf{i} \in \mathbb{Z}^2 : \phi_k(2^k\boldsymbol{x} - \mathbf{i}) \neq 0\}$. Since ϕ_k is compactly supported, $\#\Omega_{\boldsymbol{x}} \leq C$ with a number $C > 0$ independent of k and $\boldsymbol{x}$. Thus, using the fact that ϕ has the same support as ϕ_k and applying (6.9), we get

$$\sum_{\mathbf{i}\in\mathbb{Z}^2} \phi_k(2^k\boldsymbol{x} - \mathbf{i})(\mathbf{i}2^{-k} - \boldsymbol{x})^{\boldsymbol{\gamma}} = \sum_{\mathbf{i}\in\Omega_{\boldsymbol{x}}} (\phi_k(2^k\boldsymbol{x} - \mathbf{i}) - \phi(2^k\boldsymbol{x} - \mathbf{i}))(\mathbf{i}2^{-k} - \boldsymbol{x})^{\boldsymbol{\gamma}}.$$

Since the number of elements in $\Omega_{\boldsymbol{x}}$ is finite and

$$|\mathbf{i}2^{-k} - \boldsymbol{x}| \leq c2^{-k}, \quad \forall \mathbf{i} \in \Omega_{\boldsymbol{x}}, \tag{6.10}$$

taking into account that $\|\phi_k - \phi\|_\infty = O(2^{-2k})$, we easily obtain

$$\Big| \sum_{\mathbf{i}\in\Omega_x} \phi_k(2^k\boldsymbol{x} - \mathbf{i})(\mathbf{i}2^{-k} - \boldsymbol{x})^{\boldsymbol{\gamma}} \Big| \leq c2^{-k(\gamma_1+\gamma_2+2)}, \qquad \forall \boldsymbol{\gamma} \in \bar{\Gamma}_{4,5}.$$

Note that (6.10) and the fact that ϕ_k is uniformly bounded allow us to obtain the required bound on the second term in (6.8) (the one containing the Taylor remainder terms), so concluding the proof. ■

Under the hypotheses of Theorem 6.13 we can thus claim that the non-stationary Modified BLISS has approximation order six. The same result easily follows from Proposition 3.18 which, however, appeared later than the result in Theorem 6.13.

6.1.3 C^1 regularity and special reproduction properties

In this section we show that, if the parameter sequence $\{w^{(k)},\, k \in \mathbb{N}_0\}$ is suitably chosen, then the limits of the non-stationary Modified BLISS are C^1 and a superset of the exponential polynomial space $\mathcal{W}_1^2$ can be reproduced. We start by showing which conditions are required on $\{w^{(k)},\, k \in \mathbb{N}_0\}$ to achieve C^1 regularity.

Proposition 6.14 *Let $t \in [0,\pi) \cup \mathrm{i}\mathbb{R}^+$ and $\{v^{(k)},\, k \in \mathbb{N}_0\}$ be defined as in* (3.12)-(3.13)*. The non-stationary Modified BLISS with k-th level symbol $\mathrm{c}_{v^{(k)},w^{(k)}}(z_1,z_2)$ produces C^1 limits for all sequences $\{w^{(k)},\, k \in \mathbb{N}_0\}$ such that*

$$\lim_{k\to+\infty} w^{(k)} = w \in \left(\frac{29 - \sqrt{6673}}{4608}, \frac{121}{384(375 + \sqrt{140383})} \right) \simeq (-0.0114, 4.2032 \cdot 10^{-4}). \tag{6.11}$$

Proof: Since $\lim_{k\to+\infty} v^{(k)} = 1$, under the assumption in (6.11), the non-stationary scheme having k-th level symbol $\mathrm{c}_{v^{(k)},w^{(k)}}(z_1,z_2)$ is asymptotically similar to the stationary scheme with symbol $\mathrm{c}_w(z_1,z_2)$ which, in view of Proposition 6.7, is of class C^1. To prove the claim we

thus need to show that the non-stationary Modified BLISS satisfies approximate sum rules of order 2. Note that, since $\mu_k = 0$, then $\sum_{k=0}^{\infty} \mu_k$ is trivially convergent. Hence, we need to prove only that

$$\sum_{k=0}^{\infty} 2^k \, \delta_k < +\infty \qquad \text{with} \qquad \delta_k = \max_{0 \le \gamma_1+\gamma_2 \le 1} \max_{(\epsilon_1,\epsilon_2)\in\Xi'} 2^{-k(\gamma_1+\gamma_2)} \left| D^{(\gamma_1,\gamma_2)} \, \mathrm{c}_{v^{(k)},w^{(k)}}(\epsilon_1,\epsilon_2) \right|.$$

Recalling Proposition 6.10 we already know that the non-stationary Modified BLISS reproduces, and thus generates, the space $\mathcal{W}_1^2$ for all choices of $t \in [0,\pi) \cup \mathrm{i}\mathbb{R}^+$ and $\{w^{(k)},\, k \in \mathbb{N}_0\}$ fulfilling (6.11). This means that the k-th level symbol $\mathrm{c}_{v^{(k)},w^{(k)}}(z_1,z_2)$ satisfies

$$\mathrm{c}_{v^{(k)},w^{(k)}}(\epsilon_1,\epsilon_2) = D^{(1,0)}\mathrm{c}_{v^{(k)},w^{(k)}}(\epsilon_1,\epsilon_2) = D^{(0,1)}\mathrm{c}_{v^{(k)},w^{(k)}}(\epsilon_1,\epsilon_2) = 0 \qquad \text{for all } (\epsilon_1,\epsilon_2) \in \Xi^{'}.$$

As a consequence, $\delta_k = 0$ and $\sum_{k=0}^{\infty} 2^k \delta_k < +\infty$, that is approximate sum rules of order 2 are satisfied. Therefore the claim follows from Proposition 3.17. ■

Among all possible sequences $\{w^{(k)},\, k \in \mathbb{N}_0\}$ satisfying the property in (6.11) we can choose two specific expressions such that the non-stationary Modified BLISS reproduces two particular spaces of exponential polynomials that contain $\mathcal{W}_1^2$ as a special subset.

Proposition 6.15 *Let $t \in [0,\pi) \cup \mathrm{i}\mathbb{R}^+$ and $\{v^{(k)},\, k \in \mathbb{N}_0\}$ be defined as in* (3.12)-(3.13)*. If the k-th level free parameter $w^{(k)}$ is defined as*

$$a) w^{(k)} = -\frac{2(v^{(k)})^2 + 5v^{(k)} + 1}{128(v^{(k)})^2(2v^{(k)}-1)(v^{(k)}+1)^3} \tag{6.12}$$

or

$$b) w^{(k)} = -\frac{(2v^{(k+1)}+1)^3\left(8(v^{(k+1)})^3 - 5v^{(k+1)} + 1\right)}{2048(v^{(k+1)})^6\left(2(v^{(k+1)})^2-1\right)^2(v^{(k+1)}+1)^3(2v^{(k+1)}-1)\left(4(v^{(k+1)})^2-3\right)}, \tag{6.13}$$

with $v^{(k+1)}$ as in (3.13)*, then the non-stationary Modified BLISS is C^1 convergent and reproduces the space of bivariate exponential polynomials*

$$a) \quad \mathrm{span}\{1, x, y, x^2, xy, y^2, x^3, x^2y, xy^2, y^3, e^{\pm tx}, e^{\pm ty}, e^{\pm t(x\pm y)}\} \tag{6.14}$$

or

$$b) \quad \mathrm{span}\{1, x, y, e^{\pm tx}, e^{\pm ty}, e^{\pm t(x\pm y)}, e^{\pm \frac{t}{2}x}, e^{\pm \frac{t}{2}y}, e^{\pm \frac{t}{2}(x-y)}\}, \tag{6.15}$$

with respect to the parametrization in (2.6) *with $\boldsymbol{\tau} = 0$.*

Proof: We start by observing that the choices of $w^{(k)}$ in (6.12) and (6.13) guarantee C^1 convergence since

$$\lim_{k\to+\infty} w^{(k)} = \begin{cases} a) & -\frac{1}{128} \\ b) & -\frac{27}{4096} \end{cases} \in \left(\frac{29-\sqrt{6673}}{4608}, \frac{121}{384(375+\sqrt{140383})}\right) \simeq (-0.0114, 4.2032\cdot 10^{-4}).$$

Moreover, since from Proposition 6.10 we already know that reproduction of the space $\mathcal{W}_1^2$ is ensured, we can limit our attention to show reproduction of all exponential polynomials in (6.14) and (6.15) which do not already belong to the space in $\mathcal{W}_1$. We recall once again that, since the scheme is interpolatory, it is sufficient to prove only the generation of these exponential polynomials. In view of Proposition 3.6, the claim is obtained by observing that:

- when using $w^{(k)}$ in (6.12), we get $D^{(\gamma_1,\gamma_2)}\mathrm{c}_{v^{(k)},w^{(k)}}(\epsilon_1,\epsilon_2)=0$ for all $(\gamma_1,\gamma_2)\in\mathbb{N}_0^2$ such that $2\le\gamma_1+\gamma_2\le 3$ and for all $(\epsilon_1,\epsilon_2)\in\Xi'$;
- when using $w^{(k)}$ in (6.13), we get $\mathrm{c}_{v^{(k)},w^{(k)}}(\nu_1,\nu_2)=0$

$$\begin{aligned}\forall(\nu_1,\nu_2)\in\mathcal{V}_{k,\Theta}= \quad & \{(e^{\pm\frac{t}{2^{k+2}}},-1),(-e^{\pm\frac{t}{2^{k+2}}},1),(-e^{\pm\frac{t}{2^{k+2}}},-1),(1,-e^{\pm\frac{t}{2^{k+2}}}),\\ & (-1,e^{\pm\frac{t}{2^{k+2}}}),(-1,-e^{\pm\frac{t}{2^{k+2}}}),(e^{\frac{t}{2^{k+2}}},-e^{-\frac{t}{2^{k+2}}}),(-e^{\frac{t}{2^{k+2}}},e^{-\frac{t}{2^{k+2}}}),\\ & (-e^{\frac{t}{2^{k+2}}},-e^{-\frac{t}{2^{k+2}}}),\\ & (e^{-\frac{t}{2^{k+2}}},-e^{\frac{t}{2^{k+2}}}),(-e^{-\frac{t}{2^{k+2}}},e^{\frac{t}{2^{k+2}}}),(-e^{-\frac{t}{2^{k+2}}},-e^{\frac{t}{2^{k+2}}})\},\end{aligned}$$

with $t\in[0,\pi)\cup\mathrm{i}\mathbb{R}^+$.

■

6.1.4 C^2 regularity and exceptional reproduction properties

In this section we show that the k-th level parameter

$$w^{(k)}=-\frac{2v^{(k)}+1}{128(v^{(k)})^3(2v^{(k)}-1)(v^{(k)}+1)^3} \tag{6.16}$$

provides a non-stationary Modified BLISS scheme characterized by C^2-regularity and reproduction of an even larger superset of the exponential polynomial space $\mathcal{W}_1^2$. To show these results, we denote by $w_*^{(k)}$ the parameter $w^{(k)}$ in (6.16) and observe that the k-th level symbol $\mathrm{c}_{v^{(k)},w_*^{(k)}}(z_1,z_2)$ fulfills the very special factorization

$$\mathrm{c}_{v^{(k)},w_*^{(k)}}(z_1,z_2)=\frac{1}{z_1^5z_2^5}\,\mathrm{B}_{3,3,3}^{(k)}(z_1,z_2)\,\mathrm{m}^{(k)}(z_1,z_2)$$

where

$$\mathrm{B}_{3,3,3}^{(k)}(z_1,z_2)=\frac{(1+z_1)\,(1+z_2)\,(1+z_1z_2)\,(z_1^2+2v^{(k)}z_1+1)\,(z_2^2+2v^{(k)}z_2+1)\,(z_1^2z_2^2+2v^{(k)}z_1z_2+1)}{16(v^{(k)}+1)^3},$$

and

$$\begin{aligned}\mathrm{m}^{(k)}(z_1,z_2) &= (\mathrm{m}_1^{(k)}z_2^2+\mathrm{m}_2^{(k)}z_2+\mathrm{m}_1^{(k)})(z_1^4z_2^2+1)\\ &+ (\mathrm{m}_2^{(k)}z_2^3+\mathrm{m}_3^{(k)}z_2^2+\mathrm{m}_3^{(k)}z_2+\mathrm{m}_2^{(k)})(z_1^3z_2+z_1)\\ &+ (\mathrm{m}_1^{(k)}z_2^4+\mathrm{m}_3^{(k)}z_2^3+\mathrm{m}_4^{(k)}z_2^2+\mathrm{m}_3^{(k)}z_2+\mathrm{m}_1^{(k)})z_1^2,\end{aligned}$$

with

$$\begin{aligned}\mathrm{m}_1^{(k)}&=-\frac{(2v^{(k)}+1)}{8(v^{(k)})^3(2v^{(k)}-1)}, \quad \mathrm{m}_2^{(k)}=\frac{(2v^{(k)}+1)^2}{8(v^{(k)})^3(2v^{(k)}-1)},\\ \mathrm{m}_3^{(k)}&=-\frac{(2v^{(k)}+1)^2}{4(v^{(k)})^2(2v^{(k)}-1)}, \quad \mathrm{m}_4^{(k)}=\frac{3(2v^{(k)}+1)}{v^{(k)}(2v^{(k)}-1)}+1.\end{aligned}$$

Proposition 6.16 *Let $t\in[0,\pi)\cup\mathrm{i}\mathbb{R}^+$ and $\{v^{(k)},\,k\in\mathbb{N}_0\}$ be defined as in* (3.11)-(3.12)*. The non-stationary Modified BLISS having k-th level symbol $\mathrm{c}_{v^{(k)},w_*{}^{(k)}}(z_1,z_2)$, with $w_*^{(k)}$ denoting the parameter $w^{(k)}$ in* (6.16)*, produces C^2 limit functions.*

Proof: Since $\lim_{k\to+\infty} v^{(k)} = 1$ and $\lim_{k\to+\infty} {w_*}^{(k)} = -\frac{3}{1024}$, the non-stationary Modified BLISS having k-th level symbol $\mathrm{c}_{v^{(k)},{w_*}^{(k)}}(z_1, z_2)$ is asymptotically similar to the stationary scheme with symbol $\mathrm{c}_{-\frac{3}{1024}}(z_1, z_2)$, which we already know to be C^2 (see Proposition 6.8). Therefore, the proof simply consists in showing that the non-stationary Modified BLISS satisfies approximate sum rules of order 3. First we observe that, since $\mu_k = 0$, $\sum_{k=0}^{\infty} \mu_k$ is trivially convergent. We thus need to prove only that

$$\sum_{k=0}^{\infty} 4^k\, \delta_k < +\infty \qquad \text{with} \qquad \delta_k = \max_{0\le\gamma_1+\gamma_2\le 2} \max_{(\epsilon_1,\epsilon_2)\in\mathcal{Z}} 2^{-k(\gamma_1+\gamma_2)} \left| D^{(\gamma_1,\gamma_2)}\, \mathrm{c}_{v^{(k)},{w_*}^{(k)}}(\epsilon_1, \epsilon_2) \right|.$$

As already shown in Proposition 6.14, the k-th level symbol $\mathrm{c}_{v^{(k)},{w_*}^{(k)}}(z_1, z_2)$ satisfies

$$\mathrm{c}_{v^{(k)},{w_*}^{(k)}}(\epsilon_1, \epsilon_2) = D^{(1,0)}\mathrm{c}_{v^{(k)},{w_*}^{(k)}}(\epsilon_1, \epsilon_2) = D^{(0,1)}\mathrm{c}_{v^{(k)},{w_*}^{(k)}}(\epsilon_1, \epsilon_2) = 0 \qquad \text{for all } (\epsilon_1, \epsilon_2) \in \Xi',$$

in view of the fact that the non-stationary Modified BLISS reproduces the space $\mathcal{W}_1$ for all sequences $\{w^{(k)},\, k \in \mathbb{N}_0\}$ satisfying the property in (6.6) (see Proposition 6.10). Now, if we consider directional derivatives $D^{(\gamma_1,\gamma_2)}$ such that $\gamma_1 + \gamma_2 = 2$, we find that

$$\max_{(\epsilon_1,\epsilon_2)\in\Xi'} \left| D^{(1,1)}\mathrm{c}_{v^{(k)},{w_*}^{(k)}}(\epsilon_1, \epsilon_2) \right| = \frac{(v^{(k)} - 1)^2((v^{(k)})^2 + 3v^{(k)} + 1)}{(v^{(k)})^3(v^{(k)} + 1)}$$

and

$$\begin{aligned} \max_{(\epsilon_1,\epsilon_2)\in\Xi'} \left| D^{(2,0)}\mathrm{c}_{v^{(k)},{w_*}^{(k)}}(\epsilon_1, \epsilon_2) \right| &= \max_{(\epsilon_1,\epsilon_2)\in\Xi'} \left| D^{(0,2)}\mathrm{c}_{v^{(k)},{w_*}^{(k)}}(\epsilon_1, \epsilon_2) \right| \\ &= 2\frac{(v^{(k)} - 1)^2((v^{(k)})^2 + 3v^{(k)} + 1)}{(v^{(k)})^3(v^{(k)} + 1)}. \end{aligned}$$

As a consequence

$$\begin{aligned} \delta_k &= \max_{0\le\gamma_1+\gamma_2\le 2} \max_{(\epsilon_1,\epsilon_2)\in} 2^{-k(\gamma_1+\gamma_2)} \left| D^{(\gamma_1,\gamma_2)}\, \mathrm{c}_{v^{(k)},{w_*}^{(k)}}(\epsilon_1, \epsilon_2) \right| \\ &= 4^{-k}\, 2\, \frac{(v^{(k)} - 1)^2((v^{(k)})^2 + 3v^{(k)} + 1)}{(v^{(k)})^3(v^{(k)} + 1)} \end{aligned}$$

and, since $v^{(k)} \in \mathbb{R}^+$ for all $k \in \mathbb{N}_0$ and $\lim_{k\to+\infty} v^{(k)} = 1$, it is immediate to see that

$$\sum_{k=0}^{\infty} 4^k\, \delta_k = 2 \sum_{k=0}^{\infty} \frac{(v^{(k)} - 1)^2\,((v^{(k)})^2 + 3v^{(k)} + 1)}{(v^{(k)})^3\,(v^{(k)} + 1)} \le \begin{cases} 5 \displaystyle\sum_{k=0}^{\infty} \frac{(v^{(k)} - 1)^2}{(v^{(k)})^3} & \text{if} \quad v^{(k)} \in (0, 1], \\ 5 \displaystyle\sum_{k=0}^{\infty} (v^{(k)} - 1)^2 & \text{if} \quad v^{(k)} \in [1, +\infty). \end{cases}$$

The convergence of the above series follows straightforwardly by recalling the ratio criterion and the fact that $\lim_{k\to+\infty} \frac{v^{(k+1)}-1}{v^{(k)}-1} < 1$ for all choices of $v^{(0)} \in (0, 1) \cup (1, +\infty)$, and $\lim_{k\to+\infty} \frac{v^{(k)}}{v^{(k+1)}} < 1$ for all choices of $v^{(0)} \in (0, 1)$, so obtaining

$$\lim_{k\to+\infty} \left(\frac{v^{(k+1)} - 1}{v^{(k)} - 1} \right)^2 < 1$$

and

$$\lim_{k\to+\infty}\frac{(v^{(k+1)}-1)^2}{(v^{(k+1)})^3}\frac{(v^{(k)})^3}{(v^{(k)}-1)^2}=\lim_{k\to+\infty}\left(\frac{v^{(k+1)}-1}{v^{(k)}-1}\right)^2\lim_{k\to+\infty}\left(\frac{v^{(k)}}{v^{(k+1)}}\right)^3<1.$$

Hence, approximate sum rules of order 3 are satisfied and the claim is proven. ■

The choice of the parameter $w^{(k)}$ in (6.16) not only provides the highest smoothness for the non-stationary Modified BLISS, but also allows the reproduction of the largest space of exponential polynomials.

Proposition 6.17 *If the free parameter $w^{(k)}$ is defined as in* (6.16)*, then the non-stationary Modified BLISS reproduces the space of bivariate exponential polynomials*

$$\text{span}\{1,x,y,e^{\pm tx},e^{\pm ty},e^{\pm t(x\pm y)},xe^{\pm tx},ye^{\pm tx},xe^{\pm ty},ye^{\pm ty},xe^{\pm t(x-y)},ye^{\pm t(x-y)}\},\ t\in[0,\pi)\cup\mathrm{i}\mathbb{R}^+, \tag{6.17}$$

with respect to the parametrization $\{\mathbf{T}^{(k)},k\in\mathbb{N}_0\}$ in (2.6) *with $\tau=0$.*

Proof: From Proposition 6.16 we already know that the scheme defined by the parameter $w^{(k)}$ in (6.16) is convergent and of class C^2. Moreover, from Proposition 6.10 we also know reproduction of the space $\mathcal{W}_1^2$. Therefore we can limit our attention to show reproduction of all exponential polynomials in (6.17) which do not already belong to the space $\mathcal{W}_1^2$. We recall once again that, since the scheme is interpolatory, it suffices to prove only the generation of these exponential polynomials. In view of Proposition 3.6, the claim is obtained by observing that the symbol $\mathrm{b}_{v^{(k)},w^{(k)}}(z_1,z_2)$ with $w^{(k)}$ in (6.16) verifies $D^{(\gamma_1,\gamma_2)}\mathrm{b}_{v^{(k)},w^{(k)}}(\nu_1,\nu_2)=0$ for all $(\gamma_1,\gamma_2)\in\{(1,0),(0,1)\}$ and

$$\begin{aligned}\forall(\nu_1,\nu_2)\in\mathcal{V}_{k,\Theta}=\ &\{(e^{\pm\frac{t}{2^{k+1}}},-1),(-e^{\pm\frac{t}{2^{k+1}}},1),(-e^{\pm\frac{t}{2^{k+1}}},-1),(1,-e^{\pm\frac{t}{2^{k+1}}}),(-1,e^{\pm\frac{t}{2^{k+1}}}),\\&(-1,-e^{\pm\frac{t}{2^{k+1}}}),(e^{\frac{t}{2^{k+1}}},-e^{-\frac{t}{2^{k+1}}}),(-e^{\frac{t}{2^{k+1}}},e^{-\frac{t}{2^{k+1}}}),(-e^{\frac{t}{2^{k+1}}},-e^{-\frac{t}{2^{k+1}}}),\\&(e^{-\frac{t}{2^{k+1}}},-e^{\frac{t}{2^{k+1}}}),(-e^{-\frac{t}{2^{k+1}}},e^{\frac{t}{2^{k+1}}}),(-e^{-\frac{t}{2^{k+1}}},-e^{\frac{t}{2^{k+1}}})\},\end{aligned}$$

with $t\in(0,\pi)\cup\mathrm{i}\mathbb{R}^+$. ■

In Figure 6.4 we have used the non-stationary Modified BLISS with $w^{(k)}$ in (6.13) and $w^{(k)}$ in (6.16) to show the reproduction of some special trigonometric surfaces like the generalized cylinder and the helicoid.

6.1.5 Positive and negative aspects

As proven in Proposition 6.10, the non-stationary BLISS scheme reproduces $\mathcal{W}_1^2$ and thus it is able to produce exact spheres and ellipsoids as limit of the subdivision process. To gain this accuracy in the limit surface, we need to consider a high number of control points in the initial mesh. In fact, as already pointed out in Remark 6.11, to exactly reproduce an sphere as in Figure 6.3 we have to start from a mesh containing 28 control points, where some of them collapse in the sphere poles due to the regular topology of the initial mesh. The involvement of a high number of points makes the subdivision process slow, while the choice of a regular topology in the control mesh and the fact that many points collapse in the poles make the use of the limit surfaces as deformable 3D models very complicate. In fact, the

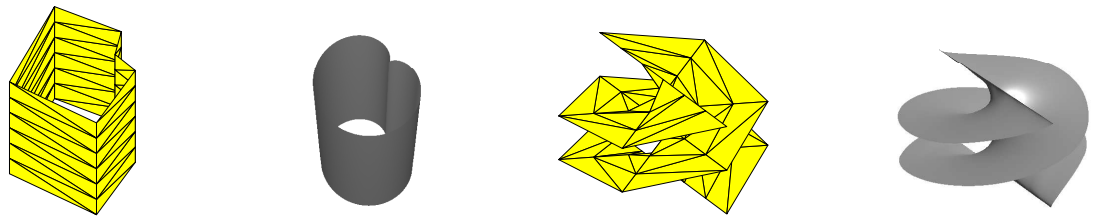

Figure 6.4: Results obtained applying 5 steps of the non-stationary Modified BLISS with $w^{(k)}$ in (6.13) (left) and $w^{(k)}$ in (6.16) (right) to the given initial meshes.

segmentation process consists in moving the points toward the boundary of the biomedical object to be segmented. Thus, if in the poles there are hundreds of points identified in one, the displacement of these 'collapsed' points becomes very difficult, since we have to move hundreds of points to the same position.
A possible way to overcome these problems is to consider an initial mesh that allows for extraordinary vertices, thus avoiding numerous collapsing points in the poles. Moreover, starting the subdivision process on an arbitrary manifold topology mesh we could reduce the number of initial control points and thus make the subdivision faster. On the contrary, the use of arbitrary manifold topology meshes does not allow for the exact reproduction of ellipsoids, thus in the limit we could only obtain an approximation of an ellipsoid.
Finally, depending on the application and on the goal we want to gain, we could choose between the accuracy given by the non-stationary BLISS scheme applied on regular meshes or the efficiency obtained using arbitrary manifold topology meshes. In the following section, we study the latter case.

6.2 A non-stationary subdivision scheme producing optimal approximations of ellipsoids

In this section, we present a new non-stationary primal subdivision scheme defined on arbitrary manifold topology triangular meshes, suitable for the construction of 3D deformable models. Differently from the BLISS scheme presented in Section 6.1, which is defined only on regular meshes, we here propose a non-stationary scheme that allows also for extraordinary vertices, thus avoiding the collapse of hundreds of points in the poles, but losing the capability of exactly generating/reproducing ellipsoids. We start by describing the new non-stationary subdivision scheme both on regular meshes and on arbitrary manifold topology meshes. Then, we analyze its main properties and we compare the limit surfaces produced considering only regular meshes with those ones produced when allowing for extraordinary vertices. We show that the latter limit surfaces could be used as deformable 3D models and some examples on real biomedical images are shown.

6.2.1 Construction of the non-stationary BLOB scheme

In correspondence to the regular regions of a triangular mesh, the action of the subdivision scheme is described by the k-th level subdivision mask

$$\mathbf{a}^{(k)} = \begin{pmatrix} 0 & 0 & 0 & \alpha_5^{(k)} & \alpha_3^{(k)} & \alpha_3^{(k)} & \alpha_5^{(k)} \\ 0 & 0 & \alpha_3^{(k)} & \alpha_2^{(k)} & \alpha_4^{(k)} & \alpha_2^{(k)} & \alpha_3^{(k)} \\ 0 & \alpha_3^{(k)} & \alpha_4^{(k)} & \alpha_6^{(k)} & \alpha_6^{(k)} & \alpha_4^{(k)} & \alpha_3^{(k)} \\ \alpha_5^{(k)} & \alpha_2^{(k)} & \alpha_6^{(k)} & \alpha_1^{(k)} & \alpha_6^{(k)} & \alpha_2^{(k)} & \alpha_5^{(k)} \\ \alpha_3^{(k)} & \alpha_4^{(k)} & \alpha_6^{(k)} & \alpha_6^{(k)} & \alpha_4^{(k)} & \alpha_3^{(k)} & 0 \\ \alpha_3^{(k)} & \alpha_2^{(k)} & \alpha_4^{(k)} & \alpha_2^{(k)} & \alpha_3^{(k)} & 0 & 0 \\ \alpha_5^{(k)} & \alpha_3^{(k)} & \alpha_3^{(k)} & \alpha_5^{(k)} & 0 & 0 & 0 \end{pmatrix}, \tag{6.18}$$

whose non-zero entries are

$$\begin{aligned} \alpha_1^{(k)} &= \frac{4(v^{(k)})^2 + 2v^{(k)} + 1}{4(v^{(k)}+1)^2}, & \alpha_2^{(k)} &= \frac{2v^{(k)}+1}{8(v^{(k)}+1)^2}, \\ \alpha_3^{(k)} &= \frac{2v^{(k)}+1}{16(v^{(k)}+1)^3}, & \alpha_4^{(k)} &= \frac{(2v^{(k)}+1)^2}{8(v^{(k)}+1)^3}, \\ \alpha_5^{(k)} &= \frac{1}{16(v^{(k)}+1)^3}, & \alpha_6^{(k)} &= \frac{(2v^{(k)}+1)(4(v^{(k)})^2+6v^{(k)}+3)}{16(v^{(k)}+1)^3}, \end{aligned} \tag{6.19}$$

with $v^{(k)}$ as in (3.11). The associated k-th level symbol is therefore

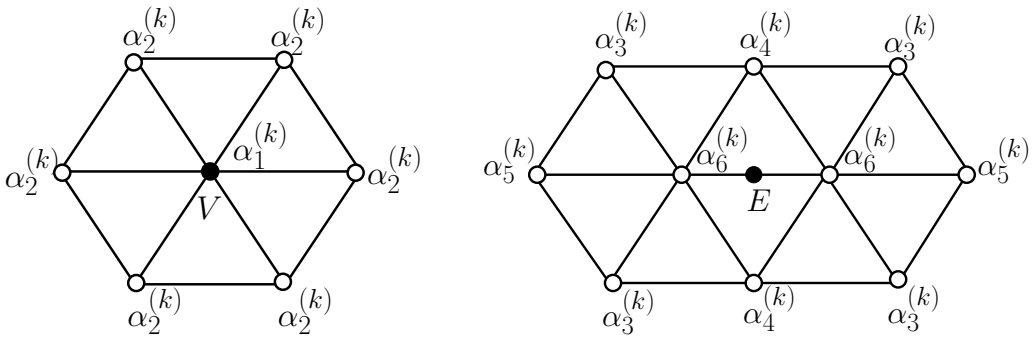

(a) Vertex-point stencil (b) Edge-point stencil

Figure 6.5: Stencils for vertex-point and edge-point rules of the BLOB scheme to be used in the regular regions of the mesh.

$$\mathrm{a}^{(k)}(z_1, z_2) = \frac{(1+z_1)\,(1+z_2)\,(1+z_1z_2)\,(z_1^2+2v^{(k)}z_1+1)\,(z_2^2+2v^{(k)}z_2+1)\,(z_1^2z_2^2+2v^{(k)}z_1z_2+1)}{16(v^{(k)}+1)^3 z_1^3 z_2^3}, \tag{6.20}$$

and the resulting refinement rules yield the so-called vertex-point and edge-point stencils illustrated in Figure 6.5. Indeed, such pictures show the local linear combinations of vertices of the coarser mesh that must be used to create a new vertex of the finer mesh to be located

in correspondence to either an old vertex or an old edge. Since the size and structure of the vertex-point rule is the same as the one used in Loop's subdivision scheme [95] shown in Figure 2.5, while the size and structure of the edge-point rule are the same as the one used in the modified Butterfly scheme [139] shown in Figure 2.6 , the new scheme is named the BLOB (Butterfly-Loop Optimal Blending) subdivision scheme.

To make the non-stationary BLOB scheme suitable for the construction of 3D deformable models, we need to allow the starting mesh to contain also extraordinary vertices. In particular, as will be better explained in the following, we are interested in applying the BLOB scheme to an initial mesh given by an octahedron, that is a polyhedron made of 8 triangular faces and 6 vertices all having valence 4. Thus the definition of the regular vertex-point stencil should be extended to the case when the old vertex is of valence 4, and the definition of the regular edge-point stencil to old edges where one or both endpoints are extraordinary vertices of valence 4. These stencils are illustrated in Figure 6.6. The rule for the computation of the edge-point with both extreme vertices of valence 4 (see Figure 6.6 (c)) is used only in the first step of the subdivision process. In fact, in the following steps the extraordinary vertices are isolated, and thus the regular rule (Figure 6.5 (b)) and the one for the case of the extreme vertices with different valences (Figure 6.6 (b)) are used. In addition, the rule for the computation of the vertex-point of valence 4 (see Figure 6.6 (a)) is used six times in each step of subdivision, since the octahedron has six vertices of valence 4, and they are kept during all the subdivision process.

As a consequence, the k-th level subdivision matrix $\tilde{S}_k$ describing the action of the BLOB scheme in the vicinity of an extraordinary vertex of valence 4, has the form in (2.21) with

$$\tilde{M}_0^{(k)} = \begin{pmatrix} \alpha_6^{(k)} & \alpha_5^{(k)} & \alpha_3^{(k)} \\ \alpha_1^{(k)} & \alpha_2^{(k)} & \alpha_3^{(k)} \\ \alpha_6^{(k)} & \alpha_3^{(k)} & \alpha_4^{(k)} \end{pmatrix}, \qquad \tilde{M}_1^{(k)} = \begin{pmatrix} \beta_5^{(k)} & 0 & 0 \\ \alpha_2^{(k)} & 0 & 0 \\ \alpha_6^{(k)} & \alpha_3^{(k)} & \alpha_5^{(k)} \end{pmatrix},$$
$$\tilde{M}_2^{(k)} = \begin{pmatrix} \beta_6^{(k)} & 0 & 0 \\ 0 & 0 & 0 \\ \alpha_3^{(k)} & 0 & 0 \end{pmatrix}, \qquad \tilde{M}_3^{(k)} = \begin{pmatrix} \beta_5^{(k)} & 0 & \alpha_3^{(k)} \\ \alpha_2^{(k)} & 0 & \alpha_2^{(k)} \\ \alpha_3^{(k)} & 0 & \alpha_5^{(k)} \end{pmatrix}, \tag{6.21}$$

and

$$\tilde{a} = \beta_1^{(k)}, \qquad \tilde{\mathbf{b}} = (\beta_2^{(k)}, 0, 0)^T, \qquad \tilde{\mathbf{c}} = (\beta_7^{(k)}, \alpha_2^{(k)}, \alpha_4^{(k)})^T$$

with

$$\beta_1^{(k)} = \frac{45(v^{(k)})^2 + 18v^{(k)} + 1}{48(v^{(k)}+1)^2}, \qquad \beta_2^{(k)} = \frac{3(v^{(k)})^2 + 78v^{(k)} + 47}{192(v^{(k)}+1)^2},$$
$$\beta_3^{(k)} = \frac{(2v^{(k)}+3)(2v^{(k)}+1)}{8(v^{(k)}+1)^2}, \qquad \beta_4^{(k)} = \frac{1}{8(v^{(k)}+1)^2},$$
$$\beta_5^{(k)} = \frac{16(v^{(k)})^2 + 18v^{(k)} + 5}{32(v^{(k)}+1)^3}, \qquad \beta_6^{(k)} = \frac{2v^{(k)}+5}{64(v^{(k)}+1)^3},$$
$$\beta_7^{(k)} = \frac{32(v^{(k)})^3 + 64(v^{(k)})^2 + 54v^{(k)} + 15}{64(v^{(k)}+1)^3}.$$

Remark 6.18 *The k-th level weights $\beta_3^{(k)}$ and $\beta_4^{(k)}$ do not appear in the subdivision matrix, since they are related to the edge-point stencil in case of an edge with both end-point vertices of valence 4 and thus they are used only in the first step of the subdivision process.*

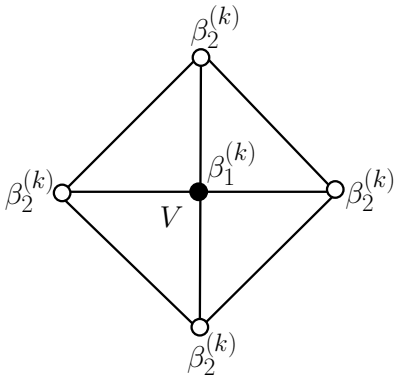

(a) Vertex-point rule for vertex of valence 4.

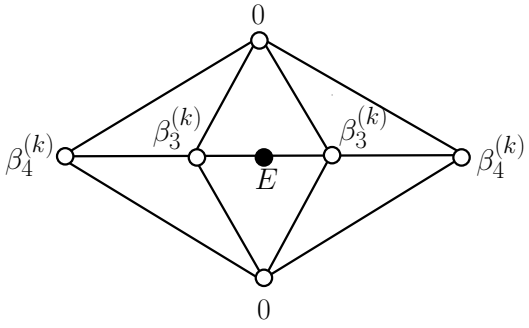

(b) Edge-point rule for an edge with both end-point vertices of valence 4.

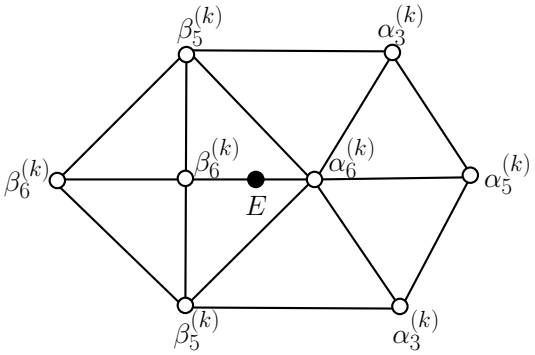

(c) Edge-point rule for an edge with one end-point vertex of valences 4 and the other of valence 6.

Figure 6.6: Stencils for vertex-point and edge-point rules involving extraordinary vertices of valence 4.

6.2.2 Generation and reproduction properties of the non-stationary BLOB scheme

In this section we start by analyzing the generation and reproduction properties of the BLOB scheme on regular meshes. This analysis is based on the results recalled in Section 3.1.

Proposition 6.19 *The non-stationary BLOB subdivision scheme generates exponential polynomials from the space* $EP^s_{(\Gamma_1,\Theta)}$ *in* (3.8)*, that is*

$$EP_{(\Gamma_1,\Theta)} = span\{1,\, x,\, y,\, e^{\pm tx},\, e^{\pm ty},\, x\, e^{\pm tx},\, y\, e^{\pm ty}, x\, e^{\pm ty},\, y\, e^{\pm tx},\\ e^{\pm t(x+y)},\, e^{\pm t(x-y)},\, x\, e^{\pm t(x-y)},\, y\, e^{\pm t(x-y)}\},$$

and reproduces linear polynomials from the space Π_1^2 *with respect to the parametrization* $\{\mathbf{T}^{(k)}, k \in \mathbb{N}_0\}$ *in* (2.6) *with* $\boldsymbol{\tau} = 0$*.*

Proof: We consider the space of exponential polynomials $EP^2_{(\Gamma_1,\Theta)}$, in (3.8) and the set

$$\begin{aligned}\mathcal{V}_{k,\Theta} = \quad & \{(-1,1),(1,-1),(-1,-1),(-e^{\frac{\pm t}{2^{k+1}}},1),(e^{\frac{\pm t}{2^{k+1}}},-1),(-e^{\frac{\pm t}{2^{k+1}}},-1),(-1,e^{\frac{\pm t}{2^{k+1}}}),\\ & (1,-e^{\frac{\pm t}{2^{k+1}}}),(-1,-e^{\frac{\pm t}{2^{k+1}}}),(-e^{\frac{\pm t}{2^{k+1}}},e^{\frac{\pm t}{2^{k+1}}}),(e^{\frac{\pm t}{2^{k+1}}},-e^{\frac{\pm t}{2^{k+1}}}),(-e^{\frac{\pm t}{2^{k+1}}},-e^{\frac{\pm t}{2^{k+1}}}),\\ & (-e^{\frac{\pm t}{2^{k+1}}},e^{\frac{-\pm t}{2^{k+1}}}),(e^{\frac{\pm t}{2^{k+1}}},-e^{\frac{-\pm t}{2^{k+1}}}),(-e^{\frac{\pm t}{2^{k+1}}},-e^{\frac{-\pm t}{2^{k+1}}})\}.\end{aligned}$$

The k-th level symbol $\mathrm{a}^{(k)}(z_1,z_2)$ in (6.20) is such that $D^{(\gamma_1,\gamma_2)}\mathrm{a}^{(k)}(\nu_1,\nu_2)=0$ for all $(\nu_1,\nu_2)\in\mathcal{V}_{k,\Theta}$ and $(\gamma_1,\gamma_2)\in\Gamma_1=\{(\gamma_1,\gamma_2)\in\mathbb{N}_0^2 : 0\le\gamma_1+\gamma_2\le 1\}$. Thus, in view of Proposition 3.6, the BLOB scheme generates $EP^2_{(\Gamma_1,\Theta)}$. On the other hand

$$\mathrm{a}^{(k)}(1,1)=4 \qquad D^{(1,0)}\mathrm{a}^{(k)}(1,1)=0 \qquad D^{(0,1)}\mathrm{a}^{(k)}(1,1)=0,$$

thus, from Proposition 2.9, the non-stationary BLOB scheme reproduces Π^2_1. ■

Exact and approximating ellipsoids

Similarly to the analysis of the non-stationary BLISS scheme in Section 6.1, the generation of the space $\mathcal{W}^2_1$, subspace of $EP^2_{(\Gamma_1,\Theta)}$, guarantees that the non-stationary BLOB scheme produces an exact ellipsoid starting from a regular mesh whose vertices are 3D points sampled from an ellipsoid in correspondence to equally spaced parameter values. Such initial control mesh is shown in Figure 6.7 (a) and it is the same used for the non-stationary BLISS scheme to produce an exact sphere (see Figure 6.3). We recall that this regular control mesh is described by 28 vertices, where the vertices of the first and last line are assumed to be topologically identical to define the poles. Although the distinct points of the starting mesh are indeed 14, the subdivision rules do not care about the topological identification, and thus they are indeed applied to the regular control mesh consisting of 28 points.

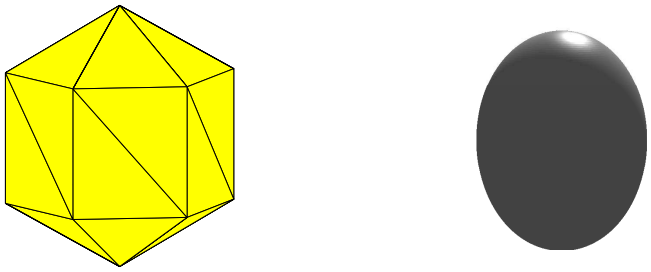

(a) Initial regular mesh (b) Exact ellipsoid

Figure 6.7: Exact ellipsoid generation via non-stationary BLOB scheme starting from a regular triangular mesh with poles.

As already pointed out in Section 6.1.5, the use of regular meshes to construct exact ellipsoids requires more initial control points than those would be effectively needed if we could allow the starting mesh to contain extraordinary vertices. For instance, if we could start the refinement process with an octahedron (see Figure 6.8), 6 initial vertices could be sufficient to obtain an ellipsoidal shape in the limit. This difference in the number of control points becomes

even more significant if we compare the number of vertices defining the k-th level subdivided meshes. Precisely, the k-th level mesh obtained from the initial 28-point regular mesh with poles by applying the regular refinement rules in Figure 6.5 contains $18 \cdot 4^k + 9 \cdot 2^k + 1$ vertices. On the other hand, the number of vertices in the k-th level mesh obtained from the octahedron by applying the extraordinary refinement rules in Figure 6.6 is only $4^{k+1} + 2$. In Table 6.1 we compare these two numbers for subdivision levels $k = 0, ..., 8$.

Level k	♯ Vertices of the subdivided regular mesh with poles	♯ Vertices of the subdivided octahedron
0	28	6
1	91	18
2	325	66
3	1225	258
4	4753	1026
5	18721	4098
6	74305	16386
7	296065	65538
8	1181953	262146

Table 6.1: Comparison between the number of vertices of the k-th level meshes obtained from the initial 28-point regular mesh with poles and the octahedron.

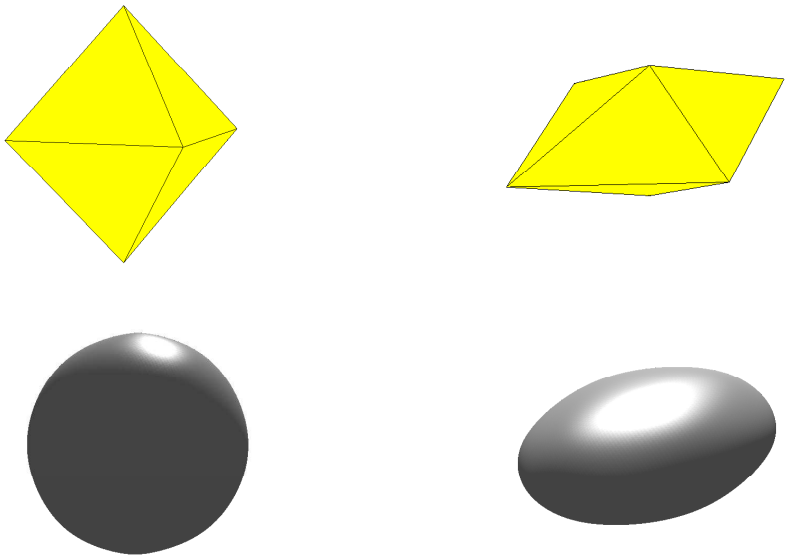

Figure 6.8: Octahedrons as initial triangular meshes (first row) and approximating sphere and ellipsoid (second row) obtained by the non-stationary BLOB scheme with extraordinary rules.

Now, let us take the octahedron as initial starting mesh. In particular, Figure 6.8 shows the approximated sphere and ellipsoid that we obtain from the corresponding octahedrons in the first row, by applying the non-stationary BLOB scheme with extraordinary refinement rules and setting $t = \frac{\pi}{2}$. We see that the non-stationary BLOB scheme produces a very accurate approximation of the corresponding exact sphere and ellipsoid. Moreover, if we apply the BLOB scheme to a 'distorted' octahedron (i.e. a polyhedron defined by 6 vertices not equally-spaced on a sphere or an ellipsoid), we obtain a limit surface with a blob-like shape (see Figure 6.9).

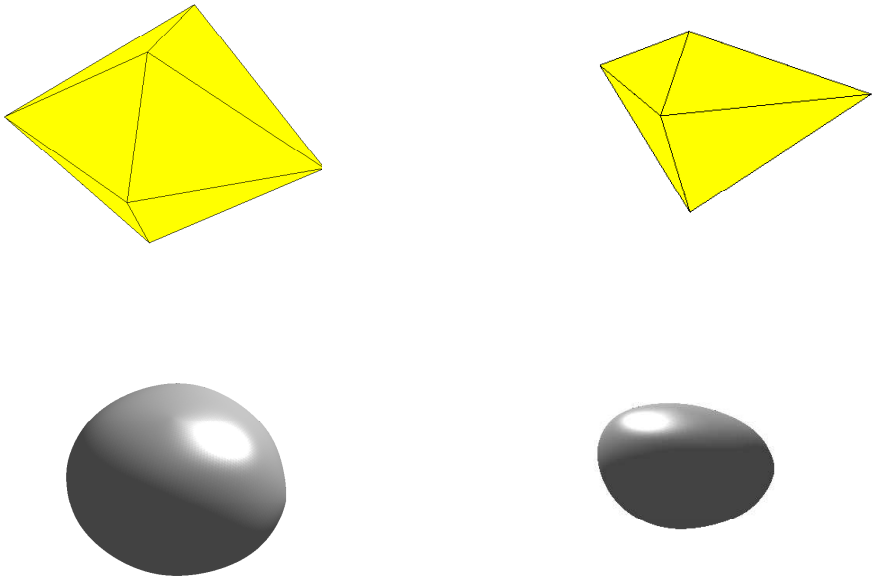

Figure 6.9: Distorted octahedron as initial triangular meshes (first row) and corresponding blob-like kimit surfaces (second row) obtained by the non-stationary BLOB scheme with extraordinary rules.

If we refine the regular octahedron using another bivariate subdivision scheme for triangular meshes of arbitrary manifold topology, such as the well-known Loop's scheme [95], the limit shape that we obtain in the limit is much more distant from the unit sphere that we would like to recover (see Figure 6.10). We see that the non-stationary BLOB scheme produces a better approximation. Precisely, let $\mathbf{C}$ be the center of gravity of the octahedron, i.e. the center of the sphere, and $\#\mathbf{f}^{(k)}$ the number of points defining the subdivision mesh at the k-th step. For all $k \geq 1$, we define

$$m_k = \min_{i=1,\ldots,\#\mathbf{f}^{(k)}} |\mathbf{C} - f_i^{(k)}| \quad \text{and} \quad M_k = \max_{i=1,\ldots,\#\mathbf{f}^{(k)}} |\mathbf{C} - f_i^{(k)}|.$$

A subdivision scheme produces a good approximation of a sphere if

$$error_k = M_k - m_k, \quad \forall k$$

is small. The error produced by the non-stationary BLOB scheme starting from the octahedron and after $k = 6$ steps of refinement is $1.06 \cdot 10^{-2}$, while the error produced by Loop's

scheme is $8.44 \cdot 10^{-2}$. To obtain approximately the same error using Loop's scheme, we need to consider a starting mesh with more control points, precisely, a mesh defined by 258 points (see Figure 6.11), obtaining an approximation error of $1.09 \cdot 10^{-2}$. This fact means that to obtain the same accuracy, the non-stationary BLOB scheme could use less control points than Loop's scheme and thus it results to be more efficient.

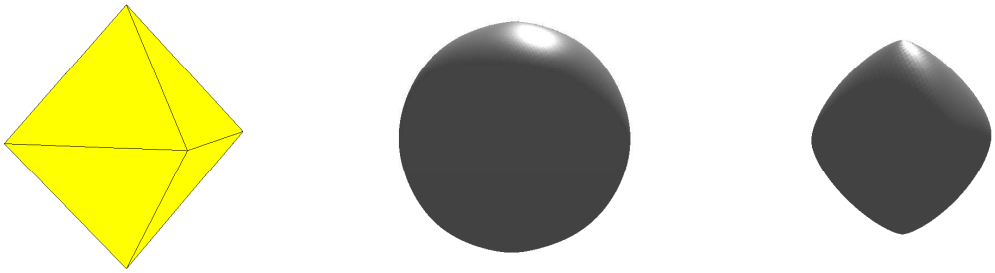

(a) Initial control mesh (b) BLOB's scheme limit surface (c) Loop's scheme limit surface

Figure 6.10: (a) The octahedron as initial control mesh, (b) the approximation of the unit sphere obtained by using the non-stationary BLOB scheme, (c) the approximation of the unit sphere obtained by using Loop's scheme.

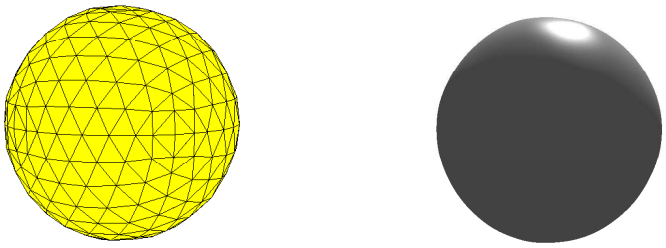

(a) Initial control mesh (b) Loop's scheme limit surface

Figure 6.11: (a) Initial mesh composed by 256 vertices, (b) the approximation of the unit sphere obtained by using Loop's scheme.

6.2.3 Affine invariance property of the non-stationary BLOB scheme

When the BLOB scheme is applied to regular regions of the mesh, the property of affine invariance follows straightforwardly from the capability of reproducing Π_1^2, as stated in Proposition 6.19. Near extraordinary vertices, affine invariance is also achieved since the entries in each row of the k-th level matrix S_k defined in (6.21) sum up to 1.

6.2.4 Convergence and smoothness properties of the non-stationary BLOB scheme

In this section, we analyze the convergence and smoothness properties of the BLOB scheme when applied to triangular meshes containing both vertices of valence 6 and 4. In order to apply the results recalled in Section 3.2, we need to derive the stationary counterpart of the non-stationary BLOB scheme, that is obtained by computing the limit of its local rules when $k \to +\infty$. Since $\lim_{k\to+\infty} v^{(k)} = 1$ for all $t \in [0,\pi) \cup \mathrm{i}\mathbb{R}^+$, it follows that, in correspondence to regular regions of the mesh, the stationary counterpart of the BLOB scheme is identified by the mask

$$\mathbf{a} := \lim_{k\to+\infty} \mathbf{a}^{(k)} = \begin{pmatrix} 0 & 0 & 0 & \frac{1}{128} & \frac{3}{128} & \frac{3}{128} & \frac{1}{128} \\ 0 & 0 & \frac{3}{128} & \frac{3}{32} & \frac{9}{64} & \frac{3}{32} & \frac{3}{128} \\ 0 & \frac{3}{128} & \frac{9}{64} & \frac{39}{128} & \frac{39}{128} & \frac{9}{64} & \frac{3}{128} \\ \frac{1}{128} & \frac{3}{32} & \frac{39}{128} & \frac{7}{16} & \frac{39}{128} & \frac{3}{32} & \frac{1}{128} \\ \frac{3}{128} & \frac{9}{64} & \frac{39}{128} & \frac{39}{128} & \frac{9}{64} & \frac{3}{128} & 0 \\ \frac{3}{128} & \frac{3}{32} & \frac{9}{64} & \frac{3}{32} & \frac{3}{128} & 0 & 0 \\ \frac{1}{128} & \frac{3}{128} & \frac{3}{128} & \frac{1}{128} & 0 & 0 & 0 \end{pmatrix}, \tag{6.22}$$

and the associated symbol is

$$\mathrm{a}(z_1, z_2) := \lim_{k\to+\infty} \mathrm{a}^{(k)}(z_1, z_2) = \frac{1}{128\, z_1^3 z_2^3} (z_1+1)^3 (z_2+1)^3 (z_1 z_2+1)^3. \tag{6.23}$$

Differently, in the neighborhood of extraordinary vertices, the refinement rules of the stationary counterpart of the BLOB scheme are encoded in the subdivision matrix $\tilde{S} := \lim_{k\to+\infty} \tilde{S}_k$ of the form in (2.21), where $\tilde{a} = \frac{1}{3}$, $\tilde{\mathbf{b}} = \left[\frac{1}{6}, 0, 0\right]^T$, $\tilde{\mathbf{c}} = \left[\frac{165}{512}, \frac{3}{32}, \frac{9}{64}\right]^T$, and

$$\begin{gathered} \tilde{M}_0 = \begin{pmatrix} \frac{39}{128} & \frac{1}{128} & \frac{3}{128} \\ \frac{7}{16} & \frac{3}{32} & \frac{3}{32} \\ \frac{39}{128} & \frac{3}{128} & \frac{9}{64} \end{pmatrix}, \qquad \tilde{M}_1 = \begin{pmatrix} \frac{39}{256} & 0 & 0 \\ \frac{3}{32} & 0 & 0 \\ \frac{39}{128} & \frac{3}{128} & \frac{1}{128} \end{pmatrix}, \\ \tilde{M}_2 = \begin{pmatrix} \frac{7}{512} & 0 & 0 \\ 0 & 0 & 0 \\ \frac{3}{128} & 0 & 0 \end{pmatrix}, \qquad \tilde{M}_3 = \begin{pmatrix} \frac{39}{256} & 0 & \frac{3}{128} \\ \frac{3}{32} & 0 & \frac{3}{32} \\ \frac{3}{128} & 0 & \frac{1}{128} \end{pmatrix}. \end{gathered} \tag{6.24}$$

Convergence and smoothness in the regular regions of the mesh

We first consider the application of the non-stationary BLOB scheme to regular regions of the mesh. In order to exploit Proposition 3.17, we first need the following result.

Proposition 6.20 *The stationary counterpart of the BLOB scheme produces C^4 limit surfaces when applied to regular triangular meshes.*

Proof: The claimed result follows by observing that the Laurent polynomial $\mathrm{a}(z_1, z_2)$ in (6.23) is the symbol of the C^4 and Π_5^2-generating subdivision scheme proposed in [70, Example 5, case 3]. ■

In light of Proposition 6.20 we can thus prove the next result.

Proposition 6.21 *The non-stationary BLOB scheme produces C^4 limit surfaces when applied to regular triangular meshes.*

Proof: We start by observing that the BLOB scheme is asymptotically similar to the C^4 convergent stationary scheme with symbol $\mathrm{a}(z_1, z_2)$ in (6.23). Then, we continue by proving that the BLOB scheme satisfies approximate sum rules of order 5. Indeed, since $\mu_k = 0$, $\sum_{k=0}^{\infty} \mu_k$ is trivially convergent. We thus need to prove only that

$$\sum_{k=0}^{\infty} 2^{4k}\, \delta_k < +\infty \qquad \text{with} \qquad \delta_k = \max_{0\le\gamma_1+\gamma_2\le 4} \max_{(\epsilon_1,\epsilon_2)\in\Xi'} 2^{-k(\gamma_1+\gamma_2)} \left| D^{(\gamma_1,\gamma_2)}\, \mathrm{a}^{(k)}(\epsilon_1, \epsilon_2) \right|.$$

Recalling Proposition 6.19 we already know that the BLOB scheme generates the space $EP_{(\Gamma_1,\Theta)}$ in (3.8). This means that its k-th level symbol $\mathrm{a}^{(k)}(z_1, z_2)$ satisfies

$$\mathrm{a}^{(k)}(\epsilon_1, \epsilon_2) = D^{(1,0)}\mathrm{a}^{(k)}(\epsilon_1, \epsilon_2) = D^{(0,1)}\mathrm{a}^{(k)}(\epsilon_1, \epsilon_2) = 0 \qquad \text{for all } (\epsilon_1, \epsilon_2) \in \Xi'$$

Thus, for the computation of δ_k we can just consider

$$\max_{2\le\gamma_1+\gamma_2\le 4} \max_{(\epsilon_1,\epsilon_2)\in\Xi'} 2^{-k(\gamma_1+\gamma_2)} \left| D^{(\gamma_1,\gamma_2)}\, \mathrm{a}^{(k)}(\epsilon_1, \epsilon_2) \right|$$

which yields

$$\max_{2\le\gamma_1+\gamma_2\le 4} \max_{(\epsilon_1,\epsilon_2)\in\Xi'} 2^{-k(\gamma_1+\gamma_2)} \left| D^{(\gamma_1,\gamma_2)}\, \mathrm{a}^{(k)}(\epsilon_1, \epsilon_2) \right| = \begin{cases} 2^{-4k} \frac{3\left|(v^{(k)}-1)(v^{(k)}-5)\right|}{(v^{(k)}+1)^2} & \text{if} \quad v^{(k)} < \frac{7}{3}, \\ 2^{-4k} \frac{6(v^{(k)}-1)^2}{(v^{(k)}+1)^2} & \text{if} \quad v^{(k)} \ge \frac{7}{3}. \end{cases}$$

Focussing first on the case $v^{(k)} < \frac{7}{3}$ we find that

$$\sum_{k=0}^{\infty} 2^{4k}\delta_k = \sum_{k=0}^{\infty} \frac{3\left|(v^{(k)}-1)(v^{(k)}-5)\right|}{(v^{(k)}+1)^2}.$$

Thus, recalling the definition of $v^{(k)}$ in (3.11), we can exploit the fact that (see (3.16))

$$|1 - v^{(k)}| \le c 2^{-2k}, \tag{6.25}$$

which implies

$$\sum_{k=0}^{\infty} 2^{4k}\delta_k = \sum_{k=0}^{\infty} \frac{3\left|(v^{(k)}-1)(v^{(k)}-5)\right|}{(v^{(k)}+1)^2} \le c \sum_{k=0}^{\infty} \left|v^{(k)} - 1\right| < +\infty,$$

with c a positive constant. With a similar reasoning we can also show that, when $v^{(k)} \ge \frac{7}{3}$,

$$\sum_{k=0}^{\infty} 2^{4k}\delta_k = \sum_{k=0}^{\infty} \frac{6(v^{(k)}-1)^2}{(v^{(k)}+1)^2} \le c \sum_{k=0}^{\infty} (v^{(k)} - 1)^2 < +\infty,$$

with c a positive constant. Hence, the claimed result follows in light of Proposition 3.17. ■

Convergence in the vicinity of extraordinary vertices

To prove that the non-stationary BLOB scheme produces limit surfaces that are at least convergent at extraordinary vertices of valence 4, we first need the following result concerning the stationary counterpart of the BLOB scheme.

Proposition 6.22 *The stationary counterpart of the BLOB scheme is convergent at extraordinary vertices of valence 4.*

Proof: The local subdivision matrix $\tilde{S}$ has eigenvalues that, sorted by modulus, verify the inequalities $1 = \lambda_0 > \lambda_1 = \lambda_2 = 0.3776 > |\lambda_i|$, $\forall i \geq 3$ and $\boldsymbol{x}_0 = [1, \ldots, 1]^T$. Thus, from Theorem 2.25 the claim follows. ■

Now, in light of Proposition 6.22 we can prove the next result.

Proposition 6.23 *The non-stationary BLOB scheme is convergent at extraordinary vertices of valence 4.*

Proof: From Propositions 6.20 and 6.22, the stationary counterpart of the BLOB scheme is C^4 continuous on regular meshes and convergent at extraordinary vertices. Hence assumption (i) of Theorem 3.25 is satisfied. Moreover, the masks of the non-stationary BLOB subdivision scheme and its stationary counterpart in (6.18) and (6.22) satisfy

$$\lim_{k \to +\infty} \frac{\|\mathbf{a}^{(k+1)} - \mathbf{a}\|}{\|\mathbf{a}^{(k)} - \mathbf{a}\|} = \frac{1}{4}.$$

Thus the two schemes are asymptotically equivalent and assumption (ii) is verified, too. Finally, using the explicit form of the subdivision matrices in (6.21) and (6.24), we can show that

$$\|S_k - S\| = \left| \frac{-29(v^{(k)})^2 + 14v^{(k)} + 15}{24(v^{(k)} + 1)^2} \right|,$$

obtaining

$$\lim_{k \to +\infty} \frac{\|S_{k+1} - S\|}{\|S_k - S\|} = \frac{1}{4} < \lambda_1 = 0.3776,$$

so concluding the proof. ■

6.2.5 The 3D deformable model obtained from the BLOB scheme and its applications

The non-stationary BLOB subdivision scheme can be efficiently exploited for the construction of deformable models with spherical topology. We explicitly model it by the triangular mesh obtained with the proposed subdivision scheme after 4 iterations (see Figure 6.12 (e)). Specific subdivision points, not necessary from the 4-th iteration, are used as the parameters of the model and they allow for a user-friendly interaction. The deformable model can be deformed manually by locally moving the parameters or automatically through the minimization of an energy functional [82, 83]. In general, the functional consists in an image energy, which is based on the information contained in the data (gradient, homogeneity...). This energy term

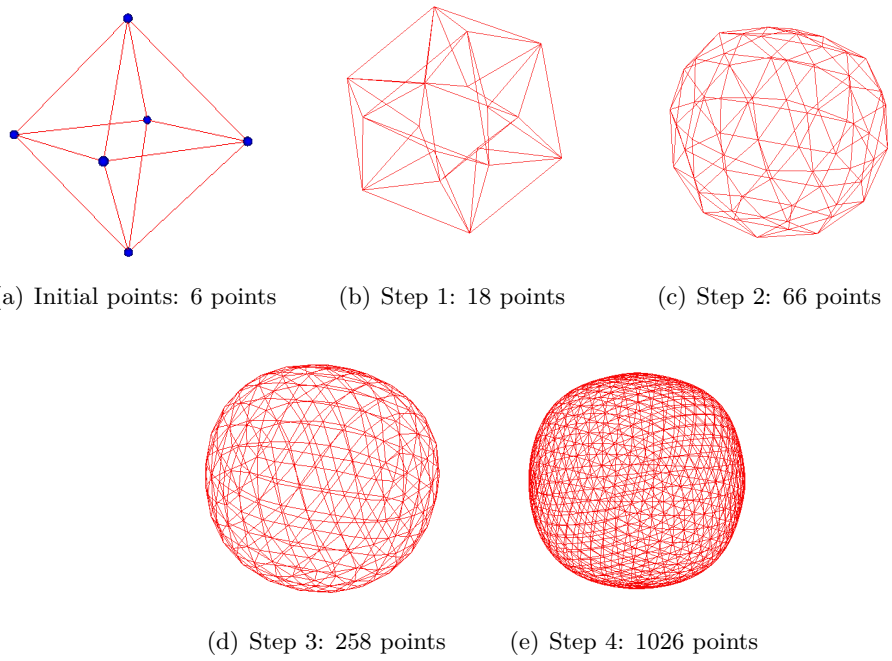

(a) Initial points: 6 points (b) Step 1: 18 points (c) Step 2: 66 points

(d) Step 3: 258 points (e) Step 4: 1026 points

Figure 6.12: Illustration of the subdivision scheme that approximates a sphere from an octahedron (a). Blue spheres: initial points; (b)-(e): the four first steps.

$\mathcal{E}$ is a function of the parameters Σ of the model and an optimization algorithm is used to find the optimum $\boldsymbol{\sigma}_{\text{opt}}$, which is described by $\boldsymbol{\sigma}_{\text{opt}} = \arg\min \mathcal{E}(\boldsymbol{\sigma})$. The use of few parameters yields to a fast optimization. However, the ability of the model to approximate a shape with accuracy increases when the number of parameters increases. In practice, a trade off has to be made between accuracy and fast optimization. Hence, according to the complexity of the shape of the object of interest, we choose as parameters the initial points (see Figure 6.12(a)) or the subdivision points at step 1, 2, 3 or 4 (see Figure 6.12 (b)-(e)). In the following, we illustrate the use of the new deformable model based on the non-stationary BLOB scheme through different applications[1].

Manual Segmentation of *Caenorhabditis Elegans* Embryos

Caenorhabditis elegans are widely used models in the study of metabolic diseases [135]. The *C. elegans* embryos shown in Figure 6.13 have blob-like shapes and so have few details. We manually segment one of them using only the 6 initial points as parameters. Thanks to the user interaction we adjust the location of the parameters to accurately segment the embryo. The result of the segmentation is given in Figure 6.13.

[1]The figures showing the application of our new deformable model on real biomedical images have been performed in collaboration with Prof. M. Unser and his Ph.D. students A. Badoual and D. Schmitter from the Biomedical Imaging Group, Ecole Polytechnique Fédérale de Lausanne (EPFL), Lausanne, Switzerland.

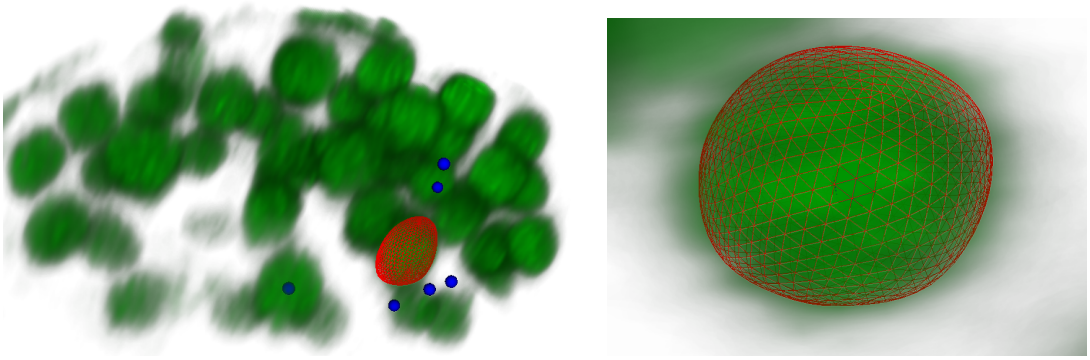

Figure 6.13: Segmentation of *Caenorhabditis elegans* embryos. Right: segmentation of a *C. elegans* embryo by manually moving the parameters (blue spheres). Left: zoom on the segmentation outcome. Photo courtesy of Rahul Sharma, Institute of Cell Biology, University of Bern, Switzerland.

Automatic nuclei segmentation

Nuclei segmentation is important to characterize their symmetry, mean intensity, or curvature. These characteristics are crucial to diagnose diseases such as neurological disorders or cancer. We segmented the nucleus of a neuron of a rat in 3D microscopy images [31]. The shape of the nucleus has many details (concavities). Hence, we used as parameters the 66 subdivision points obtained at the 2nd subdivision step. The initialization is shown in Figure 6.14. We detected the contours using an energy based on gradient information and we minimized it using a Powell-like line-search method [114]. The outcome is illustrated in Figure 6.15.

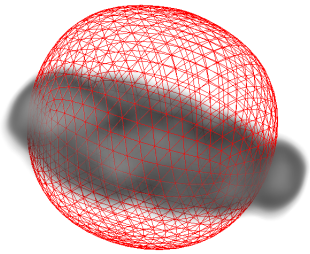

Figure 6.14: Initialization of a nucleus of a neuron.

Automatic brain segmentation

Brain segmentation algorithms are challenging because the brain is a structure with many concavities such as grooves or lobes. Segmentation algorithms are used in medicine to detect temporal morphological changes in relation with neurological diseases [125]. We performed a segmentation on a 3D MRI scan of a human brain using 66 subdivision points as parameters. We initialized the deformable model with an approximate sphere (see Figure 6.16) and we

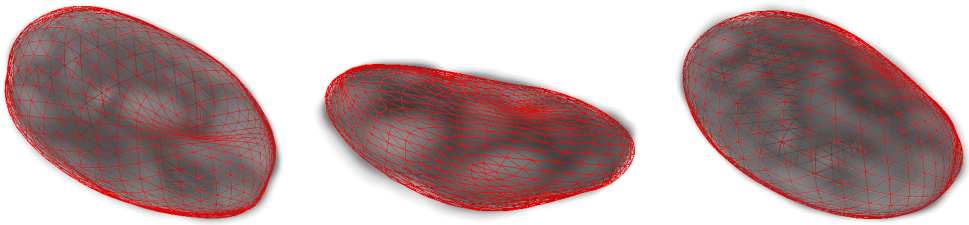

Figure 6.15: Segmentation of a nucleus of a neuron in 3D microscopy images

used the same energy as the one used in Section 6.2.5. The segmentation result is illustrated in Figure 6.17.

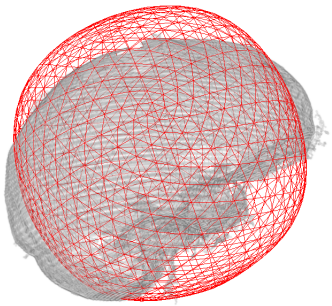

Figure 6.16: Initialization of brain.

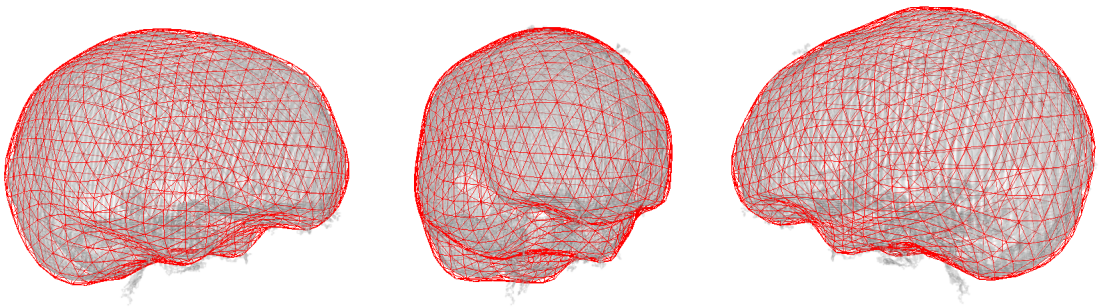

Figure 6.17: Segmentation of a brain in a 3D MRI volume

User-interactive modeling

The triangular mesh can be deformed manually by moving subdivision points. For instance, this allows one to adjust the result of an automatic segmentation. We illustrate how a surface can manually be modified, starting from an approximate sphere to design a shape of interest.

The modeling of a bone structure is shown in Figure 6.18 (right). Different steps of this deformation are shown in Figure 6.18.

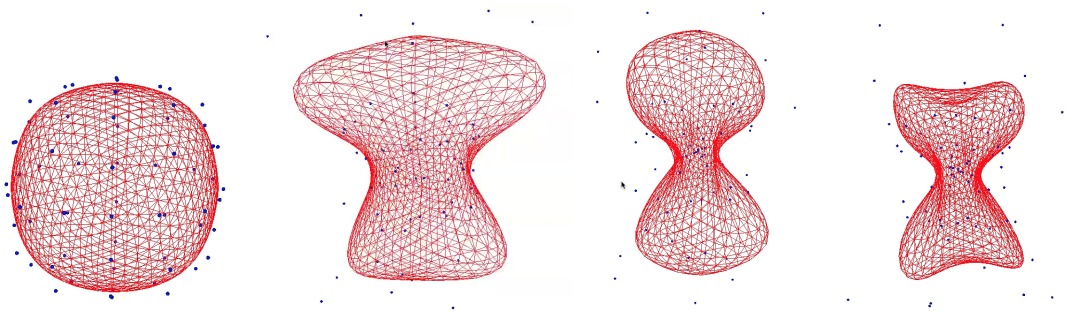

Figure 6.18: Deformation of the sphere by user interaction. Blue spheres: parameters.

Chapter 7

Interpolation of quad-meshes via approximating subdivision schemes

As presented in Section 1.2, subdivision schemes could be classified as approximating or interpolatory schemes. Interpolatory schemes are widely required in interactive design and geometric modeling since the vertices of the original control mesh defining the surface are also points of the limit surface, and thus one can control the surface in a more intuitive manner. Unfortunately, interpolatory schemes do not produce limit surfaces of good quality because, since no vertex is ever moved once it is computed, any distortion generated in the early refinement steps persists in the limit (see e.g. Figure 7.12). On the contrary, approximating schemes produce limit surfaces with a better quality than the interpolatory ones. For this reason, to interpolate a mesh with a higher quality surface, many interpolating methods relying on approximating subdivision schemes were proposed. The easiest method to construct a limit interpolating curve or surface using an approximating scheme is to compute a new set of control points by solving a simple linear system, which involves the so-called limit stencil of the subdivision scheme, in such a way that the approximating scheme applied to the new control points produces a limit curve/surface that passes through the original control points. This method is used in [68, 101] to construct interpolating limit surfaces based on Doo-Sabin's and Catmull-Clark's subdivision and in [120] to design interpolating limit curves based on a non-stationary version of cubic B-splines. Other interpolating methods which exploit the limit stencil are proposed in [40, 41], and they are based on Doo-Sabin's and Catmull-Clark's subdivision, respectively.

We here present an efficient algorithm for constructing interpolating curves or surfaces starting from any kind of approximating subdivision scheme, that is univariate or bivariate schemes with stationary or non-stationary rules. As in the previously cited works, the interpolation is gained exploiting the limit stencil of the approximating subdivision scheme. Notice that, in the stationary case the computation of the limit stencil is well-known and it is obtained exploiting linear algebra tools; on the other hand, in the non-stationary case there is no a general method to find the limit stencil, but it could be computed with both linear algebra and geometrical approaches. The basic idea of our interpolatory algorithm is to compute a new control mesh for which the limit surface interpolates the vertices of the original mesh. This new control mesh is derived from one subdivision step with a modified geometric rule which involves the computation of the limit stencil. In the following, we refer to this procedure as the preprocessing step, which could be described by a simple formula depending on a

local free shape parameter. Moreover, if we use a non-stationary subdivision scheme we gain an additional free tension parameter to adjust the shape of the subdivision surface.

7.1 The limit stencil

Since the algorithm we present in this chapter could be applied both to stationary and non-stationary schemes, we here use the more general non-stationary notation, which easily reduces to the stationary one if the scheme is level independent.
Let $\mathbf{f}^{(0)} = \{f_i^{(0)}, i \in \mathbb{Z}^s\}$ be a set of initial control points. A convergent symmetric uniform subdivision scheme $\{\mathcal{S}_k, k \in \mathbb{N}_0\}$, associated to a local subdivision matrix $\{S_k, k \in \mathbb{N}_0\}$, is described by the refinement rules

$$\mathbf{f}^{(k+1)} = S_k \mathbf{f}^{(k)} = S_k \cdot S_{k-1} \mathbf{f}^{(k-1)} = ... = S^{(k+1)} \mathbf{f}^{(0)}, \qquad S^{(k+1)} = S_k \cdots S_0, \tag{7.1}$$

which for all $k \in \mathbb{N}_0$ generate the refined data sequence $\mathbf{f}^{(k+1)}$ starting from the initial data $\mathbf{f}^{(0)}$. At the end of the subdivision process, i.e. for $k \to +\infty$, the positions of the so-called limit points $\mathbf{f}^{(\infty)}$ are described by

$$\mathbf{f}^{(\infty)} = \left(\prod_{j=0}^{+\infty} S_j \right) \mathbf{f}^{(0)} = S^{(\infty)} \mathbf{f}^{(0)}.$$

From a practical point of view, in order to find the exact limit position of the control points, we could not apply the subdivision rules infinity times to the initial data, but we could study the behavior of the matrix $S^{(\infty)}$, whose coefficients define the rule to compute the limit points.

Remark 7.1 *In case of a univariate subdivision scheme, we choose an arbitrary ordering of the initial control points and we write the subdivision rules in a matrix form. The size of the k-th level subdivision matrix $S_k \in \mathbb{R}^{N \times N}$ depends on how many points are involved in the subdivision rules, i.e. how many old points give a contribution to compute m new points, where m is the arity of the scheme. In case of a bivariate subdivision scheme, the k-th level subdivision matrix $S_k \in \mathbb{R}^{N \times N}$ could be constructed as explained in Section 2.3, where the dimension N depends on the valence n of the considered vertex or face and on the number of rings involved in the refinement rules (see equation* (2.19)*).*

To study the behavior of the local limit matrix

$$S^{(\infty)} = \lim_{k \to +\infty} \prod_{j=0}^{k} S_j,$$

we could distinguish two cases: S_k depending or not on the level k. We analyze these two cases separately.

7.1.1 Independence on k: stationary subdivision schemes

If S_k does not depend on the level k, i.e. the rules of the subdivision scheme are stationary, then $S_k = S$ for all $k \in \mathbb{N}_0$ and thus

$$S^{(\infty)} = \lim_{k \to +\infty} \prod_{j=0}^{k} S = \lim_{k \to +\infty} S^{k+1}.$$

We apply the Jordan decomposition (see Section 2.3.1) to S, such that $S^{k+1} = XJ^{k+1}X^{-1}$, where $J^{k+1} = diag(J_1^{(k+1)}, \dots, J_{\overline{r}}^{k+1})$ with each block J_r of the form in (2.27), X is a full matrix with the generalized right eigenvectors $\boldsymbol{x}_i$ of S on the columns and X^{-1} is a full matrix with the generalized left eigenvectors $\tilde{\boldsymbol{x}}_i^T$ of S on the rows. Thus, we have

$$S^{(\infty)} = X \left(\lim_{k \to +\infty} J^{k+1} \right) X^{-1}.$$

Since we consider a convergent subdivision scheme, it follows that the largest eigenvalue of S is unique and equal to 1, with all the other eigenvalues less then 1, i.e.

$$1 = \lambda_0 > |\lambda_i|, \ i = 1, \dots \overline{r}.$$

Moreover, the eigenvector associated to λ_0 is $\boldsymbol{x}_0 = [1, \dots, 1]^T$ (see Theorem 2.25). Recalling Remark 2.24, it follows that

$$S^{(\infty)} = X \lim_{k \to +\infty} \begin{pmatrix} 1 & \mathbf{0} & \dots & \mathbf{0} \\ \mathbf{0} & J_1 & \ddots & \mathbf{0} \\ \vdots & \ddots & \ddots & \vdots \\ \mathbf{0} & \cdots & \mathbf{0} & J_{\overline{r}} \end{pmatrix} X^{-1} = X \begin{pmatrix} 1 & 0 & \cdots & 0 \\ 0 & 0 & \cdots & 0 \\ \vdots & \ddots & \ddots & \vdots \\ 0 & \cdots & \cdots & 0 \end{pmatrix} X^{-1} = \boldsymbol{x}_0 \tilde{\boldsymbol{x}}_0^T = \begin{pmatrix} \tilde{\boldsymbol{x}}_0^T \\ \tilde{\boldsymbol{x}}_0^T \\ \vdots \\ \tilde{\boldsymbol{x}}_0^T \end{pmatrix}.$$

Finally, the row vector $\tilde{\boldsymbol{x}}_0^T$ is called the limit stencil.

7.1.2 Dependence on k: non-stationary subdivision

On the other hand, if the local k-level matrix S_k depends on the subdivision level, i.e. the rules of the subdivision scheme are non-stationary or level-dependent, then the computation of the limit position becomes more complicate. We could proceed as in the stationary case, with a linear algebra approach, computing the Jordan decomposition of S_k as $S_k = X_k J_k X_k^{-1}$ and studying the behavior of

$$S^{(\infty)} = \lim_{k \to +\infty} \prod_{j=0}^{k} X_j J_j X_j^{-1}.$$

Another possibility is to proceed using a geometrical point of view, studying the behavior of the points during the subdivision process and following their displacements to find their limit position, as shown in [120]. In both the cases, we could not propose a general approach: each non-stationary subdivision scheme has its particular behavior.

7.2 Interpolation algorithm

In this section we present a general algorithm able to produce interpolating curves and surfaces as limits of subdivision processes based on an approximating scheme $\{\mathcal{S}_k, k \in \mathbb{N}_0\}$ and using the so called preprocessing step.
Let $\mathbf{a}^{(\infty)}$ be the limit stencil computed as in Section 7.1 associated to the approximating scheme $\{\mathcal{S}_k, k \in \mathbb{N}_0\}$. Starting from the set of control points $\mathbf{f}^{(0)}$, we apply on them a preprocessing step to compute a new control polyline/mesh. This preprocessing step is a local process and it is composed by two different parts:

Part 1. For each point $f_i^{(0)}$, we construct the 0-level local subdivision matrix $S_0 \in \mathbb{R}^{N\times N}$ and we compute

$$\tilde{f}_{i,j}^{(0)} = \sum_{h=0,\dots,N-1} S_0(j,h) f_{i+h}^{(0)}, \qquad \text{with} \quad j = 0,\dots,N-1, \tag{7.2}$$

where $S_0(j,h)$ is the element at line j and column h of the matrix S_0.

Part 2. We compute the vertices of the new control polyline/mesh $\mathbf{g}^{(0)}$, such that for all i

$$g_{i,j}^{(0)} = f_i^{(0)} + \alpha_i(\tilde{f}_{i,j}^{(0)} - \mathcal{L}(\tilde{f}_{i,0}^{(0)})), \qquad \alpha_i \in \mathbb{R}, \quad j = 0,\dots,N-1, \tag{7.3}$$

where $\mathcal{L}(\tilde{f}_{i,0}^{(0)})$ is the limit point associated to $\tilde{f}_{i,0}^{(0)}$ and defined by the limit stencil $\mathbf{a}^{(\infty)}$, such that

$$\mathcal{L}(f_{i,0}) = \sum_{h=0,\dots,N-1} \mathrm{a}_h^{(\infty)} f_{i,h}, \qquad \text{with} \qquad \sum_{h=0,\dots,N-1} \mathrm{a}_h^{(\infty)} = 1. \tag{7.4}$$

It follows that from each point $f_i^{(0)}$ of the starting control polyline/mesh, we define N new points $g_{i,j}^{(0)}$. Once the preprocessing step is completed, the interpolating limit curve/surface is obtained just applying the subdivision scheme $\mathcal{S}_k$ to the preprocessed polyline/mesh $\mathbf{g}^{(0)}$.

Theorem 7.2 *Applying the subdivision scheme $\mathcal{S}_k$ to the control points $\mathbf{g}^{(0)}$, we obtain a limit curve/surface that interpolates the vertices of $\mathbf{f}^{(0)}$, for all $\alpha_i \in \mathbb{R}$.*

Proof: For each new vertex $g_{i,0}^{(0)}$ we compute its limit position, that is, for all i,

$$\begin{aligned}\mathcal{L}(g_{i,0}^{(0)}) &= \sum_{h=0,\dots,N-1} \mathrm{a}_h^{(\infty)} g_{i,h}^{(0)} = \sum_{h=0,\dots,N-1} \mathrm{a}_h^{(\infty)} \left(f_i^{(0)} + \alpha_i(\tilde{f}_{i,h}^{(0)} - \mathcal{L}(\tilde{f}_{i,0}^{(0)})\right) \\ &= \sum_{h=0,\dots,N-1} \mathrm{a}_h^{(\infty)} f_i^{(0)} + \alpha_i \sum_{h=0,\dots,N-1} \mathrm{a}_h^{(\infty)} \tilde{f}_{i,h}^{(0)} - \alpha_i \sum_{h=0,\dots,N-1} \mathrm{a}_h^{(\infty)} \mathcal{L}(\tilde{f}_{i,0}^{0}).\end{aligned}$$

Recalling (7.4), we obtain

$$\mathcal{L}(g_{i,0}^{(0)}) = f_i^{(0)} + \alpha_i \sum_{h=0,\dots,N-1} \mathrm{a}_h^{(\infty)} \tilde{f}_{i,h}^{(0)} - \alpha_i \mathcal{L}(\tilde{f}_{i,0}^{(0)}) = f_i^{(0)} + \alpha_i \mathcal{L}(\tilde{f}_{i,0}^{(0)}) - \alpha_i \mathcal{L}(\tilde{f}_{i,0}^{(0)}) = f_i^{(0)}.$$

This means that in the limit the vertices of $\mathbf{g}^{(0)}$ converges to $\mathbf{f}^{(0)}$, thus the limit curve/surface interpolates the vertices $\mathbf{f}^{(0)}$. ■

The procedure described to design interpolating limit curves and surfaces using an approximating subdivision scheme $\{\mathcal{S}_k, k \in \mathbb{N}_0\}$ could be summarized in the following algorithm.

Algorithm 2 *INPUT: initial control polyline/mesh $\mathbf{f}^{(0)}$ and an approximating subdivision scheme $\{\mathcal{S}_k, k \in \mathbb{N}_0\}$,*

1. *compute the set of points $\tilde{\mathbf{f}}^{(0)}$ as in* (7.2),
2. *compute $\mathbf{g}^{(0)}$ as in* (7.3),
3. *apply $\{\mathcal{S}_k, k \in \mathbb{N}_0\}$ to $\mathbf{g}^{(0)}$.*

OUTPUT: limit curve/surface interpolating $\mathbf{f}^{(0)}$.

7.2.1 The local free parameter α_i

In Theorem 7.2 we prove that Algorithm 2 produces interpolating limit curves/surfaces for all values of $\alpha_i \in \mathbb{R}$. This free parameter is a local parameter related to the i-th point of the control polyline/mesh. The choice of α_i influences the position of the points $\mathbf{g}^{(0)}$ and, consequently, the behavior of the limit curve/surface. In particular, for some values of α_i the control polyline/mesh $\mathbf{g}^{(0)}$ intersects itself and thus the limit curve/surface inherits this intersection or presents some deformations. In the following we derive sufficient conditions on α_i to guarantee that the limit curve/surface does not present these distortions. We consider the curve case, since it is more manageable, but we will see that the results in the univariate case could be easily extended to the bivariate case. We start by noticing that if $\alpha_i < 0$, a

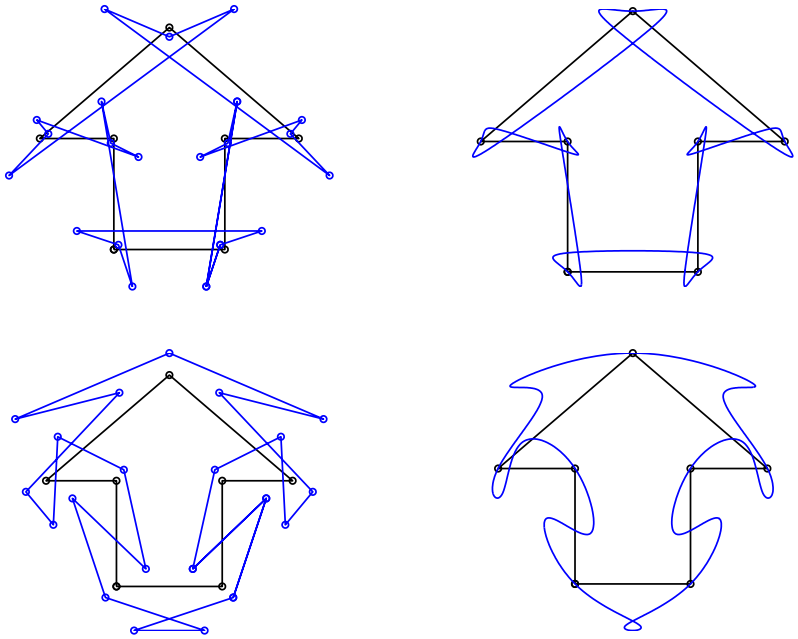

Figure 7.1: Preprocessed polylines and interpolating limit curves obtained with $\alpha_i = -1,\ \forall i$ (top line) and $\alpha_i = 2.5,\ \forall i$ (bottom line), using stationary cubic B-spline with rules in (7.5).

part of the polyline $\mathbf{g}^{(0)}$ falls inside the control polyline $\mathbf{f}^{(0)}$, thus to gain the interpolation property the limit curve has to intersect itself. On the other hand, if $\alpha_i > 0$ it may happen that two consecutive points of $\mathbf{g}^{(0)}$ are exchanged determining self-intersection or distortions in the limit curve. These behaviors are presented in Figure 7.1, where, in particular, we show the preprocessed control polylines and the limit curves obtained using the stationary cubic B-spline scheme with rules

$$\begin{cases} f_{2i}^{(k+1)} &= \frac{1}{8} f_{i-1}^{(k)} + \frac{3}{4} f_i^{(k)} + \frac{1}{8} f_{i+1}^{(k)}, \\ f_{2i+1}^{(k)} &= \frac{1}{2} f_i^{(k)} + \frac{1}{2} f_{i+1}^{(k)}, \end{cases} \tag{7.5}$$

and Algorithm 2 with $\alpha_i = -1, \forall i$ (top line) and $\alpha_i = 2.5, \forall i$ (bottom line). We see that these values of α_i imply self-intersections and distortions in the limit curves.
To find admissible values for α_i, let us consider Figure 7.2 as example, where we suppose

$N = 3$. From $f_0^{(0)}$ we compute $\tilde{f}_{0,0}^{(0)}, \tilde{f}_{0,1}^{(0)}, \tilde{f}_{0,2}^{(0)}$ using (7.2) and we consider the related limit point $\mathcal{L}(\tilde{f}_{0,0}^{(0)})$. In the same way, starting from $f_2^{(0)}$ we compute $\tilde{f}_{2,0}^{(0)}, \tilde{f}_{2,1}^{(0)}, \tilde{f}_{2,2}^{(0)}$ with limit point $\mathcal{L}(\tilde{f}_{2,0}^{(0)})$ (see Figure 7.2 (a)). The dot lines indicate the directions of the displacements $\tilde{f}_{i,j}^{(0)} - \mathcal{L}(\tilde{f}_{i,0}^{(0)})$, $i = 0, 2$, $j = 0, 1, 2$, on which the points $g_{i,j}^{(0)}$ lie. Fixing a value of α_0 and α_2, and using (7.3), we compute the position of the points $g_{0,0}^{(0)}, g_{0,1}^{(0)}, g_{0,2}^{(0)}$ related to $f_0^{(0)}$ and the points $g_{2,0}^{(0)}, g_{2,1}^{(0)}, g_{2,2}^{(0)}$ related to $f_2^{(0)}$. If α_0 and α_2 are 'too large' the points $g_{0,2}^{(0)}$ and $g_{2,1}^{(0)}$ could be exchanged, i.e. $g_{0,2}^{(0)}$ is between $g_{2,1}^{(0)}$ and $g_{2,0}^{(0)}$ and not between $g_{0,0}^{(0)}$ and $g_{2,1}^{(0)}$ (see Figure 7.2 (b)). To avoid this, we have to choose α_0 and α_2 in such a way that

$$\alpha_0|\tilde{f}_{0,2}^{(0)} - \mathcal{L}(\tilde{f}_{0,0}^{(0)})| \leq \frac{1}{2}|f_0^{(0)} - f_2^{(0)}|\cos(\phi_{0,2}), \quad \text{and} \quad \alpha_2|\tilde{f}_{2,1}^{(0)} - \mathcal{L}(\tilde{f}_{2,0}^{(0)})| \leq \frac{1}{2}|f_0^{(0)} - f_2^{(0)}|\cos(\phi_{2,0}),$$

where $\phi_{0,2}$ is the angle between the edge $f_0^{(0)} f_2^{(0)}$ and the segment $f_0^{(0)} g_{0,2}^{(0)}$ and $\phi_{2,0}$ is the angle between the edge $f_2^{(0)} f_0^{(0)}$ and the segment $f_2^{(0)} g_{2,1}^{(0)}$. This condition guarantees that $g_{0,2}^{(0)}$ and $g_{2,1}^{(0)}$ are not exchanged. But it may happen that they are aligned along the perpendicular to the edge $f_0^{(0)} f_2^{(0)}$ (see Figure 7.2 (c)). To exclude also this case it is sufficient to require

$$\alpha_0|\tilde{f}_{0,2}^{(0)} - \mathcal{L}(\tilde{f}_{0,0}^{(0)})| \leq \frac{1}{2}|f_0^{(0)} - f_2^{(0)}| \quad \text{and} \quad \alpha_2|\tilde{f}_{2,1}^{(0)} - \mathcal{L}(\tilde{f}_{2,0}^{(0)})| \leq \frac{1}{2}|f_0^{(0)} - f_2^{(0)}|,$$

thus obtaining two points that are neither exchanged, nor on the perpendicular to the corresponding edge (see Figure 7.2 (d)). This study should be done for each point and each edge. We generalize the previous reasoning as in the following.

- Given a control polyline $\mathbf{f}^{(0)} = \{f_i^{(0)}, i \in \mathbb{Z}\}$, for each point $f_i^{(0)}$, let $f_{\ell_1}^{(0)}$ and $f_{\ell_2}^{(0)}$ be the two points that are connected with $f_i^{(0)}$ by an edge. We denote

$$E_i := \min_{\ell \in L} \|f_i^{(0)} - f_\ell^{(0)}\|_2, \qquad \text{with} \qquad L = \{\ell_1, \ell_2\} \tag{7.6}$$

and

$$D_i := \max_{j=0,\ldots,N-1} \|\tilde{f}_{i,j}^{(0)} - \mathcal{L}(\tilde{f}_{i,0}^{(0)})\|_2. \tag{7.7}$$

If α_i satisfies

$$0 \leq \alpha_i \leq \frac{1}{2}\frac{E_i}{D_i}, \quad \forall i \tag{7.8}$$

then the limit curve is not self-intersecting.

From this reasoning and in light of equation (7.3), it is clear that the local parameter α_i suggests how much distant we move from the control mesh $\mathbf{f}^{(0)}$. This will be underlined in the numerical experiments in Section 7.4. The conditions found in (7.8) are also applicable in the surface setting with same minor changes, as follows.

- Given a control mesh $\mathbf{f}^{(0)} = \{f_i^{(0)}, i \in \mathbb{Z}^2\}$, for each point $f_i^{(0)}$, let $f_{\ell_1}^{(0)}, \ldots, f_{\ell_m}^{(0)}$ be the m points that share a face with $f_i^{(0)}$. We denote,

$$E_i := \min_{\ell \in L} \|f_i^{(0)} - f_\ell^{(0)}\|_2, \qquad L = \{\ell_1, \ldots, \ell_m\}$$

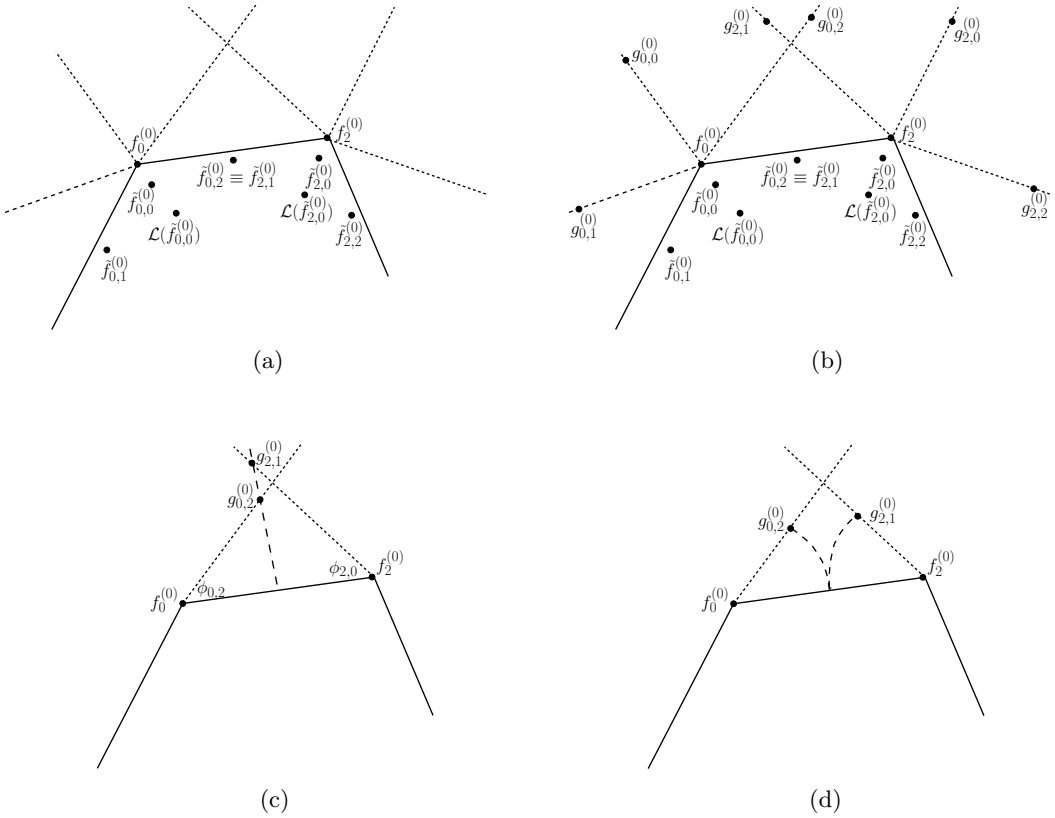

Figure 7.2: Illustrative example on how we should choose α_i.

and

$$D_i := \max_{j=0,\dots,N-1} \|\tilde{f}_{i,j}^{(0)} - \mathcal{L}(\tilde{f}_{i,0}^{(0)})\|_2.$$

If α_i satisfies

$$0 \leq \alpha_i \leq \frac{1}{2}\frac{E_i}{D_i}, \quad \forall i \tag{7.9}$$

then the limit surface is not self-intersecting.

In Figure 7.3, we propose an example on how we could choose the parameters α_i. We consider a closed polyline defined by the control points $f_i^{(0)}, i = 0, \dots, 6$ and we display the lengths of the edges, that is the values $\|f_i^{(0)} - f_\ell^{(0)}\|_2$ (see Figure 7.3 (left)). In Figure 7.3 (right) we show the points $\tilde{f}_{i,j}$ (blue dots) computed with a step of stationary cubic B-splines with rule in (7.5) and the limit points obtained exploiting the limit stencil $\mathbf{a}^{(\infty)} = \left[\frac{1}{6}, \frac{2}{3}, \frac{1}{6}\right]$ (red dots). The dot lines represent the connections between each point $\tilde{f}_{i,j}$ and the correspondent limit point. The quantities $\|\tilde{f}_{i,j}^{(0)} - \mathcal{L}(\tilde{f}_{i,0}^{(0)})\|_2$ are indicated. Now, we exploit equations (7.6)-(7.7)-(7.8) to

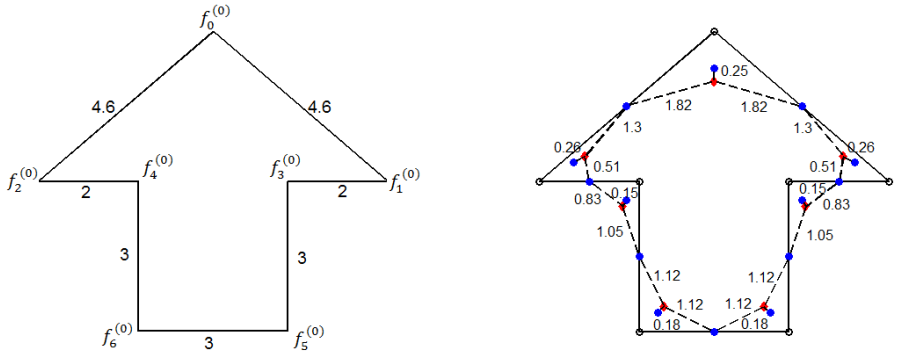

Figure 7.3: Left: initial control points $f_i^{(0)}$ and length of each edge. Right: new points $\tilde{f}_{i,j}^{(0)}$ obtained with one step of stationary cubic B-spline scheme in (7.5) (blue dots) and correspondent limit points (red dots).

find $\alpha_i, i = 0, \dots, 6$. We have

$$\begin{array}{rlrlrl} E_0 &= 4.6 & D_0 &= 1.82 & \alpha_0 &\leq 1.26 \\ E_1 = E_2 &= 2 & D_1 = D_2 &= 1.3 & \alpha_1 = \alpha_2 &\leq 0.77 \\ E_3 = E_4 &= 2 & D_3 = D_4 &= 1.5 & \alpha_3 = \alpha_4 &\leq 0.67 \\ E_5 = E_6 &= 3 & D_5 = D_6 &= 1.12 & \alpha_5 = \alpha_6 &\leq 1.34 \end{array}$$

Thus, choosing the values of α_i satisfying these conditions, any self-intersection or distortion is avoided (see, e.g. Figure 7.4).

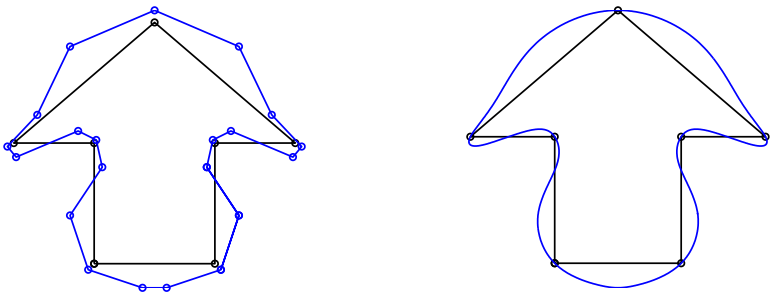

Figure 7.4: Preprocessed polyline and interpolating limit curve obtained with $\alpha = [1.2, 0.7, 0.7, 0.6, 0.6, 1.2, 1.2]$ and using the cubic B-spline with rules in (7.5). The points and the coefficients α_i are ordered from top to bottom.

7.3 Comparison with other methods

Many methods have been proposed to construct interpolating limit curves/surfaces starting from an approximating scheme. In general, these methods differentiate for the definition of the new control points. The methods shown in [40, 41] are similar to our construction of the new control polyline/mesh. In these works, the authors construct the new control mesh using

a modified rule based on Doo-Sabin's and Catmull-Clark's schemes and exploiting their limit stencils. However, the geometric rules proposed are strictly connected with the subdivision scheme used, and not easily generalizable to all subdivision rules. On the contrary, the algorithm we present is extremely general and could be applied to any kind of subdivision scheme: univariate or bivariate subdivision schemes, with stationary or non-stationary rules. In the following, we focus on the comparison with the most immediate method, i.e. the solution of a linear system, underlying differences and similarities.

7.3.1 Solution of a linear system

The easier way to construct a new control polyline in order to obtain interpolating curves/surfaces using an approximating scheme is the solution of a linear system of the form

$$A^{(\infty)}\mathbf{h}^{(0)} = \mathbf{f}^{(0)}, \tag{7.10}$$

where $A^{(\infty)}$ is a square matrix with rows defined by the limit stencil $\mathbf{a}^{(\infty)}$, $\mathbf{f}^{(0)}$ is the vector of the starting control points and $\mathbf{h}^{(0)}$ is the new control polyline/mesh. In particular, the algorithm is defined as follows.

Algorithm 3 *INPUT: initial control polyline/mesh* $\mathbf{f}^{(0)}$ *and an approximating subdivision scheme* $\{\mathcal{S}_k, k \in \mathbb{N}_0\}$*,*

1. *solve the linear system in* (7.10) *to find* $\mathbf{h}^{(0)}$*,*
2. *apply* $\{\mathcal{S}_k, k \in \mathbb{N}_0\}$ *to* $\mathbf{h}^{(0)}$*.*

OUTPUT: limit curve/surface interpolating $\mathbf{f}^{(0)}$*.*

As already recalled, Algorithm 3 is used in many works in literature (see e.g. [68, 101, 120]). To find the exact solution of the linear system could be very expensive if the initial polyline/mesh is made of a high number of control vertices. Moreover, it may happen that the produced limit curve/surface presents some undulations or distortions, thus requiring a shape fairing. For example, Halstead et al. [68] propose a method for generating fair Catmull-Clark's surfaces by first interpolating a set of given mesh vertices, and then fairing the surface by minimizing a quadratic norm that combines thin plate and membrane energies. The similarity between our proposal and Algorithm 3 is the use of the limit stencil. However, we can underline many differences. First of all, we do not require the solution of a linear system, but we work locally on a few number of vertices. Then, using Algorithm 3 the new control polyline/mesh is defined by the same number of points of the starting vector $\mathbf{f}^{(0)}$, while the algorithm we propose constructs the preprocessed control polyline/mesh which is define by N-times the number of the initial control points. Moreover, our definition of the new control polyline/mesh $\mathbf{g}^{(0)}$ in (7.3) allows us to gain a free local parameter α_i that could be used to model the shape of the final limit curve/surface (see Section 7.4), thus avoiding the need of a shape fairing.
In the following, we present a simple example based on a non-stationary version of cubic B-spline scheme to show differences and similarities of our interpolating algorithm and the method in (7.10).

Interpolation via a non-stationary cubic B-spline scheme

In [120], the authors proposed a non-stationary version of the cubic B-spline with rules

$$\begin{cases} f_{2i}^{(k)} &= \frac{\beta_k}{8} f_{i-1}^{(k)} + \left(1 - \frac{\beta_k}{4}\right) f_i^{(k)} + \frac{\beta_k}{8} f_{i+1}^{(k)}, \\ f_{2i+1}^{(k)} &= \frac{1}{2} f_i^{(k)} + \frac{1}{2} f_{i+1}^{(k)}, \end{cases} \qquad \beta_k = \frac{2}{1 + \cos\left(\frac{t}{2^{k+1}}\right)}, \quad t \in [0, \pi) \cup \mathrm{i}\mathbb{R}^+, \tag{7.11}$$

and limit stencil given by

$$\left[\frac{1-\gamma}{2}, \gamma, \frac{1-\gamma}{2}\right], \quad \text{with} \quad \gamma = \cot\left(\frac{t}{2}\right)\left(\frac{1}{t} - \cot t\right). \tag{7.12}$$

From the subdivision rules in (7.11), it is easy to see that three old points are involved in the computation of two new points, thus $N = 3$. Let us consider a control polyline given by 5 points (see Figures 7.5 and 7.6). Using Algorithm 2, the preprocessed polyline $\mathbf{g}^{(0)}$ is computed as

$$g_{i,j}^{(0)} = f_i^{(0)} + \alpha_i(\tilde{f}_{i,j}^{(0)} - \mathcal{L}(\tilde{f}_{i,0}^{(0)})), \quad j = 0, 1, 2$$

i.e.

$$\begin{cases} g_{i,0}^{(0)} &= f_i^{(0)} + \alpha_i(\tilde{f}_{i,0}^{(0)} - \mathcal{L}(\tilde{f}_{i,0}^{(0)})), \\ g_{i,1}^{(0)} &= f_i^{(0)} + \alpha_i(\tilde{f}_{i,1}^{(0)} - \mathcal{L}(\tilde{f}_{i,0}^{(0)})), \\ g_{i,2}^{(0)} &= f_i^{(0)} + \alpha_i(\tilde{f}_{i,2}^{(0)} - \mathcal{L}(\tilde{f}_{i,0}^{(0)})). \end{cases}$$

Calling $f_{\ell_1}^{(0)}$ and $f_{\ell_2}^{(0)}$ the two points near $f_i^{(0)}$, we exploiting the subdivision rules in (7.11) obtaining

$$\begin{cases} \tilde{f}_{i,0}^{(0)} &= \dfrac{\beta_k}{8} f_{\ell_1}^{(0)} + \left(1 - \dfrac{\beta_k}{4}\right) f_i^{(0)} + \dfrac{\beta_k}{8} f_{\ell_2}^{(0)}, \\ \tilde{f}_{i,1}^{(0)} &= \dfrac{1}{2} f_{\ell_1}^{(0)} + \dfrac{1}{2} f_i^{(0)}, \\ \tilde{f}_{i,2}^{(0)} &= \dfrac{1}{2} f_i^{(0)} + \dfrac{1}{2} f_{\ell_2}^{(0)}, \end{cases}$$

and the limit stencil in (7.12)

$$\begin{aligned} \mathcal{L}(\tilde{f}_{i,0}^{(0)}) &= \gamma \tilde{f}_{i,0}^{(0)} + \frac{1-\gamma}{2}(\tilde{f}_{i,1}^{(0)} + \tilde{f}_{i,2}^{(0)}) \\ &= \left[\frac{1+\gamma}{2} + \gamma\frac{\beta_0}{4}\right] f_i^{(0)} + \left(\gamma\frac{\beta_0}{8} + \frac{1-\gamma}{4}\right)(f_{\ell_1}^{(0)} + f_{\ell_2}^{(0)}) \end{aligned}.$$

Combining these formulas, we obtain

$$\begin{cases} g_{i,0}^{(0)} &= \left[1 + \alpha_i(1-\gamma)\left(\frac{1}{2} - \frac{\beta_0}{4}\right)\right] f_i^{(0)} + \alpha_i(1-\gamma)\left(\frac{\beta_0}{8} - \frac{1}{4}\right)(f_{\ell_1}^{(0)} + f_{\ell_2}^{(0)}) \\ g_{i,0}^{(0)} &= \left[1 + \alpha_i\frac{\gamma}{2}\left(\frac{\beta_0}{2} - 1\right)\right] f_i^{(0)} + \alpha_i\left(\frac{1+\gamma}{4} - \gamma\frac{\beta_0}{8}\right) f_{\ell_1}^{(0)} - \alpha_i\left(\gamma\frac{\beta_0}{8} + \frac{1-\gamma}{4}\right) f_{\ell_2}^{(0)} \\ g_{i,2}^{(0)} &= \left[1 + \alpha_i\frac{\gamma}{2}\left(\frac{\beta_0}{2} - 1\right)\right] f_i^{(0)} - \alpha_i\left(\gamma\frac{\beta_0}{8} + \frac{1-\gamma}{4}\right) f_{\ell_1}^{(0)} + \alpha_i\left(\frac{1+\gamma}{4} - \gamma\frac{\beta_0}{8}\right) f_{\ell_2}^{(0)}. \end{cases}$$

On the contrary, using Algorithm 3, from [120] we have that the new control polyline $\mathbf{h}^{(0)}$ is computed as

$$h_i^{(0)} = \frac{1}{5}\sum_{j=0}^{4} f_i^{(0)} \sum_{\ell=0}^{4} \frac{\cos(2\pi\ell(j-i)/5)}{(1-\omega_\ell)\gamma + \omega_\ell}, \quad \text{with} \quad \omega_\ell = \frac{1}{2}\left(\cos\left(\frac{2\pi\ell}{5}\right) + \cos\left(\frac{8\pi\ell}{5}\right)\right),$$

and γ as in (7.12). It is clear that the new control polylines $\mathbf{g}^{(0)}$ and $\mathbf{h}^{(0)}$ are different. If Algorithm 3 is more intuitive (it is just the solution of a linear system), Algorithm 2 is more flexible. In fact, the latter allows us to define many different control polylines $\mathbf{g}^{(0)}$ depending on the choice of α_i (see Figure 7.5), while Algorithm 3 defines only one control polyline $\mathbf{h}^{(0)}$ and thus one limit curve as shown in Figure 7.6.

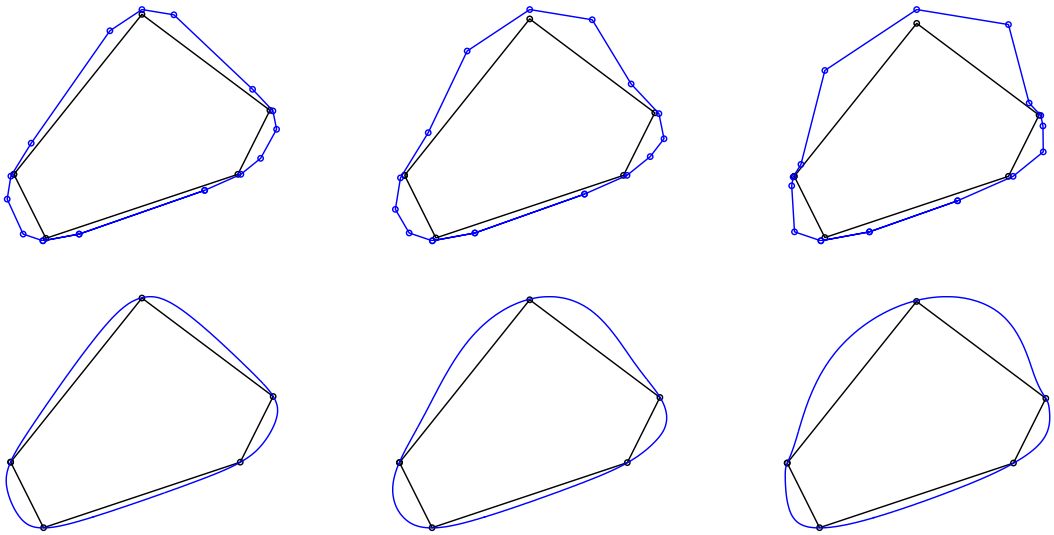

Figure 7.5: Preprocessed polylines and interpolating limit curves obtained via Algorithm 2 using the non-stationary extension of the cubic B-spline scheme with rules in (7.11) where $t = \frac{\pi}{2}$ and $\alpha = [0.5, 0.5, 0.5, 0.5]$ (left), $\alpha = [0.7, 0.6, 1, 0.6, 0.7]$ (center), $\alpha = [0.2, 0.7, 1.5, 0.3, 0.8]$ (right). The points and the parameters α_i are ordered from left to right.

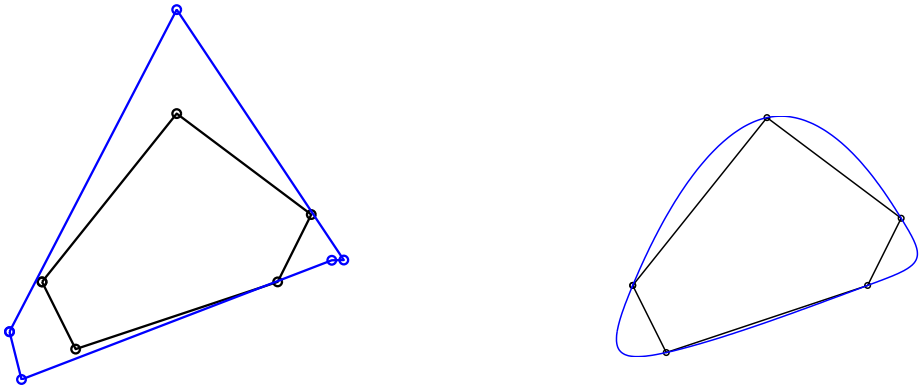

Figure 7.6: Preprocessed polyline and interpolating limit curve obtained via Algorithm 3 using the non-stationary extension of the cubic B-spline scheme with rules in (7.11) where $t = \frac{\pi}{2}$.

7.4 Numerical applications

We conclude the presentation of the new interpolatory algorithm shown in Section 7.2 with some numerical examples. As already pointed out, this algorithm could be applied to stationary and non-stationary subdivision schemes. We start with a stationary example based on Catmull-Clark's subdivision scheme, to show the influence of the local parameter α_i. Then, we propose some examples based on non-stationary subdivision schemes, both for curves and for surfaces.

7.4.1 Stationary Catmull-Clark's subdivision scheme

The refinement rules characterizing stationary Catmull-Clark's scheme are presented in Section 2.4 and the relative stencils are shown in Figure 2.8. The limit position of a vertex point is given by rules [41, 68]

$$V^{(\infty)} = \frac{n^2 V + 4\sum_{j=1}^{n} E_j + \sum_{j=1}^{n} F_j}{n(n+5)},$$

see Figure 7.7. Thus, ordering the points as $[V, E_1, F_1, E_2, F_2, \ldots, E_n, F_n]$ the limit stencil is

$$\mathbf{a}^{(\infty)} = \left[\frac{n}{n+5}, \frac{4}{n(n+5)}, \frac{1}{n(n+5)}, \frac{4}{n(n+5)}, \frac{1}{n(n+5)}, \ldots, \frac{4}{n(n+5)}, \frac{1}{n(n+5)}\right].$$

We apply Algorithm 2 using Catmull-Clark's subdivision scheme. In particular, in Figure 7.8

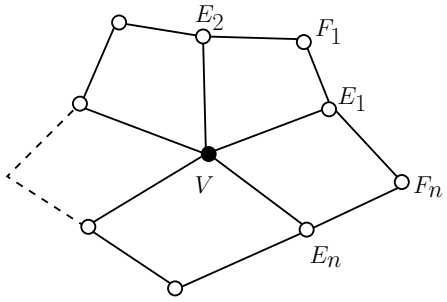

Figure 7.7: Limit stencil of Catmull-Clark's scheme.

we show the limit surface obtained by applying Algorithm 2 with $\alpha_i = 0.7$ for all i, compared with the surface generated with $\alpha_i = 0.7$ for all i except one point with $\alpha_i = 2$. We see that the parameter α_i suggests how much distant we move from the control mesh.

7.4.2 Non-stationary cubic B-spline scheme

In [120], a non-stationary version of the cubic B-spline scheme is proposed with subdivision rules in (7.11), where the correspondent limit stencil in (7.12) is computed using a geometrical approach. In Figure 7.5 we already showed some examples of limit curves obtained using Algorithm 2 with the non-stationary rules of cubic B-spline. We see that the use of local parameters α_i allows us to locally control the limit curve. In particular, the possibility to choose different parameters results to be very useful when the control polyline has short and

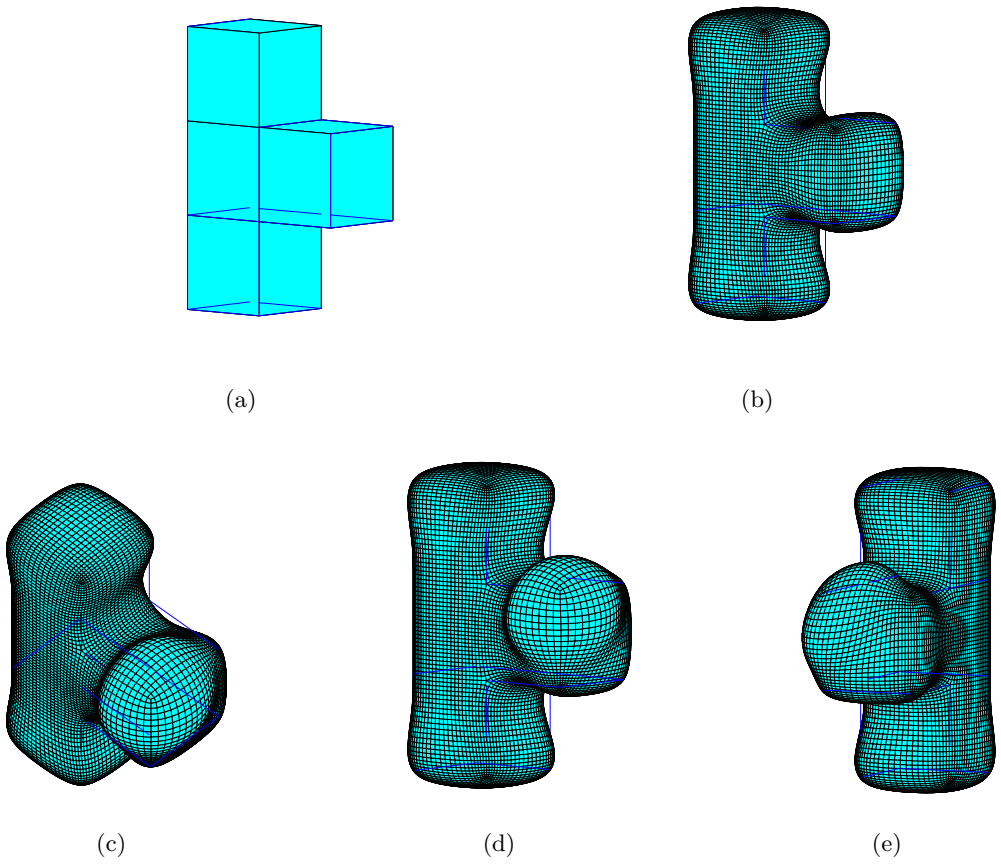

Figure 7.8: (a) Initial control mesh, (b) interpolatory limit surface obtained applying Algorithm 2 with $\alpha_i = 0.7$ for all i via stationary Catmull-Clark's subdivision scheme, (c)-(e) Different views of the interpolatory limit surface obtained applying Algorithm 2 with $\alpha_i = 0.7$ for all i except one point with $\alpha_i = 2$ via stationary Catmull-Clark's subdivision scheme.

long edges. In fact, in this way, since the parameter α_i has to satisfy the constraint in (7.8), we could choose a small α_i if the point $f_i^{(0)}$ is the extreme point of a short edge, conversely we could choose a large α_i if $f_i^{(0)}$ is the extreme point of two long edges. The locality of the parameter let us choose a different α_i for each point of the starting control polyline/mesh $\mathbf{f}^{(0)}$.

7.4.3 Non-stationary Chaikin's subdivision scheme

A non-stationary version of Chaikin's scheme is identified by the refinement rules [61]

$$\begin{cases} f_{2^{k+1}i}^{(k+1)} &= w^{(k)} f_{2^k i-1}^{(k)} + (1-w^{(k)}) f_{2^k i}^{(k)}, \\ f_{2^{k+1}i+1}^{(k+1)} &= (1-w^{(k)}) f_{2^k i}^{(k)} + w^{(k)} f_{2^k i+1}^{(k)}. \end{cases} \tag{7.13}$$

with $w^{(k)} = \frac{1}{2(1+v^{(k)})}$ and $v^{(k)} = \cos\left(\frac{t}{2^{k+1}}\right)$, $t \in [0,\pi) \cup \mathrm{i}\mathbb{R}^+$ as in (3.11).
To design interpolating limit curves using the non-stationary Chaikin's scheme, we first need to find the limit stencil. Here, we show a geometrical approach to solve the problem.

Proposition 7.3 *The limit stencil of the non-stationary extension of Chaikin's scheme with rules on* (7.13) *is* $\mathbf{a}^{(\infty)} = \left[\frac{1}{2}, \frac{1}{2}\right]$.

Proof: We study the evolution of the point $f_i^{(0)}$ and in particular we analyze the behavior of the sequence of points $\{f_{2^{k+1}i}^{(k+1)}\}_{k\in\mathbb{N}_0}$ generated by the rules in (7.13) to find its limit for $k \to +\infty$.
From (7.13) we can rewrite the rule of the new even point $f_{2^{k+1}i}^{(k+1)}$ as

$$f_{2^{k+1}i}^{(k+1)} = w^{(k)} f_{2^k i-1}^{(k)} + (1-w^{(k)}) f_{2^k i}^{(k)} = f_{2^k i}^{(k)} - w^{(k)} D_{2^k i}^{(k)}$$

with $D_{2^k i}^{(k)} = f_{2^k i}^{(k)} - f_{2^k i-1}^{(k)}$. Iterating we thus have

$$f_{2^{k+1}i}^{(k+1)} = f_{2^k i}^{(k)} - w^{(k)} D_{2^k i}^{(k)} = f_{2^{k-1} i}^{(k-1)} - w^{(k-1)} D_{2^{k-1} i}^{(k-1)} - w^{(k)} D_{2^k i}^{(k)} = \ldots = f_i^{(0)} - \sum_{\ell=0}^{k} w^{(\ell)} D_{2^\ell i}^{(\ell)},$$

where

$$\begin{aligned} D_{2^\ell i}^{(\ell)} &= f_{2^\ell i}^{(\ell)} - f_{2^\ell i-1}^{(\ell)} \\ &= w^{(\ell-1)} f_{2^{\ell-1} i-1}^{(\ell-1)} + (1-w^{(\ell-1)}) f_{2^{\ell-1} i}^{(\ell-1)} - (1-w^{(\ell-1)}) f_{2^{\ell-1} i-1}^{(\ell-1)} - w^{(\ell-1)} f_{2^{\ell-1} i}^{(\ell-1)} \\ &= (1-2w^{(\ell-1)}) D_{2^{\ell-1} i}^{(\ell-1)} = \ldots = \left(\prod_{j=0}^{\ell-1} (1-2w^{(j)})\right) D_i^{(0)}. \end{aligned}$$

Thus we find

$$f_{2^{k+1}i}^{(k+1)} = f_i^{(0)} - \gamma^{(k)} D_i^{(0)} \qquad \text{where} \qquad \gamma^{(k)} = \sum_{\ell=0}^{k} w^{(\ell)} \prod_{j=0}^{\ell-1} (1-2w^{(j)}). \tag{7.14}$$

Now, we observe that $1-2w^{(j)} = 1 - \frac{1}{1+v^{(j)}} = \frac{v^{(j)}}{1+v^{(j)}} = \frac{\cos\left(\frac{t}{2^{j+1}}\right)}{1+\cos\left(\frac{t}{2^{j+1}}\right)} = \frac{1}{2}\cos\left(\frac{t}{2^{j+1}}\right) \frac{1}{\cos^2\left(\frac{t}{2^{j+2}}\right)}$, and hence

$$\prod_{j=0}^{\ell-1} (1-2w^{(j)}) = \frac{1}{2^\ell} \prod_{j=0}^{\ell-1} \cos\left(\frac{t}{2^{j+1}}\right) \frac{1}{\left(\prod_{j=0}^{\ell-1} \cos\left(\frac{t}{2^{j+2}}\right)\right)^2} = \frac{1}{2^\ell} \prod_{j=1}^{\ell} \cos\left(\frac{t}{2^j}\right) \frac{\cos^2\left(\frac{t}{2}\right)}{\left(\prod_{j=1}^{\ell+1} \cos\left(\frac{t}{2^j}\right)\right)^2}.$$

Since $\prod_{j=1}^{\ell} \cos\left(\frac{t}{2^j}\right) = \frac{\sin(t)}{2^\ell \sin\left(\frac{t}{2^\ell}\right)}$, it follows that $\prod_{j=0}^{\ell-1} (1-2w^{(j)}) = \cot\left(\frac{t}{2}\right) \tan\left(\frac{t}{2^{\ell+1}}\right)$. The latter implies that

$$\gamma^{(k)} = \sum_{\ell=0}^{k} \frac{1}{2(1+v^{(\ell)})} \cot\left(\frac{t}{2}\right) \tan\left(\frac{t}{2^{\ell+1}}\right) = \cot\left(\frac{t}{2}\right) \sum_{\ell=0}^{k} \frac{\tan\left(\frac{t}{2^{\ell+2}}\right)}{2\cos\left(\frac{t}{2^{\ell+1}}\right)} = \frac{1}{2} - \cot\left(\frac{t}{2}\right) \tan\left(\frac{t}{2^{k+2}}\right).$$

Finally, since $\lim_{k\to\infty}\gamma^{(k)}=\frac{1}{2}$, then from (7.14) we have

$$\lim_{k\to\infty} f_{2^{k+1}i}^{(k+1)} = f_i^{(0)} - \frac{1}{2}D_i^{(0)} = \frac{1}{2}(f_{i-1}^{(0)} + f_i^{(0)}),$$

thus the limit stencil is $\mathbf{a}^{(\infty)} = \left[\frac{1}{2}, \frac{1}{2}\right]$. ■

Applying Algorithm 2 using the non-stationary Chaikin's scheme with rules in (7.13), we are able to design interpolating limit curves with different shapes, thanks to the two free parameters α_i and t (see Figure 7.9). In particular, we choose the same value α_i for all the control points $f_i^{(0)}$ in such a way that condition (7.8) is satisfied for all i. We see that when α_i is small, we have less flexibility for the limit shape in order to obtain the property of interpolation, while if α_i is large the limit curve has more space to modify itself to gain the interpolation property. On the contrary, as we could expect, the parameter t plays as a tension parameter passing from values of t in $[0,\pi)$ to values in $\mathrm{i}\mathbb{R}^+$ we obtain shapes that are closer and closer to the initial control polyline.

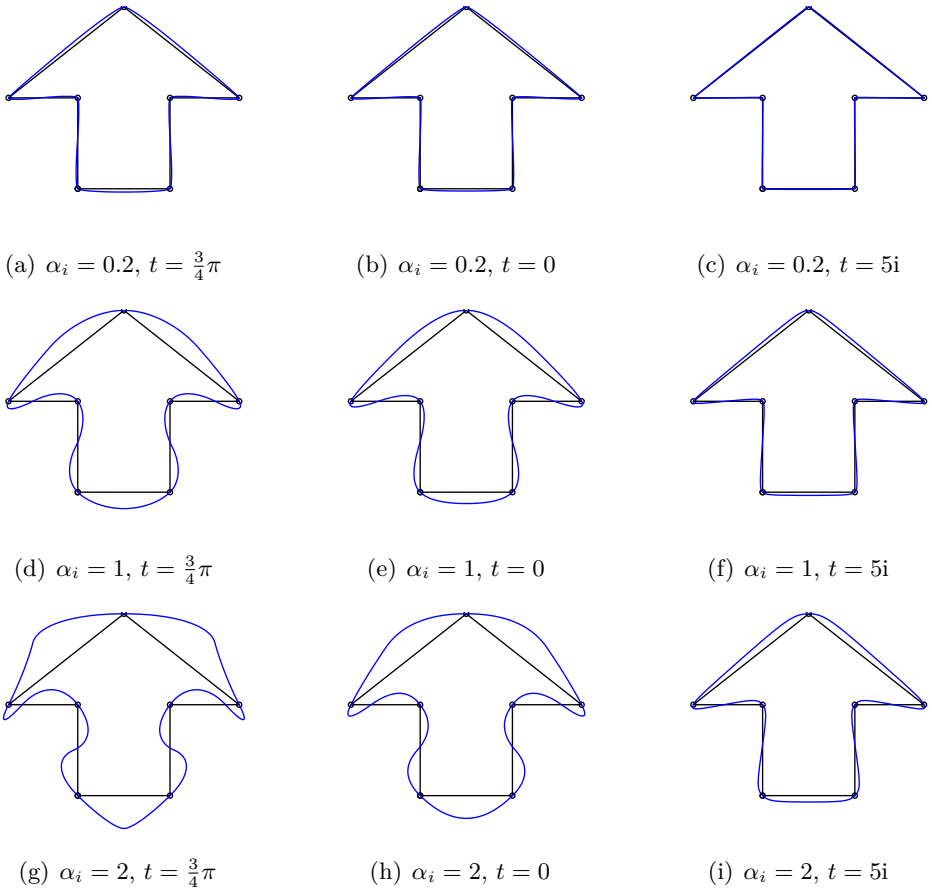

(a) $\alpha_i = 0.2$, $t = \frac{3}{4}\pi$ (b) $\alpha_i = 0.2$, $t = 0$ (c) $\alpha_i = 0.2$, $t = 5\mathrm{i}$

(d) $\alpha_i = 1$, $t = \frac{3}{4}\pi$ (e) $\alpha_i = 1$, $t = 0$ (f) $\alpha_i = 1$, $t = 5\mathrm{i}$

(g) $\alpha_i = 2$, $t = \frac{3}{4}\pi$ (h) $\alpha_i = 2$, $t = 0$ (i) $\alpha_i = 2$, $t = 5\mathrm{i}$

Figure 7.9: Interpolatory limit curves obtained using interpolatory Algorithm 2 with non-stationary Chaikin's scheme. From top to bottom: increasing values of $\alpha_i \in \mathbb{R}^+$ satisfying condition (7.8); from left to right: different values of $t \in [0,\pi) \cup \mathrm{i}\mathbb{R}^+$.

7.4.4 Non-stationary Doo-Sabin's subdivision scheme

In [63], a non stationary version of Doo-Sabin's scheme is proposed, described by the rules

$$f_\ell^{(k+1)} = \alpha_n^{(k)} f_\ell^{(k)} + \beta_n^{(k)}(f_{\ell-1}^{(k)} + f_{\ell+1}^{(k)}) + \gamma_n^{(k)} \sum_{j=1, j\neq\{\ell-1,\ell,\ell+1\}}^{n} f_j^{(k)}, \quad \ell = 1,\dots,n, \tag{7.15}$$

where

$$\alpha_n^{(k)} = \frac{1 + nv_k(1+v_k)}{n(1+v_k)^2}, \quad \beta_n^{(k)} = \frac{nv_k + 2}{2n(1+v_k)^2}, \quad \gamma_n^{(k)} = \frac{1}{n(1+v_k)^2},$$

with $v^{(k)} = \cos\left(\frac{t}{2^{k+1}}\right)$ and $t \in [0,\pi) \cup \mathrm{i}\mathbb{R}^+$ as in (3.11). To apply the interpolation method, we need to compute the limit stencil related to this scheme. In the following, we show two different methods to compute the limit stencil.

Proposition 7.4 *The limit stencil of the non-stationary version of Doo-Sabin's scheme with rules in* (7.15) *is* $\mathbf{a}^{(\infty)} = \left[\frac{1}{n}, \frac{1}{n}, \dots, \frac{1}{n}\right]$*, where* n *is the face valence.*

Proof via a linear algebra approach. We consider the k-level subdivision matrix S_k defined as

$$S_k = circ(\alpha_n^{(k)}, \beta_n^{(k)}, \underbrace{\gamma_n^{(k)}, \dots, \gamma_n^{(k)}}_{n-3 \text{ times}}, \beta_n^{(k)}).$$

We compute the Jordan decomposition of $S_k = X_k J_k X_k^{-1}$, finding that X_k and X_k^{-1} are independent on the level k, thus $S_k = X J_k X^{-1}$. In particular the first column of X is the vector of ones, i.e. $\boldsymbol{x}_0 = [1,\dots,1]^T$, while the first line of X^{-1} is given by $\tilde{\boldsymbol{x}}_0^T = \frac{1}{n}[1,\dots,1]$. Thus, we have

$$S^\infty = X \left(\lim_{k\to+\infty} \prod_{j=0}^{k} J_j \right) X^{-1}, \qquad \text{with} \quad \lim_{k\to+\infty} \prod_{j=0}^{k} J_j = \begin{pmatrix} 1 & 0 & \cdots & 0 \\ 0 & 0 & \cdots & 0 \\ \vdots & \ddots & \ddots & \vdots \\ 0 & \cdots & \cdots & 0 \end{pmatrix}.$$

Finally the limit stencil is

$$\mathbf{a}^{(\infty)} = \big[\underbrace{\frac{1}{n}, \frac{1}{n}, \dots, \frac{1}{n}}_{n \text{ times}}\big].$$

Proof via a geometrical approach. Introducing the auxiliary notation

$$\tilde{\alpha}_n^{(k)} := \frac{(v^{(k)})^2}{(1+v^{(k)})^2}, \qquad \tilde{\beta}_n^{(k)} := \frac{v^{(k)}}{(1+v^{(k)})^2}, \qquad \tilde{\gamma}_n^{(k)} := \frac{1}{(1+v^{(k)})^2},$$

we can equivalently rewrite (7.15) as

$$f_\ell^{(k+1)} = \tilde{\alpha}_n^{(k)} f_\ell^{(k)} + \tilde{\beta}_n^{(k)} \left(M_\ell^{(k)} + M_{\ell+1}^{(k)} \right) + \tilde{\gamma}_n^{(k)} A^{(k)}, \tag{7.16}$$

with $M_\ell^{(k)} := \frac{f_{\ell-1}^{(k)} + f_\ell^{(k)}}{2}$ and

$$A^{(k)} := \frac{1}{n} \sum_{j=1}^{n} f_j^{(k)} = \frac{1}{n} \sum_{j=1}^{n} M_j^{(k)}. \tag{7.17}$$

Then, combining (7.16) with (7.17) we obtain

$$\begin{aligned} A^{(k+1)} &= \frac{1}{n}\sum_{\ell=1}^{n} f_\ell^{(k+1)} = \frac{1}{n}\sum_{\ell=1}^{n}\left(\tilde{\alpha}_n^{(k)} f_\ell^{(k)} + \tilde{\beta}_n^{(k)}\left(M_\ell^{(k)} + M_{\ell+1}^{(k)}\right) + \tilde{\gamma}_n^{(k)} A^{(k)}\right) \\ &= (\tilde{\alpha}_n^{(k)} + 2\tilde{\beta}_n^{(k)} + \tilde{\gamma}_n^{(k)})A^{(k)}, \end{aligned} \tag{7.18}$$

and, in light of the fact that $\tilde{\alpha}_n^{(k)} + 2\tilde{\beta}_n^{(k)} + \tilde{\gamma}_n^{(k)} = 1$, we arrive at showing that

$$A^{(k+1)} = A^{(0)}, \qquad \forall k \in \mathbb{N}_0. \tag{7.19}$$

Exploiting (7.19), (7.16) and (7.18) we start writing

$$\begin{aligned} R_\ell^{(k+1)} &= f_\ell^{(k+1)} - A^{(0)} = f_\ell^{(k+1)} - A^{(k+1)} \\ &= \tilde{\alpha}_n^{(k)} f_\ell^{(k)} + \tilde{\beta}_n^{(k)}\left(M_\ell^{(k)} + M_{\ell+1}^{(k)}\right) + \tilde{\gamma}_n^{(k)} A^{(k)} - (\tilde{\alpha}_n^{(k)} + 2\tilde{\beta}_n^{(k)} + \tilde{\gamma}_n^{(k)})A^{(k)} \\ &= \tilde{\alpha}_n^{(k)} R_\ell^{(k)} + 2\tilde{\beta}_n^{(k)} Q_\ell^{(k)}, \end{aligned} \tag{7.20}$$

with $Q_\ell^{(k)} = \frac{M_\ell^{(k)} + M_{\ell+1}^{(k)}}{2} - A^{(k)}$ and observe that, by definition (see also Figure 7.10), $||Q_\ell^{(k)}||_2 \leq ||R_\ell^{(k)}||_2$, $\forall k \in \mathbb{N}_0$. As a consequence, since $\tilde{\alpha}_n^{(k)} \geq 0$ and $\tilde{\beta}_n^{(k)} \geq 0$ for all $k \in \mathbb{N}_0$, then

$$||R_\ell^{(k+1)}||_2 \leq \tilde{\alpha}_n^{(k)}||R_\ell^{(k)}||_2 + 2\tilde{\beta}_n^{(k)}||Q_\ell^{(k)}||_2 \leq (\tilde{\alpha}_n^{(k)} + 2\tilde{\beta}_n^{(k)})||R_\ell^{(k)}||_2,$$

and, iterating, $||R_\ell^{(k+1)}||_2 \leq \prod_{j=0}^{k}(\tilde{\alpha}_n^{(j)} + 2\tilde{\beta}_n^{(j)})\ ||R_\ell^{(0)}||_2$. Now, since $\tilde{\alpha}_n^{(j)} + 2\tilde{\beta}_n^{(j)} < 1$ for all $j \in \mathbb{N}_0$ $\prod_{j=0}^{\infty}(\tilde{\alpha}_n^{(j)} + 2\tilde{\beta}_n^{(j)}) = 0$ and thus $\lim_{k\to\infty} ||R_\ell^{(k+1)}||_2 = 0$. By definition of $R_\ell^{(k+1)}$, it easily follows that

$$\lim_{k\to\infty} ||f_\ell^{(k+1)} - A^{(0)}||_2 = 0,$$

thus $\mathbf{f}^{(\infty)} = \frac{1}{n}\sum_{j=1}^{n} f_j^{(0)}$ and the limit stencil is $\mathbf{a}^{(\infty)} = \left[\frac{1}{n}, \ldots, \frac{1}{n}\right]$. ■

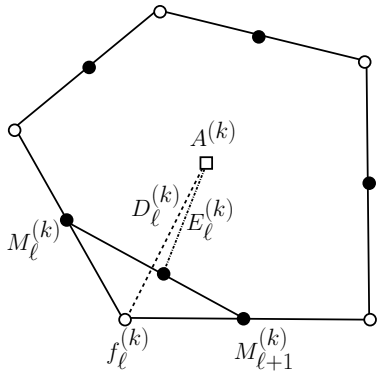

Figure 7.10: Distance between a vertex $f_\ell^{(k)}$ and its centroid $A^{(k)}$ compared with the distance between the midpoint of the segment $M_\ell^{(k)}, M_{\ell+1}^{(k)}$ and the same centroid $A^{(k)}$.

Once the limit stencil is computed, we are able to apply the interpolation Algorithm 2. Since the approximating subdivision used is non-stationary, we have two free parameters, α_i and

t, that allow the user to adjust the shape of the limit surfaces. In Figure 7.11, we show the interpolating limit surfaces obtained starting from a cube and choosing different values of the free parameters α_i and t. Since all the edges of the cube are all equal, we fix the same value α_i for all the points $f_i^{(0)}$, satisfying condition (7.9). As in the Chaikin's example, we

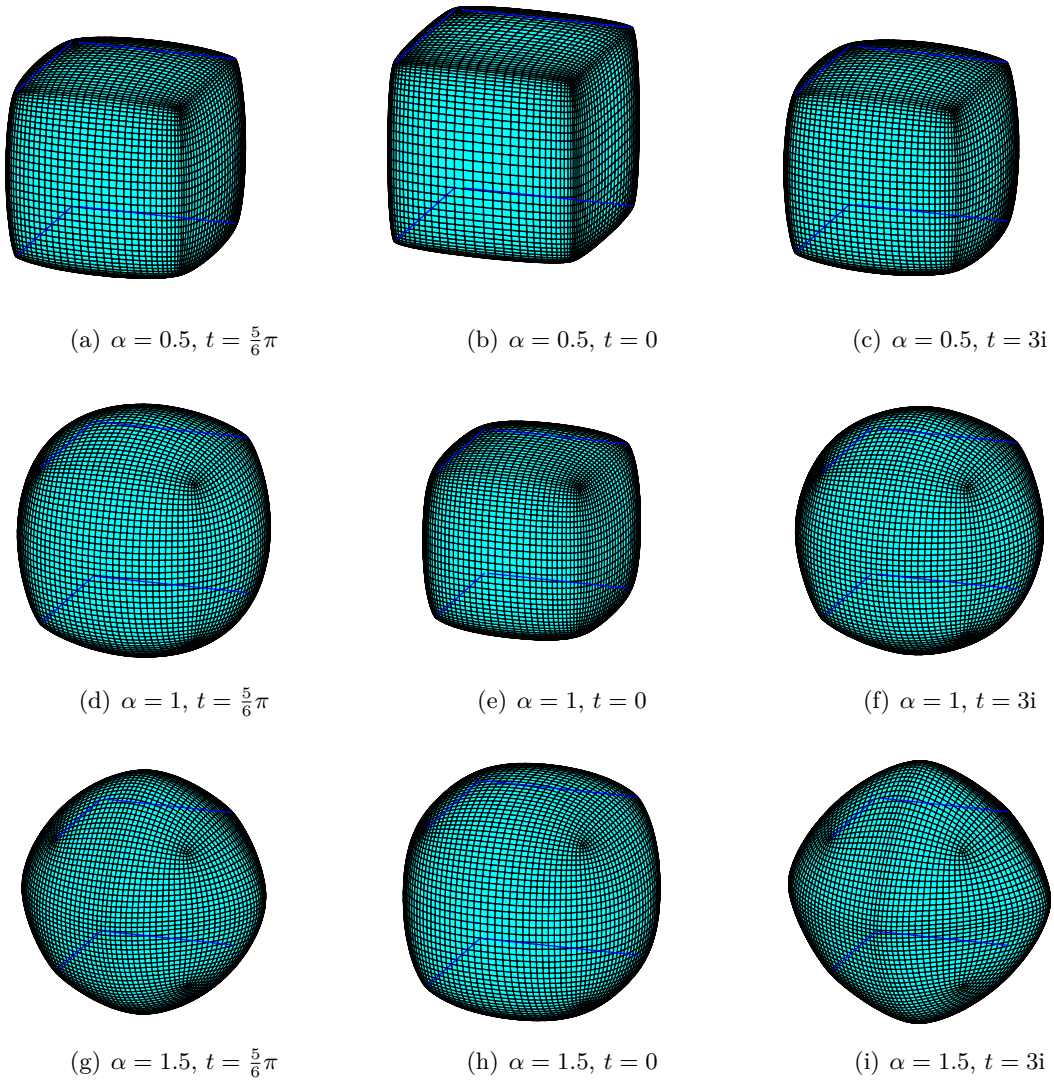

(a) $\alpha = 0.5$, $t = \frac{5}{6}\pi$ (b) $\alpha = 0.5$, $t = 0$ (c) $\alpha = 0.5$, $t = 3\mathrm{i}$

(d) $\alpha = 1$, $t = \frac{5}{6}\pi$ (e) $\alpha = 1$, $t = 0$ (f) $\alpha = 1$, $t = 3\mathrm{i}$

(g) $\alpha = 1.5$, $t = \frac{5}{6}\pi$ (h) $\alpha = 1.5$, $t = 0$ (i) $\alpha = 1.5$, $t = 3\mathrm{i}$

Figure 7.11: Interpolatory limit surfaces obtained via Algorithm 2 and using a non-stationary version of Doo-Sabin's scheme with rules in (7.15). From top to bottom: increasing values of $\alpha \in \mathbb{R}^+$ satisfying condition (7.9); from left to right: different values of $t \in [0, \pi) \cup \mathrm{i}\mathbb{R}^+$.

notice that t plays as a tension parameter, in fact passing from values of t in $[0, \pi)$ to values in $\mathrm{i}\mathbb{R}^+$ we obtain shapes that are closer and closer to the initial control mesh. Regarding the parameter α_i, we see that when α_i is small, we have less flexibility for the limit shape in order to obtain the property of interpolation, while if α_i is large the limit surface has more space to modify itself to gain the interpolation property. In fact, from (7.3), it is clear that the parameter α_i suggests how much distant we are from the control mesh $\mathbf{f}^{(0)}$ that we want

to interpolate.

Remark 7.5 *We underline that, the use of non-stationary subdivision rules allow us to gain the free parameter t that does not appear in the stationary case, and thus we can obtain many different kind of shapes. In fact, with stationary Chaikin's scheme [16] and stationary Doo-Sabin's scheme (see Section 2.4) we could design only the curve and surfaces in the central column of Figures 7.9 and 7.11, i.e. the ones related to* $t = 0$*, where only* α_i *can be used to model the limit shapes. With the non-stationary rules we gain an extra parameter an thus more flexibility in the limit surfaces.*

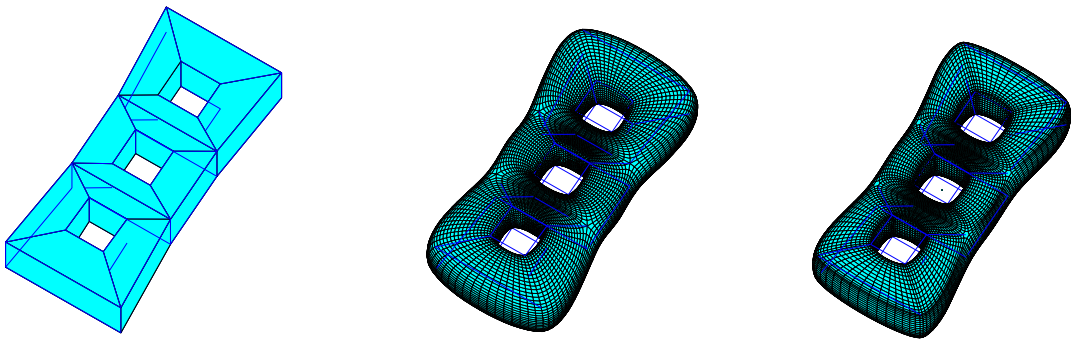

(a) Initial mesh

(b) Kobbelt's scheme

(c) Doo-Sabin's scheme with $t = \frac{5}{6}\pi$ and $\alpha_i = 0.5$

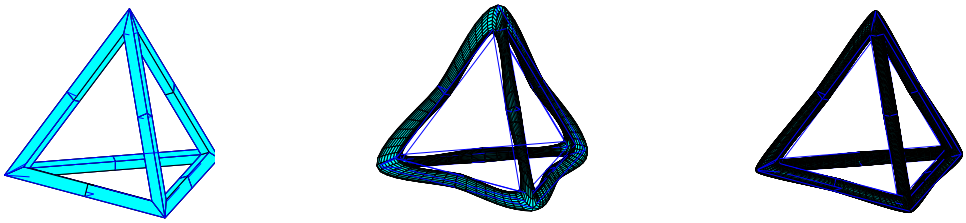

(d) Initial mesh

(e) Kobbelt's scheme

(f) Doo-Sabin's scheme with $t =$ i and $\alpha_i = 0.3$

Figure 7.12: Comparison between interpolatory limit surfaces. From left to right: initial control mesh, Kobbelt's scheme results, non-stationary Doo-Sabin's scheme results with our interpolating algorithm.

The possibility of modeling the limit shape using the two free parameters results in an improvement in the quality of the interpolating limit surfaces produces by non-stationary approximating subdivision schemes via Algorithm 2 in comparison with the surfaces produces by interpolatory subdivision schemes. In Figure 7.12 we show comparisons between the limit surfaces obtained using the interpolatory subdivision scheme proposed by Kobbelt (see Section 2.4.5) and the surface obtained using Algorithm 2 with non-stationary Doo-Sabin's scheme. We notice that with a suitable choice of the free parameters, the surfaces obtained via Doo-Sabin's scheme have less undulations and imperfections than the limit surfaces obtain

with Kobbelt's scheme and the first ones are closer and more faithful to the initial control meshes.

Conclusion

In the first part of this thesis (Chapters 1-3), we recalled the principal notions regarding univariate and bivariate, stationary and non-stationary subdivision schemes, together with the methods to analyze their main properties. These methods have been exploited in the following chapters to construct and analyze new subdivision schemes or generalizations of existent subdivision schemes. In particular, Chapter 4 concerned with univariate subdivision schemes, while Chapters 5 and 6 studied bivariate subdivision schemes in the stationary and non-stationary setting, respectively. Finally, the property of interpolation of curves and surfaces has been analyzed in Chapter 7.
The first goal of this thesis is to provide a complete review of all the techniques appeared in literature in the last years to analyze convergence, generation and reproduction capabilities, approximation order and smoothness properties of a stationary or non-stationary subdivision scheme. Particular attention was given to the linear algebra tools useful for the smoothness analysis of a subdivision surface described on arbitrary manifold topology meshes. In details, in Section 2.3, we recalled all the necessary conditions proposed in literature which are required on the eigenvalues of a stationary subdivision matrix in order to obtain limit surfaces that are C^1 continuous with bounded curvature and optimal shrinkage (see Table 2.1). Regarding the non-stationary setting, we showed the first proposal of sufficient conditions to check the convergence of non-stationary subdivision schemes near an extraordinary vertex or face (see Theorem 3.25).
After the review of all the techniques useful for the analysis of subdivision schemes, the second goal of this thesis is to exploit them for the construction of new subdivision schemes or generalizations of existent subdivision schemes, in order to iprove further properties of known schemes in literature. In particular, in the univariate case, the combined 4-point scheme resulted to be a generalization of many independent schemes proposed in literature; the stationary 5-point scheme and its non-stationary extension provided a C^2 piecewise uniform subdivision scheme; the non-stationary version of (i) Lane-Riesenfeld algorithm, (ii) Hormann-Sabin's scheme and (iii) Dubuc-Deslauriers $2n$-point scheme allowed a more extensive use of these three fundamental families of stationary subdivision schemes, thanks to the additional capability of generating and reproducing conic sections.
In the bivariate setting, the necessary conditions required on the eigenvalues of a stationary subdivision matrix have been used to study a strategy to define the free weights of an extraordinary stencil. In particular, a complete analysis of interpolatory schemes generalizing the tensor-product version of the Dubuc-Deslauriers 4-point scheme to quadrilateral meshes of arbitrary manifold topology has been developed and it has led to a particular choice for the stencil weights that improved previous results presented in literature. Moreover, we also proposed a general computational strategy, applicable to all stationary subdivision schemes

defined on arbitrary manifold topology meshes, in order to determine the range of variability of the extraordinary stencil weights which has been tested on variants of Loop's scheme. In addition, we showed that the use of non-stationary rules allows us to produce limit surfaces with particular shapes, such as approximating or exact ellipsoids, that could be used for the segmentation of biomedical images. Finally, a new general interpolatory algorithm has been proposed to construct interpolating limit curves and surfaces using stationary or non-stationary approximating subdivision schemes. This method signed a great improvement in the design of interpolatory curves and surfaces since it avoids not desired ripples and distortions and thus it produces limit shapes with a higher quality than the ones obtained with interpolatory subdivision schemes.

From this discussion, it is clear that many open problems remain. First of all, we need to complete the analysis of non-stationary subdivision scheme defined on arbitrary manifold topology meshes. In fact, Theorem 3.25 concerns only convergence near an extraordinary element. This result could be extended, finding sufficient conditions for tangent plane continuity and boundedness of curvature of a non-stationary subdivision scheme at the limit point of an extraordinary vertex or face. A second step could be an extension of the notions of generation and reproduction of spaces of (exponential) polynomials to the case of extraordinary elements. As a consequence, exploiting these two missing results, it could be possible to define a new subdivision scheme able to produce in the limit exact ellipsoids starting from meshes with arbitrary manifold topology. This scheme would be used for biomedical imaging segmentation and would improve both the non-stationary BLISS scheme and the non-stationary BLOB scheme proposed in Chapter 6.

Bibliography

[1] N. Aghdaii, H. Younesy, H. Zhang, 5-6-7 Meshes: remeshing and analysis, Computers & Graphics 36 (2012) 1072-1083.

[2] G. Albrecht, L. Romani, Convexity preserving interpolatory subdivision with conic precision, Applied Mathematics and Computation 219 (2012) 4049-4066.

[3] S. Amat, K. Dadourian, R. Donat, J. Liandrat, J.C. Trillo, Error bounds for a convexity-preserving interpolation and its limit function, Journal of Computational and Applied Mathematics 211 (2008) 36-44.

[4] S. Amat, R. Donat, J.C. Trillo, Proving convexity preserving properties of interpolatory subdivision schemes through reconstruction operators, Applied Mathematics and Computation 219 (2013) 7413-7421.

[5] L-E. Andersson , N.F. Stewart, Introduction to the mathematics of subdivision surfaces, SIAM 2010.

[6] A. Badoual, P. Novara, L. Romani, D. Schmitter, M. Unser, Subdivision-based 3D deformable models for the segmentation of volumetric biomedical images, in preparation.

[7] A.A. Ball, D.J.T. Storry, A matrix approach to the analysis of recursively generated B-spline surfaces, Computer Aided Design 18 (1986) 437-442.

[8] C. Beccari, G. Casciola, L. Romani, A non-stationary uniform tension paramater controlled interpolating 4-point scheme reproducing conics, Computer Aided Geometric Design 24 (2007) 1-9.

[9] C. Beccari, G. Casciola, L. Romani, Shape controlled interpolatory ternary subdivision, Applied Mathematics and Computation 215 (2009) 916-927.

[10] D.A. Bini, G. Latouche, B. Meini, Numerical methods for structured Markov chains, Numerical Mathematics and Scientific Computation, Oxford Science Publication Oxford University Press, New York (2005).

[11] Z. Cai, Convexity preservation of the interpolating four-point C^2 ternary stationary subdivision scheme, Computer Aided Geometric Design 26 (2009) 560-565.

[12] V. Caselles, R. Kimmel, G. Sapiro, Geodesic active contours, International Journal of Computer Vision 22 (1997) 61-79.

[13] T.J. Cashman, K. Hormann, U. Reif, Generalized Lane-Riesenfeld algorithms, Computer Aided Geometric Design 30 (2013) 398-409.

[14] E. Catmull, J. Clark, Recursively generated B-spline surfaces on arbitrary topological meshes, Computer Aided Design 10 (1978) 350-355.

[15] A.S. Cavaretta, W. Dahmen, C.A. Micchelli, Stationary subdivision, Memories of the American Mathematical Society 453 (1991) 1-185.

[16] G.M. Chaikin, An algorithm for high-speed curve generation, Computer Graphics and Image Processing 3 (1974) 346-349.

[17] P. Chalmoviansky, B. Jüttler, A non-linear circle-preserving subdivision scheme, Advances in Computational Mathematics 27 (2007) 375-400.

[18] M. Charina, Finiteness conjecture and subdivision, Applied and Computational Harmonic Analysis 36 (2014) 522-526.

[19] M. Charina, C. Conti, Polynomial reproduction of multivariate scalar subdivision schemes, Journal of Computational and Applied Mathematics, 240 (2013) 51-61.

[20] M. Charina, C. Conti, N. Guglielmi, V. Protasov, Regularity of non-stationary subdivision: a matrix approach, Numerische Mathematik (2016).

[21] M. Charina, C. Conti, L. Romani, Reproduction of exponential polynomials by multivariate non-stationary subdivision schemes with a general dilation matrix, Numerische Mathematik 127 (2014) 223-254.

[22] D.R. Chen, R.Q. Jia, S.D. Riemenschneider, Convergence of vector subdivision schemes in Sobolev spaces, Applied and Computational Harmonic Analysis 12 (2002) 128-149.

[23] B. Clark, N. Ray, X. Jiao, Surface mesh optimization, adaption and untangling with high-order accuracy, Proceedings of the 2st international meshing round table (2013) 385-402.

[24] C. Conti, N. Dyn, C. Manni, M. L. Mazure, Convergence of univariate non-stationary subdivision schemes via asymptotical similarity, Computer Aided Geometric Design 37 (2015) 1-8.

[25] C. Conti, K. Hormann, Polynomial reproduction for univariate subdivision scheme of any arity, Journal of Approximation Theory 163 (2011) 413-437.

[26] C. Conti, J-L. Merrien, L. Romani, Dual Hermite subdivision schemes of de Rham-type, BIT 54 (2014) 955-977.

[27] C. Conti, L. Romani, Affine combination of B-spline subdivision masks and its non-stationary counterparts, BIT 50 (2010) 269-299.

[28] C. Conti, L. Romani, Algebraic conditions on non-stationary subdivision symbols for exponential polynomial reproduction, Journal of Computational and Applied Mathematics 236 (2011) 543-556.

[29] C. Conti, L. Romani, M. Unser, Ellipse-preserving Hermite interpolation and subdivision, Journal of Mathematical Analysis and Applications 426 (2015) 211-227.

[30] C. Conti, L. Romani, J. Yoon, Approximation order and approximate sum rules in subdivision, Journal of Approximation Theory 207 (2016) 380-401.

[31] S. da Silveira, B. Schneider, C. Cifuentes-Diaz, D. Sage, T. Abbas-Terki, T. Iwatsubo, M. Unser, P. Aebischer, Phosphorylation does not prompt, nor prevent, the formation of α-synuclein toxic species in a rat model of Parkinson's disease, Human Molecular Genetics 18 (2009) 872-887.

[32] I. Daubechies, J.C. Lagarias, Sets of matrices all infinite products of which converge, Linear Algebra and Its Applications 161 (1992) 227-263.

[33] P. Davis, Circulant Matrices, J. Wiley and Sons, New York (1979).

[34] B. De Leener, S. Kadoury, J. Cohen-Adad, Robust, accurate and fast automatic segmentation of the spinal cord, NeuroImage 98 (2014) 528–536.

[35] G. de Rham, Sur une courbe plane, Journal de Mathématiques Pures et Appliqués 35 (1956) 25-42.

[36] V. Del Prete, F. Di Benedetto, M. Donatelli, S. Serra-Capizzano, Symbol approach in a signal-restoration problem involving block Toeplitz matrices, Journal of Computational and Applied Mathematics 272 (2014) 399-416.

[37] R. Delgado-Gonzalo, P. Thévenaz, C.S. Seelamantula, M. Unser, Snakes with an ellipse-reproducing property, IEEE Transaction in Image Processing, 21 (2012) 1258-1271.

[38] R. Delgado-Gonzalo, N. Chenouard, M. Unser, Spline-based deforming ellipsoids for interactive 3D bioimage segmentation, IEEE Transaction in Image Processing 22 (2013) 3926-3940.

[39] C. Deng, W. Ma, A unified interpolatory subdivision scheme for quadrilateral meshes, ACM Transactions on Graphics 32 (2013) 1-11.

[40] C. Deng, X. Yang, Interpolation over arbitrary topology meshes using Doo-Sabin surfaces, Shape Modeling International (2009) 52-57.

[41] C. Deng, X. Yang, A simple method for interpolating meshes of arbitrary topology by Catmull-Clark surfaces, The Visual Computer 26 (2010) 137-146.

[42] G. Deslauriers, S. Dubuc, Symmetric iterative interpolation processes, Constructive Approximation 5 (1989) 49-68.

[43] N.A. Dodgson, M.A. Sabin, A circle-preserving variant of the fourpoint subdivision scheme, in: M. Daehlen, K. Morken, L.L. Schumaker (Eds.), Mathematical Methods for Curves and Surfaces (2005) 275–286.

[44] N. A. Dodgson, I. P. Ivrissimtzis, M. A. Sabin,On the support of recursive subdivision, ACM Transactions on Graphics 23(4) (2004) 1043-1060.

[45] M. Donatelli, P. Novara, L. Romani, Tangent plane continuity of non-stationary subdivision schemes at the limit point of extraordinary vertices and faces, in progress.

[46] M. Donatelli, P. Novara, L. Romani, S. Serra-Capizzano, D. Sesana, Surface subdivision algorithms and structured linear algebra: a computational approach to determine bounds of extraordinary rule weights, in progress.

[47] A. Dorostkar, M. Neytcheva, S. Serra-Capizzano, Spectral analysis of coupled PDEs and of their Schur complements via the notion of Generalized Locally Toeplitz sequences, in revision for Computer Methods in Applied Mechanics and Engineering (2015).

[48] D. Doo, M.A. Sabin, Behaviour of recursive subdivision surfaces near extraordinary points, Computer-Aided Design 10 189-194 (1978).

[49] S. Dubuc, Interpolation through an iterative scheme Journal of Mathematical Analysis and Applications 114 (1986) 185-204.

[50] S. Dubuc, J-L. Merrien, Convergent vector and Hermite subdivision schemes, Constructive Approximation 23 (2005) 1-22.

[51] A. Dufour, R. Thibeaux, E. Labruyere, N. Guillen, J.-C. Olivo-Marin, 3-D Active meshes: Fast discrete deformable models for cell tracking in 3-D time-lapse microscopy, IEEE Transactions on Image Processing 20 (2011) 1925-1937.

[52] N. Dyn, Subdivision schemes in Computer-Aided-Geometric Design, Advances in Numerical Analysis, Vol. II, Wavelets, Subdivision Algorithms and Radial Basis Functions, W. Light (ed.), Clarendon Press, Oxford (1992) 36-104.

[53] N. Dyn, Analysis of convergence and smoothness by the formalism of Laurent polynomials, in Tutorials on Multiresolution in Geometric Modelling, A. Iske, E. Quak, and M. Floater eds., Springer (2002) 51-68.

[54] N. Dyn, J.A. Gregory, D. Levin, A butterfly subdivision scheme for surface interpolation with tension control, ACM Transaction on Graphics 9(2) (1990) 160-169.

[55] N. Dyn, F. Kuijt, D. Levin, R. van Damme, Convexity preservation of the four-point interpolatory subdivision scheme, Computer Aided Geometric Design 16 (1999) 789-792.

[56] N. Dyn, D. Levin, Analysis of asymptotically equivalent binary subdivision schemes, Journal of Mathematical Analysis and Applications 193 (1995) 594-621.

[57] N. Dyn, D. Levin, Subdivision schemes in geometric modelling, Acta Numerica 11 (2002) 73-144.

[58] N. Dyn, D. Levin, J.A. Gregory, A 4-point interpolatory subdivision scheme for curve design, Computer Aided Geometric Design 4 (1987) 257-268.

[59] N. Dyn, D. Levin, A. Luzzatto, Exponentials reproducing subdivision schemes, Foundations of Computational Mathematics 3 (2003) 187-206.

[60] N. Dyn, D. Levin, M. Marinov, Geometrically controlled 4-point interpolatory schemes, Advances in Multiresolution for Geometric Modelling (2005) 302-315.

[61] M. Fang, W. Ma, G. Wang, A generalized curve subdivision scheme of arbitrary order with a tension parameter, Computer Aided Geometric Design 27 (2010) 720-733.

[62] M. Floater, G. Muntingh, Exact regularity of pseudo-splines, arXiv:1209.2692v2 (2012).

[63] M. Fang, W. Ma, G. Wang, A generalized surface subdivision scheme of arbitrary order with a tension parameter, Computer Aided Geometric Design 49 (2014) 8-17.

[64] C. Garoni, S. Serra-Capizzano, D. Sesana, Spectral analysis and spectral symbol of d-variate $\mathbf{Q}_p$ Lagrangian FEM stiffness matrices, SIAM Journal on Matrix Analysis and Applications 36 1100-1128 (2015).

[65] I. Ginkel, G. Umlauf, Loop subdivision with curvature control, Eurographics Symposium on Geometry Processing (2006).

[66] L. Gori, F. Pitolli, E. Santi, Refinable ripplets with dilation $M = 3$, Jaen Journal on Approximation 3 (2011) 173–191.

[67] L. Gori, F. Pitolli, E. Santi, On a class of shape-preserving refinable functions with dilation 3, Journal of Computational and Applied Mathematics 245 (2013) 62-74.

[68] M. Halstead, M. Kass, T. DeRose, Efficient, fair interpolation using Catmull-Clark surfaces, Proceedings of ACM Siggraph (1993) 35-33.

[69] Y. Hao, R. Wang, C. Li, Analysis of a 6-point binary subdivision scheme, Applied Mathematics and Computation 218 (2011) 3209-3216.

[70] B. Han, Classification and construction of bivariate subdivision schemes, Proceedings on Curves and Surfaces Fitting: Saint-Malo 2002 (A. Cohen, J.-L. Merrien, and L. L. Schumaker eds.) (2003) 187-197.

[71] M.F. Hassan, N.A. Dodgson, Ternary and three-point univariate subdivision schemes, Curve and Surface Fitting: Saint-Malo 2002 (A. Cohen, J.-L. Merrien, and L. L. Schumaker, eds.) (2003) 199-208.

[72] M. F. Hassan, I. P. Ivrissimitzis, N. A. Dodgson, M. A. Sabin, An interpolating 4-point C^2 ternary stationary subdivision scheme, Computer Aided Geometric Design 19 (2002) 1-18.

[73] S. Hed, Analysis of subdivision schemes for surface generation, Tel Aviv University (1992) M.Sc. thesis.

[74] K. Hormann, M.A. Sabin, A family of subdivision schemes with cubic precision, Computer Aided Geometric Design 25 (2008) 41-52.

[75] M. Jacob, T. Blu, M. Unser, Efficient energies and algorithms for parametric snakes, IEEE Transactions on Image Processing 13 (2004) 1231-1244.

[76] B. Jeong, H. Kim, Y. Lee, J. Yoon, Exponential polynomial reproducing property of non-stationary symmetric subdivision schemes and normalized exponential B-splines, Advances in Computational Mathematics 38 (2013) 647-666.

[77] B. Jeong, Y.J. Lee, J. Yoon, A family of non-stationary subdivision schemes reproducing exponential polynomials, Journal of Mathematical Analysis and Applications 402 (2013) 207-219.

[78] R. Q. Jia, Q. Jiang, Spectral analysis of the transition operators and its applications to smoothness analysis of wavelets, SIAM Journal on Matrix Analysis and Applications 24 (2003) 1071-1109.

[79] R. Q. Jia, D. Riemenschneider, D-X. Zhou, Vector subdivision schemes and multiple wavelets, Mathematics of Computation 67 (1998) 1533-1563.

[80] X.Q. Jin, Developments and applications of block Toeplitz iterative solvers, Combinatorics and Computer Science, 2. Kluwer Academy Publication Group, Dordrecht, Science Press Beijing, Beijing, 2002.

[81] K. Karciauskas. J. Peters, Bicubic polar subdivision, ACM Transactions on Graphics 26(4) (2007).

[82] M. Kass, A. Witkin, D. Terzopoulos, Snakes: Active contour models, International Journal of Computer Vision 1 (1987) 321-331.

[83] M. Kaus, V. Pekar, C. Lorenz, R. Truyen, S. Lobregt, J. Weese, Automated 3D PDM construction from segmented images using deformable models, IEEE Transactions on Medical Imaging 22 (2003) 1005-1013.

[84] L. Kobbelt, Interpolatory subdivision on open quadrilateral nets with arbitrary topology, Proceedings of Eurographics, Computer Graphic Forum 15 (1996) 409-420.

[85] L. Kobbelt, $\sqrt{3}$-subdivision, Proceedings of the 27th annual conference on Computer graphics and interactive techniques SIGGRAPH '00 (2000) 103-112.

[86] F. Kuijt, Convexity preserving interpolation - Stationary nonlinear subdivision and splines, Ph.D. Thesis University of Twente (1998).

[87] F. Kuijt, R. van Damme, Convexity preserving interpolatory subdivision schemes, Constructive Approximation 14 (1998) 609-630.

[88] F. Kuijt, R. van Damme, Shape preserving interpolatory subdivision schemes for nonuniform data, Journal of Approximation Theory 114 (2002) 1-32.

[89] J.C. Lagarias, Y. Wang, The finiteness conjecture for the generalized spectral radius of a set of matrices, Linear Algebra and Its Application 214(1) (1995) 17-42.

[90] J.M. Lane, R.F. Riesenfeld, A theoretical development for the computer generation and display of piecewise polynomial surfaces, IEEE Transactions on Pattern Analysis and Machine Intelligence 2 (1980) 35-46.

[91] A. Levin, Polynomial generation and quasi interpolation in stationary non uniform subdivision, Computer Aided Geometric Design 20 (2003) 41-60.

[92] G. Li, W. Ma, A method for constructing interpolatory subdivision schemes and blending subdivisions, Computer Graphic Forum 26 (2007) 185-201.

[93] G. Li, W. Ma, H. Bao, A new interpolatory subdivision scheme for quadrilateral meshes, Computer Graphic Forum 24 (2005) 3-16.

[94] X. Li, J. Zheng, An alternative method for constructing interpolatory subdivision from approximating subdivision, Computer Aided Geometric Design 29 (2012) 474-484.

[95] C. Loop, Smooth Subdivision Surfaces Based on Triangles. M.S. Mathematics thesis University of Utah (1987).

[96] C. Loop, Bounded curvature triangle mesh subdivision with the convex hull property, The Visual Computer 18 (2002) 316-325.

[97] C. Loop, Smooth ternary subdivision of triangle meshes, Curve and Surface Fitting: Saint-Malo 2002 (A. Cohen, J.L. Merrien and L.L. Schumaker eds.) (2003) 295-302.

[98] C. Loop, J. Stam, Quad/Triangle Subdivision, Computer Graphics Forum 22 (2003) 79-86.

[99] A. Myles, K. Karciauskas, J. Peters, Extending Catmull-Clark Subdivision and PCCM with Polar Structures, IEEE Proceedings of the 15th Pacific Conference on Computer Graphics and Applications (2007) 313-320.

[100] G. Mustafa, J. Deng, P. Ashraf, N.A. Rehman, The mask of odd points n-ary interpolating subdivision scheme, Journal of Applied Mathematics Article ID 205863 (2012).

[101] A. H. Nasri, Polyhedral subdivision methods for free-form surfaces, ACM Transactions on Graphics 6 (1987) 29-37.

[102] P. Novara, Interpolation of polylines by non-stationary Chaikin's scheme, MASCOT Proceedings 2015, IMACS Series in Computational and Applied Mathematics 20 (2016).

[103] P. Novara, L. Romani, Building blocks for designing arbitrarily smooth subdivision scheme with conic precision, Journal of Computational and Applied Mathemathics 279 (2015) 67-79.

[104] P. Novara, L. Romani, On extraordinary rules of quad-based interpolatory subdivision schemes, Computer Aided Geometric Design 35 (2015) 225-242.

[105] P. Novara, L. Romani, Complete characterization of the regions of C^2 and C^3 convergence of combined ternary 4-point subdivision schemes, Applied Mathematics Letters, 62 (2016) 84-91.

[106] P. Novara, L. Romani, On the interpolating 5-point ternary subdivision scheme: a revised proof of convexity-preservation and an application-oriented extension, in press on Mathematics and Computers in Simulation.

[107] P. Novara, L. Romani, Local parameter-depending interpolation over arbitrary topology quad-meshes, in preparation.

[108] P. Novara, L. Romani, J. Yoon, Improving smoothness and accuracy of Modified Butterfly subdivision scheme, Applied Mathematics and Computation 272 (2016) 64-79.

[109] J. Pan, S. Lin, X. Luo, A combined approximating and interpolating subdivision scheme with C^2 continuity, Applied Mathematics Letters 25 (2012) 2140-2146.

[110] J. Peters, U. Reif, The simplest subdivision scheme for smoothing polyhedra, ACM Transactions on Graphics 16 (1997) 420-431.

[111] J. Peters, U. Reif, Shape characterization of subdivision surfaces - basic principles, Computer Aided Geometric Design 21 585-599 (2004).

[112] J. Peters, U. Reif, Subdivision Surfaces, (2008) Springer.

[113] J. Peters, L-J. Shiue, Combining 4- and 3- directional subdivision, ACM Transactions on Graphics 23 (2004) 980-1003.

[114] W. Press, S. Teukolsky, W. Vetterling, and B. Flannery, Numerical recipes: The art of scientific computing. Cambridge University Press, third ed., 1986.

[115] V. Protasov, Spectral factorizations of 2-block Toeplitz matrices and refinement equations, St. Petersburg Mathematic Journal 18 (2007) 607-646.

[116] K. Rehan, S. Siddiqi, A family of ternary subdivision schemes for curves, Applied Mathematics and Computation 270 (2015) 114-123.

[117] U. Reif, A unified approach to subdivision algorithms near extraordinary vertices, Computer Aided Geometric Design 12 (1995) 153-174.

[118] O. Rioul, Simple regularity criteria for subdivision schemes, SIAM Journal on Mathematical Analysis 23 (1992) 1544-1576.

[119] L. Romani, From approximating subdivision schemes for exponential splines to high-performance interpolating algorithms, Journal of Computational and Applied Mathematics 224 (2009) 383-396.

[120] L. Romani, V. Hernandez-Mederos, J.Estrada-Sarlabous, Exact evaluation of a class of non-stationary approximating subdivision algorithms and related applications, IMA Journal of Numerical Analysis 36 (2016) 380-399.

[121] G.C. Rota, W.G. Strang, A note on the joint spectral radius, Indagationes 22 (1960) 379-381.

[122] M. A. Sabin, Subdivision of Box-splines, in Tutorials on Multiresolution in Geometric Modelling, A. Iske, E. Quak, and M. Floater eds., Springer (2002) 51-68.

[123] S. Schaefer, J. Warren, A factored interpolatory subdivision scheme for quadrilateral surfaces, in Curve and Surface Fitting: Saint-Malo 2003 (A. Cohen, J.L. Merrien and L.L. Schumaker eds.) 373-382.

[124] D. Schmitter, R. Delgado-Gonzalo, G. Krueger, M. Unser, Atlas-free brain segmentation in 3D proton-density-like mri images, International Symposium on Biomedical Imaging (ISBI) (2013) 629-632.

[125] D. Schmitter, C. Gaudet-Blavignac, D. Piccini, M. Unser, New parametric 3D snake for medical segmentation of structures with cylindrical topology, in Proceedings of the 2015 IEEE International Conference on Image Processing (ICIP'15) (2015).

[126] J. Stam, Exact evaluation of Catmull-Clark subdivision surfaces at arbitrary parameter values, In SIGGRAPH '98: Proceedings of the 25th annual conference on Computer graphics and interactive techniques, ACM Press (1998) 395-404.

[127] V. Surazhsky, C. Gotsman, Explicit surface remeshing, Symposium on computational geometry (2003) 20-30.

[128] G. Székely, A. Kelemen, C. Brechbhler, G. Gerig, Segmentation of 2D and 3D objects from MRI volume data using constrained elastic deformations of exible fourier contour and surface models, Medical Image Analysis 1 (1996) 19-24.

[129] J. Tan, Y. Yao, H. Cao, L. Zhang, Convexity preservation of five-point binary subdivision scheme with a parameter, Applied Mathematics and Computation 245 (2014) 279-288.

[130] J. Tan, X. Zhuang, L. Zhang, A new four-point shape-preserving C^3 subdivision scheme, Computer Aided Geometric Design 31 (2014) 57-62.

[131] G. Umlauf, Analyzing the characteristic map of triangular subdivision schemes, Constructive Approximation 16 (2000) 145-155.

[132] L. Velho, D. Zorin, 4-8 subdivision scheme, Computer Aided Geometric Design 18 (2001) 397-427.

[133] V. Vidal, G. Lavoue, F. Dupont, Low budget and high fidelity relaxed 567-remeshing, Computer & Graphics 47 (2015) 16-23.

[134] V. Vidal, C. Wolf, F. Dupont, Combinatorial mesh optimization, Visual Computation 28 (2012) 511-25.

[135] D. Wustner, A. Larsen, N. Faergeman, J. Brewer, and D. Sage, Selective visualization of fluorescent sterols in caenorhabditis elegans by bleach-rate-based image segmentation, Traffic 11 (2010) 440-454.

[136] H. Zheng, M. Hu, G. Peng, Constructing $(2n-1)$-point ternary interpolatory subdivision schemes by using variation of constants, IEEE Proceedings of the International Conference on Computational Intelligence and Software Engineering (2009) 1-4.

[137] D. Zorin, Stationary subdivision and multiresolution surface representations, PhD thesis, Pasadena, California (1997).

[138] D. Zorin, A method for analysis of C^1-continuity of subdivision surfaces, SIAM Journal of Numerical Analysis 35 (2000) 1677-1708.

[139] D. Zorin, P. Schröder, W. Sweldens, Interpolating subdivision for meshes with arbitrary topology. In Proceedings of 23rd International Conference on Computer Graphics and Interactive Techniques (SIGGRAPH96) (1996) 189-192.

Acknowledgements

I would like to thank my supervisor Prof.ssa Lucia Romani for guiding me on my Research journey.
A huge thank you is also due to my co-supervisor Prof. Marco Donatelli for allowing me to pursue my interests during this Ph.D. Thank you so much for all your kindness and help especially during the last few months.
I would like to thank all those who have collaborated with me during the past three years: Stefano Serra-Capizzano, Debora Sesana and Jungho Yoon. Thanks to Michael Unser and his Ph.D students from EPFL for their hospitality during my stay in Lausanne. Thanks to Maria Charina for a wonderful month in Vienna. Thanks to Costanza Conti and Maria Antonia Cotronei for their kindness and valuable advices.
Finally, I would like to thank the anonymous referees for their helpful suggestions to improve this thesis.

Now I would prefer to continue in Italian ...

Un enorme grazie va a tutti i miei compagni di dottorato, di Como e di Milano, con cui ho condiviso questi anni di lavoro e confronto, ma anche di divertimento e amicizia. Un ringraziamento speciale a Mari, la migliore scoperta di questo dottorato, e a Elena, con cui ho condiviso nove anni di matematica.
Un grazie alle mie Amiche di sempre, per aver festeggiato i miei successi e per avermi supportato nei giorni più difficili.
Grazie alla mia famiglia, Mamma e Papà, Alberto e Susy, per essere sempre dalla mia parte.
Infine, grazie a Mattia. Ti ho incontrato durante il primo anno di dottorato e hai stravolto tutti i miei programmi. Averti accanto mi rende felice.